The University Of Sheffield.

Department of Immunity, Infection and Cardiovascular Disease
The Medical School, Royal Hallamshire Hospital

Characterisation of the Pathophysiological Role of Chloride Ion Channels in Human Leukocytes Function

Hani Mansour M Alothaid

Submitted as a thesis for the degree of Doctor of Philosophy in Cellular and Molecular Medicine

Supervised by

Dr. Louise Robson and Dr. Richmond Muimo

June 2018

Dedication

I dedicate this work to my parents with my sincerest gratitude and love: I miss them every day. Also to my wife, Shuruq Almabar, for her patience during the PhD journey.

Acknowledgments

I would like to express my deepest gratitude to my supervisors, Dr. Richmond Muimo and Dr. Louise Robson for their support and guidance, care, patience, and for providing me with an excellent atmosphere in which to perform my research. My sincere thanks also to Dr. Mark Thomas, Dr. Andrew Streets (my personal tutor), Dr. Rahaf Issa, Dr. Mohammed Nassar and Dr. Rachid Tazi-Ahnini, who have all helped me immeasurably throughout the process.

I owe a debt to the following people: Abdullah Talari, Mohammed Aldughaim, Jonathan Kilby, Benjamin Durham, Bezaleel Mambwe, Antonio Lapenna, Mohammed Moamin, P. Anujan, Md Mohasin, Ali Jaafar, Majid Almansouri, Bandar Baothman, Mahmoud Habibullah, Hassan Alshamrani, Khalaf Alshamrani, Fawaz Alqahtani and Ali Shukur, who as good colleagues were always willing to help and offer their best advice and suggestions.

Many thanks to my best friends, Mahmud Hassan and Azeez Yusuf, with whom I spent many days and nights from a distance.

I would also like to thank my mother, father, sisters, brothers, and my wife's parents and many other friends here in the UK and in Saudi Arabia. They were constant in their support and encouraged me during my studies abroad.

Finally, a big and special thank you goes to my wife and my children for their love and patience. They were always there to cheer me up and stood by me through the good and difficult times. My research would not have been possible without their support.

Hani,

June 2018

About the author

I am a Saudi Arabian government-sponsored PhD candidate in Cellular and Molecular Medicine (Immunopathophysiology) at The University of Sheffield. My biomedical training began at Manchester Metropolitan University where I gained a BSc (Hons) in Biomedical Science and graduated with second class honours. My passion for biomedicine and desire for research excellence prompted my decision to continue my education and training in Molecular Medicine (MSc), graduating with Merit from The University of Sheffield. Recently, I have been appointed as a lecturer in the Department of Laboratory Medicine, in the Faculty of Applied Medical Sciences at Albaha University in Saudi Arabia. My work on CF disease immunological changes will continue beyond this PhD through collaboration with Prof. Hanaa Banjar, a Consultant of Paediatric Pulmonology and CF at King Faisal Specialist Hospital and Research Centre (KFSH&RC) in Riyadh, Saudi Arabia.

Doctoral Development Programme (DDP) and related activities

Throughout my PhD journey, I have attended DDP modules to advance my research skills. I successfully completed the following core modules: Research Ethics and Integrity (FCM6100); Research Training: Literature Review (MED6950); Research Training: Techniques, Safety and Report (MED6960); and Introduction to EndNote (LIB102).

In addition to many internal seminars and workshops, I also attended the following external courses:

Short course: Immunology for clinicians and scientists. 28th – 30th November 2016, Imperial College, **London.**

Conference: Protein-Protein Interactions Conference. 5th – 6th December 2016, Science Chemistry Innovation (SCI), **London.**

Symposium: Lifecourse Biology: From development to disease and the clinic. 13th – 15th September 2017, The Bateson Centre, **Sheffield.**

Short course: Biological Basis of Cancer Therapy: Pharmacology, Chemotherapy & Molecular Biology. 13th – 17th November 2017, School of Oncology, Christie Hospital, **Manchester.**

Workshop: Bone and joint biology: Basic course in bone and cartilage biology and disease. 23rd – 24th November 2017, Bone Research Society, **Sheffield.**

In the **Centre of Student Skills and Development in Sheffield**, I attended three workshops: (1) Reading for Memory Workshop; (2) Academic Writing Workshop and; (3) Dissertation Planning Workshop.

With **Sheffield Teaching Assistant (LTS) programmes**, I actively participated and attended the following workshops: (1) Confidentiality & Data Protection; (2) Assessment & Feedback; (3) Laboratory Demonstrating; (4) Lecturing; (5) Research Supervision; (6) Academic Culture: Transitions & Expectations; and (7) Teaching Design and Delivery.

With the **Sustainability Group at the University of Sheffield**, I attended a 6-lecture series in Sustainability Skills & Education (SusSEd) and received confirmation of completion.

Published Abstracts and Presentations

Internally:

Alothaid, H., Robson, L. & Muimo, R. (September 2015). PKA-mediated regulation of calcineurin as a switch in cell secretion. Oral presentation presented in the medical school.

Alothaid, H., Robson, L. & Muimo, R. (June 2016). cAMP/PKA-mediated regulation of PP2B as a switch in immune cells secretion. Poster presentation presented in the Medical School Research Meeting.

Externally:

Alothaid, H., Robson, L. & Muimo, R. (July 2016). cAMP/PKA-mediated regulation of calcineurin as a switch in cell secretion. *Protein Phosphatases Conference.* **Colorado, USA.**

Alothaid, H., Robson, L. & Muimo, R. (May 2017). PKA-dependent calcineurin as a switch in immune cells secretion. *ICCF 2017: 19th International Conference on Cystic Fibrosis.* **London, UK.**

Alothaid, H., Robson, L. & Muimo, R. (July 2017). Lipopolysaccharides from *Pseudomonas aeruginosa* activates chloride channels in monocytes. *Europhosphatase 2017: Phosphatases in cell fates and decisions.* **Paris, France.**

Alothaid, H., Robson, L. & Muimo, R. (November 2017). *Pseudomonas aeruginosa* bacteria activates chloride ion channels in immune cells. *International Conference on Immunology and Immunotechnology.* **Barcelona, Spain** (Youngest Investigator Award).

Alothaid, H., Robson, L. & Muimo, R. (March 2018). Cl^- channels play a role in mediating cytokines release during *Pseudomonas aeruginosa* infection. *Middle East Cystic Fibrosis Association Conference.* **Izmir, Turkey.**

Alothaid, H., Robson, L. & Muimo, R. (April 2018). Chloride ion channels play role in mediating immune response during *Pseudomonas aeruginosa* infection. *ICMD 2018: International Conference on Molecular Diagnostics.* **London, UK.**

Manuscripts in preparation

Alothaid, H.[1], Robson, L.[2] & Muimo, R.[1] **Role of Chloride Ion Channels in Human Monocyte Function.** [1] Department of Infection, Immunity and Cardiovascular Disease, The Medical School, University of Sheffield, Sheffield, UK, S10 2RX. [2] Department of Biomedical Science, University of Sheffield, Sheffield, UK, S10 2TN.

Essential laboratory training and practical skills acquired

Throughout my PhD journey, I have gained many skills and have been trained in various techniques.

In terms of safe working practices, I completed first aid training, a general safety course, out of hours training, fire training, waste training and risk assessment with COSHH training also covered.

More specific to the experimentation process, I completed the following training courses: designing and making experimental solutions and buffers, common lab calculations, culture of mammalian cell lines and primary human cells maintenance, use of balances/pH meters, and other basic and general equipment training.

Finally, the following training was also necessary for the completion of this present research: protein quantification from cells, biochemical studies such as immunoprecipitation, sodium dodecyl sulfate polyacrylamide gel electrophoresis and western blots, functional assays using patch clamp techniques, use of basic and advanced microscopes, phagocytosis and survival phagocytosed assays, FITC-dextran fluorescent assay, enzyme-linked immunosorbent assay, MTS cytotoxicity assays, cytometric bead array by Flow cytometry, and cell migration assays.

Research Skills and Personal Development

Over the course of my PhD journey, I have not simply developed my scientific skills and knowledge but have also developed a great many ancillary skills. These are described below.

I have become competent in the use of Excel and databases and thus in data analysis and presentation. I have also learned to use the specialist software PClamp and GraphPad Prism to conduct general statistical and mathematical analysis.

I have been fortunate enough to acquire additional general bioscience knowledge through attendance at external and internal seminars, short courses and conferences. Guidance and support were always provided by my supervisors in terms of detailed knowledge related to the PhD programme and project.

I have been able to engage in critical analysis of papers through regular discussion with supervisors and have developed my writing skills through the submission of abstracts, writing of literature reviews and thesis planning. Detailed feedback on various aspects of my PhD (abstracts, first year report, literature review, thesis plan and final thesis) has significantly contributed to my ability to self-critique.

My presentation and poster preparation skills have been honed through practice, as well as development of note-taking skills in seminars. Of great use has been the improvement in my cooperation and collaboration skills developed through lab work with colleagues and monthly supervisory meetings. Additionally, I was involved in laboratory demonstrations for MSc students between April – August 2017.

My planning and organisational skills have been greatly enhanced by heeding the advice of my supervisors in structuring my work on a weekly basis. I have also developed time management, patience and the ability to work under pressure. I have had to become adaptable and resilient due to unsuccessful experiments and have learned to succeed by troubleshooting and repeating experiments several times. Guidance and support on this was usually provided by my supervisors.

LIST OF CONTENTS

LIST OF FIGURES

LIST OF TABLES

LIST OF MAIN ABBREVIATIONS

°C	degree Celsius
ABC	ATP binding cassette
ANOVA	analysis of variance
AnxA2	annexin A2
ASL	airway surface liquid
ATP	adenosine triphosphate
ATPase	adenosine triphosphatase
BAPTA-AM	1,2-Bis (2-aminophenoxy) ethane-N,N,N′,N′-tetraacetic acid tetrakis (acetoxymethyl ester)
BSA	bovine serum albumin
Ca^{2+}	calcium
cAMP	cyclic adenosine monophosphate
CaM	calmodulin
CaN	calcineurin
CBA	cytometric bead array
CF	cystic fibrosis
CFTR	cystic fibrosis transmembrane conductance regulator
CFTR(inh)-172	CFTR inhibitor
CFU	colony-forming unit
Cl^-	chloride
CO_2	carbon dioxide
Cs^+	caesium
CsA	cyclosporin
dH_2O	distilled water
DIDS	4,4'-Diisothiocyano-2,2'-stilbenedisulfonic acid
DMSO	dimethyl sulfoxide
E. coli	*Escherichia coli*
ELISA	enzyme-linked immunosorbent assay
ENaC	epithelial sodium channel
EPAC	exchange factor directly activated by cAMP
FBS	foetal bovine serum
FC	flow cytometry
Fig.	figure
FSK	forskolin
G_{in}	whole-cell inward conductance
G_{out}	whole-cell outward conductance
H_2O	water
HBSS	Hanks' balanced salt solution
HCO_3^-	bicarbonate
HPBM	human peripheral blood monocyte
HRP	horseradish peroxidase
IB	immunoblot
IBMX	isobutylmethylxanthine
IL-1β	Interleukin 1 beta
IMS	industrial methylated spirits
IP	immunoprecipitation
I-V	current-voltage relationship
K	potassium
KCl	potassium chloride

kDa	kilo Dalton
LPS	lipopolysaccharide
MDM	HPBM-derived macrophage
Mg	magnesium
mg	milligram
min	minute
MOI	multiplicity of infection
mRNA	messenger RNA
ms	millisecond
MTS	3-(4,5-dimethylthiazol-2-yl)-5-(3-carboxymethoxyphenyl)-2-(4-sulfophenyl)-2H-tetrazolium, inner salt
mV	millivolt
MW	molecular weight unit
Na_2HPO_4-$7H_2O$	sodium phosphate dibasic heptahydrate
NaCl	sodium chloride
NaOH	sodium hydroxide
NBD	nuclear binding domain
Nig	nigericin
nM	nanomolar
O	oxygen
OD	optical density
ORCC	outwardly rectifying chloride channel
P. aeruginosa	*Pseudomonas aeruginosa*
pA	pico-Ampere, a unit of electric current measurement
PAO1	strain of *Pseudomonas aeruginosa*
PBMC	peripheral blood mononuclear cell
pF	pico-Farad, a unit of capacitance
pg	pictogram
PKA	protein kinas A
PKC	protein kinas C
PKI	protein kinase A inhibitor
PMA	phorbol 12-myristate 13-acetate
PP2B	protein phosphatase 2B (calcineurin)
qPCR	quantitative polymerase chain reaction
rpm	revolution per min
SDS-PAGE	sodium dodecyl sulfate polyacrylamide gel electrophoresis
SEM	standard error of the mean
T-75	75 cm^2 tissue culture flask
THP-1	human monocytic cell line
TMB	3,3′,5,5′-Tetramethylbenzidine
TNF-α	tumour necrosis factor alpha
WB	western blot
µM	micromolar
µS	microsiemens

Abstract

Cystic fibrosis (CF) is a disease that arises due to dysfunction in the cystic fibrosis transmembrane conductance regulator (CFTR) protein, causing thickening of mucus and bacteria colonisation of the airways. The disease has a prevalence of 151 per 100,000 people in the UK. In the airway, CFTR has been shown to form a functional complex with S100A10 – a calcium (Ca^{2+}) binding protein – and annexin A2 – a Ca^{2+}-regulated membrane-binding protein – in a cAMP/PKA-dependent manner to mediate cell secretion. In endothelial cells, activation of calcineurin (CaN)-like phosphatase by cAMP/PKA has been shown to enhance the release of von Willibrand factor (vWF) from Weibel-Palade bodies (WPBs). This study thus aims to establish the extent and importance of regulation of chloride (Cl^-) channels (CFTR and outwardly rectifying Cl^- ion channel (ORCC)) via cAMP-dependent pathways and LPS in the release of pro-inflammatory cytokines, phagocytosis of bacteria and survival of phagocytosed bacterial cells by immune cells.

We have successfully demonstrated interaction of CaN, S100A10 and AnxA2 in PMA-treated monocytic THP-1 cells in response to cAMP/PKA activation. PKA was also found to regulate Cl^- channels (CFTR and ORCC) in these cells. In addition, LPS from *P. aeruginosa*, but not *E. coli*, was found to induce Cl^- conductance via CFTR/ORCC in both PMA-treated monocytic THP-1 cells and human peripheral blood monocytes (HPBMs). This Cl^- transport requires PKA and CaN. Investigation into the role of Cl^- on phagocytotic ability of the immune cells showed that Cl^- channels are important for successful phagocytosis and killing of *P. aeruginosa* by PMA-treated monocytic THP-1 cells and HPBMs-derived macrophages (MDMs). In addition, LPS induced the release of both IL-1β and TNF-α from HPBMs. However, PKA/CaN appears not to be involved in CFTR/ORCC-mediated cytokine release. Further investigation showed that while PKA/CaN is not required for CFTR-mediated inflammatory responses and the phagocytotic ability of immune cells, Ca^{2+} and EPAC2 are absolutely required in a PKA-independent manner.

In conclusion, LPS from *P. aeruginosa* activates CFTR/ORCC, and this is facilitated by PKA/CaN activity. Moreover, EPAC2 and Ca^{2+} may be the requisite factors for CFTR/ORCC-mediated inflammatory response to occur in immune cells.

CHAPTER 1

General Introduction

1 GENERAL INTRODUCTION

1.1 CHLORIDE CHANNELS

Ion channels are key molecules that regulate signal transduction across biological membranes. The mechanism by which ions are transported was first discovered by Erwin Neher and Bert Sakmann in the 1970s using the patch clamp technique (1). Following this, the primary structure of an ion channel and transporter was discovered via molecular cloning in the 1980s, providing more specific insight into the functions of these proteins in maintaining homeostasis and other key cellular processes (2). The control of ion movement into and out of cells governs a range of biological activities that are important for health and may play a role in disease processes (3). Chloride (Cl^-) channels are a diverse group of anion-selective channels with different functional and structural characteristics. They are proteinaceous pores in biological membranes that enable passive diffusion of anions along the electrochemical gradient. These channels can conduct other anions, including iodide and nitrate, but are known as Cl^- channels since Cl^- is the most abundant anion in living organisms. Cl^- channels are responsible for the regulation of a great variety of processes and biological components. Examples include neuronal responses, skeletal, cardiac and smooth muscle cells, cell volume, transepithelial salt transport, acidification of cell compartments, and the cell cycle and cell death (4).

Cl^- channels are also implicated in health and disease. For instance, myotonia congenita is caused by inherited mutations in the *ClC-1* gene (5), and Cl^- conductance via ClC-1 channels is severely compromised in these patients. Another Cl^- channel, ClC-5, is implicated in Dent's disease, a syndrome characterised by kidney stones, proteinuria and hypercalciuria (6). Finally, and of most significance to this present research, is the cystic fibrosis transmembrane conductance regulator (CFTR), a major Cl^- channel that is responsible for development of cystic fibrosis (CF), another inherited disease that leads

to an early death (5). Thus, Cl^- channels are highly relevant to the development of several human diseases, and as such, a thorough understanding of these ion channels and their biological implications is of great medical, scientific and societal importance.

1.1.1 Structure and biological function of Cl^- ion channels

Cl^- transport is needed to regulate cell volume through modification of cell osmotic stability as well as for transepithelial transport of solutes across multiple cell types in the body (4). Changes in Cl^- concentrations may be the regulating factor of numerous cell functions: such as regulation of volume and homeostasis, transepithelial transport and electrical excitability in specific cell populations (4).

Together with other ion transporters, Cl^- channels regulate the composition and volume of the cytoplasm. For example, in regulating the cytoplasmic pH, Na^+/H^+ exchangers require a parallel Cl^- channel to recycle the participating chloride ions (7). Cl^- channels also play a role in acidification of intracellular compartments, a process which occurs via adenosine triphosphatases (ATPase), a vacuolar proton that acts together with Cl^- conductance (8). However, Cl^- channels are not very selective and allow easy passage of most inorganic anions and even some larger organic anions (9). Therefore, the term Cl^- channel may be somewhat misleading and anion channels would perhaps be more accurate as a descriptor of function (9).

It is still unclear how many separate Cl^- channel families exist. This uncertainty, in part, arises from disagreements surrounding the choice of criteria for classification. However, the larger families include the ClC family with nine members that can function in the plasma membrane and intracellular compartments: the CFTR channel, the ligand-gated GABA- and glycine-receptor Cl^- channels, and the CLIC family, the latter of which is thought to encode calcium (Ca^{2+})-activated Cl^- channels (4). All of these are known to have a structural-functional correlation with disease development.

1.1.2 CFTR

CFTR belongs to the ABC subfamily C (ABCC7) that acts as an ion channel (10, 11), and is localised to the apical regions of epithelial cells (12). Mutations in CFTR are responsible for CF; therefore, this ion channel is one of the most heavily-researched ABC transporters. CFTR is encoded by the *CFTR* gene, first discovered by Dr Lap Chee's research group in 1989 (13). The protein product of the gene is a 1480-residue length membrane protein with a typical ABC transporter structure but with an additional regulatory region (R) and extended N- and C-termini. ABC transporters have a common structure with two transmembrane domains (TMDs) and two nucleotide-binding domains (NBDs) (Fig. 1-1). Therefore, CFTR motifs arranged as TMD1-NBD1-R-TMD2-NBD2 (14). CFTR forms an ion channel at apical epithelial cell membranes with limited selectivity (15). It also facilitates bicarbonate (HCO_3^-) movement, sharing the transport pathway with Cl^- (14).

Adenosine triphosphate (ATP) binds to the two NBD domains forming the NBD dimer. This is then communicated to the TMD domains resulting in a conformational change. When the NBD dimer forms, the CFTR anion pore opens. Upon ATP hydrolysis, the channel returns to its closed state (16). This allows anion flow and is mainly dependent on the electrochemical potential – the concentration gradient and electrical potential difference across the membrane (17). In CF this channel function is compromised with reduced Cl^- efflux. NBD dimerisation facilitates the formation of an outwards pore by the TMD domains with the R domain facilitating regulation via protein kinase A (PKA) through phosphorylation (18).

The cyclic adenosine monophosphate (cAMP)-regulated CFTR is an ion channel and a regulator of other channels, including epithelial Na^+ channel (ENaC) and Cl^- intracellular channels-1 (CLIC1) (19). CFTR has also been found to regulate other channels like the

renal outer medullary potassium channel (ROMK2), the sodium-proton exchanger, and aquaporins (14). Therefore, the CFTR channel has a diverse range of functions and is therefore an important consideration in the study of health and disease.

The electrophysiological properties of the epithelia are modified depending on CFTR-mediated anion secretion (Cl^- and HCO_3^-) and ENaC-mediated sodium (Na^+) absorption (20). CFTR has three phases: open, closed, and open-ready. The latter of these prevents Cl^- flux but can rapidly transform into the open phase (21). CFTR channel activity is also regulated by PKA phosphorylation of the R region and the availability of intracellular ATP (22, 23). At rest, the R region is thought to be dephosphorylated (24). Rich et al. (1991) have shown that deletion of the R region leads to a permanently open channel; however, CFTR inhibition is needed to conserve cellular ATP levels. CFTR can be activated by other protein kinases, such as protein kinase C (PKC), while phosphorylation of the R residue for activation can occur on any of nine phosphorylation sites and have an additive effect on channel activity (25, 14). ATP-binding is needed to open the channel, and ATP hydrolysis is associated with channel closure. Therefore, CFTR only requires ATP-binding to undergo conformational changes allowing its opening. In addition, the CFTR gating cycle of about 1 second correlates to the estimated turn-over rate of ATP (26). Non-hydrolysable ATP prolongs channel opening delaying ATP physiological activities, however this is not permanent (14).

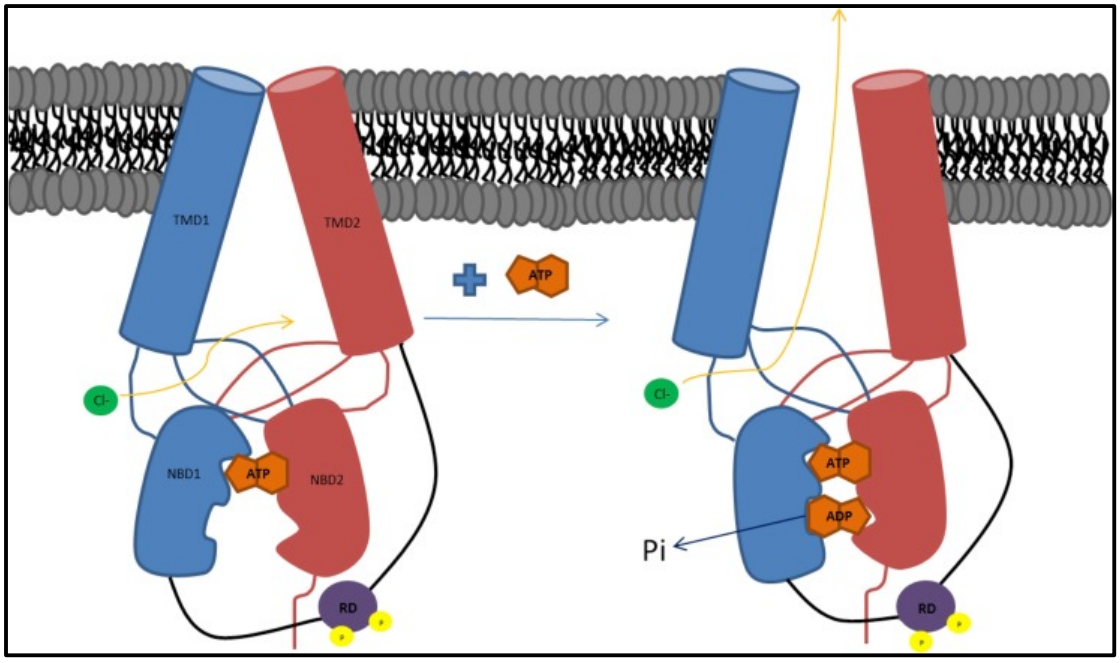

Figure 1-1. The mechanism of CFTR anion channel gating.

Schematic representation of the possible structural changes that can lead to the opening of the CFTR protein channel via ATP binding and hydrolysis-driven conformational changes, allowing the flow of the Cl^- through the opening. Adapted from Wang Y, *et. al.;* Meng X, *et. al.* (27, 28).

1.1.3 Outward rectifying Cl^- channels

Early studies of CF revealed that the properties of Na^+ and Cl^- channels are altered in CF epithelia. This indicated CFTR's regulatory function (29). The first example of such a channel regulated by CFTR was the outwardly rectifying Cl^- ion channel (ORCC). CFTR is thought to be needed for activation of ORCC and it is hypothesised that CFTR mediates the transportation of other small regulatory molecules out of the cell which can then activate other proteins (4). Activation of ORCC in healthy epithelia occurs via cAMP. In both unhealthy and CF epithelia the ORCC is known to be stimulated by extracellular ATP (30).

There is a relationship between CFTR and ORCC whereby both are activated by cAMP under depolarising potentials: a net negative charge inside the cell compared to the external environment. Heterotrimeric G proteins inhibit cAMP-activated Cl^- channel currents in airway epithelial cells (31). It is suggested that CFTR modulates ORCC via guanosine-5'-triphosphate (GTP)-binding proteins and through intermediate purinergic receptor regulation, although this mechanism may be regulated by ATP or uridine-5'-triphosphate (UTP) activation of purinergic receptors (32). GTP-binding proteins modulate ion channels both directly and indirectly through a pathway involving protein kinases (33).

1.2 Regulation of ORCC and CFTR channels

The goal of CFTR regulation is to enable its translocation to the plasma membrane where its function and stability are controlled, thereby enabling CFTR to act as a Cl^- channel and perform the anion secretion needed for hydration of the epithelium. As with all other proteins with physiological/cellular functions, several factors influence regulation of CFTR activities. Some of these involve activation of pathways that enable long-term and transient direct interaction with second messengers, such as cAMP or different proteins

(discussed below). Similarly, ORCC regulation is of importance in the regulation of Cl^- owing to its regulation by CFTR and anion movement in and out of the cell. This has potential implications for health and disease.

1.2.1 ATP, Adenylate cyclase and cAMP regulation of CFTR and ORCC

cAMP is one of the most important and conserved second messengers for many pathways. It regulates numerous cellular processes including metabolism, secretion, cell fate, gene transcription and CFTR activation and function. The production of cAMP from ATP is initiated by numerous ligands binding to G_s protein-coupled receptors at the cell membrane. This activates adenylyl cyclases (ACs), enzymes which are responsible for the generation of cAMP from ATP (34). The freshly produced cAMP activates PKA which in turn activates plasma membrane-bound CFTR. This facilitates ATP-binding, leading to channel activation. In the presence of ATP, CFTR is open and active, enabling Cl^- efflux from the cell. For channel closure, ATP is then converted to adenosine diphosphate (ADP) (34, 35). Therefore, ATP is involved in CFTR activation via cAMP produced by ACs. Later, ATP interacts with the active channel enabling it to open and Cl^- efflux to occur.

Similarly, whole cell and single channel patch-clamp analyses have shown that CFTR activation leads to transport of ATP out of the cell. This stimulates ORCC via a purinergic receptor-dependent signalling mechanism in a cAMP-dependent manner (31). Therefore, the role of cAMP in the activation and regulation of both CFTR and ORCC, as demonstrated experimentally, seems crucial to their regulation of cellular functions.

1.2.2 The involvement of the PKA-dependent pathway

ACs produce cAMP, whose main function is to regulate protein phosphorylation. The first defined recipient of this regulation is PKA, a heterotetrameric holoenzyme with two regulatory (R) and two catalytic (C) units. Low intracellular cAMP levels are associated

with inactive PKA, but when cAMP levels are high, two molecules of cAMP bind to each R unit, releasing C units. These C units are responsible for phosphorylation of the serine (S) or threonine (T) residues within the R-R-X-S/T-X sequence (36).

The PKA holoenzyme occurs as cytoplasmic type I PKA and particulate type II PKA. Numerous A-kinase anchoring proteins (AKAPs) have been identified which facilitate the binding of PKA, protein phosphatase 2B (PP2B or CaN) and PKC to different cell membranes. This allows the formation of large macromolecular signalling complexes which include cAMP, Ca^{2+}, phospholipid and calmodulin (CaM)-dependent pathways (35).

The CFTR domain organisation is TMD1-NBD1-R-TMD2-NBD2. The R-domain is highly charged with numerous residues which can be phosphorylated by the cAMP-dependent PKA. This allows activation of CFTR by PKA which adds phosphate groups to the residues within the R region of CFTR thereby inducing its conformational change (36, 37).

The PKA-dependent activation of ORCC has also been evaluated in the literature. Direct effects of PKA on activation of ORCC have been hypothesised based on interruption of PKA activity and subsequent restoration (4). For instance, the expression of recombinant CF genes in bronchial epithelium corrects defective Cl^- secretion and induces the appearance of small, linear Cl^- conductance channels. Furthermore, recombinant genes lead to restoration of PKA activation of ORCC (38).

1.2.3 PKC phosphorylation of CFTR

Like PKA, PKC is a protein kinase with regulatory functions over CFTR. Phosphorylation of CFTR by PKC has been predicted to occur at the NBD1 of CFTR as well as the regulatory domain. The regulatory function of PKC over CFTR is, however, indirect as this phosphorylation occurs to enhance the activation of CFTR by PKA (39).

It has been hypothesised that once phosphorylated by PKC, there is hydrolysis of ATP at the NBD1 and NBD2 domains of CFTR such that the hydrolysis at the NBD1 results in opening of the channel that closes the channel at the NBD2 (40). As shown in a mutational study by Chappe, Hinkson (39), removal of all PKC phophorylation residues drastically reduced the activity of PKA on CFTR whilst only partially reducing PKC activity. PKC residues T582, T604 and S686 in CFTR were found to be strongly required for PKA activation of CFTR. These residues are located in a highly conserved region among different species, highlighting the possible regulatory importance of the residues to CFTR function.

1.2.4 CFTR phosphorylation by other kinases

One of the functional implications of CFTR regulation is to maintain its membrane localisation as this is crucial to its function. Spleen tyrosine kinase (SYK) is a cytoplasmic tyrosine kinase with immunomodulatory functions, especially in leukocyts (41, 42). Phosphorylation of CFTR by SYK has been shown through mutagenesis to result in decrease in CFTR localisation to the plasma membrane. The role of SYK is known to be tied to casein kinase II (CK2), a serine-threonine kinase proven to regulate trafficking of secreted proteins. Phosphorylation of CFTR by CK2 is known to regulate CFTR biogenesis and its function at the apical membrane in epithelial cells (43, 42). Phosphorylation of CFTR at the Y512 residue has been demonstrated to be required for CK2 phosphorylation of CFTR at sequence PGTIKENIIFGVSY$_{512}$DEYRYR (42). As such, it is possible that phosphorylation of CFTR by CK2 after SYK phosphorylation may occur to upregulate CFTR protein expression of the otherwise downregulated CFTR in physiological conditions where there is demand for CFTR.

1.2.5 Calcineurin

CFTR is also associated with a large multi-protein complex comprised of cAMP/PKA/calcineurin (CaN) and annexin A2 (AnxA2)-S100A10 (44, 45). CaN is a serine/threonine protein phosphatase that is regulated by Ca^{2+} and CaM (46). It is responsible for coupling Ca^{2+} signalling to various processes such as inflammation and lymphocyte activation. Recently, CaN is found to be regulated by PKA in a Ca^{2+}-independent manner (see Fig. 1-2) (47). Therefore, cAMP activates PKA and this phosphorylates and activates both CFTR and CaN and form a complex that also includes AnxA2 and S100A10 (44).

```
001 MAGASELGTGPGAAGGDGDDSLYPIAVLIDELRNEDVQLRLNSIKKLSTIALALGVERTRSELLPF
067 LTDTIYDEDEVLLALAEQLGNFTGLVGGPDFAHCLLPPLENLATVEETVVRDKAVESLRQISQEHT
133 PVALEAYFVPLVKRLASGDWFTSRTSACGLFSVCYPRASNAVKAEIRQQFRSLCSDDTPMVRRAAA
200 SKLGEFAKVLELDSVKSEIVPLFTSLASDEQDSVRLLAVEACVSIAQLLSQDDLETLVMPTLRQAA
266 EDKSWRVRYMVADRFSELQKAMGPKITLNDLIPAFQNLLKDCEAEVRAAAAHKVKELGENLPIEDR
332 ETIIMNQILPYIKELVSDTNQHVKSALASVIMGLSTILGKENTIEHLLPLFLAQLKDECPDVRLNI
398 ISNLDCVNEVIGIRQLSQSLLPAIVELAEDAKWRVRLAIIEYMPLLAGQLGVEFFDEKLNSLCMAW
464 LVDHVYAIREAATNNLMKLVQKFGTEWAQNTIVPKVLVMANDPNYLHRMTTLFCINALSEACGQEI
530 TTKQMLPIVLKMAGDQVANVRFNVAKSLQKIGPILDTNALQGEVKPVLQKLGQDEDMDVKYFAQEA
597 ISVLALA

XXXX Myristoylation site
XXXX cAMP/cGMP Protein dependent kinase phosphorylation site
XXXX PKA phosphorylation site
XXXX CK2 and PKC phosphorylation site
```

Figure 1-2. Amino acid sequence of CaN and possible regulatory sequences.
Sequence of CaN subjected to prosite scan at http://prosite.expasy.org/. CK2 and PKC phosphorylation sites are possible for both serine and threonine residues. PKA phosphorylation site is highlighted purple as cAMP protein kinase site. PKA activities can also be regulated through CK2 as shown by Rebholz H, *et. al.* (48). Thus, activation of CaN by PKA can either be direct or indirect by involving another protein kinase.

CaN is a heterodimer consisting of a catalytic sub-unit (CaN-A) and a Ca^{2+}-binding regulatory sub-unit (CaN-B) (46). High cytosolic Ca^{2+} concentrations induce conformational changes in CaN-B and thereby activate CaN-A and CaM function. In airway and gut epithelia, CaM is regulated by PKA via PKA-mediated phosphorylation of CaN. This leads to CaM complex formation with AnxA2-S100A10 and CFTR (Fig. 1-3) (44).

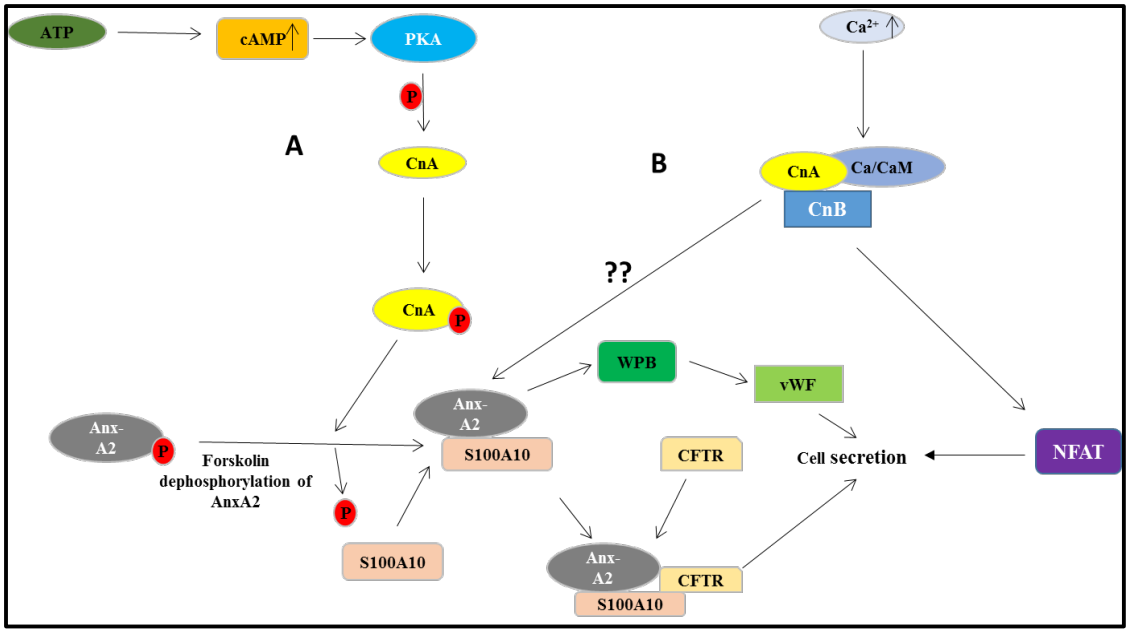

Figure 1-3. CaN activation by cAMP/PKA and interaction with CaM for cell secretion.

(A) Activation of CaN-like phosphatase activity by cAMP/PKA has been shown to enhance the release of von Willibrand factor (vWF) from Weibel-Palade bodies (WPB). This is affected through the complex formed between S100A10 and AnxA2 by dephosphorylation of AnxA2. This cAMP/PKA activity likely works through activation of CaN phosphatase in regulating AnxA2 and S100A10 complex formation. S100A10 and AnxA2 have also been shown in the past to aid cell secretion through interaction with CFTR. **(B)** Ca^{2+}/CaM also activate CaN in a different pathway that is regulated by Ca^{2+} levels. These pathways (cAMP/PKA and CaM-dependent activation of CaN) may all be working in concert to aid cell secretion.

CaN regulates signal transmission from the cytosol to the nucleus via dephosphorylation and translocation of nuclear factor of activated T cells (NFAT) into the nucleus where they activate numerous physiological and developmental processes. CaN also plays a vital role in the activation of lymphocytes and so regulates the immune response (49). CaN also appears to be activated by lipopolysaccharides (LPS) in ventricular myocytes, implicating CaN activity in low-grade inflammatory processes regulated by LPS (50). Furthermore, inactivation of CaN leads to decreased responsiveness to LPS in macrophages and dendritic cells, a process that protects against LPS-induced toxicity, supporting the link between LPS-mediated inflammation and CaN-dependent toxicity and

apoptosis (51). In addition, CaN confers Ca^{2+} sensitivity to the function of the CFTR channel. This occurs as a complex of CFTR and CaN together with other proteins.

1.2.6 Effect of PP2C phosphatase activity on CFTR

CaN (PP2B) is a Ca^{2+}-dependent phosphatase known to regulate CFTR in a cAMP-dependent manner, as described above. However, PP2C is another protein phosphatase that is Manganese cation (Mn^{2+})- or Magnesium cation (Mg^{2+})-dependent and has been proposed to play a regulatory role in the inactivation of CFTR. This conclusion is based on findings that okadaic acid, as an inhibitor of PP1, PP2A and PP2B but not PP2C, was unable to prevent deactivation of CFTR Cl^- conductance (52). Travis, Berger (53) showed that a recombinant PP2C protein and co-expression of CFTR and PP2C in an epithelia cell line was able to dephosphorylate and deactivate CFTR. Based on the distinct response of PP2C to inhibitors in comparison with other phospahtases against CFTR, PP2C may be a worthwhile regulatory target for phosphatase.

1.2.7 Involvement of AnxA2 and S100A10 in the pathway

CFTR activity is partially dependent on complex formation with other molecules. The CFTR complex requires AnxA2 and S100A10 to form a functional complex that is Ca^{2+}-dependent and cAMP-dependent (see Fig. 1-3 above). As the AnxA2-S100A10 complex plays a role in Cl^- transport and in integrating Ca^{2+} and cAMP signalling in airway epithelial cells (54), consideration of both molecules and their functional dependence within the complex are considered in this study.

1.2.7.1 AnxA2

AnxA2 is a member of the annexin family of proteins that bind to negatively charged phospholipids in cell membranes in a Ca^{2+}-dependent manner. The carboxylic acid (COOH)-terminal core of annexin contains Ca^{2+}-binding sites, and the NH_2-terminal allows protein-protein interactions (55, 56). Annexins share sequence homology with the

CFTR region that is commonly deleted in the F508Δ-CFTR mutant. This region is also implicated in endo- and exocytosis (56).

Phosphorylation of AnxA2 prevents complex formation with S100A10 and is mediated by high Ca^{2+} concentrations in the cytosol (57). However, dephosphorylation and activation of AnxA2 is a cAMP-dependent process that facilitates interaction with S100A10 and regulation of the Cl^- flux (54). Therefore, both Ca^{2+}- and cAMP-dependent pathways coordinate to regulate the AnxA2-S100A10 and CFTR interaction via phosphorylation and dephosphorylation of AnxA2. The phosphorylation of AnxA2 depends on Ca^{2+}, thus preventing interaction with S100A10 (54).

AnxA2 also has a role in the host defence system against infection, as illustrated through the LPS-mediated inflammatory state induced through toll-like receptor 4 (TLR4) (58). More specifically, AnxA2 has been shown to facilitate internalisation of TLR4 (via MYD88), leading to translocation into endosomes. This process results in TRIF-related adaptor molecule (TRAM)-dependent signalling, which releases anti-inflammatory cytokines. Conversely, deficiency has been shown to prolong TLR4 signalling and is associated with pro-inflammatory cytokine release (58). AnxA2-S100A10 tetramers have also been shown to modulate macrophage function, including inflammatory and phagocytic activity via TLR4. More specifically, wild type tetramers activate macrophages, while knockout of TLR4 inhibits this response (59).

1.2.7.2 S100A10

S100A10 is a member of the S100 protein family of small Ca^{2+}-binding proteins which regulate both intra- and extracellular proteins. Although all other annexins need Ca^{2+} to facilitate their binding to S100 ligands, AnxA2 can bind S100A10 independently of Ca^{2+}. This complex formation is modulated by post-translational modifications of AnxA2. However, it has recently been suggested that cAMP and PKA regulate this complex

formation together with CaN, which then facilitates the interaction of the AnxA2-S100A10 complex with CFTR (54). The AnxA2-S100A10 complex links to cell membranes and vesicles to regulate the membrane associations and ion channels. AnxA2 preferentially binds to anionic phospholipids while S100A10 acts as a bridge to link the complex to ion channels and cytoskeletal proteins such as actin (54).

1.2.8 Exchange protein directly activated by cAMP (EPAC)

CFTR-mediated ion transport is known to be stimulated when the subcortical levels of cAMP rise, resulting in activation of PKA. This then leads to phosphorylation and activation of CFTR. In addition to cAMP playing a vital role in the PKA activation needed for CFTR activation, cAMP is also important in regulating CFTR plasma membrane stability, mediated through stabilisation of the actin cytoskeleton (60). Although cAMP-dependent PKA activation of CFTR represents a major regulatory mechanism of CFTR functions, guanine nucleotide-exchange factors can be activated by cAMP as well. One example is EPAC1 which provides a PKA independent pathway for maintaining CFTR stabilisation at the plasma membrane. cAMP mediates activation by preventing endocytosis and recycling in endosomes independent of PKA activities through facilitation of the interaction of CFTR with Na^+/H^+ exchanger regulatory factor (NHERF1) (61). Lobo et al. (61) also demonstrated that downregulation of NHERF1 completely abolishes the interaction between EPAC1 and CFTR in the human airway epithelial cell line and that enhancement of EPAC1 and CFTR interaction rescues CFTR function in a CF model epithelial cell line with F508Δ-CFTR. As such, EPAC, NHERF1 and CFTR seem to be acting as a multiprotein complex in this instance to facilitate CFTR physiological function. This finding may be crucial to developing a treatment target for CF.

EPACs respond to cAMP by regulating cell-cell interactions, cell-matrix adhesion, cell cytoskeleton and cell polarisation. These processes are deregulated in CF (62). EPAC1 binds cAMP and migrates to the plasma membrane where it is immobilised through its binding to ezrin-radixin-moesin complexes (ERM). CFTR is also bound to ERM that attaches the channel to the actin cytoskeleton (37). Therefore, EPACs binding to cAMP enables cAMP to localise to the same compartment as CFTR (in which PKA is activated) and in turn, phosphorylate and activate CFTR.

More recently, EPACs have been found to directly stabilise CFTR at the plasma membrane and this occurs via the PDZ adaptor protein NHERF1 (61). PDZ domain proteins are scaffold-based regulatory proteins that occur in specific cell compartments of polarised epithelial cells (63). CFTR directly interacts with NHERF1 via its C-terminus thereby facilitating the formation of a regulatory complex including CFTR, Ezrin and PKA at the plasma membrane of epithelial cells (Fig. 1-4) (64). EPAC also activates CaN and may indirectly influence this pathway (Fig. 1-5) (65).

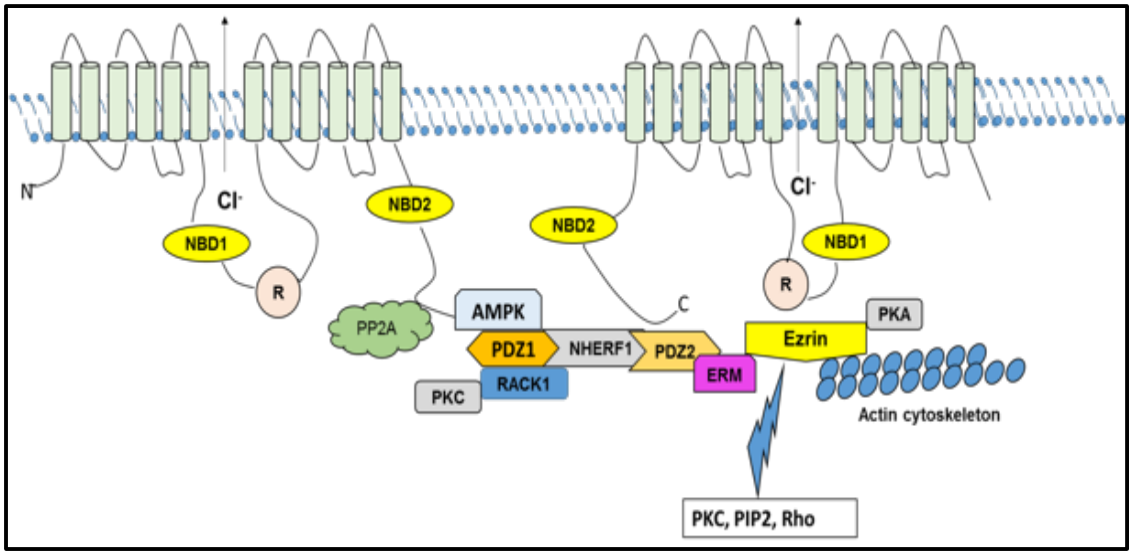

Figure 1-4. PKA regulation of CFTR-mediated Cl^- transport.

Different proteins interact either directly or indirectly with CFTR to either inhibit or enhance the activities of the channel. Activation of PP2A causes the phosphatase to dephosphorylate AMP kinase (AMPK), thus activating it. Activated AMPK phosphorylates PDZ1 to facilitate interaction with NHEFR1. This then binds to PDZ2 for anchoring of a second CFTR channel by Ezrin. This process thus allows for membrane dimerisation of CFTR. ERM = ezrin, radixin, moesin binding domain; NBD = nucleotide-binding domain; R = regulatory domain of CFTR. Adapted from Li H, *et. al.* (49, 66).

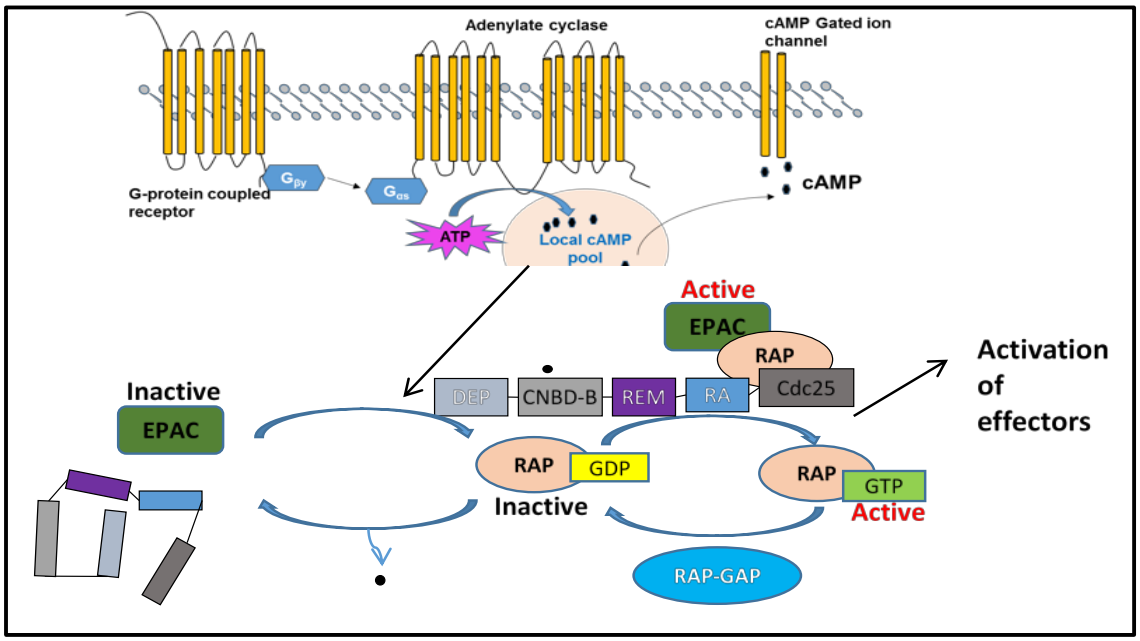

Figure 1-5. Mechanism of EPAC activation by cAMP.

Synthesis of cAMP by adenylyl cyclase is mediated by the G-protein coupled receptor (GPCR). The cAMP eventually binds with the cyclic nucleotide–binding domain (CNBD-B) of EPAC. This induces a conformational change that facilitates binding of EPAC with RAP GTPase to activate EPAC which is independent of PKA. This induces a biological effect. Adapted from Lezoualc'h, *et. al.* (67).

1.2.9 Calcium-activated potassium channel (KCa3.1)

One of CFTR's major functions involves regulation of transepithelial fluid and Na^+/Cl^- transport in the kidney, airways and sweat ducts (68). Defects in CFTR result in depletion of the airway surface liquid (ASL) which then results in sticky mucous secretion and dysfunctional bacterial clearance. However, the bulk of the transepithelial Cl^- transport required to maintain adequate ASL volume must be coupled to a rising K^+ conductance for recycling of the K^+ entering the cell through the Na^+/ K^+ pump. This is in addition to maintenance of the electrical driving force required for anion transport out across the apical membrane. KCa3.1 protein is an important channel known to regulate Cl^- secretion due to the finding of a previous study demonstrating that 1-Ethylbenzimidazolinone (1-EBIO), a KCa3.1 channel inducer, could stimulate cAMP dependent Cl^- secretion in tissue sections from CF patients (69). This finding thus supports that of Wang, Haanes (70) who showed that KCa3.1 produces the driving force required to maintain Cl^- efflux by CFTR in epithelial cells. In addition, a recent yeast-2-hybrid study has shown that KCa3.1 may regulate CFTR-mediated Cl^- transport through direct interaction of the two proteins (71).

1.3 CFTR PATHOPHYSIOLOGY IN CF

CF is the most common lethal autosomal recessive condition in Europe with 1 in 2000/3000 new-borns affected and a 4% carrier rate in the United Kingdom (72). The discovery of the *CFTR* gene in the early 1990s provided the first clue as to the molecular basis of CF development. In healthy individuals, functional CFTR acts as an ATP- and cAMP-regulated Cl^- channel. It is found on the apical membranes of respiratory and endocrine glandular epithelium including the lungs, liver, gut, pancreas, reproductive tissues, bone marrow cells and immune cells (13, 73-76). Sequelae associated with CF include CF-related diabetes mellitus (sharing characteristics of both type 1 and type 2

diabetes mellitus), malabsorption syndromes, male infertility, and a higher incidence of bacterial infections of the airways (75). The hallmarks of CF are thick and dehydrated airway mucus, pancreatic dysfunction, bile duct obstruction, infertility, high sweat Cl^- levels, intestinal obstruction, and chronic sinusitis. The major complication that arises due to any of these conditions is chronic bacterial infections, especially *Staphylococcus aureus (S. aureus)* and *Pseudomonas aeruginosa (P. aeruginosa),* which slowly destroy the lung parenchyma causing pulmonary hypertension, bronchiectasis, and eventually, cardio-respiratory failure and death (77).

Forty years ago, the life expectancy of children with CF was restricted to adolescence, but this has been improved to the 4^{th} decade of life due to rigorous management strategies (78). These include chest physiotherapy which enables clearance of mucus, healthy nutrition, and early use of antimicrobials (usually targeting *S. aureus* and *P. aeruginosa*) to mitigate the spread of infection. However, these treatment strategies only address the manifestation of the disease and not the cause – the ion channel defect. There are numerous therapeutic strategies that have been proposed to either correct the defective cellular processing of the CFTR (79), or improve upon the Cl^- channel function and even to replace defective genes (72, 79). These will be addressed later in this chapter.

1.3.1 Cellular defects in CF

Healthy individuals have a lining of fluid (ASL) over the respiratory epithelium, as well as lipid-rich surfactants, which are bactericidal, and alveolar macrophages (80). The ASL is made up of periciliary liquid covered by the mucus layer that is secreted by goblet and Clara cells. The role of the mucus is to trap microorganisms which are then removed by the mucociliary escalator. The periciliary fluid secretion is regulated by Na^+ absorption by the apical membrane ENaC, transporting Na^+ into the epithelial cells. In addition, Cl^- and water are secreted into the periciliary fluid by the CFTR. This process maintains the

ASL in which the cilia bathe (81). However, with CF, ASL is depleted and mucociliary action is inhibited. Dehydration of the ASL (due to disrupted CFTR function) thus impedes mucus clearance (82) leading to airway acidification and further dehydration (83, 84). These are optimal conditions for bacterial colonisation, recurrent infections, and chronic inflammation leading to irreversible damage to the airway epithelium – the main cause of morbidity and mortality in CF (72, 81). In addition to dense mucus in the lungs, pathogen colonisation of the airways and severe inflammation cause progressive and irreversible damage to the structure of the lungs along with pancreatic and bile duct defects, infertility and diabetes (85, 86).

1.3.2 Genetic basis for CF disease

The outcomes of *CFTR* mutations lead to a phenotype of varying severity. Modifier genes and the environment also play key roles in regulating *CFTR* gene expression and activity. (87-89). CF disease is caused by mutations found in chromosome 7 in the region that codes for the CFTR protein (7q31.2) (11). To date, approximately 2000 different genetic mutations have been identified and are currently divided into 6 classes (90, 74, 91): Class I mutations are frameshift, splicing, or nonsense mutations. These cause premature termination codons (PTC) that dramatically reduce or even eliminate *CFTR* expression. Class II mutations cause misfolding, early protein degradation by the endoplasmic reticulum (ER), and compromised protein biogenesis that results in low CFTR cell surface expression levels. Delta F508 (F508Δ) deletion changing the secondary and tertiary protein structure and resulting in the inability of Cl^- channels to respond to higher cAMP levels in epithelial cells through opening. Defective expression, trafficking or function of CFTR impairs Cl^- secretion. Thus, intracellular Na^+ concentration increases. Patients with the F508Δ mutation have destabilised CFTR structure and folding which leads to its degradation. However, approximately 1% of the translated protein reaches the

plasma membrane (92, 93) and is functional but displays altered gating with prolonged channel closure or shorter opening (94). Class III mutations affect CFTR channel gating and function in terms of a reduced probability of opening. Class IV mutations change channel conductance by compromising the ion conduction pore function. Class V mutations do not affect protein conformation but influence its abundance due to promoter or splicing abnormalities. Finally, class VI mutations affect channel stability at the plasma membrane after endoplasmic reticulum (ER) quality checks by affecting channel conformation or adding internalisation signals. This causes a higher plasma membrane turn-over or reduced expression on the apical epithelium (see Fig. 1-6 for a visual representation of all classes).

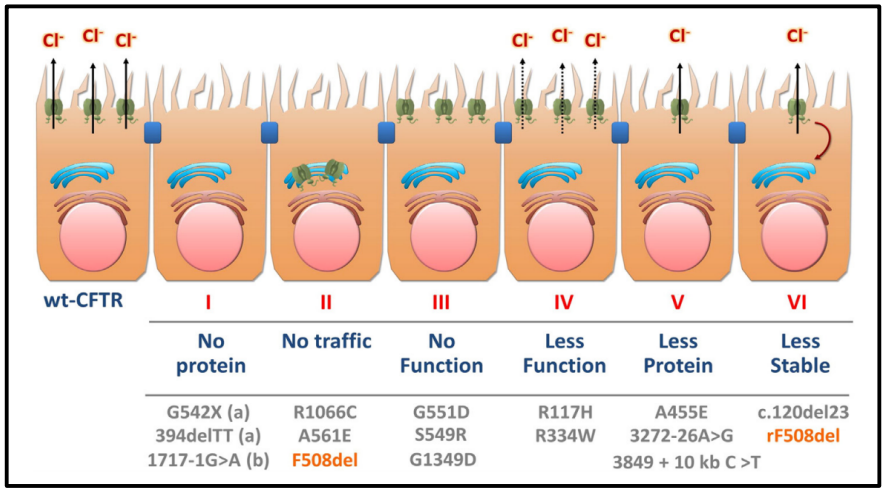

Figure 1-6. Classes of CFTR mutations in epithelial cells. Obtained from Amaral and Farinha (95).

The effects of these mutations on functional impairment and clinical severity are still unclear for most mutations although they have been well-characterised for a proportion of these mutations. Indeed, it has been noted that there is a great deal of work needed to link the genetic and clinical aspects of CF pathology, particularly given the wide range of gene mutations now identified in patients (76). However, this classification has been of great importance in the development of treatment strategies (11, 91).

1.4 THE ROLE OF CFTR IN AIRWAYS

The *CFTR* gene encodes a Cl^- channel that also acts as a regulator of other transmembrane proteins thereby maintaining the healthy function of the lung epithelium. In CF, the airway epithelium is disorganised and dysfunctional with an altered influx of water and ions to the bronchioles, accompanied by bacterial infections and dramatic inflammation (96). Therefore, the potential role of CFTR in modifying airway function for normal airways or during disease through susceptibility to infection/inflammation is a topic of interest.

1.4.1 Pulmonary ion channels in good health and disease conditions

Cl^- channels are found on intracellular organils, such as lysosomes and endosomes, and in the plasma membrane where they regulate cell volume, transport of salt and water, and the excitability to neuronal cells (97). In epithelial cells, ENaCs enable the passive influx of Na^+ through the apical plasma membrane. Na^+ and potassium (K^+) are actively transport from the cell via ATPase. The generated osmotic gradient is needed for water transport into and out of the cell. This is mediated by CFTR which regulates Cl^- influx and efflux (97).

Defective Cl^- transport is associated with CF due to the disease being caused by mutations in the *CFTR* gene. This mutations express themselves through defective CFTR channel activity (98). CFTR is located at the plasma membrane of apical epithelial cells in the airways where it is responsible for maintaining the salt-water transport balance (98).

The compromise in CFTR activity is explained by a model which suggests that reduced Cl^- reabsorption via CFTR causes diminished Na^+ uptake through the ENaC. This leads to high salt concentrations in the luminal space, thereby preventing the secretory functions of epithelial cells. The second model suggests that Na^+ absorption via ENaC is higher and so Cl^- reabsorption is also increased via CFTR-independent mechanisms.

This leads to airway dehydration and defective mucociliary transport, as described previously (99, 74, 97). Both models of defective sodium chloride (NaCl) reabsorption support the theory of compromised pulmonary activity of CF; however, there is a strong consensus that Cl^- transport through CFTR in the airway epithelia is also compromised (5).

Ca^{2+}-activated Cl^- channels (CaCC) complement CFTR activity with CFTR upregulation. This then leads to CaCC down-regulation and vice versa. CFTR is responsible for maintaining airway ASL homeostasis whereby CaCCs manage Cl^- secretion and ASL height in response to extracellular stimuli (82).

In addition to environmental and genetic factors, compromised CFTR is also thought to contribute to bronchiectasis: the abnormal and irreversible dilation of the bronchi. However, the exact mechanism by which CFTR facilitates this is still not clear (5). Furthermore, CFTR may play a role in modulating immune function, which is an important consideration in CF patients who are more vulnerable to persistent bacterial infection in the airways, secondary to ASL and mucociliary deficits. In patients with CF, a loss of CFTR is associated with a decrease in innate immune responses, including the release of interleukin-6 (IL-6) and IL-8 pro-inflammatory cytokines which is mediated through TLR4 expression in the airways (100). This finding may explain the potential for chronic bacterial infections in the lungs of CF patients.

1.4.1.1 Fluid secretion and mucociliary clearance in the airways

In the lungs, mucociliary clearance is part of the innate immune system and is needed to maintain healthy airways. Both ciliary beat and ion transport contribute to the removal of inhaled pathogens and particles. Therefore, the ciliated cells have a central role since they provide the cilia beat and regulate the ion channel function which regulates transepithelial

water flow. This is needed for management of the periciliary liquid that lies below the mucus layer. Together they form the ALS (101).

The composition of the periciliary liquid relies on Na^+ reabsorption in the basolaterally-located ATPase and the apically-located ENaCs and Cl^- channels (102). In CF, Cl^- secretion is reduced and Na^+ absorption is increased due to defective CFTR function. This leads to reduced volume and height of periciliary liquid, impaired ciliary beat, accumulation of mucus in the airways, and inflammation due to compromised pathogen removal (101).

Pathogens and particles are trapped in the mucus which is transported by the ciliary beat. Impaired ciliary beat compromises this innate immune function of the lung and respiratory infections are thus more likely to occur (102). The ASL also contains immunoprotective proteins including the Clara cell secretory protein and the surfactant proteins secreted by epithelial cells (103). The surfactant proteins SP-A and SP-D recognise pathogens and activate the innate immune response (103). In CF, inhaled bacteria such as *P. aeruginosa* and fungi such as *Aspergillus fumigatus* are the major causes of severe inflammation owing to increased pathogen colonisation of the airway (101, 102).

1.4.2 CF and pulmonary infection

Initially, the primary organisms thought to infect the airways of children afflicted with CF were *Haemophilus influenzae* and *S. aureus,* whereas *P. aeruginosa* and *Burkholderia cepacia* were proposed to be the main pathogens present in adults (Fig. 1-7) (104). More recently, newer diagnostic methods and techniques have enabled better analysis and identification of the pathogens associated with CF (105). This has led to the discovery of pathogens and microbes responsible for disease progression and poor outcome. In addition, each patient has a different combination of pathogens consisting of bacteria,

fungi and viruses (106). Therefore, it is now clear that the initial pathogens thought to be responsible for damage to the lung environment and disease progression are now considered normal microbiota (107). *P. aeruginosa* is the most common pathogen in CF. It is able to utilise nitrite in anoxic environments as well as ferment arginine and pyruvate as sources of energy (108, 109). Moreover, these oxygen-limited regions induce dramatic physiological changes to *P. aeruginosa* including modifications to the outer membrane which allow better antibiotic tolerance (109). *P. aeruginosa* thrives in the airways of CF patient because their respiratory system is not completely aerobic. The compromised Cl^- secretion leads to dehydration of the ASL. This causes reduced ciliary action and compromised clearance of mucus combined with the development of mucus plugs that obstruct the airways creating a niche suitable for microbes (110).

It is essential that each patient's pathogen composition is determined since co-infection with certain microbes can dramatically alter patient outcome. This has been demonstrated with a drosophila model of mono-infection versus co-infections with *P. aeruginosa* (111). It has also been shown in a murine model that *P. aeruginosa* biofilm formation was influenced by its co-infection with *Burkholderia cenocepaci* in the mouse lung (112). Different combinations of bacteria in a CF lung microbiome are known to alter the disease outcome through influencing host immune response to other bacteria. In addition, bacteria alteration of physiological conditions either favours or inhibits viability of other bacteria in the microbiome (113), posing different risks to the patient depending on their individual coinfections.

However, not all microorganisms present in the lungs directly contribute to disease. This was demonstrated by the discovery of the presence of the rhinovirus in the respiratory tract of infants and children which was thought not to influence disease progression (106). However, in adults, an increased rhinovirus load has been associated with the worsening

of the disease (114). Similar findings have been published for *Candida albicans* and *Streptococcus* (114, 115, 107). Therefore, it is essential that the microbiota of each CF patient is well characterised and the interactions between the different microorganisms and the individual microorganisms with the host environment are identified since these shed more light on the disease progression and patient outcome.

As fetal CF lungs do not show any inflammation until after birth, it is assumed that defective CFTR is not responsible for initiating inflammation but it may contribute to the inflammatory process in response to infection (116). It is also assumed that the composition of the ASL is altered in CF patients with a higher salt concentration. This concentration inactivates defences and is optimal for bacterial growth (82, 97). In addition, the higher salt concentration of the ASL and periciliary fluid leads to its dehydration and increased viscosity that impairs clearance of the mucociliary fluid. This promotes chronic infection, activating and intensifying the already chronic inflammatory response (110). This excessive and persistent inflammation is responsible for the irreversible tissue damage present in older CF patients (117).

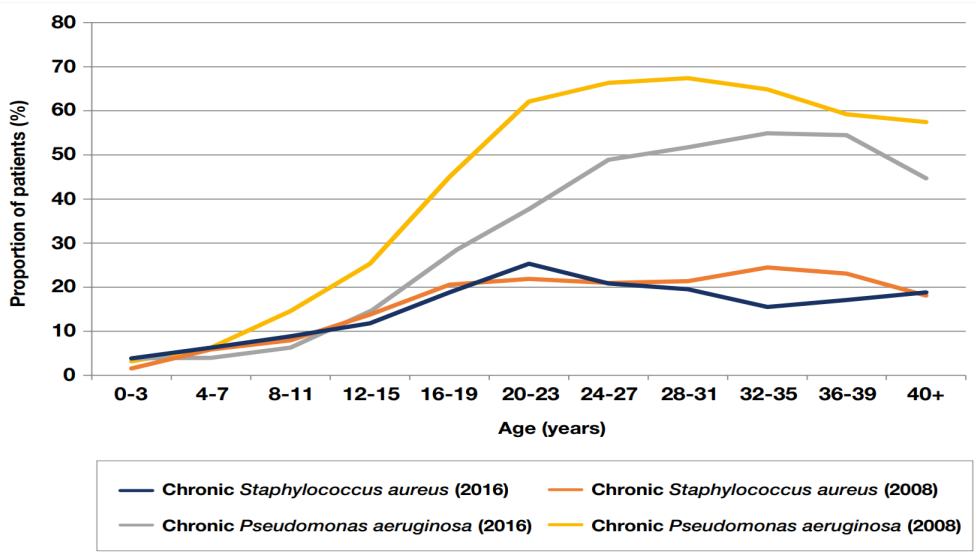

Figure 1-7. UK Cystic Fibrosis Registry Annual Data Report 2016.

Lung infections monitored in patients between 2008 and 2016. n=6082 in 2008, n=9695 in 2016.

1.4.3 Pro-inflammatory cytokine profiles in the airways

Inflammation has more recently been identified as one of the major contributing factors to tissue remodelling, destruction, and loss of function in CF (118). Chronic bacterial infections, especially *P. aeruginosa*, play a major role in defining the disease progression of CF. These bacterial infections are thought to begin early in the disease's development, even before symptoms occur (119).

Chronic airway inflammation is proposed to be triggered by the accumulation of mucus in the airways which leads to damage to the lung tissue without any bacterial infection (120). Studies of animal models of CF and in infants with CF have shown that sterile inflammatory lung disease occurs before symptom development and prior to any infection (121). These findings are supported by investigations using animal models which show high myeloid infiltration and dendritic cell polarisation with abnormal macrophage phenotypes. This suggested that inflammation was present in the lungs of the mice without their having experienced exposure to any pathogens (122). Neutrophil infiltration has also been implicated during early chronic inflammation without any exposure to infection (123). Therefore, it has been proposed that inflammation may facilitate the development of infections at a later stage of CF (123).

Moreover, chronic infections with *P. aeruginosa* have been shown to be responsible for the airway remodelling and fibrosis identified in CF patients (124). In CF, there is a complex balance between pro-inflammatory and anti-inflammatory factors, with pro-inflammatory cytokines present in the ASL at higher concentrations compared to healthy individuals (125). These anti-inflammatory cytokines include IRAP, TNFsR and IL-10 which inhibit macrophage production of tumour necrosis factor-alpha (TNF-α), IL-1β, IL-6 and IL-8 (126). However, this increase in anti-inflammatory cytokines is not enough to mitigate the effects of the pro-inflammatory cytokines in the ASL of CF patients.

Therefore, persistent inflammation occurs (125). Despite the ongoing chronic inflammation in the airways of CF patients, most tissue damage is due to the higher infiltration of neutrophils which are responsible for bacterial clearance. They also release reactive oxygen species (ROS) and secrete proteases which damage the lung tissue (127).

Animal studies have shown that chronic *P. aeruginosa* infections with a corresponding pulmonary T helper cell 1 (IFN-γ-producing) response exhibit a lower mortality, faster bacterial clearance, and milder lung inflammation compared to mice with a predominantly T helper cell 2 (IL-4, IL-5, IL-10-producing) response (128, 129). In addition, similar observations were made with CF patients in which those with the highest IFN-γ levels had the best lung function (130). It was therefore proposed that the balance between granulocyte-macrophage colony-stimulating factor (GM-CSF) and granulocyte colony-stimulating factor (G-CSF) determines the type of dendritic cell that primes T cells to new antigens, and that this process is responsible for the type of immune response exhibited (125).

Studies of CF patients with chronic *P. aeruginosa* infections performed six months prior to their death identified higher levels of circulating C-reactive protein (CRP), TNF-α and elastase complex (a correlate of neutrophil activity) (125). These results show that the high level of inflammation in the lungs is reflected in the systemic circulation.

1.4.4 Role of airway epithelium in the innate immune response

CF is characterised by excessive inflammation in the lungs with high neutrophil infiltration observed in adults and children who have not been exposed to any infections (106). Neutrophils, monocytes and macrophages are responsible for proteolytic degradation of elastin followed by dramatic lung tissue damage (131). It is currently thought that the excessive neutrophil infiltration and activity in the lungs is due to both

deregulated cytokine production by the airway epithelial cells and deregulated neutrophil activity (132).

The airway epithelium acts as the interface or physical barrier between pathogens and the immune system. Signalling pathways responsible for pro-inflammatory cytokine production are upregulated in CF airway epithelia (35). This has been demonstrated by exposure of CF epithelial cells to *P. aeruginosa* in *in vitro* cultures which induced the activation of the pro-inflammatory transcription factor nuclear factor-κB (NF-κB), leading to the expression of IL-8 (132). IL-8 is a chemoattractant for neutrophils (126), and IL-1β and TNF-α have also been shown to stimulate neutrophil chemoattraction in endothelial cells of the airways (133). Animal studies have demonstrated that infection with *P. aeruginosa* and other pathogens greatly upregulates NF-κB expression in the airway epithelium, and this is associated with inflammation in the lungs (134).

Therefore, it is hypothesised that functional CFTR is needed to facilitate healthy neutrophil development and function. Further investigations have identified a defect in phagocytosis in the CF neutrophils (135). Moreover, there is a higher proportion of mast cells in the lungs of CF patients and these secrete high levels of the pro-inflammatory cytokine IL-6. IL-6 stimulates the development of more neutrophils in the bone marrow and blocks the regulatory T cells (132). In addition, during infection, there is an increase in oxidative processes which leads to ROS formation. The ROS is not effectively neutralised in CFTR epithelium due to the minimal levels of glutathione (136, 137).

1.5 THE ROLE OF Cl^- CHANNELS IN THE IMMUNE RESPONSE

As a major Cl^- channel, CFTR is known to regulate other Cl^- channels such as ORCCs. Its activities have been linked with the immune response to bacterial infection, as in CF. However, other Cl^- channels play crucial roles with physiological consequences which

impact the immune system. One of the most characterised Cl^- channels with a known role in immune cells, such as lymphocytes, is the volume-regulated anion channel (VRAC). VRAC, also known as a swell-regulated Cl^- channel, is responsible for regulating the swelling of specific cell types in response to Cl^- movement across the cell in a process termed regulatory volume decrease (RVD) (138). Cl^- channels (ClCs) are a group of ion channels known to be involved in the recruitment and activation of specific immune cells, such as eosinophils and neutrophils, during inflammation characteristic of allergy and asthma (139). Transmembrane member 16A (TMEM16A), also known as Anoctamin 1 (Anoc1), is an ORCC that is known to be responsible for Ca^{2+}-mediated Cl^- transport in different cell types. Indeed, Cl^- transport through the ion channel has been shown to regulate mucus secretion and cytokine expression during inflammation. TMEM16A expression has also been shown to be increased in response to induced asthmatic conditions in cultures producing hypersecretion of mucus typical of a T helper cell 2 response of the respiratory system (140). As such, it has been proposed that pharmacological stimulation of TMEM16A can induce hypersecretion of mucus that can compensate for the dysfunctional mucus production in CF (141). Based on this, understanding of the immune function of Cl^- channels may be effective in developing therapeutic targets for treatment of CF.

1.5.1 The immune system's response to infection in CF

There are three components to the innate and adaptive immune defence in the lungs: (1) the mucociliary escalator; (2) the effects of surfactant proteins and antimicrobial compounds and; (3) the cellular contributions of epithelial cells, neutrophils, monocytes, macrophages, dendritic cells and lymphocytes (132).

Circulating monocytes differentiate to alveolar macrophages – key players in the removal of pathogens in the lung. They are also involved in antigen presentation to T cells. Studies

show that macrophages of CF patients are incapable of destroying pathogens (142, 143). However, the mechanisms of macrophages – opsonisation and inadequate levels of phagocytosis – appear to be intact, which suggests that CFTR influences other mechanisms that are associated with pathogen clearance (132).

Although T cell, neutrophil and macrophage levels are all elevated in CF lungs, the proportion of activated neutrophils and macrophages is low (144, 131). Activation of immune cells may relate to gene expression pathways, and it has been shown that gene expression pathways are also deregulated in CF monocytes. The mitogen-activated protein kinase (MAPK)/extracellular-signal-regulated kinase (Erk) pathway is hypersensitive in CF monocytes, and this is involved in cell division, apoptosis and cytokine synthesis. This pathway is also associated with the pro-inflammatory actions of NF- κB signalling, secondary to CFTR mutations or deficit in experimental models (117). However, despite the activation of MAPK/Erk, CF monocytes produce less IL-8 than is needed for neutrophil recruitment, suggesting other deficits in signalling pathways. Therefore, during infections, neutrophil recruitment is inadequate, compromising pathogen clearance (145).

1.5.2 Role of Cl^- channels in the functioning of monocytes and macrophages

Monocytes and macrophages are major components of the immune system that act as the immune effector cells protecting the host from microbes. Monocytes migrate to target tissues and differentiate into macrophages where they bind oxidised low-density lipoproteins (LDL) which facilitate the secretion of pro-inflammatory cytokines. Cl^- channels have been associated with the acidification of phagosomes, an important factor facilitating the microbial function of phagocytes. Alveolar macrophages in CF mice show effective phagocytosis of invading pathogens but are incapable of destroying the engulfed microbes. This is thought to be due to ineffective acidification of lysosomes, a process

regulated by CFTR. Therefore, after fusion of phagosomes and lysosomes, to form phagolysosomes, the poorly acidified environment does not support enzyme activity and so the bacteria are not destroyed. Indeed, the environment is conducive to bacterial growth (146). These findings have been supported with studies from CF patients and CF ferrets (147) as well as by other studies that support the defective acidification process and conclude that this has other implications leading to defective pathogen elimination (148).

The presence of ORCC in monocytes has also been confirmed using experimental data and is thought to be partly responsible for monocyte migration in addition to modifying Ca^{2+} influx (149). However, the contribution of this mechanism to monocyte function in patients with CF is under-explored.

1.5.3 Bacteria phagocytosis in CF

Toll like receptor 4 (TLR4) is an important component of immune cells used in the identification of pathogens, especially Gram-negative bacteria. Immune cells such as macrophages bind to LPS on bacteria such as *P. aeruginosa* using TLR4 to facilitate phagocytosis of the bacteria (150). Compromised lysosomal turnover of TLR4 in CF monocytes is associated with a limited response to LPS, which abrogates the inflammatory response expected upon LPS signalling (151, 122). It has been shown that phagocytosis of bacteria in CF patients' immune cells may be inhibited, suggesting inadequate immunological responses to the presence of bacteria (152). In addition, CFTR has been found to contribute to modifying the pH in phagosomes: the acidification of lysosomal and phagosomal compartments is compromised in CF macrophages (153). This leads to the inability of alveolar macrophages to destroy engulfed pathogens and explains how engulfed bacteria can still survive in CF macrophages. The consequences of this for CF patients are an exaggerated inflammatory response induced by infection with inadequate pathogen clearance. Therefore, the anomalies in monocytes and

macrophages of CF patients are directly due to CFTR defects but may also be influenced by the lack of activation of macrophages by T cells. Thus, the innate immune response is incapable of pathogen removal (132).

1.5.4 Inflammasome

The inflammasome is needed for detection and degradation of pathogenic bacteria in the cytosol within the macrophage through induction of caspase-1 expression (154, 155). Toll-like receptors (TLRs) are membrane-bound receptors found on the cell membrane and on the membranes of intracellular vesicles such as endosomes. TLRs are important for the recognition of pathogens but they are not able to distinguish between pathogenic and non-pathogenic bacteria. Nucleotide-binding oligomerisation domain-like receptors (NOD-like receptors, or NLRs), also called NALPs, are intracellular pattern-recognition receptors that recognise pathogen-associated molecular patterns needed to activate the host immune response (156, 157). NLRs have recently been discovered and are components of a multi-protein complex together with caspase-1 and apoptosis-associated speck-like protein (ASC) that form the inflammasome. This is essential for the induction of the inflammatory process (156). NLRP3 inflammasome assembly is triggered by the presence of bacteria, their toxins and nucleic acids in the cytosol (158) leading to activation of caspase-1. The NLRP3/caspase-1 activation pathway promotes neutrophil activation and attraction in the airways (159). Intracellular potassium efflux due to bacteria-induced cell and organelle membrane perturbations also activates inflammasome assembly (see Fig. 1-8) (160).

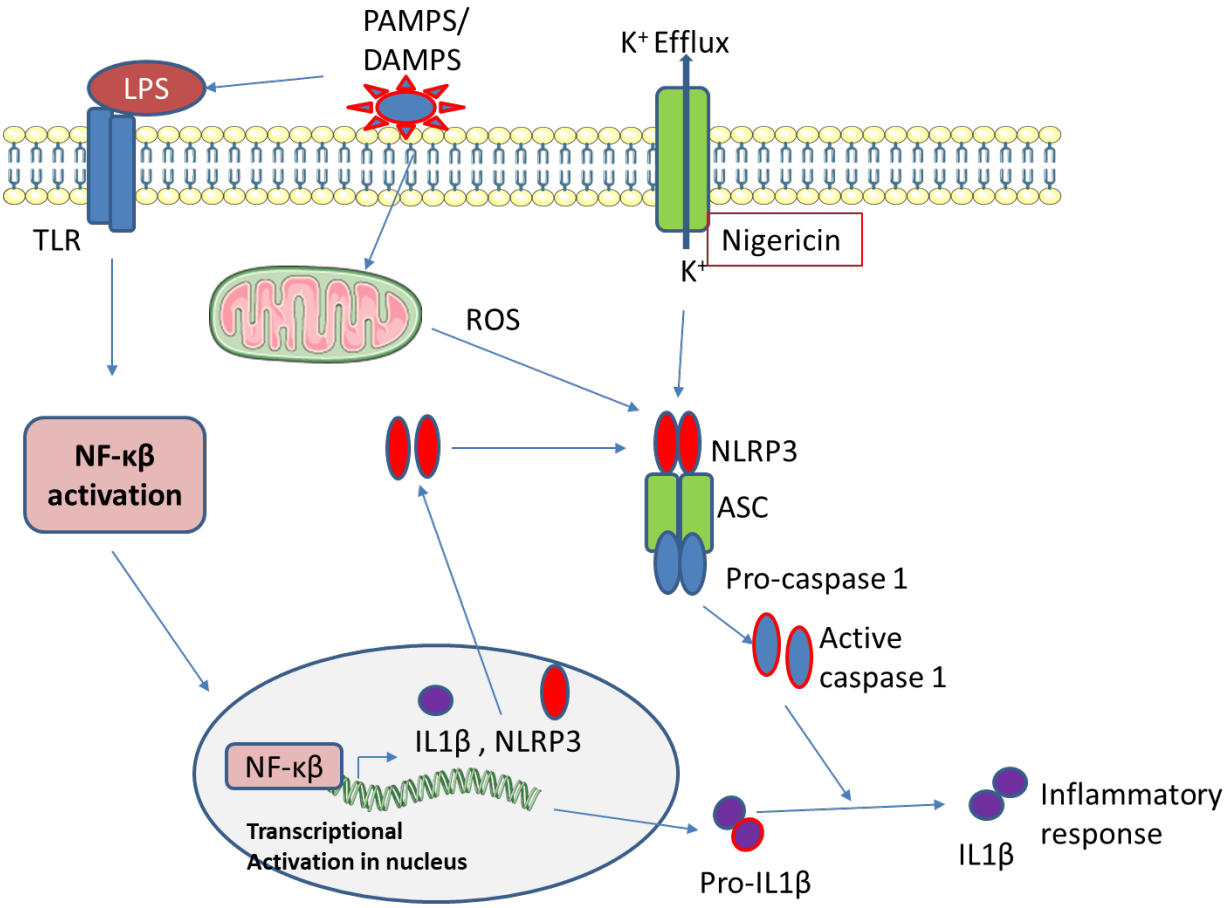

Figure 1-8. NLRP3 inflammasome activation.

The NLRP3 inflammasome complex is made up of pro-caspase-1, NLRP3 and an adaptor protein - apoptosis-associated speck-like protein containing a CARD (ASC). The formation of this complex is regulated by a two-step mechanism which involves binding of LPS to TLRs for activation of NF-kβ which enters the nucleus to activate transcription of pro-IL-1β and NLRP3 genes. The second stimulus is binding of other pathogen/danger-associated molecular patterns (PAMP or DAMPs) to TLRs or entry into the cell and binding with subcellular structures, such as the mitochondria or lysosomes, to induce aggregation of the protein complex comprising the inflammasome. The inflammasome is responsible for proteolysis of pro-caspase 1 into the active caspase. This then cleaves pro-IL-1β to mature IL-1β to induce inflammatory responses. Adapted from Kawana N, *et. al.* (161).

1.5.4.1 The biological role of caspase-1 during infection

Inactive caspase-1 or pro-caspase-1 is present in the cytosol of phagocytic cells and is activated by the family of NLRs in response to infection. It initiates a pro-inflammatory, non-apoptotic form of cell death (157). On the other hand, active caspase-1 promotes the cleavage and activation of the pro-inflammatory cytokines pro-IL-1β and pro-IL-18 (see Fig. 1-8) (154, 156). IL-1β plays a role in numerous immune reactions including recruitment of inflammatory cells, and IL-18 is implicated in the production of interferon-γ and the cytolytic activity of natural killer cells (162). Caspase-1 also cleaves other protein substrates, pro-caspase-7 being one such example (157). In addition, caspase-1 is involved in the membrane repair essential for cell survival after damage from bacterial toxins that form pores (163).

1.5.5 Cytokine release by immune cells

Dysregulated inflammasome activity is responsible for airway infections and inflammation. In CF, airway epithelial cells are responsible for the exaggerated pro-inflammatory cytokine response to infection. However, it remains unclear whether this abnormal immune response is due to a defect in CFTR signalling or if it is a response to chronic infection by multiple microorganisms simultaneously (164). The NLRP3 inflammasome activity triggers secretion and activation of IL-1β and IL-18 in addition to TNF-α. These amplify the innate inflammatory response to pathogens (164).

1.5.5.1 Interleukin 1 beta (IL-1β)

IL-1β is mainly released by macrophages and monocytes for the recruitment of inflammatory cells and amplifying the pro-inflammatory cytokine response (165). IL-1β signalling activates pathogenic IL-17A secreting by T cells ($CD4^+$) which manage the balance between Th17 and regulatory T cells needed to combat fungal infections in CF lungs (166). However, the inflammasome/IL-1β pathway can lead to excessive

inflammation, which is a further detrimental contributor to the CF pathology (167, 168). Therefore, downregulation of this pathway may, in some cases, be beneficial for the management of CF. It has been shown that NLRP3/caspase-1 pathways can mediate the release of IL-1β as part of a response to pulmonary pathogens and particle infiltration, leading to inflammation, although NLRP3/capase-1 independent IL-1β pathways also operate in this process (159).

1.5.5.2 TNF-α and other cytokines involved

In CF, there is an imbalance between the pro-inflammatory and anti-inflammatory cytokines. TNF-α is one of the most well-researched pro-inflammatory cytokines and is thought to be produced by resident macrophages as well as invading monocytes (169). TNF-α is a mediator of the acute inflammatory response and stimulates neutrophils and monocytes to sites of infection. It also modifies vascular endothelial cell permeability to immune cells to facilitate immune capabilities in tissue (170). An abnormal *TNF-α* gene has been associated with the severity of CF, highlighting the importance of the regulation of this cytokine over the clinical course of CF (170). An important anti-inflammatory protein is IL-10 as it balances the effects of the pro-inflammatory proteins. However, the levels of IL-10 have been found to decrease with age in CF patients.

Chemotactic cytokines or chemokines attract immune cells to the site of inflammation (171). The best-studied of these with regards to CF is CXCL8 (IL-8). CXCL8 interacts with C-X-C Motif Chemokine Receptor 1 (CXCR1) and CXCR2 to attract neutrophils, thereby inducing degranulation and superoxide production (169). However, in CF patients, CXCR1 is proteolytically cleaved in the airways, eliminating CXCL8-mediated anti-inflammatory effects (169).

1.6 PROJECT BACKGROUND, HYPOTHESIS AND AIMS

CF is a disease that affects respiratory function and has a prevalence of 151 per 100,000 people in the UK. The disease arises due to dysfunction in the CFTR protein, causing mucus lodging and bacteria colonisation of the airways and intestinal linings. In the airway, CFTR has been shown to form a functional complex with S100A10 and AnxA2 – a membrane phospholipid – in a cAMP/PKA-dependent pathway, leading to Cl^- secretion (44, 172). This complex is regulated by CaN. Furthermore, in endothelial cells, activation of calcineurin (CaN)-like phosphatase by cAMP/PKA has been shown to enhance the release of von Willibrand factor (VWF) from Weibel-Palade bodies (WPBs).

1.6.1 Hypothesis

Cl^- channels (CFTR and ORCC) play a significant role in the functions of immune cells including the release of pro-inflammatory molecules, bacteria phagocytosis and survival of phagocytosed bacteria.

1.6.2 Objectives

The aims of this study were:

i. To establish the extent and importance of formation of multiprotein complex formed of AnxA2, S100A10 and CFTR through cAMP/PKA/CaN in immune cells.

ii. To study the importance of PKA and CaN in the regulation of CFTR and ORCC in immune cells using patch clamp analysis.

iii. To investigate whether Cl^- channels can be activated by LPS in immune cells using patch clamp analysis under different inhibitor exposure conditions, such as chemical inhibition of CFTR, using CFTR(inh)-172.

iv. To investigate whether activation of Cl^- channels by LPS from *P. aeruginosa* requires cAMP.

v. To investigate the role of cAMP and LPS-activated Cl^- channels in the release of pro-inflammatory cytokines by immune cells via the monitoring of cytokine release using ELISA and a cytometric bead array (CBA) system.

vi. To investigate the impact of CFTR and ORCC functions on pro-inflammatory cytokine release, bacteria phagocytosis and survival of phagocytosed bacterial cells by immune cells.

vii. To investigate cellular pathways by which cAMP impacts pro-inflammatory cytokine release and bacteria phagocytosis by immune cells.

CHAPTER 2

General materials and methods

2 INTRODUCTION

This chapter provides a detailed account of the common methods and overview of the techniques used in the present research. Methods that are specific to a particular investigation are detailed in the appropriate chapter.

2.1 MATERIALS

2.1.1 Cell Lines

Two cell lines were utilised in this study: the human bronchial epithelial cell line (16HBE14o$^-$) obtained from Dr. Louise Robson's lab, and the human monocytic cell line (THP-1) obtained from UoS in-house cell bank. The former represents a positive control and was included in our lab's studies to demonstrate the cAMP/PKA-dependent activation of CaN (44, 173). 16HBE14o$^-$ is ideal for use in this present study as it is derived from airway epithelia and has been well-studied in CF. It is also easy to obtain and provides a proper representation of the signalling events that are responsible for secretion in the airway. In addition, the cell has the ability to preserve its morphological properties after several passages and possesses a good level of CFTR mRNA expression (174).

The second cell line, THP-1, is derived from the peripheral blood of a monocytic leukaemia patient. Typically, after production from the bone marrow, monocytes circulate for around 3-4 days after which they move into the tissues in response to certain signals. However, during infection, they can quickly migrate to the affected tissue locations where they are divided into dendritic cells and macrophages for the phagocytosis of bacterial cells. They constitute approximately 2-10% of all human leukocytes and play crucial roles such as the replenishment of macrophage population and the immune system's response to infection (175).

2.1.2 Human primary cells

Human peripheral blood monocytes (HPBMs) and HPBMs-derived macrophages (MDMs) were used in this study as they have been shown to express CFTR and ORCC (149, 147). Macrophages are the major phagocytic cells in human blood and form part of the innate immune response in mammals. Found in all tissues, their primary function is to engulf cells that do not express the proteins found in healthy cells such as in cancer cells, cell debris, bacteria and viruses (176).

The ethical approval for using HPBMs and MDMs from healthy volunteers was granted by the Sheffield National Research Ethics Service (NRES) Committee, Yorkshire and the Humber, Health Research Authority, NHS. The ethics reference is (07/Q2305/7). HPBMs isolation was performed under sterile conditions in a microflow class II cabinet.

2.1.3 Other materials

More details regarding other materials used in this study and suppliers have been listed in the following table (Table 2.1).

Table 2.1. List of the main equipment, chemicals and reagents used in this study.

Item	Manufacturer	Storage Temp	Stock Conc.
10 cm dishes	Thermo Scientific		
20% Sodium Dodecyl Sulfate (SDS)	Fisher Scientific	Room-Tem. (RT)	20%
4,4'-Diisothiocyanatostilbene-2,2'-disulfonic acid disodium salt hydrate (DIDS)	Sigma-Aldrich	4°C	
8-pCPT-2'-O-Me-cAMP	Sigma-Aldrich	4°C	
96 Well EIA/RIA plates	Costar		
Absolute Alcohol	VWR Chemicals	RT	
Acrylamide (ProtoGel 30%(w/v) Acrylamide: 0.8% (w/v) Bis-Acrylamide stock solution (37.5:1)	GENEFLOW	RT	
Adenosine triphosphate powder (ATP)	Sigma-Aldrich	4°C	
AEBSF Hydrochloride BioChemia	AppliChem	4°C	

Item	Manufacturer	Storage Temp	Stock Conc.
Alexa Fluor 647-anti cAMP antibody	Perkin Emler, Inc	4°C	
All kits and reagents used in CBA experiment	BD Biosciences	4°C	
Amersham Hyperfilm™ ECL (High performance chemiluminescence film)	GE Healthcare		
Ammonium Persulfate - APS	Sigma-Aldrich	-20°C	10%
Annexin A2 antibody	Prof. Gerke– Germany	4°C	
Annexin II (C-16) sc-1924 (goat polyclonal antibody)	Santa Cruz Biotechnology, INC	4°C	200 µg/ml
BAPTA-AM	Sigma-Aldrich	4°C	
Beta Actin (β-Actin) antibody	Sigma-Aldrich	-20°C	200 µg/ml
Biotin cAMP	Perkin Emler, Inc	4°C	
Blue Protein standard range	Bio-Labs	-20°C	
Bovine Serum Albumin (BSA)	Sigma-Aldrich	-20°C	20 mg/ml
$CaCl_2$	Sigma-Aldrich	RT	
c-AMP detection buffer	Perkin Emler, Inc	4°C	
c-AMP standard	Perkin Emler, Inc	4°C	50 nM/ml
CD14 MicroBeads, human	Miltenyi Biotec	2-8°C	
Cell counting slides, dual-chamber	Bio-Rad		
Cell culture plastic ware	Star Lab		
Centrifuge 5417 R	Eppendorf		
CFTR(inh)-172	Sigma-Aldrich	4°C	
Class II Microbiological safety cabinet	UniMat-BS		
CO_2 Incubator	Panasonic		
CsCl	Sigma-Aldrich	4°C	
CsOH	Sigma-Aldrich	4°C	
Cyclosporin A (CsA)	Sigma-Aldrich	4°C	
Dimethyl Sulfoxide (DMSO)	Sigma-Aldrich	RT	
Distilled water (dH_2O)			
EGTA	Sigma-Aldrich	4°C	
EPAC2 antibody	Santa Cruz Biotech., INC	4°C	200 µg/ml
ESI-05	Sigma-Aldrich	4°C	
ESI-09	Sigma-Aldrich	4°C	
Eu-W8044 Labeled streptavidin	Perkin Emler, Inc	4°C	
FBS (Fetal bovine serum)	Sigma-Aldrich	-20°C	
Ficoll-Paque plus	GE Healthcare Ltd.	RT	1.077 g/ml
Forskolin	LKT laboratories, Inc.	-20°C	
Freezer (-80°C)	Ultima REVCO		

Item	Manufacturer	Storage Temp	Stock Conc.
Gentamicin	Gibco by life technologies	RT	50 mg⁄mL
Hank's Balanced Salt Solution (HBSS) with $CaCl_2$ and $MgCl_2$	Gibco by life technologies	4°C	
HEPES	Sigma-Aldrich	RT	
Human IL-1 beta DuoSet ELISA Kit	R&D systems	4°C	
IBMX (3-Isobutyl-1-methylxanthine)	SIGMA	-20°C	
KCl	Sigma-Aldrich	RT	
Laminar hood	UniMat-BS		
L-Glutamine	Sigma-Aldrich	-20°C	200 mM
LPS from E. coli, Serotype 055:B5	Enzo	4°C	1 mg/ml
LPS from Pseudomonas aeruginosa 10	Sigma-Aldrich	4°C	100 mg/ml
LS Columns	Miltenyi Biotec	RT	
Lysogeny broth (LB) agar	Sigma-Aldrich	RT	
Lysogeny broth (LB) media	Fisher Scientific	RT	
MACS buffer	Miltenyi Biotec	2-8°C	
MACS cell separation system	Miltenyi Biotech, Bergisch Gladbach	4°C	
MACS MultiStand	Miltenyi Biotec	RT	
Magnetic stirrer (stir and heat)	BIBBY – HB502		
Medium 199	Sigma-Aldrich	4°C	
Methanol	VWR Chemicals	RT	
$MgCl_2$	Sigma-Aldrich	4°C	100 mM
$MgSO_4$	Sigma-Aldrich	RT	
Micro pipettes	Eppendorf		
Monocyte CD14/FITC	DAKO	2-8°C	1:1000
N,N,N',N'-Tetramethyl-ethylenediamine (TEMED)	SIGMA	RT	
Nigericin	Sigma-Aldrich	4°C	
Osmometer	CAMLAB		
Paper Developer	ILFORD PQ UNIVERSAL	RT	
PBS (Phosphate buffered saline) 1X - pH7.4	Gibco by life technologies	RT	1X
PE anti-Human CD16	PharMingen	2-8°C	1:1000
Penicillin-Streptomycin	Sigma-Aldrich	-20°C	
pH meter - 3305	JENWAY		

Item	Manufacturer	Storage Temp	Stock Conc.
Phenylmethanesulfonylfluoride or Phenylmethylsulfonyl fluoride (PMSF)	Sigma-Aldrich	-20°C	
Phorbol 12-myristate 13-acetate (PMA)	Sigma-Aldrich	-20°C	1 mg/ml
Pipettes	Fisherbrand		
PKA inhibitor fragment (6-22) amide	APExBIO	-20°C	
Plastic coverslips (13 mm)	Agar Scientific Ltd.		
Polyclonal goat anti-mouse immunoglobulin HRP	Dako	4°C	1 g/L
Polyclonal goat anti-rabbit immunoglobulin HRP	Dako	4°C	0.250 g/L
Polyclonal rabbit anti-goat immunoglobulin HRP	Dako	4°C	0.50 g/L
Polypropylene conical tubes 50 ml	Falcon		
Power PAC 1000	Bio-Rad		
PP2B- Aα (D-9): sc-17808 (mouse clonal antibody)	Santa Cruz Biotech., INC	4°C	200 µg/ml
PP2B-A (H-209) sc-9070 (rabbit clonal antibody)	Santa Cruz Biotech., INC	4°C	200 µg/ml
PP2B-B1 (C-17)sc-6119 (goat polyclonal antibody)	Santa Cruz Biotech., INC	4°C	200µg/ml
PP2B-B1/2 (D-1): sc-373803 (mouse clonal antibody)	Santa Cruz Biotech., INC	4°C	200 µg/ml
Protease inhibitor cocktail tablets (*cOmplete*)	Roche Ltd	4°C	
Protein G sepharose	GE Healthcare	4°C	
P-Serine antibody polyclonal (P-Ser-polyclonal)	Cell Signaling	-20°C	
P-Threonine antibody polyclonal (P-Thr-polyclonal)	Cell Signaling	-20°C	
Quick start Bradford 1x Dye reagent	Bio-Rad	4°C	
Rapid Fixer	ILFORD HYPAM	RT	
Resolving gel buffer (1.5M Tris-HCl pH 8.8)	Bio-Rad	RT	1X
RPMI 1640 medium	Sigma-Aldrich	4°C	
S100A10	Prof. Gerke– Germany	4°C	
Saponin	Sigma-Aldrich	-20°C	1.020 g/mL
SDS gel apparatus	GENEFLOW		
Shaker	HeidolphPolymax1040		
Skim Milk powder	Fluka Analytical	RT	
Sodium Chloride (NaCl)	VWR Chemicals	RT	
Sodium Deoxycholate	Sigma-Aldrich	RT	
Sodium Hydroxide (NaOH)	Fisher Chemical	RT	

Item	Manufacturer	Storage Temp	Stock Conc.
Spectrophotometer, J6300	Jenway		
Stacking gel buffer (0.5M Tris-HCl pH 6.8)	Bio-Rad	RT	1X
SuperSignal West Pico Luminol Enhancer solution	Thermo Scientific	RT	
SuperSignal West Pico Stable Peroxide solution	Thermo Scientific	RT	
T-75 flasks sterile	Thermo Scientific		
TMB solution (HRP substrate for ELISA)	Interchim	4°C	
TRIS/Glycine/SDS (0.25M Tris, 1.92M Glycine, 1% SDS)	GENEFLOW	RT	10X
TRIS/Glycine/SDS (0.25M Tris, 1.92M Glycine)	GENEFLOW	RT	10X
Triton X-100	BDH	RT	
Trizmahydrochloride solution 1M, pH 8.0	SIGMA	RT	
Trypan blue solution (T8154)	Sigma-Aldrich	RT	0.4%
Trypsin-EDTA solution	Sigma-Aldrich	-20°C	1X
TWEEN 20 detergent	Calbiochem	15-30°C	
Water bath	Clifton Range		
Weighing balance	GENEFLOW		

2.2 METHODS

2.2.1 Cell culture

THP-1 cells were cultured in RPMI-1640 medium and 16HBE14o$^-$ was cultured in medium-199, containing 10% foetal bovine serum (FBS). This was followed by the addition of penicillin (100 U/ml), streptomycin (0.1 mg/ml) and 1% L-glutamine (2 mM), an essential amino acid that is required by nearly all mammalian cells grown in culture.

Prior to the cell culture procedure, the reagents trypsin and phosphate buffered saline (PBS), along with the media, were kept in a water bath at 37ºC for 30 to 40 min. The flow hood (cabinet) was switched on and sterilised with 70% industrial methylated spirits (IMS) as were all reagent bottles before being placed in the flow hood. Cell lines were cultured to approximately 85-90% confluence and the cells were passaged. In order to passage 16HBE14o$^-$, the media on these cells were aspirated and the cells were rinsed with sterile PBS containing 137 mM NaCl, 8 mM Na_2HPO_4-$7H_2O$, 2.7 mM KCl and 2 mM KH_2PO_4 in a litre of solution at pH 7.4. The PBS was then aspirated and cells were detached from the flask using 1 ml of pre-warmed sterile trypsin, an enzyme that breaks down proteins in the extracellular matrix (177). The flask was incubated at a temperature of 37ºC, 95% humidity and 5% CO_2 for 5-10 min. The cells were then re-suspended by aspirating repeatedly up and down before being transferring into a 50 ml tube which was filled with fresh media to the 40-45 ml level. The tube was then centrifuged at 1000 revolutions per minute (rpm) and 4°C for 4 min to separate the trypsin from the cells and to separate dead from healthy cells. Subsequently, the cells were re-suspended in 9 ml of medium and then 3 ml of this cell suspension was transferred into a new 75 cm^2 tissue culture flask (T-75) that contained 7 ml of fresh media (total volume 10 ml). The new flask was then placed into the incubator until its next use.

THP-1 cells were grown as suspensions and passaged by centrifuging the suspension in a 10 ml tube at 1000 rpm for 5 min and discarding the supernatant to wash the cells with PBS before centrifuging the suspension again for 5 min at 1000 rpm. The PBS was decanted after centrifuging and the cells were suspended by adding 10 ml of culture media into the tube, mixing together and adding 5 ml of the suspension into 5 ml of fresh culture media in a T-75 flask. The new flask was then placed into the incubator until the next use.

2.2.1.1 Isolation of human peripheral blood monocytes (HPBMs)

To isolate and study HPBMs, peripheral blood mononuclear cells (PBMCs) were harvested from the freshly collected blood using informed consent taken from at least two healthy donors. These cells were placed in blood bags which contained EDTA. The reason behind using samples from different two donors was to confirm the findings through biological repeats, ensuring greater accuracy of results through the use of distinct samples that can then capture random variations. One of the biggest challenges experienced when isolating HPBMs is the interference of mixed populations and lymphoid cells. To that end, several procedures of separation were utilised for isolating monocytes from the peripheral blood, albeit with inconsistent success rates. A number of such methods take advantage of these cells' adherent properties, whereas others rely upon the variations in the expression of cell size, cell surface antigen, and the density between other leukocytes and monocytes. However, it is often the case that either the purity or monocyte number are compromised in the process (178).

Due to time and financial constraints, we primarily utilised adherence methods. The results obtained used this method were confirmed using HPBMs isolated by positive selection with $CD14^{+}$. PBMCs were isolated through the use of Ficoll-Paque by decanting the blood into two sterile falcon tubes (the quantity being 25 ml from each). The blood was centrifuged for 30 min at 1500 × g. This mix was separated into four layers, the

second of which (creamy coloured) was sifted from the top to a 50 ml sterile tube (Fig. 2-1). This tube was once again centrifuged at 1000 × g for a period of 10 min. Thereafter, the supernatants were emptied, and the pellets were dislodged with gentle tapping. The cells from both tubes were combined with sterile PBS before they were centrifuged again in the same manner and for the same duration (10 min at 1000 x g). After discarding the supernatant, the pellet was re-suspended in fresh 10 ml of RPMI-1640 +10% FBS + 1% L-glutamine. Subsequently, the suspension was diluted to a ratio of 1:20 and counted to provide a specific density and concentration to the cells, which were seeded at 3 ml volume in 6-well plates. Thereafter, the isolation of HPBMs from PBMCs took place either via positive selection (e.g. with $CD14^+$) specifically using MACS system and following the manufacturer's protocol, or via plastic adherence. For the latter, that is, plastic adherence, $5x10^6$ PBMCs per well were placed into 12-well plates. In addition, the cells were permitted to adhere within a 5% CO_2 incubator for 2-3 hours at a temperature of 37°C in 1 ml RPMI-1640 comprised of L-glutamine which, in turn, was supplemented with 100 U/ml penicillin, 10% (v/v) fetal calf serum and 1 mg/ml streptomycin. Whilst it is possible for PBMCs to also adhere, the majority of them were unable to do so as strongly as HPBMs and were removed relatively easily by four vigorous and extensive washes. Approximately 25% of the cells remaining within the first 24 hours of culture were denoted by lymphocytes. However, after a period of 48 hours in serum-low culture, lymphocytes were reduced substantially (1-2%) on untreated plastic surfaces and tissue culture-treated (179). However, for confirmation purposes, we tested the purity of the plastic adherence HPBMs; the cells were checked via flow cytometry in the basis of CD14 as well as CD16 staining in order to derive intermediate ($CD14^+/CD16^+$), extremely pure classical ($CD14^+/CD16^-$) and nonclassical ($CD14^-/CD16^+$) HPBMs subsets. In line with expectations, classical HPBMs comprised most of the overall total HPBMs - approximately 65 to 75%. Meanwhile intermediate

HPBMs ranged anywhere between 15 and 20% whereas non-classical ranged from close to 5 to 10% of these cells following an isolation period of 48 hours. Both methods described here have been used in experiments of this current research for further confirmation and undertook a comparison between the results obtained from HPBMs which were isolated via adherence and the findings from selectively isolated HPBMs (pure $CD14^{+}$). No substantial differences were found between these results which confirms that our method of separating HPBMs from PBMCs via adherence signifies the correct cell for our studies.

For HPBMs-derived macrophages (MDMs), HPBMs were incubated with completed RPMI-1640 media for 14 days to enable complete differentiation into macrophages. The medium was refreshed every 4 days. This differentiation process included numerous changes as the cell developed. These included increases in size of between 5 - 10 times, organelles augmenting in complexity and quantity, and phagocytic ability amongst others. It is critical to note that not all macrophages (Langerhans cells and cerebrum microglia, for example), have been developed and derived from HPBMs (180).

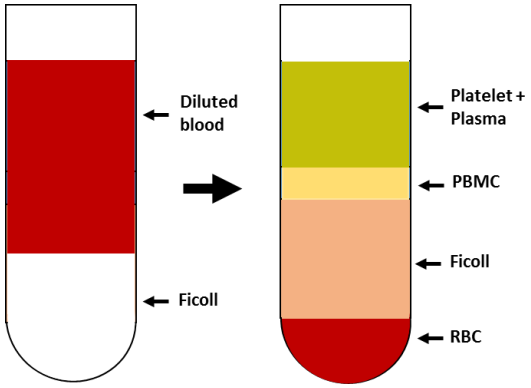

Figure 2-1. Preparation of PBMCs isolation from whole human blood.

2.2.1.2 Freezing and thawing cell lines

From a single T-75 flask, 16HBE14o$^-$ cells were trypsinised and suspended again in culture medium. The THP-1 cells were non-adherent cells and suspension was comprised of unattached THP-1 cells or 16HBE14o$^-$ transferred to a Falcon tube before being centrifuged for 5 min at 1000 rpm. The supernatant was then extracted, after which the pellet was re-suspended in freezing media (1 ml) that comprised 90% FBS and 10% dimethyl sulfoxide (DMSO). Finally, it was transferred to a cryovial and stored at a temperature of -80°C for 2 days and then transferred into liquid nitrogen for long-term storage.

Later, when needed, a cryovial of frozen cells was removed from the freezer and thawed in a warm bath at 37ºC. They were yet again suspended in pre-warmed medium (10 ml) and moved to a T-75 flask before being placed in an incubator (37ºC). The following day, the media was replaced to remove any excess DMSO from the flask.

2.2.1.3 Cell count using haemocytometer

In order to obtain an accurate cell count, a suspension of cultured single cells was used. The content of the tube was diluted in PBS at 1:20 (950 µl PBS + 50 µl cells) in a bijou bottle. A grease-free coverslip and a haemocytometer were cleaned using IMS in the flow hood. After cleaning, approximately 10 µl cell suspension was dropped on the haemocytometer. The cover slip was then placed over the haemocytometer and the four side squares were counted using a microscope (see Fig. 2-2). The number of cells was estimated using the formula below:

Cell number/ml = (cell count/4) x 20 (dilution factor) x 10,000

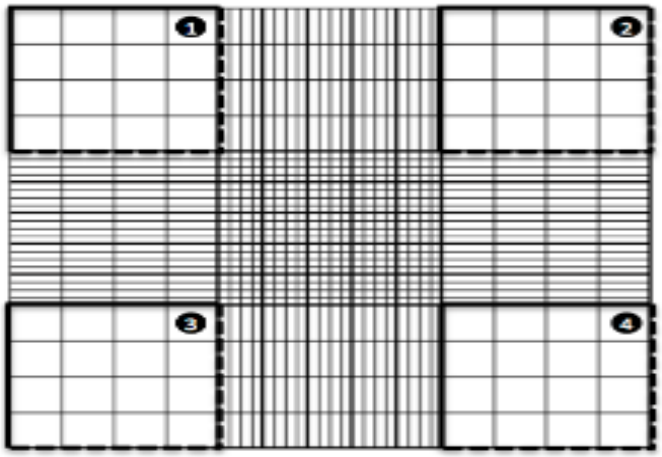

Figure 2-2. Haemocytometer for cell count.

2.2.1.4 Phorbol 12-myristate 13-acetate (PMA) treatment for THP-1 cells

PMA is a specific activator of protein kinase C (PKC) which induces differentiation of adherent monocytes by causing cell cycle arrest and activation of NF-kβ dependent gene transcription (181). The condition for PMA treatment of THP-1 cells to allow them to differentiate and adhere (PMA-treated monocytic THP-1 cells) was implemented in 3 phases. The cells were treated in 200 nM of PMA (see table 2.2) and placed in an incubator (37ºC) overnight. On the second day of incubation with PMA, the medium was replaced with fresh PMA-free media and again left to incubate overnight. On the third day, these adherent monocytes were harvested and used.

Table 2.2. Final concentration of PMA.

	Mass concentration	Molecular weight	Molarity	Final Concentration
PMA	**1 mg/ml**	**616.83 g/mol**	**1.62 mM**	**200 nM**

2.2.2 Electrophoresis and western blot

2.2.2.1 Conditions for forskolin, 3-isobutyl-1-methylxanthine and protein kinase A inhibitor for immunoprecipitation

16HBE14o$^-$ and THP-1 cells in the T-75 flasks were passaged in the manner explained previously. Typically, at 80% confluence, cells grown in the T-75 flask were passaged and 2 ml of cell suspension was added after centrifugation to a 10 cm dish which contained 3 ml of fresh medium. The cells were then incubated to grow and adhere to the point where experimental treatments could be carried out. Specifically, this was when the cells grew on plates to at least 80% confluence for epithelial cells or after 3 days of PMA treatment for THP-1.

Of the plates used, a control plate which was left untreated was grown in a culture medium alone. Treated cells (16HBE14o$^-$ and PMA-treated monocytic THP-1 cells) were grown in a complete medium and treated using forskolin (FSK) at 10 μM and 3-isobutyl-1-methylxanthine (IBMX) at 100 μM for 30 min. The medium was aspirated and the cells were then harvested by scraping after the addition of 1 ml of trypsin into a 10 ml tube. The cells were then rinsed with ice cold PBS and centrifuged as previously (5 min at 1000 x g). These cells were then lysed and the protein in the lysate was quantified using Bradford assay (section 2.2.2.3). The remaining pellets were then frozen at a temperature of -80°C for subsequent use. The lysate was prepared for immunoprecipitation (IP) and western blot (WB) and was then utilised to identify and separate proteins on the basis of molecule size. Notably, the charged particles in uniform pores move to the opposite electrode when they are affected by the electric field (182).

Two other sets of cell samples were prepared in 10 cm dishes, with one being treated with protein kinase A inhibitor (PKI) for 5 min and the other treated with PKI for 5 min followed by FSK/IBMX for a length of 30 min using the concentrations outlined in table 2.3. below and following the procedure mentioned above. The cells were first rinsed with

ice cold PBS harvested by scraping after having been incubated with trypsin for 5 min and prepared for western blotting.

FSK, a labdane diterpene, is used to increase cAMP intracellular level through activation adenylyl cyclase, an enzyme that converts ATP to cAMP. IBMX on the other hand, is a phosphodiesterase inhibitor which degrades phosphodiester bonds in ATP, thus inhibiting ATP degradation raising level of ATP. IBMX can thus raise cAMP levels by making ATP available for conversion into cAMP. Several studies have used these two compounds to synergistically raise intracellular cAMP levels (183-185).

Table 2.3. Concentrations of PKI, FSK and IBMX for cell treatment.

Chemical Component	Stock Concentration	Final Concentration
FSK	12 mM	10 μM
IBMX	50 mM	100 μM
PKI	535.3 μM	100 nM

2.2.2.2 Cell lysate preparation and extraction

For both western blot protocol and immunoprecipitation, all cells, both treated and untreated, were harvested using trypsin or scraping. Non-adherent cells were centrifuged with the medium to pellet the cells. The supernatant was discarded and the cells were washed with cold PBS and centrifuged to pellet cells. The cell pellets were then lysed using 200 μl of 1× radioimmunoprecipitation assay (RIPA) buffer containing 150 mM NaCl, 1.0% NP-40 or Triton X-100, 0.5% sodium deoxycholate, 0.1% SDS (sodium dodecyl sulfate) and 50 mM Tris at pH 8.0 on ice for 10 min (Table 2.4). RIPA buffer destroys cell membranes and intracellular membranes so that individual proteins in the cell can be present in one homogenous mixture in order to allow each protein to individually migrate in electrophoretic gel. Given that cellular proteins are in contact; it is necessary to add a protease inhibitor to the RIPA buffer before it is used to inhibit the

proteases from degrading proteins in lysate. One *cOmplete* protease inhibitor tablet (Roche Ltd, UK) was dissolved in 2 ml distilled water before being added to RIPA buffer to make 25×. The lysate was centrifuged at 15000 rpm for 5 min at 4°C to precipitate cell debris and membranes. The supernatant was then transferred to a 2 ml Eppendorf tube, leaving the pellet behind.

Table 2.4. Concentration of components of RIPA buffer.

RIPA Buffer Components	Stock Concentration	Final Concentration
Sodium chloride (NaCl)	1 M	150 mM
Triton X-100	100%	1%
Sodium Deoxycholate	5%	0.50%
Sodium dodecyl sulfate (SDS)	20%	0.10%
Tris pH 8.0	1 M	50 mM

2.2.2.3 Protein quantification using Bradford assay

To ensure that the amount of protein loaded onto SDS gel was error-free such that electrophoretic bands obtained were relative to the expression level, the protein in each lysate was quantified. The quantification was done using Bradford protein assay, a spectroscopic assay that uses the colouration of protein samples to measure the concentration. First, a standard curve was plotted using a series of dilutions containing BSA of known concentration in varying volumes of RIPA buffer and a fixed volume of 1× Bradford reagent, as indicated in table 2.5. Following this, for the quantification of lysate, 5 µl of sample was added to 250 µl of the Bradford buffer and this was then added in triplicates to a 96-well plate to take the average of the 3 values.

Table 2.5. Concentration of reagents for standard curve of Bradford Assay.

Tube	Standard (µl)	Final Conc. (µg/µl)	Volume of the standard needed per well (µl)	Bradford buffer volume per well
1	100 RIPA + 100µl BSA	20	5	250 µl
2	100 from Tube 1 mixed with 100 RIPA	10	5	250 µl
3	100 from Tube 2 mixed with 100 RIPA	5	5	250 µl
4	100 from Tube 3 mixed with 100 RIPA	2.5	5	250 µl
5	100 from Tube 4 mixed with 100 RIPA	1.25	5	250 µl
6	100 from Tube 5 mixed with 100 RIPA	0.625	5	250 µl
7	100 from Tube 6 mixed with 100 RIPA Mix, then discard 100 from this tube	0.312	5	250 µl
8	Blank (100 RIPA buffer)	0	5	250 µl

2.2.2.4 Gel preparation and SDS polyacrylamide gel electrophoresis (SDS-PAGE)

A resolving gel was first prepared with proportions depending on the size of the protein of interest (see table 2.6). A higher level of acrylamide was used for the detection of smaller proteins and a lower level for larger proteins. Tetramethyl-ethylenediamine (TEMED) was not added until the liquid was ready to be poured into the cast as TEMED catalyses the gel formation. The liquid solution was then added into the cast using a 1000 µl pipette with extra care taken to ensure that there were no bubbles created in the process. The resolving gel was allowed to solidify before the stacking gel was added, as indicated in table 2.7. The liquid was dispensed onto the resolving gel and a comb was placed in the cast to provide the shape of the well onto which the proteins were loaded.

Table 2.6. Ingredients for making SDS-PAGE Gel (resolving).

Resolving Gel	**8%**	**10%**	**12%**	**15%**
1.5 M Tris-HCI buffer, pH 8.8	2.5 ml	2.5 ml	2.5 ml	2.5 ml
Acrylamide	2.67 ml	3.33 ml	4 ml	5 ml
Ammonium Persulfate (APS) 10%	100 µl	100 µl	100 µl	100 µl
10% Sodium Dodecyl Sulfate (SDS)	100 µl	100 µl	100 µl	100 µl
Distilled water (dH_2O)	4.62 ml	3.96 ml	3.29 ml	2.29 ml
Tetramethyl-ethylenediamine (TEMED)	10 µl	10 µl	10 µl	10 µl
Total Volume	**10 ml**	**10 ml**	**10 ml**	**10 ml**

Table 2.7. Ingredients for making SDS-PAGE Gel (stacking gels).

Stacking Gel (5%)	**10 ml**	**5 ml**
0.5 M Tris-HCI buffer, pH 6.8	2.5 ml	1.25 ml
Acrylamide	1.3 ml	650 µl
Ammonium Persulfate (APS) 10%	50 µl	25 µl
10% Sodium Dodecyl Sulfate (SDS)	100 µl	50 µl
Distilled water (dH_2O)	5.99 ml	3 ml
Tetramethyl-ethylenediamine (TEMED)	10 µl	5 µl

2.2.2.4.1 Tris buffered saline (TBS) solution (10×)

In order to make 1 L of TBS (10×), 80.06 g of NaCl (1.37 M) and 24.23 g of Tris Base (MW=121.1 g) were added to nearly 800 ml of deionised water. After the solutes were completely dissolved, the pH was then adjusted to a level of 7.6 with HCl. This solution was mixed with deionised water to a volume of 1 L. This was kept at room temperature and then diluted to 1× working concentration before its use.

2.2.2.4.2 TBS-Tween 20 (TBS-T) solution (1×)

The 1× TBS-T solution was made by blending 100 ml of 10× TBS-T with 900 ml of deionised water and 0.5 ml of Tween 20 (0.05%). In recognition of the fact that Tween

20 will stick to the pipette tip in wake of viscosity, special care was taken to ensure that the appropriate amount of Tween 20 was added to the mixture. It was stored at room temperature until its use.

2.2.2.5 Electrophoresis and western blot (WB) technique

After casting the gel, a running buffer containing 1× Tris-glycine (25 mM Tris base, 190 mM glycine and 0.1% SDS) was prepared. Protein in the lysates was denatured in 1×laemmli buffer and then placed in a heating block for denaturation and depolarisation at 75°C for 5 min (186). The SDS gel was submerged in the running buffer and 100 µg of lysates were loaded onto the wells of the gel with 6 µl of ladder on the first lane. The gel was run at 100-200V for 1 hour to 1.5 hours and monitoring of the migration was done at every interval until the protein front (blue dye) reached the bottom of the gel.

The migrated bands were transferred semi-dryly onto an activated polyvinylidenediflouride (PVDF) membrane. A 1× transfer buffer was prepared (25 mM Tris, 190 mM glycine, 20% methanol - for proteins larger than 80 kD, SDS included at 0.1%) and the PVDF membrane was soaked in the transfer buffer to prevent bubbles forming when the gel was placed on the PVDF to transfer the protein. After the gel cast was opened, the gel was removed and placed over the PVDF membrane before being sandwiched between filter papers and gauze pads and placed into the transfer buffer. The gel was placed at the negative side while the membrane was positioned at the positive so that the protein moved onto the membrane rather than the filter paper. This was run at 100 mA for 1 hour. The PVDF is hydrophobic and needs to be pre-activated with 100% methanol for full protein binding capacity.

After the successful transfer of proteins, the PVDF was blocked in 20 ml of solution containing 5% skimmed milk in TBS-Tween (TBS-T) and placed on a shaker at room temperature for approximately 1 hour. This blocking buffer was used to block the

unreacted sites on PVDF and reduce the amount of nonspecific bind proteins (187). The membrane was immunoblotted (IB) with primary antibody at the dilution level recommended by manufacturers in a milk solution at 4°C overnight (see table 2.8). This primary antibody recognised the protein of interest and, after the membrane was incubated in primary antibody, the membrane was rinsed with TBS-T 6 times for 10 min each time. It was then incubated for 1 hour in tagged secondary antibody raised in the same species (and prepared in the same way) as the primary antibody. Subsequently, the membrane was rinsed again with TBS-T 6 times for 10 min each time. Excessive regent was removed and the membrane was covered in a plastic sheet before the addition of enhanced chemiluminescence (ECL). Notably, ECL is a sensitive enhanced, non-radioactive, luminol-based chemiluminescent substrate that was used to detect horseradish peroxidase (HRP) conjugates on the immunoblots. The ECL Western Blotting Substrate visualises and detects picogram (pg) amounts of antigen using photographic or other feasible chemiluminescent imaging methods. Thus, imaging was acquired using darkroom development techniques and image scanning methods using the BioRad Imaging System.

Table 2.8. Samples of antibodies used in this experiment.

Primary antibody	**M. W. kDa**	**Species/ Raised in**	**Type**	**Concentration**
HH7 (anti-AnxA2)	36	Mouse	Monoclonal	1:1000
Anti-Annexin II (C-16)	36	Goat	Polyclonal	1:1000
H21 (anti-S100A10)	11	Mouse	Monoclonal	1:1000
Anti-PP2B-A (H-209)	61	Rabbit	Polyclonal	1:500
Anti-PP2B-B1 (C-17)	19	Goat	Polyclonal	1:500
Anti-PP2B-B1/2 (D-1)	20	Mouse	Monoclonal	1:500
Anti-beta Actin	48	Mouse	Polyclonal	1:1000

Secondary antibodies acquired from Dako (Glostrup, Denmark) raised in the same species conjugated to HRP were used, including polyclonal goat anti-mouse immunoglobulins, polyclonal mouse anti-rabbit immunoglobulins, and polyclonal rabbit anti-goat immunoglobulins.

2.2.3 Immunoprecipitation (IP) assay

In order to ensure IP, a primary antibody against the protein of interest was incubated with lysate/cell extract at 4°C to enable binding of the antibody to the protein. For each target protein, 3 pre-clear eppendorf tubes were prepared and 200 µl of protein G sepharose slurry beads was added to the tubes. 200 µl of RIPA buffer was then added to the tube containing the beads and the tubes were gently vortexed to wash the beads. These tubes were centrifuged for 1 min at 14000 rpm and 4ºC. The supernatant was discarded and another 200 µl of RIPA buffer was added and vortexed again more gently. The tubes were centrifuged as before and the supernatant discarded. Then, 100 µl of RIPA buffer was added and vortexed before the tubes were centrifuged again. A portion of the supernatant was then discarded, leaving approximately 50% in the tube. The beads and the buffer were mixed with a pipette and 50 µl of the beads-buffer mixture was added into a new eppendorf tube which was kept on ice. 1 mg of lysate was added into a tube containing of 500 µl RIPA buffer. This tube was then covered and placed on a rotator at 4°C for 1 hour. 2 µg of antibody against the target protein was prepared and added to a new tube labelled AB. The supernatant in these tubes containing the beads was aspirated post-centrifugation and then added to tube AB. Tube AB was covered and kept in a 50 ml tube and placed for an hour on the rotator in a cold room. The contents of tube AB were then transferred into the eppendorf tube with the beads and the tube was then incubated overnight in a cold room.

The eppendorf tube was centrifuged at 14000 rpm for 1 min at 4ºC. The supernatant was decanted carefully until there was an amount which just covered the beads. 500 µl of RIPA was added and vortexed for a few seconds and centrifuged for 30 seconds at 14000 rpm. The supernatant was discarded and another 200 µl of RIPA was added and vortexed gently before being centrifuged again. The supernatant was discarded again, and the process was repeated, including discarding of all supernatant. 35 µl of 1× sample buffer was added to the tube, mixed gently and was boiled at 75°C for 5 min. Then, the tube was centrifuged again, and the supernatant was loaded onto SDS gel for western blot.

2.2.4 Cell viability and cytotoxicity assays

2.2.4.1 Trypan cell viability assay

Cell viability assay was used for drug compatibility screening and for determining the cytotoxicity of the tested chemicals. The PMA-treated monocytic THP-1 cells or HPBMs were treated in different conditions [untreated cells for control and treated cells with various inhibitors including PKI, cyclosporine A (CsA), 4,4'-Diisothiocyano-2,2'-stilbenedisulfonic acid (DIDS), CFTR inhibitor (CFTR(inh)-172) or α-[(2-(3-Chlorophenyl)hydrazinylidene]-5-(1,1-dimethylethyl)-β-oxo-3-isoxazolepropanenitrile (ESI-09)]. PMA-treated monocytic THP-1 cells or HPBMs were first detached from the plate. 10 µl of the cell suspension was taken and added to 10 µl of trypan blue within the same eppendorf. 10 µl of this mix was then loaded into an automated cell counter (TC20™, Bio-Rad) which determined the % of viable and dead cells.

2.2.4.2 3-(4,5-dimethylthiazol-2-yl)-5-(3-carboxymethoxyphenyl)-2-(4-sulfophenyl)-2H-tetrazolium, inner salt (MTS) assay

The MTS assay is a colorimetric assay for assessing cell metabolic activity. Cells were seeded at 20,000 cells/well (100 µl /well). With regard to the adherent cells, trypsinised cells were treated as normal (for instance, 500 µl for 25-T flask) and re-suspended in 5 ml of media. 500 µl of cell suspension was taken and a cell viability count analyser was

used to calculate the volume/density necessary for the purpose of seeding 20,000 cells/well. When the cells adhered to the bottom after 2 hours of seeding, the media was decanted and replaced with fresh media (for control) or media containing inhibitor (e.g. PKI, CsA, DIDS, CFTR(inh)-172 or ESI-09) at 100 µl/well. Thereafter, all 3 plates were incubated at 37ºC: the first plate was read after 3 hours of treatment to maintain the same conditions used in the other experiments, then 20 µl of MTS was added to each well and they were re-incubated again for 3 hours with MTS at 37ºC. The second plate was incubated for 18 hours with the treatments, followed by 20 µl of MTS being placed into each well and further incubation for another 3 hours with MTS at 37ºC. In the same manner, the third plate was prepared after a period of 24 hours of the treatments and then re-incubated at 37ºC for another 3 hours with 20 µl of MTS placed into each well. Thereafter, every plate was read using the microplate photometers (plate reader) at 490 nm. The well comprising media alone was used as a negative control (equivalent of blank). This experiment was repeated three times independentally.

2.2.5 Patch clamp technique

The patch clamp technique is an electrophysiology used to quantify the amount of current flowing through single or multiple ion channels on single living cells or tissue sections immersed in ionic solution (Fig. 2-3). It was developed by Neher and Sakmann in Gottingen, Germany in 1976. It uses a patch pipette filled with electrolytes and a recording electrode to read the current (using a voltage clamp) or voltage (using a current clamp) moving across the membrane of isolated cells in a tissue or membrane patch (188). In a voltage clamp, the voltage passing through the patch pipette is varied by the researcher and the current can be measured. When in a current clamp, the current is varied so that the voltage across the membrane of the isolated cell can be measured.

2.2.5.1 Whole-cell patch clamp technique

The patch clamp technique is regarded as the gold standard technique for the functional characterisation of both single and multiple ion channels on the cell membrane. In this present study, the whole-cell patch method was used to conduct all electrophysiology experiments (189). The technique was used on 16HBE14o$^-$, PMA-treated monocytic THP-1 cells and HPBMs grown on plastic coverslips. A coverslip was placed into a perspex bath kept atop an inverted microscope stage (Olympus IX70, Olympus, Southend-on-sea, Essex, UK). Thereafter, a patch pipette was pulled down to come into contact with the cell surface so as to create a high resistance seal. Thereafter, a pipette was introduced to provide pulses of suction which caused the membrane below the tip of pipette to rupture. The pipette solution diluted the cytosol and permitted electrical access in and out the cell via the cell membrane. The extracellular and intracellular solutions (bath and pipette solution, respectively) were both controlled, but only the extracellular bath solution was altered during the experiment to avoid interference with the component of the intracellular component which would have caused confounding effects (see Fig. 2-3). All the experiments were carried out at room temperature (22-25°C).

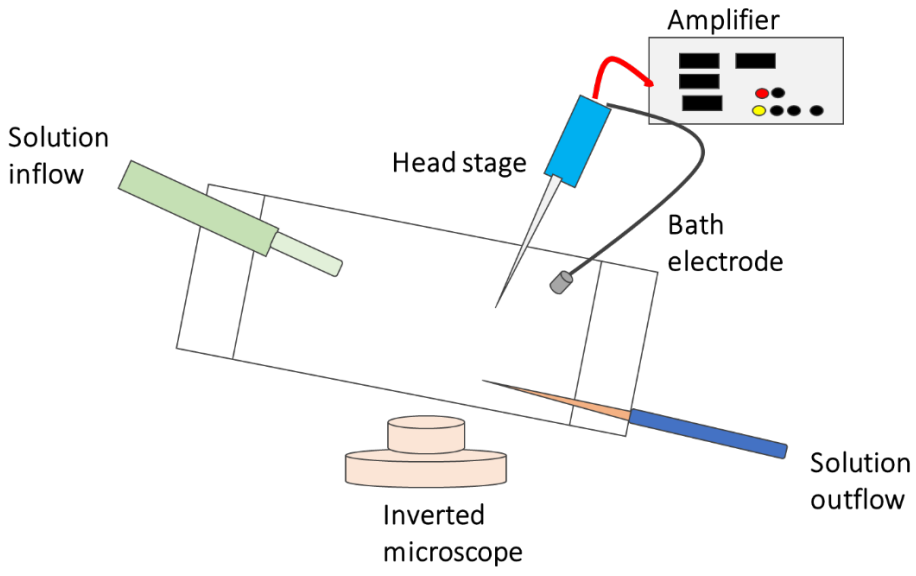

Figure 2-3. Simple set-up of a patch clamp technique.

2.2.5.2 Bath perfusion system

The delivery of bath solutions took place through a gravity driven perfusion system. Syringes were suspended over the rig which contained the extracellular experimental solutions and flowed through the polyethylene tubing which ended in a single perfusion tip entering the bath. Bulldog clips were mounted atop the polyethylene tubing and underneath the syringes in order to stop the experimental solution from flowing. Only a single experimental solution was allowed to flow from one syringe at a given point in time. Solution that flowed into the bath was taken off using suction via a glass pipette that was situated at the bath's other side. Solutions in the syringes were filtered through a 0.2 μm syringe filter to remove unwanted elements (e.g. debris and dust) which might impede the taking of a patch.

2.2.5.3 Patch pipettes

Non-heparinised micro-haematocrit capillary tubes were used to construct the patch pipettes. The tubes were pulled vertically in a two-stage micropipette puller and the capillary tube ends were flame polished to eliminate rough edges that could potentially cause damage to the chloride coating of the pipette electrodes. Then, the tube was inserted into the pipette puller and clamped to position the heated coil at the tube's central section. The pipette puller comprised an automatic stopper control making two automatic stage pulls. After being heated at a set temperature to melt and stretch the tube, the coil was cooled and automatically shifted down to the central section of the melted tube. Then it was reheated to a lower temperature, causing the tubes to melt and stretch further until 2 patch pipettes had been created.

The pipettes were filled using an intracellular pipette filtered solution. Then, bubbles were removed from the pipettes' tips with gentle flicking to prevent possible obstruction between the cell membrane and electrode. Thereafter, the pipette was placed inside the

designed holder to be subsequently attached to the headstage positioned at the right side of the bath. The pipette holder was tightened with rubber to ensure that the pipette was in place with a fully airtight seal. A manometer filled with coloured liquid was then connected to the pipette holder, allowing for the application of pressure on the pipette. Positive-pressure was gently applied to remove unwanted elements from the pipette during the process of obtaining a patch. Afterward, a negative-pressure was applied to create a seal between the two (cell and pipette).

2.2.5.4 Micromanipulators

Two manipulators accurately guided the pipette tip (via the bath solution) to establish contact with the coarse manipulator, cell membrane and the fine manipulator. After connecting both to the head stage, a three-axis coarse manipulator was utilised to bring the pipette closer to the cell. Then, the fine manipulator was used to guide the pipette to touch the cell surface.

2.2.5.5 Electrodes

Two electrodes, the recording (or pipette) electrode and reference (or bath) electrode, were used for the patch clamp. These were silver wires that had been chlorided in bleach for 15 min.

The chlorided pipette electrode was soldered to a brass pin. It was placed inside the holder of the pipette and was surrounded by 1-2 O-rings to strengthen the seal between the holder and the wire. Thereafter, the pipette holder was linked with the head stage to create a connection from the head stage all the way down to reach the pipette solution.

The reference electrode, comprising a silver-chlorided wire soldered to a gold pin, was placed in an extracellular bath solution. It was then connected to the head stage with a connecting wire.

2.2.5.6 Electronics

All the experiments used a List EPC-7 patch clamp amplifier. The currents gauged by the amplifier were low-pass filtered at 5 kilohertz (kHz) via a Bessel filter. These filtered signals were displayed on the monitor and were processed by digidata interface (Axon Instruments, Union City, California, USA) using a Windows-based compatible computer (Dell) via the pClamp 8.0 software (Axon Instruments). Voltage protocol was then driven by the computer through pClamp 8.0 software.

2.2.5.7 Other equipment used in the whole-cell patch clamp technique

This head stage was mounted atop the course manipulator and connected directly to the recording electrode through the pipette holder. It should be noted that the headstage was the amplifier's small extension and hence, acted as an interface between the electrode and the amplifier device. The Olympus I×70 inverted microscope was mounted atop a vibration-resistant table to minimise possible vibrations. It was surrounded by a Faraday cage connected to the ground which protected the recording equipment from any extraneous electronic noise. As the Faraday cage was opened on the front, an aluminium barrier was placed in front of the microscope to prevent electrical noise from interfering with the recording.

2.2.5.8 Obtaining and recording the whole-cell patch

The pClamp 8.0 software was set to 'pipres' with 0 to +20 mV/pA gain. Once the bath was filled with solution, a piece of coverslip from the incubator (containing cells) was placed in the bath. A pipette was then filled with internal solution and attached to the top of the holder. Positive pressure was applied to the pipette with a liquid manometer and was kept intact via a 3-way tap. Then, the pipette was brought down to the bath solution using a coarse manipulator and the tip of pipette was visualised by looking through the microscope at 100× magnification. When the pipette reached the bath's solution, a

resulting current deflection manifested on the monitor. The deflection's size was used to calculate the pipette's resistance. The initial difference in pipette and bath current was found to create an offset on the amplifier. However, it was neutralised by setting the pipette's current strength to zero with an offset control (on the amplifier).

After locating a single cell, the pipette was lowered carefully to the cell through the coarse manipulator. Thereafter, the microscope was altered to a higher magnification (400×), and a fine manipulator used to direct the pipette over the cell's surface. Before the pipette was able to touch the cell, a negative pressure replaced the positive pressure through the monometer's isolation, and the pipette was again brought down further to come into contact with the cell membrane. This allowed the formation of a tight seal between the cell membrane and the pipette (gigaseal). With the seal formation, the current deflection on the monitor reduced to a flat line.

Then, the computer programme was altered to 'sealres': the gain on the amplifier was turned to 0 to +20 mV/pA. The capacity transients could be seen at the beginning and end of the trace. The fast capacitance transients were then dialled off with the fast capacitance controller (C-fast) and pulses of suction were applied via the mouth to the pipette, prompting the cell membrane to rupture and the solution inside the pipette to dialyse the cell's inside portion, thereby creating a whole-cell patch. This could be viewed on the monitor and was expressed with a large increase in size of the capacitance spikes at commencement and end of the trace. These were then dialled using G-series and C-slow controllers along the amplifier. Importantly, the slow capacity compensation offered a measure of the cell's area and was considered as 1 $\mu F/cm^2$.

2.2.5.9 Voltage step protocol

The voltage step method was followed to measure current between +100 and -100 millivolts (mV) in 10 mV steps for a time span of 400 millisecond (ms). The holding

potential was -40 mV. This protocol was used in our study to functionally measure ORCC and CFTR mediated currents in 16HBE14o$^-$, PMA-treated monocytic THP-1 cells and HPBMs.

2.2.5.10 Experimental solutions

The experimental solutions' osmolality was checked using a Roebling osmometer and subsequently adjusted to 300 ± 1 mOsm·kg^{-1} H_2O using water or mannitol as appropriate.

With full specification provided in the tables below (2.9, 2.10 and 2.11), the intracellular solution (pipette) and extracellular solution (bath) were prepared, such that the conditions were similar to those of physiological ionic conditions. Importantly, clamp Ca^{2+} was reduced to a low level in both solutions to prevent activation of Ca^{2+}-activated Cl^- channels.

Table 2.9. Stock solution and molecular weights of the materials used.

Salt	Stock concentration	Weight
NaCl	1 M	-
$CaCl_2$	1 M	-
$CsCl_2$	200 mM	-
$MgCl_2$	100 mM	-
EGTA	-	380 g
ATP	-	550 g
HEPES (NaOH)	100 mM	-
HEPES (CsOH)	100 mM	-
Concentration = number of moles / volume. Stock solution of moles = mass / molecular weight (MW).		

Table 2.10. Bath solution for whole-cell patch clamp experiment.

Salt	Final concentration
NaCl	140 mM
$CaCl_2$	2 mM
$MgCl_2$	1 mM
HEPES (NaOH)*	10 mM
* pH buffer, clamp the pH to 7.4 pH units.	

Table 2.11. Pipette solution for whole-cell patch clamp experiment.

Salt	Final concentration
$CsCl_2$ ■	135 mM
$MgCl_2$	2 mM
EGTA ◊	2 mM
ATP ≡	1 mM
HEPES (CsOH)*	10 mM
■ Cs^+ blocks K^+ channels. ◊ Ca^{2+} buffer, clamp Ca^{2+} to a low level, important to prevent activation of Ca^{2+}-activated Cl^- channels. ≡ Needed to support the continued opening of CFTR (works with Mg^{2+}). * pH buffer, clamp the pH to 7.4 pH units.	

2.2.5.11 Cell preparations for whole-cell patch clamp

In splitting 16HBE14o$^-$, cells were transferred onto plastic coverslips (at 13 mm diameter) and placed in a 12-well multi-well plate. The cells were left to grow (or to attach for HPBMs) in fresh media for a period of 24-48 hours at 37°C prior to being used in electrophysiology experiments. For THP-1 cell lines, after the PMA treatment was performed, cells were seeded on coverslips in a 12-well multi-well plate before they were allowed to attach for 24 hours. The following day, the medium was refreshed with PMA-free media and the cells incubated for another 2 days (as explained earlier in the cell culture section 2.2.1).

2.2.5.12 Pre-stimulation of the cells with FSK/IBMX

In order to stimulate Cl^- channels, cells were exposed to FSK (10 μM) and IBMX (100 μM) in the bath solution for 30 min before obtaining patches (to stimulate cAMP). During the first few minutes of the patch experiment, the currents recorded from the cells (without inhibitors) were used as a control. To measure the magnitude of ORCC, DIDS (500 μM) was added to the bath under a steady state and the currents recorded for 1-3 min followed by CFTR(inh)-172 (10 μM) for 1-3 min to study CFTR function. To investigate the involvement of PKA/CaN pathway, cells were pre-incubated for 30 min with PKA inhibitor or CaN inhibitor, PKI (100 nM) and CsA (1 μM), respectively.

2.2.5.13 Pre-stimulation of the cells with LPS

In previous studies, monocytes were activated and primed by LPS to stimulate the production of pro-inflammatory cytokines so as to affect the physiological signalling pathway obtained during infection (190). In addition, LPS has been demonstrated to activate specific ion channels (191, 192). The PMA-treated monocytic THP-1 cells and HPBMs were challenged with *P. aeruginosa* LPS at 37ºC in 5% CO_2 for 30 min to investigate the impact of LPS on the function of ORCC and CFTR.

LPS from *P. aeruginosa* has a molecular mass of 10‑20 kDa. The final concentration of *P. aeruginosa* LPS used in this study was 30 µg/ml. All inhibitors were added as explained earlier in FSK/IBMX stimulation section. Briefly, DIDS (500 µM) was added to the bath perfusion for 1-3 min to study ORCC function, followed by CFTR(inh)-172 (10 µM) to specifically study CFTR function. To test the involvement of the PKA/CaN pathway, cells were pre-incubated for 30 min with either PKI (100 nM) or CsA (1 µM).

2.2.5.14 Whole-cell patch clamp analysis

The analysis of whole-cell records was carried out using P-clamp software (Clampfit 8.1), which calculated the mean current (denoted by pA) and breach voltage (denoted by mV). Thereafter, the current was normalised on the cell area by dividing it by the capacitance reading that was obtained when the slow capacity transients (C-slow) had been dialled off. Subsequently, linear regression was used to calculate the reversal potential (represented by V_{rev}) of the currents.

The calculation of both whole-cell inward (G_{in}) and outward conductances (G_{out}) was made from the current line's slope on both sides of the V_{rev} based on Ohms law. Conductances were normalised to the cell size.

Ohms law states:

$$G = \frac{I}{V}$$

Where, **G** refers to whole cell conductance (siemans), **I** denotes Whole cell current amplitude (amps) and **V** signifies Voltage (volts).

2.2.5.15 Statistical analysis for patch clamp results

The entire data was expressed as mean ± SEM (standard error of the mean). The statistical significance was examined using either paired or unpaired *t*-tests or a one-way ANOVA. A Bonferroni post hoc test was carried out and expected at 5% ($p \leq 0.05$). It should be noted that all methods of whole-cell patch clamp were adapted from Kate Louise Harris's thesis, submitted to the University of Sheffield, 2011.

2.2.6 Enzyme-linked immunosorbent assay (ELISA)

2.2.6.1 Preparation of supernatants

All solutions for this experiment, including the inhibitors and the activators, were prepared in RPMI-1640 medium and pre-warmed at 37°C for 30 min. These were then kept in a laminar flow cabinet at 20-25°C until they were added to the cells. HPBMs were seeded equally in a 6-well multi-well plate (around 1,000,000 cells/well). Before commencing the procedure, all mediums were replaced with fresh media (3 ml/well). The cells were pre-treated with the inhibitors (including DIDS, CFTR(inh)-172, PKI, CsA, ESI-09, ESI-05 and BAPTA-AM) for 30 min, followed by LPS from *P. aeruginosa* (30 µg/ml) for 2 hours to prime the cells and provide the first signal. Subsequently, nigericin (10 µM) was added and rested for 1 hour to provide the second signal and activate caspase-1 to release the cytokines such as IL-1β and TNF-α (193, 194). Cells primed with LPS only and nigericin were used as a control. The supernatants were collected and processed according to ELISA assay or stored at -80°C until the next usage.

2.2.6.2 R&D kit for the experiment

Preparation for ELISA kit from R&D was done using the following reagents:

PBS (137 mM NaCl, 2.7 mM KCl, 8.1 mM Na_2HPO_4, 1.5 mM KH_2PO_4. pH 7.2-7.4, 0.2μm was filtered). Wash Buffer: 0.05% Tween® 20 in PBS, pH 7.2-7.4. (1.5 ml T-20 into 2.5 L 1×PBS). Coating buffer containing 2.4 g Na_2CO_3, 4.8 g $NaHCO_3$ in 800 ml PBS 1× (pH 9.6) was filtered before being used or, alternatively, PBS with sodium azide was used. Reagent diluent / blocking: 1% BSA in 1×PBS (in our lab prepared as 0.5 g into 50 ml of 1×PBS). Substrate solution: 1:1 mixture of colour reagent A (H_2O_2) and colour reagent B (tetramethylbenzidine). Stop Solution: 1 M Sulphuric acid (H_2SO_4). Streptavidin-HRP: each vial containing 2.0 ml of streptavidin conjugated to horseradish-peroxidase. It was diluted to the working concentration specified on the vial label using reagent diluent (250 µl HRP into 9.75 ml of reagent diluent/blocking). Mouse anti-human IL-1β capture antibody: referring to the lot-specific C of A for the amount supplied. Each vial was reconstituted with 0.5 ml of PBS. Biotinylated goat anti-human IL-1β detection antibody: each vial was reconstituted with 1.0 ml of reagent diluent. Recombinant human IL-1β standard: each vial was reconstituted with 0.5 ml of deionised or distilled water. A seven-point standard curve using 2-fold serial dilutions in reagent diluent was recommended. Preparation of 1000 µl of high standard (the first standard point at the highest concentration) as per the assayed plate (195).

2.2.6.3 Solid phase sandwich ELISA experiment

All reagents and components were equilibrated to room temperature before use. The microplate was coated with capture purified antibody [2-5 µg/ml] in a 100 µl/well using a coating buffer-diluted capture antibody. The plate was covered tightly with parafilm and incubated overnight at room temperature**.** The following day, each well was aspirated and the plate was washed with the wash buffer 3 times. After this, 300 µl of reagent

diluent (blocking buffer) was added and incubated at room temperature for 2 hours. The samples were also prepared along with the serial dilutions for the next step. Each well was again aspirated and the plate was washed 3 times using the wash buffer. Then the plate was prepared for sample loading. If the samples were concentrated, they were diluted in a dilution buffer at a ratio of 1 to 10. Importantly, the removal of the last wash was always delayed if the next stage of assay was not fully prepared. The standard cytokine was diluted, beginning from 250 pg/ml for 7 points dilution 1:2 and the last point (no. 8) with a dilution buffer/zero. After mixing, 500 µl was taken from the 1st into the 2nd tube which contained 500 µl of dH_2O. After mixing again, 500 µl was transferred to the next tube. This was repeated until the 7th tube (Fig. 2-4). After the addition of 100 µl of serial dilution and samples, the plate was incubated for 2 hours at room temperature or overnight at 4°C. Then, the plate was aspirated and was washed 3 times with the wash buffer, as earlier explained. Subsequently, 100 µl of detection antibody was added into each well at a concentration of 200 ng/ml or 1:2000 dilution. After being covered with an adhesive strip, the plate was incubated for a period of 2 hours at room temperature to allow the detection reaction to complete. Again, the plate was aspirated and washed 3 times with wash buffer. Then, 100 µl of streptavidin-conjugated-HRP enzyme was added at 1:1000 dilution (100 µl from streptavidin-HRP mixed with reagent diluent). The plate was covered and incubated for 20 min at room temperature. After that, the plate was aspirated and washed 3 times and 100 µl of substrate solution (TMB substrate) was added to each well. The plate was re-incubated for 20 min at room temperature whilst avoiding exposure to direct light sources (see Fig. 2-5). The development of the standard and samples was checked and the reaction was stopped by adding 50 µl of stop solution to each well. The plate was tapped gently to ensure proper mixing. Upon stopping the reaction, standard dilution wells are expected to be linear (i.e. a clear gradient visible along different points of the dilution with the blank being colourless). The absorbance of

the plate was read at 450 nm using a microplate reader machine. When wavelength correction was available, the readings were taken at 540 nm or 570 nm; otherwise, readings were subtracted at 540 nm or 570 nm from the readings at 450 nm to correct optical imperfections within the plate. Thus, there is the possibility that the readings taken directly at 450 nm without correction were less accurate.

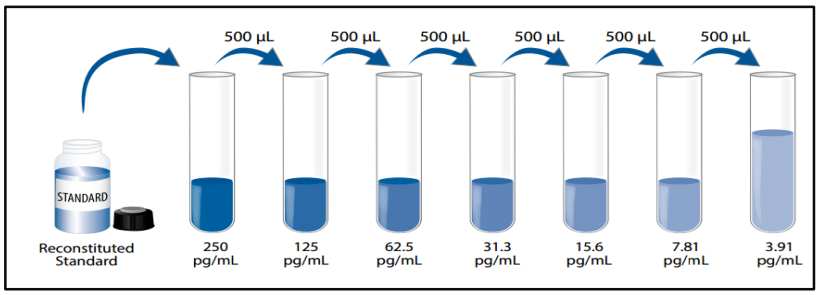

Figure 2-4. Standard dilution preparation of Solid Phase Sandwich ELISA experiment (195).

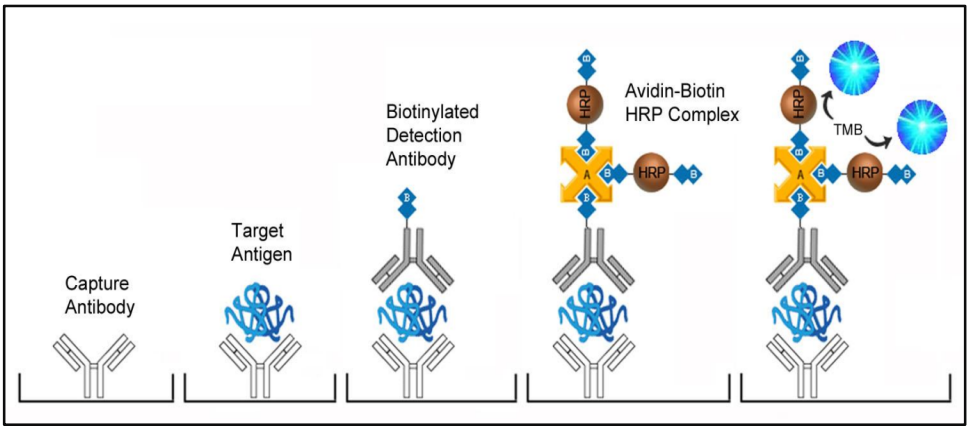

Figure 2-5. Assay summary of ELISA sandwich for IL-1β detection (195).

2.2.7 BD™ Cytometric Bead Array (CBA)

2.2.7.1 Supernatants/samples preparation

All solutions for this experiment were pre-warmed at 37°C for 30 min. These were kept in a laminar flow cabinet at 20-25°C until they were added to the cells. HPBMs were seeded equally in a 6-well multi-well plate (around 1,000,000 cells/well). Before commencing the procedure, all mediums were replaced with fresh media (e.g. 3 ml/well). The cells were pre-treated with the inhibitors (including DIDS, CFTR(inh)-172, PKI,

CsA, ESI-09, ESI-05 and BAPTA-AM) for 30 min, followed by LPS from *P. aeruginosa* (30 µg/ml) for 2 hours to prime the cells and provide the first signal. Subsequently, nigericin (10 µM) was added for 1 hour to provide the second signal and activate caspase-1 to release cytokines (in this case, IL-1β and TNF-α) (193, 194). Cells primed with LPS only and nigericin were used as a control. The supernatants were collected and then processed with CBA assay or stored at -80°C until the next usage.

2.2.7.2 BD™ reagents for the experiment

These reagents were used in this assay: human inflammatory cytokines PE detection reagent, human inflammatory cytokines standards, PE positive control detector, wash buffer (buffer reagents), assay diluent and serum enhancement buffer (196).

2.2.7.3 Culture supernatant CBA assay procedure

The human inflammation standards were reconstituted in assay diluent for 35 min and diluted with serial dilutions using assay diluent. This was mixed with 50 µl/test of human inflammation capture bead suspension. Standard dilutions and test samples were added to appropriate sample tubes (50 µl/tube). Subsequently, 50 µl of mixed beads were transferred to each assay tube for a 1 hour of incubation at room temperature and protected from light. After that, the PE detection reagent (50 µl/test) was also added and incubated for 2 hours at room temperature and protected from light. The samples were washed with 1 ml wash buffer and then centrifuged. Lastly, 300 µl of wash buffer was added to the assay tubes to allow analysis of the samples (Fig. 2-6).

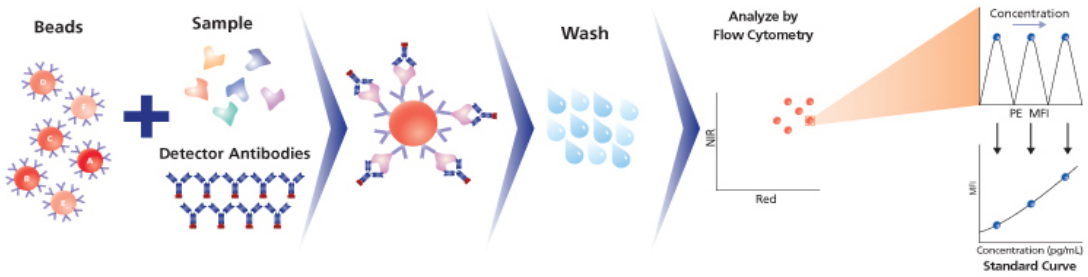

Figure 2-6. Cytometric beads array steps (196).

2.2.8 Phagocytosis and survival of *P. aeruginosa* assay

2.2.8.1 Seeding of THP-1 cell and MDMs

The media was pre-warmed to 37°C for at least 30 min and then the THP-1 cells were removed from the incubator and transferred into the cell culture cabinet under sterile conditions. The contents of each flask were transferred to a centrifuge tube and centrifuged at 200 × g for 5 min. Then, the cell pellet was re-suspended in RPMI-1640 media (+10% FBS) and the number of cells in each suspension was determined. The volume of cells and media required to obtain 400,000 cells per well (1 ml in each well) was calculated. PMA was then added to achieve a concentration of 200 nM in the cell suspension. After mixing thoroughly, 1 ml of cell suspension was transferred into each well of a 24-well plate. The plate was then incubated at 37°C, 5% CO_2 overnight. The media was removed and 1 ml PMA-free RPMI-1640 media (+10% FBS) was added then incubated again at 37°C, 5% CO_2 for 24 hours. For MDMs, freshly isolated HPBMs were seeded at 400,000 cells per well in a 24-well plate and incubated at 37°C for a period of 14 days before infection to allow complete differentiation into macrophages.

2.2.8.2 Set-up a *P. aeruginosa* bacterial culture

5 ml culture of bacteria (*P. aeruginosa* PAO1 strain provided by Dr. Mark Thomas) was prepared by transferring one bacterial colony into the 5 ml LB broth media. It was then incubated at 37°C, 5% CO_2 for 16-18 hours on the shaker at 250 rpm.

2.2.8.3 Phagocytosis of *P. aeruginosa* by PMA-treated monocytic THP-1 cells and MDMs cells

The plate of cells was transferred into the hood under sterile conditions. The media was removed from each well and 1 ml HBSS was added and then the plate was swirled before removing the liquid. This process was repeated once more. Afterwards, 500 µl of either media only or media containing CFTR(inh)-172 (10 µM), DIDS (500 µM),

CFTR(inh)-172 (10 µM) combined with DIDS (500 µM), CsA (1 µM), ESI-09 (25 µM) or ESI-05 (25 µM) was added to the corresponding well and incubated for 30 min at 37°C. Meanwhile, the bacteria were prepared for infection. The culture was removed from the incubator and placed on ice for 30 min. It was then centrifuged at 4,500 × g for 10 min at 4°C. The bacterial pellet was washed twice with PBS by decanting the supernatant and centrifuging at 4,500 × g for 10 min at 4°C. After washing, the pellet was re-suspended in 10 ml RPMI-1640 media to a colony-forming unit (CFU)/ml of ~3.5×10^8. This stock culture was used to prepare the required multiplicity of infection (MOI 10).

Then, 250 µl of MOI 10 bacterial suspension was added to each well. The plates were incubated on ice for 30 min to allow the bacteria to adhere to the cells and then transferred to a 37°C incubator for 2 hours to initiate internalisation. After incubation, the supernatants were collected, centrifuged at 13,000 rpm for 5 mins to pellet the bacteria, transferred to a fresh Eppendorf, and stored at -80°C for later use in ELISA assays. Infected cells were washed twice with 1 ml HBSS. Subsequently, 2 ml gentamicin (200 µg/ml) was added to each well. The plates were then incubated at 37°C for 60 min to kill the extracellular bacteria. The infected cells were then washed with 2 ml HBSS 3 times. After that, 500 µl of 2% saponin was added to each well and the plates incubated at 37°C for 13 min to lyse the cells and release the intracellular bacteria. PBS (500 µl) was added into each well and the cells were vigorously scraped whilst pipetting up/down to release the intracellular bacteria. Thereafter, 1:10 dilution of the lysate was prepared in 1× PBS. An agar plate was divided into 5 segments and 30 µl of each dilution was dropped on the surface. The plates were allowed to dry and incubated for 18 hours (Fig. 2-7).

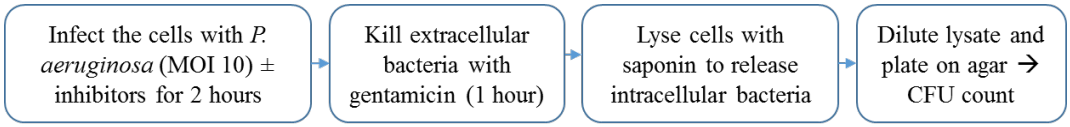

Figure 2-7. Steps to determine the effects of inhibitors on phagocytosis/engulfment.

2.2.8.4 Survival of phagocytosed *P. aeruginosa* in PMA-treated monocytic THP-1 cells and MDMs cells

The bacteria were prepared for infection as explained earlier (section 2.2.8.2). The plate of cells was then transferred to the hood under sterile conditions. The media was then removed from each well and 1 ml HBSS was added. It was then swirled before the liquid was removed. This step was repeated once more. 250 µl of MOI 10 bacterial suspension was added to each well. The plates were incubated on ice for 30 min then transferred to a 37°C incubator for 2 hours. After incubation, the bacteria were removed and the infected cells were washed with 1 ml HBSS, twice. After that, 2 ml gentamicin (200 µg/ml) was added to kill the extracellular bacteria. After incubation at 37°C for 60 min, the infected cells were washed twice with 2 ml HBSS and then 500 µl survival media was added to each well. Survival media was composed of RPMI-1640 medium + 1% FBS + 50 µg/ml gentamicin plus or minus (±) one of the inhibitors [CFTR(inh)-172 (10 µM), DIDS (500 µM), CFTR(inh)-172 (10 µM) + DIDS (500 µM), CsA (1 µM) or ESI-09 (25 µM)]. It was then incubated at 37°C for either 3 hours, 10 hours or 18 hours. The supernatants from each timepoint were centrifuged at 13,000 rpm for 5 mins to pellet any remaining bacteria, transferred to a fresh Eppendorf and stored at -80°C for later use in ELISA assays. The infected cells were washed three times with 1 ml HBSS. After this, 500 µl 2% saponin was added to each well and incubated at 37°C for 13 min to lyse the cells and release the intracellular bacteria. PBS (500 µl) was added into each well and the cells were vigorously scraped whilst pipetting up/down to release the intracellular bacteria. Thereafter, 1 in 10 dilutions was prepared of the lysate in 1× PBS. An agar plate was divided into 5 segments and 3 × 10 µl of each dilution (neat to 10^{-3}) was dropped on the surface. The plates were allowed to dry and transferred to an incubator for 18 hours (Fig. 2-8).

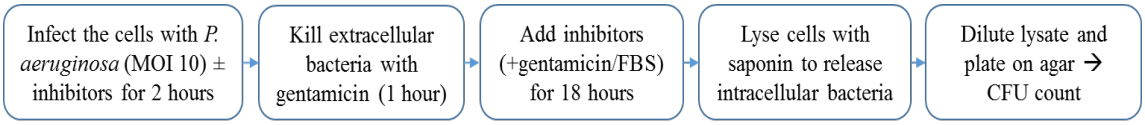

Figure 2-8. Steps to determine the effects of inhibitors on phagocytosed bacteria survival.

2.2.8.5 Colony-forming unit count

The number of colony forming units (CFU) was counted at a minimum of two dilutions. The number of viable intracellular bacteria was then determined using the following equation:

$$\boldsymbol{CFU\ (per\ ml) = average\ colony\ count \times \left(\frac{1}{0.01\ ml}\right) \times dilution\ factor}$$

2.2.9 Statistical analysis

Statistical analysis of obtained data was carried out using GraphPad Prism version 7. All data were analysed by *t*-tests and one-way analysis of variance (ANOVA) with Bonferroni correction to test for significance level. Statistically significant differences in tests were indicated for p value ≤ 0.05.

CHAPTER 3

The role of cAMP/PKA-regulated CaN in mediating Cl^- transport in immune cells

3 INTRODUCTION

CFTR protein is a type of ABC transporter on the apical side of the epithelial membrane and is instrumental in regulating biological processes like sweating saliva, secretion and tear production (197). Almost all known functions of CFTR are cAMP dependent, possibly due to its interaction with different proteins such as the PDZ motif containing proteins known to be phosphorylated by PKA (198, 199). The mechanism of action of CFTR in terms of ion transportation has been suggested to be largely dependent on its insertion and removal from the cell membrane. This activity has been associated with its interaction with PDZ proteins (200). Ion transport through CFTR and its regulated channel, ORCC, is known to be facilitated by CFTR interaction with other proteins such as AnxA2 and S100A10, forming a multiprotein complex that requires PKA and CaN-like phosphatse activity. Formation of this multiprotein complex is known to be crucial for CFTR functions, among which is the regulation of CFTR Cl^- transport. It has been found that attenuation of the multiprotein complex formation by specific pharmacologic agents, such as PKA inhibitors and CaN inhibitors, abrogates CFTR function (44). Interestingly, it has been demonstrated that F508Δ-CFTR cannot form this multiprotein complex (172), implicating the complex in CF development. S100A10 and AnxA2 interaction is known to be stabilised by forskolin (FSK)-induced dephosphorylation of AnxA2 by a CaN-like phosphatase to cause release of von Willibrand factor (vWF) and induced exocytosis of Weibel-Palade bodies (WPB) (201). Furthermore, exocytosis of WPB is the initiating factor for repair in endothelial cells in response to inflammation and vascular damage (202, 203). Thus, CFTR may also play a role in the vascular repair system when in association with AnxA2, CaN and S100A10. As such, dysfunction in the formation of this complex may hinder CFTR function and may also contribute to adverse conditions seen in CF.

As stated earlier, abrogation of S100A10 and AnxA2 interaction has been shown to interrupt CFTR function. This is likely due to inhibition of the formation of an S100A10/AnxA2/CFTR multiprotein complex. Since CaN is known to form a multiprotein complex with CFTR, its interaction with S100A10 and AnxA2 may have consequences for CFTR function such as affecting the regulation of CFTR Cl^- transport. Although the formation of an S100A10/AnxA2/CFTR multiprotein complex has been demonstrated in airway bronchial epithelial cell lines with a possible role in a CaN like phosphatase (45), there is currently no evidence for the role of CaN in the formation of this complex nor of its potential effects on CFTR function in immune cells.

3.1 AIMS OF THE STUDY

On the basis of the current state of knowledge in the field, this study aims to confirm the formation of a CFTR multiprotein complex involving S100A10, AnxA2 and CaN in PMA-treated monocytic THP-1 cells and HPBMs. Further, we studied whether the formation of this complex has any effect on the functioning of CFTR mediated Cl^- flux.

3.2 CONFIRMATION OF CaN, S100A10 AND AnxA2 IN 16HBE14o$^-$, PMA-TREATED MONOCYTIC THP-1 CELLS AND HPBMs

The secretory complex involving CaN, S100A10, AnxA2 and CFTR has been shown to play an important role in Cl^- flux in airway epithelia and endothelial cells (204, 44). This study confirms the expression and function of the proteins involved in the secretory complex S100A10-AnxA2 and CaN in PMA-treated monocytic THP-1 cells and HPBMs. The 16HBE14o$^-$ cell line was used as a positive control.

16HBE14o$^-$ and THP-1 cell lines were cultured until an approximate 80-90% confluence level before being harvested according to the process outlined in the methods chapter (2, section 2.2.1). Primary cells separated from whole blood (see chapter 2, section 2.2.1.1) were seeded in a T-75 flask. Following isolation and prior to their differentiation into macrophages, HPBMs gradually attached themselves to the plate bottom and were then ready to use within 2-3 days (205). HPBMs were not used directly after isolation as they would have been contaminated with other blood cells types such as lymphocytes. As such, aspiration of the media and washing after 2 hours of isolation was done to leave only adherent monocytes behind. The cells were harvested as described in chapter 2, section 2.2.1. Western blot analysis of lysates from 16HBE14o$^-$, PMA-treated monocytic THP-1 cells and HPBMs confirmed the expression of all the target proteins: CaN band was confirmed in the blots around 60-62 kDa (Fig. 3-1A). As expected, AnxA2 and S100A10 bands were also observed around 36 kDa and 11 kDa, respectively, in 16HBE14o$^-$, PMA-treated monocytic THP-1 cells and HPBMs (see Fig. 3-1B and C). Interestingly, probable isoforms of CaN in PMA-treated monocytic THP-1 cells and HPBMs were also observed. As seen in Fig. 3-1A, one band is visible around 60 kDa in 16HBE14o$^-$ cell lines while 2 bands are visible in PMA-treated monocytic THP-1 cells and HPBMs.

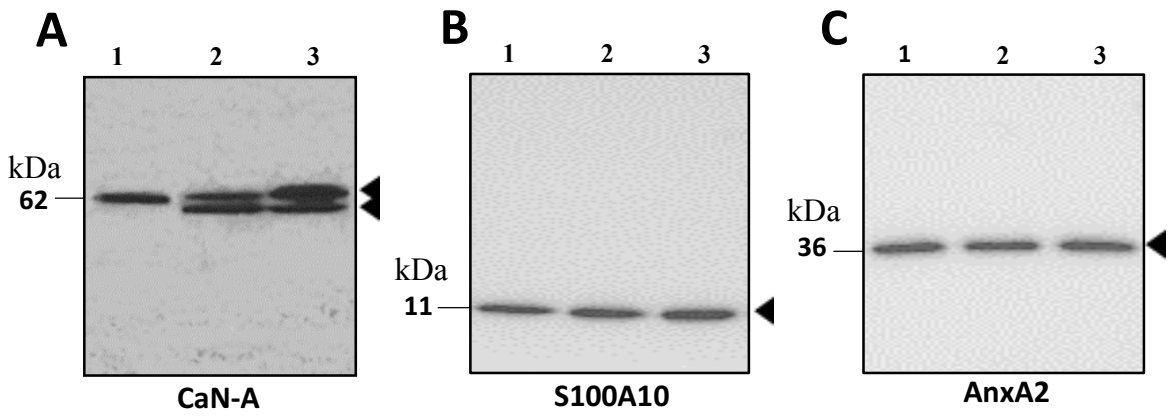

Figure 3-1. Western blot analysis of CaN, AnxA2 and S100A10 expression in 16HBE14o$^-$ cell lines, PMA-treated monocytic THP-1 cells and HPBMs.

16HBE14o$^-$ cells **(1)**, PMA-treated monocytic THP-1 cells **(2)** and HPBMs **(3)** were assessed for the expression of CaN **(A)**, S100A10 **(B)** and AnxA2 **(C)** proteins with western blotting. Lysates (100 μg) from cells harvested at 90% confluence and subjected to SDS-PAGE were resolved on either 10-12% gel for CaN or 15% gel for S100A10 and AnxA2, followed by transfer onto a PVDF membrane. The membrane blots were probed with anti-CaN (1:500) polyclonal antibody, anti-S100A10 (1:1000) and anti-AnxA2 (1:1000) monoclonal antibodies. The CaN band appeared at 62 kDa in 16HBE14o$^-$, but two bands were observed around the same size in PMA-treated monocytic THP-1 cells and HPBMs. In addition, S100A10 and AnxA2 were observed in all cells at 11 kDa and 36 kDa, respectively. (n=7)

3.3 Investigation of the potential interaction between AnxA2, S100A10 and CaN proteins in PMA-treated monocytic THP-1 cells

It has been previously demonstrated in 16HBE14o$^-$ cell lines that AnxA2, S100A10 and CaN proteins exist in complexes (44). This study confirms the expression of AnxA2, S100A10 and CaN in 16HBE14o$^-$ cells, PMA-treated monocytic THP-1 cells, and HPBMs. This suggests that the cAMP/PKA-dependent regulation of CaN and complex formation exists in monocytes, as seen in 16HBE14o$^-$. Since this interaction has been demonstrated to be enhanced or initiated in response to an increase in cAMP intracellular levels (44), the cells were treated with 10 μM of FSK and 100 μM of 3-isobutyl-1-methylxanthine (IBMX) to induce cAMP/PKA-dependent signalling in order to investigate the interactions between cAMP/PKA-dependent CaN, AnxA2 and S100A10. Protein kinase A inhibitor (PKI) was used (at 100 nM) to inhibit PKA to determine the role of PKA in complex formation.

Therefore, immunoprecipitation of AnxA2 and S100A10 in 16HBE14o$^-$ cell lines and PMA-treated monocytic THP-1 cells was carried out. The results displayed in Fig. 3-2 show co-immunoprecipitation of AnxA2 and S100A10, suggesting the likelihood of an interaction between the targeted proteins in both cell types. This conclusion is specifically based on the observation of bands around 62 kDa and 19 kDa corresponding to molecular weights of A and B subunits of CaN, respectively. This confirms that S100A10 interacts with CaN at the CaN-A subunit while AnxA2 does so at the CaN-B subunit.

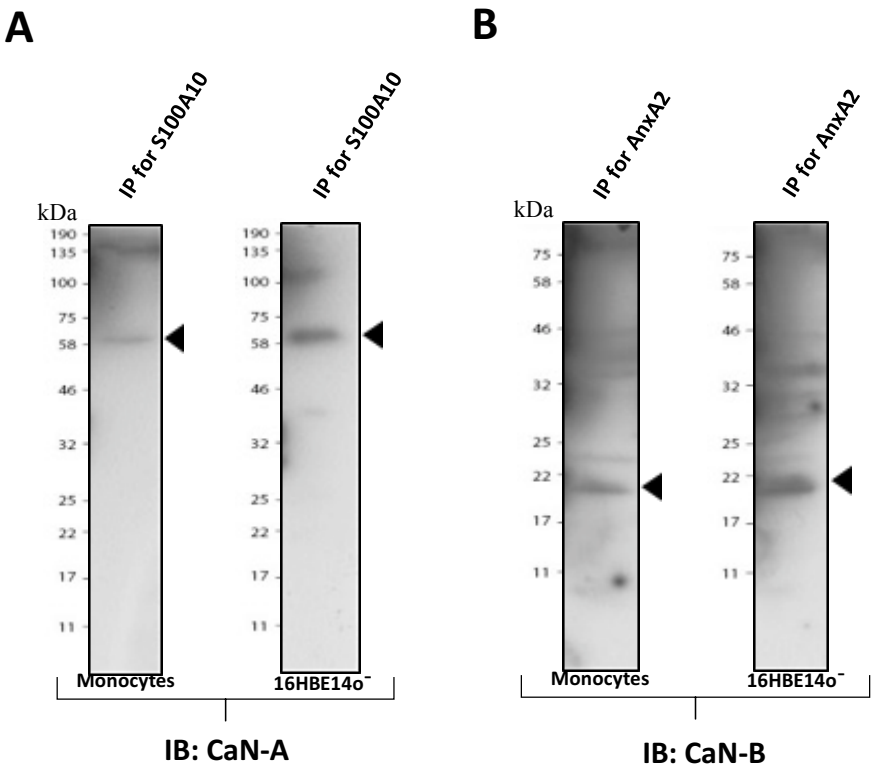

Figure 3-2. Western blot analysis of CaN in immunoprecipitation of S100A10 and AnexA2 in 16HBE14o⁻ and PMA-treated monocytic THP-1 cells in response to cAMP/PKA activities.

Cell lysates from 16HBE14o⁻ and PMA-treated monocytic THP-1 were incubated in IP beads premixed with 10 µl of **(A)** primary anti-S100A10 probed with anti-CaN-A antibody and **(B)** primary anti-AnxA2 antibody probed with anti-CaN-B antibody. (n=3)

3.4 FURTHER CONFIRMATION OF ANXA2-S100A10 AND CAN INTERACTION IN PMA-TREATED MONOCYTIC THP-1 CELLS.

Following initial confirmation of AnxA2 and S100A10 co-immunoprecipitation with CaN, the finding was validated using reverse immunoprecipitation. To do this, PMA-treated monocytic THP-1 cells were treated as described previously and the lysate collected was subjected to immunoprecipitation using anti-CaN antibody to immunoprecipitate AnxA2 or S100A10 (see Fig. 3-3). As a control, untreated THP-1 monocytes cells lysate was subjected to immunoprecipitation since this interaction had been previously confirmed in 16HBE14o$^-$ cells that were also untreated (44). The results indicated that exposure of PMA-treated monocytic THP-1 cells to PKI alone (an inhibitor of PKA) caused no interaction between either CaN and S100A10 or CaN and AnxA2. However, exposure of the cell to both PKI and FSK/IBMX caused weak interaction between AnxA2 and CaN only, and exposure to FSK/IBMX alone caused strong interaction between both S100A10 and AnxA2 with CaN. In the control unexposed PMA-treated monocytic THP-1 cells, there was no interacion between CaN and any AnxA2 and S100A10 even though CaN expression was confirmed by blotting the lystae with anti-CaN antibody. CaN expression was also confirmed in the lysate blot using CaN for PMA-treated monocytic THP-1 cells exposed to PKI and/ or FSK/IBMX. Findings here strongly suggests that interaction between S100A10 and CaN may be independent of PKA but dependent on cAMP signalling and that CaN and AnxA2 interaction is only dependent on cAMP/PKA signalling.

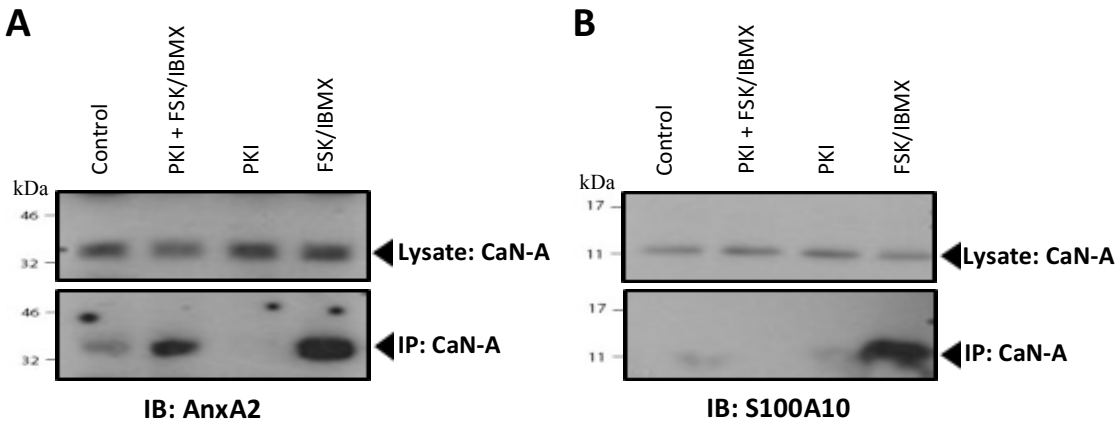

Figure 3-3. Western blot analysis for S100A10 and AnxA2 in immunoprecipitation of CaN in PMA-treated monocytic THP-1 cells in response to PKA activity.

PMA-treated monocytic THP-1 cells were treated as follows: an untreated (control) batch, a batch treated with FSK (10 μM) / IBMX (100 μM) for 30 min, a batch treated with PKI (100 nM) for 5 min, a batch with both PKI (100 nM) for 5 min and FSK (10 μM)/IBMX (100 μM) for 30 min. 1 mg of lysate was used for immunoprecipitation of CaN-A. The blots containing the CaN-A were immunoblotted with **(A)** anti-AnxA2 antibody as a control, and **(B)** anti-S100A10 antibody. Membranes A and B were developed using enhanced chemiluminescence (ECL) reagent and film. (n=4)

3.5 ACTIVATION OF cAMP/PKA PLAYS A ROLE IN S100A10, ANXA2 AND CaN INTERACTION AND THE FUNCTIONING OF Cl^- CHANNELS

After concluding that there is a strong likelihood of interaction between AnxA2, S100A10 and CaN, an investigation of the effects of this interaction on CFTR-mediated ion currents in monocytes was conducted. This was based on the proposition of Borthwick et al. (44) and Muimo (54) based on their studies of airway epithelia that CFTR interaction with AnxA2 and S100A10 requires a CaN-like phosphatase activity. Thus, these initial studies were designed to replicate the observed effect of the AnxA2, S100A10 and CaN interaction on outwardly rectifying chloride channels (ORCC) and CFTR-mediated Cl^- movement in 16HBE14o$^-$ (control cell line) and then in monocytes. The cells were stimulated with FSK (10 μM) and IBMX (100 μM) for 30 min to activate Cl^- channels through the cAMP/PKA pathway as the combination of FSK/IBMX is known to raise the cAMP levels in cells (206). In turn, CaN pathways and cAMP activation of PKA may subsequently activate Cl^- channels. To confirm whether the combination of FSK/IBMX activates Cl^- transport, whole cells records showed DIDS and CFTR(inh)-172-sensitive currents upon exposure of the cells to DIDS, a non-selective ion channel blocker, followed by CFTR(inh)-172, a specific inhibitor for CFTR channels.

The ion current across the cell was recorded as indicated in Fig. 3-4. 16HBE14o$^-$ exposed to DIDS (500 μM) evidenced a significantly lower inward and outward conducting current compared to control unexposed monocytes. In addition to this, the current was also outwardly rectifying. It was found that exposure of 16HBE14o$^-$ cells to CFTR(inh)-172 (10 μM) significantly inhibited inward and outward conducting Cl^- currents compared to whole cell currents recorded when exposed to DIDS only, suggesting that ORCC and CFTR are both involved in the mediation of Cl^- currents in 16HBE14o$^-$.

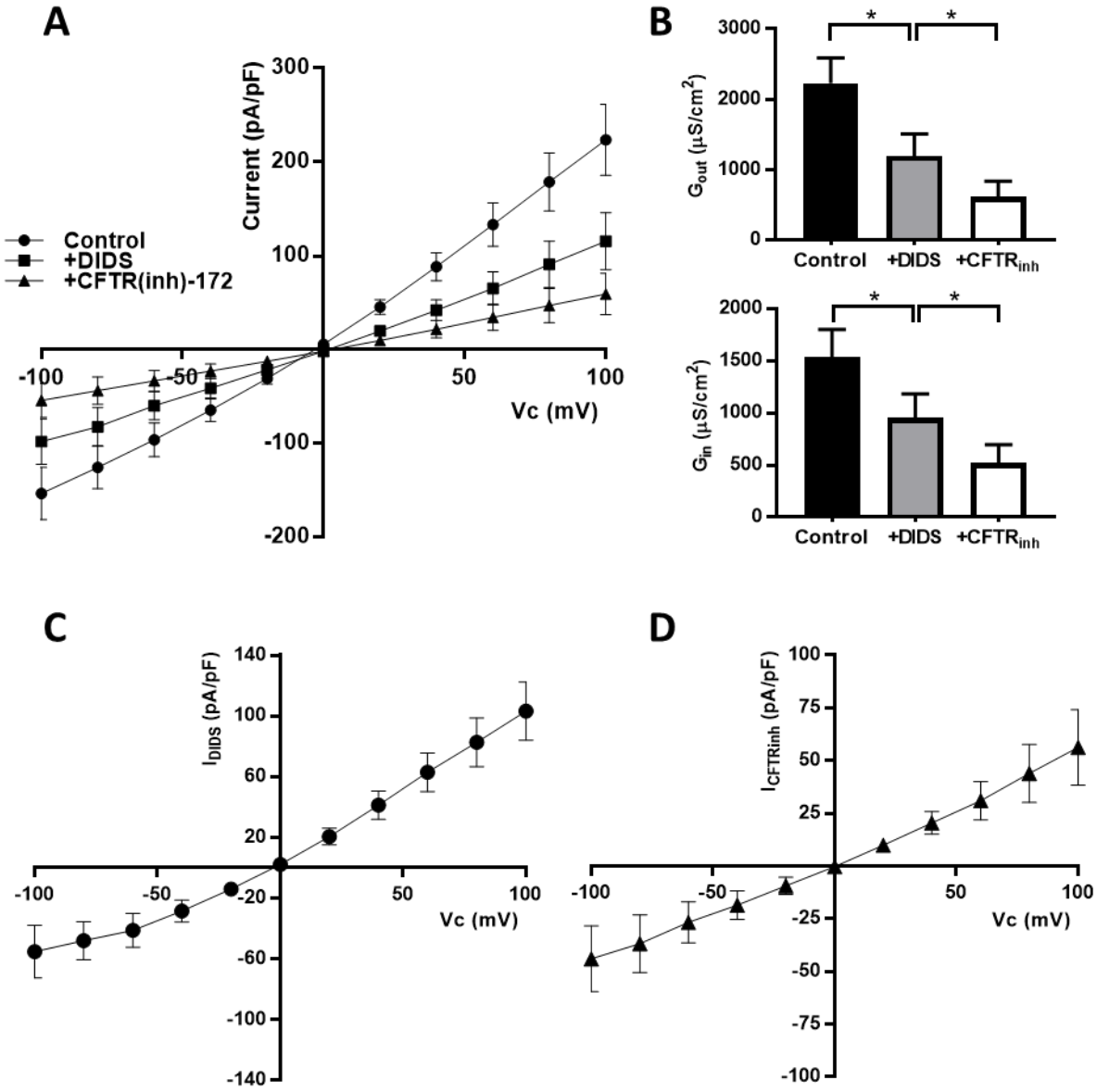

Figure 3-4. DIDS and CFTR(inh)-172 inhibited Cl^- flux in 16HBE14o$^-$ cell lines stimulated with FSK/IBMX.

Whole cell currents recorded from human bronchial epithelial cell line 16HBE14o$^-$ pre-incubated with FSK (10 µM) and IBMX (100 µM) for 30 min to activate DIDS-sensitive Cl^- channels (ORCC) and CFTR channels through the cAMP/PKA pathway. **(A)** Circles on the I-V curve signify currents recorded under control conditions. Squares signify currents remaining after the addition of DIDS (500 µM). Triangles signify current recorded in the presence of CFTR(inh)-172 (10 µM). **(B)** Indicates the mean G_{out} and G_{in} under control conditions, and in the presence of DIDS and presence of CFTR(inh)-172. The I-V curve **(C)** indicates the DIDS-sensitive outwardly-rectifying currents (I_{DIDS}), and **(D)** shows the ohmic CFTR currents ($I_{CFTRinh}$). Data are presented as mean ± SEM. (n=13). * indicates a significant difference.

3.6 PMA-UNSTIMULATED THP-1 CELL LINE DOES NOT EXPRESS S100A10

In present study, the THP-1 cell line used in investigating the potential interaction between S100A10 and CaN was briefly stimulated with PMA to induce mature monocytic phenotype (see chapter 2, section 2.2.1.4 for details). As a control, the same experiment was conducted on unstimulated THP-1 cell lines. As shown in Fig. 3-5, western blot analysis indicated that unstimulated THP-1 cells do not express S100A10 while PMA-treated THP-1 monocytic cells and 16HBE14o$^-$ cell lines do express the protein. This suggests that interaction between S100A10 and CaN is not possible in PMA-unstimulated THP-1 cell lines. A patch clamp measurement was also recorded of FSK/IBMX-stimulated Cl^- flux across unstimulated THP-1, both in the presence and absence of DIDS and CFTR(inh)-172 (Fig. 3-6). The findings showed no Cl^- flux through the THP-1 cells, suggesting dysfunctional Cl^- transport. To confirm equal protein loading, western blots containing lysates from each cell type were probed for β-actin. β-actin is a known housekeeping gene ubiquitously expressed in almost all cell types (207).

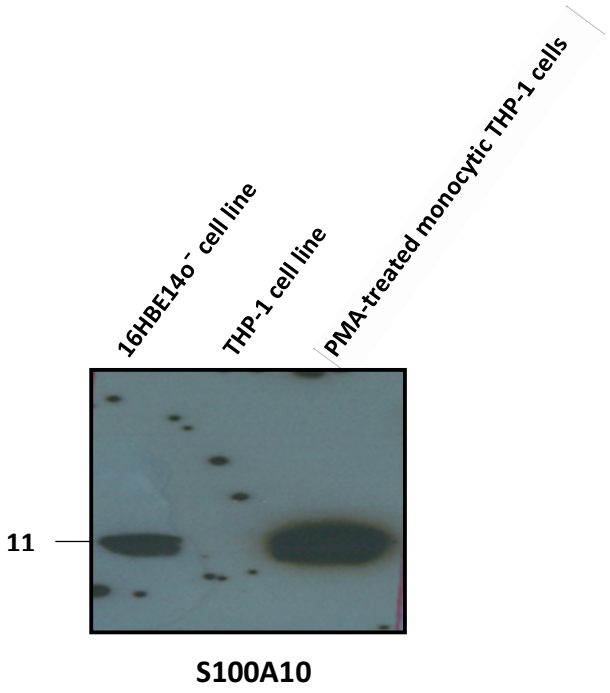

Figure 3-5. Western blot analysis of S100A10 in 16HBE14o⁻ cell lines, THP-1 cell lines and PMA-treated monocytic THP-1 cells.

16HBE14o⁻ cells, THP-1 cell and PMA-treated monocytic THP-1 cells were assessed for the presence of S100A10 proteins by western blotting. Lysates (100 μg) from cells harvested at 90% confluence and subjected to SDS-PAGE were resolved on 15% gel, followed by transfer onto a PVDF membrane. The membrane blots were probed with anti-S100A10 (1:1000) monoclonal antibodies. The S100A10 band is shown at 11 kDa in 16HBE14o⁻. Additionally, a band was observed of approximately the same size in PMA-treated monocytic THP-1 cells. Remarkably, the undifferentiated THP-1 cell line was found not to express S100A10 (n=4). To confirm protein loading, western blots containing lysates from each cell type were probed for β-actin (data not shown).

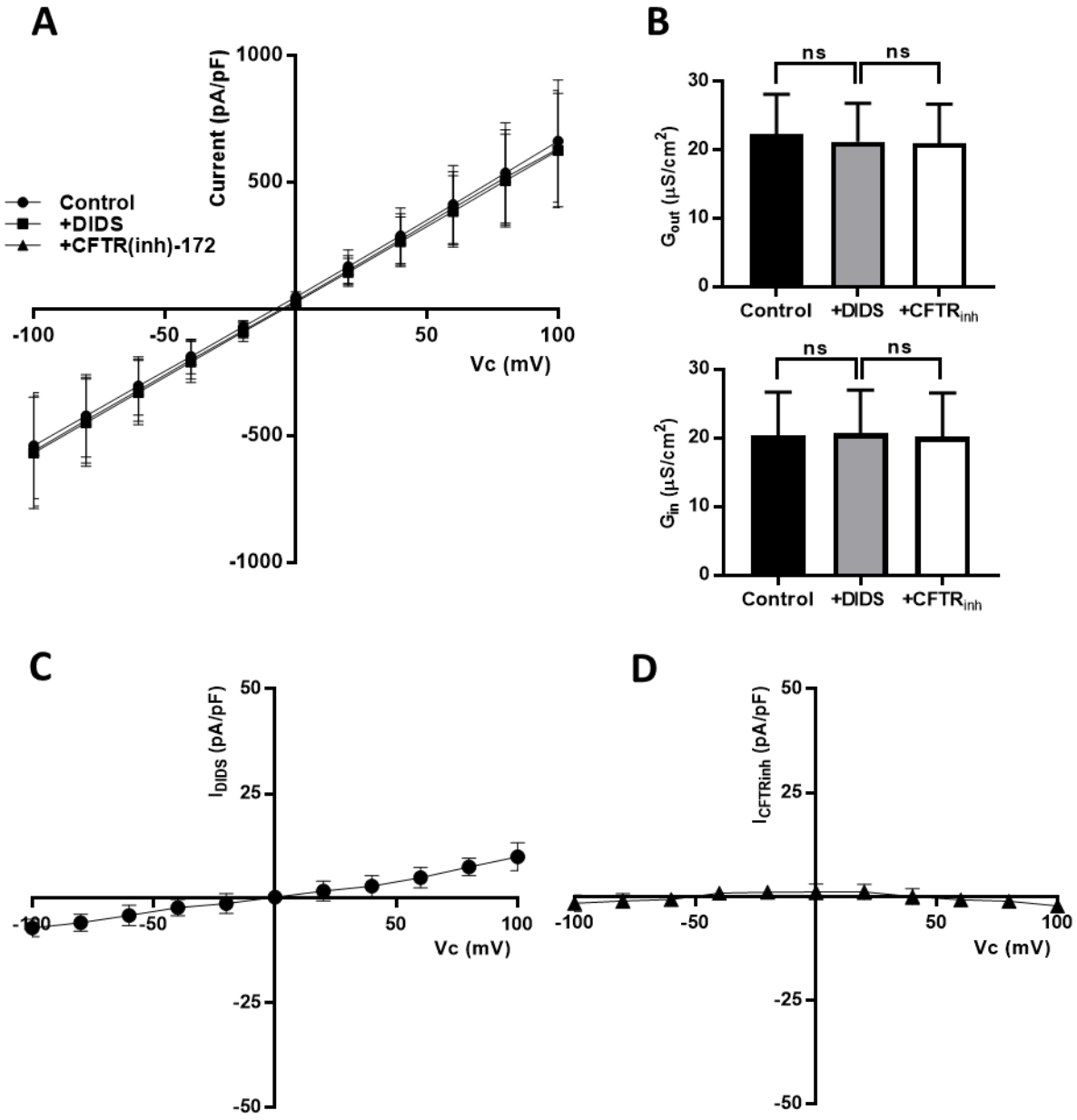

Figure 3-6. Non-effect of DIDS and CFTR(inh)-172 on undifferentiated THP-1 cells line pre-stimulated with FSK/IBMX.

Whole cell currents recorded from THP-1 cell lines pre-incubated with forskolin (10 µM) and IBMX (100 µM) for 30 min to activate DIDS-sensitive Cl^- channels (ORCC) and CFTR channels. **(A)** Circles on the I-V curve signify currents recorded under control conditions. Squares signify currents recorded in the presence of DIDS (500 µM). Triangles signify currents recorded in the presence of CFTR(inh)-172 (10 µM). **(B)** Indicated the mean G_{out} and G_{in} under control conditions, in the presence of DIDS, and the presence of CFTR(inh)-172. The I-V curve **(C)** shows the lack of DIDS-sensitive currents (I_{DIDS}). **(D)** shows the lack of CFTR(inh)-172-sensitive currents ($I_{CFTRinh}$). Data are presented as mean ± SEM. (n=20). ^{ns} indicates a non-significant difference.

After showing that inhibition of CFTR and DIDS-sensitive ORCC by CFTR(inh)-172 (10 μM) and DIDS (500 μM) respectively resulted in a drop in ion currents mediated by the Cl^- channels in 16HBE14o$^-$ as a control cells, PMA-treated monocytic THP-1 cells pre-exposed to 0.2% DMSO without FSK (10 μM)/IBMX (100 mM) stimulation were investigated. The cells were exposed to DIDS (500 μM) followed by CFTR(inh)-172 (10 μM), as done previously for 16HBE14o$^-$ cells, and the Cl^- current across the cell membrane was recorded and analysed. This was done to establish the basal effect of DIDS or CFTR(inh)-172 exposure on the Cl^- current conductance independent of FSK (10 μM) and IBMX (100 μM) activities. As a result, it was found that exposure of the PMA-treated monocytic THP-1 cells line to either of DIDS or CFTR(inh)-172 had no significant effect on both the outward and inward conductance (Fig. 3-7). Because of the low Cl^- current conductance in FSK (10 μM) and IBMX (100 μM) unstimulated PMA-treated monocytic THP-1 cell lines, this finding suggests very low or no active Cl^- channels in absence of cAMP stimulation.

The PMA-treated monocytic THP-1 cells were then stimulated with FSK (10 μM)/IBMX (100 mM) prior to exposure to DIDS (500 μM) and CFTR(inh)-172 (10 μM) to evaluate the impact of FSK/IBMX on the Cl^- channel's function. As shown in Fig. 3-8, PMA-treated monocytic THP-1 cells exposed to FSK/IBMX showed significant DIDS-sensitive outwardly rectifying currents. In addition, it was found that exposure to CFTR(inh)-172 further inhibited inward and outward conducting Cl^- currents, suggesting that cAMP-stimulated ORCC and CFTR played a major role in mediating Cl^- currents in PMA-treated monocytic THP-1 cells, as seen in 16HBE14o$^-$.

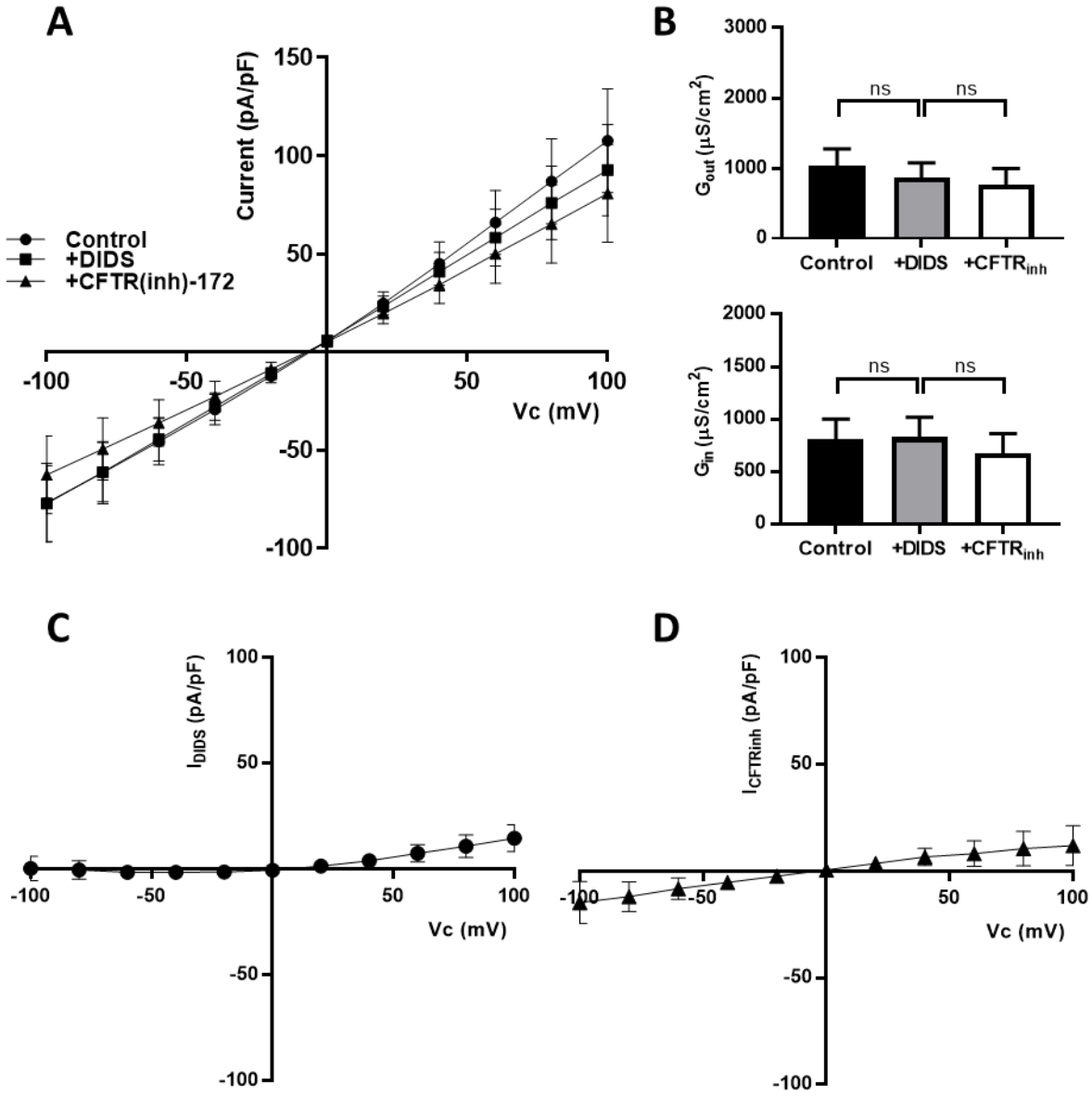

Figure 3-7. Non-effect of DIDS and CFTR(inh)-172 on PMA-treated THP-1 cells pre-incubated with vehicle (0.2% DMSO).

Whole cell currents recorded from PMA-treated THP-1 cell pre-incubated in vehicle without any stimulus for 30 min to study the activity of DIDS-sensitive Cl^- channels (ORCC) and CFTR channels under basal conditions. **(A)** Circles on the I-V curve signify currents recorded under control conditions. Squares signify currents recorded in the presence of DIDS (500 µM). Triangles signify currents recorded in the presence of CFTR(inh)-172 (10 µM). **(B)** Indicated the mean G_{out} and G_{in} under control conditions, in the presence of DIDS, and the presence of CFTR(inh)-172. The I-V curve **(C)** shows the lack of DIDS-sensitive currents (I_{DIDS}), and **(D)** shows the lack of CFTR(inh)-172-sensitive currents ($I_{CFTRinh}$). Data are presented as mean ± SEM. (n=10). ^{ns} indicates a non-significant difference.

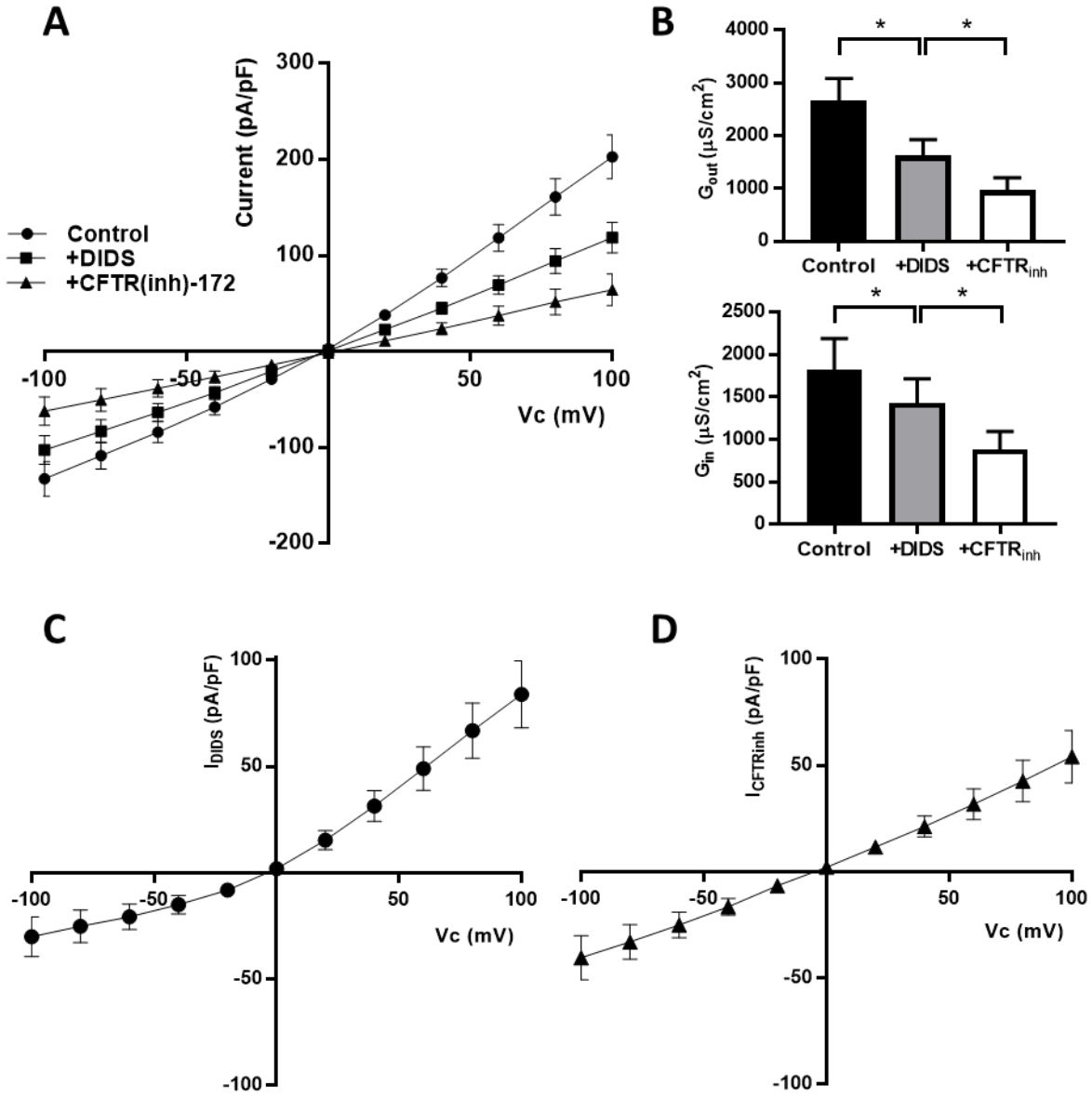

Figure 3-8. DIDS and CFTR(inh)-172 inhibited Cl^- flux in PMA-treated THP-1 cells stimulated with FSK/IBMX.

Whole cell currents recorded from PMA-treated THP-1 cell pre-incubated with FSK (10 µM) and IBMX (100 µM) for 30 min to activate DIDS-sensitive Cl^- channels (ORCC) and CFTR channels. **(A)** Circles in the I-V curve signify currents recorded under control conditions. Squares signify currents remaining after the addition of DIDS (500 µM). Triangles signify current remaining after the addition of CFTR(inh)-172 (10 µM). **(B)** Indicates the mean G_{out} and G_{in} under control conditions, in the presence of DIDS, and the presence of CFTR(inh)-172. The I-V curve **(C)** shows the DIDS-sensitive outwardly-rectifying currents (I_{DIDS}), and **(D)** shows the ohmic CFTR currents ($I_{CFTRinh}$). Data are presented as mean ± SEM. (n=18). * indicates a significant difference.

Up to this point, the findings of this current study have shown that FSK (10 μM)/IBMX (100 μM) stimulated ion currents are inhibited by 10 μM of CFTR(inh)-172 and 500 μM of DIDS in both 16HBE14o$^-$ and PMA-treated monocytic THP-1 cells. Moreover, the effect of PKA inhibition on Cl^- flux was investigated. PMA-treated monocytic THP-1 cells were pre-exposed to PKI (100 nM) to inhibit cAMP/PKA signalling activities then exposed to FSK/IBMX, as previously stated. On the basis of this experimentation, it was concluded that PKA is involved in FSK/IBMX activation and ion current conductance across the cells. Fig. 3-9 shows that PKI (100 nM)/FSK (10 μM) and IBMX (100 μM) exposure resulted in very low inward and outward Cl^- current conductance in PMA-treated monocytic THP-1 cells. DIDS and CFTR(inh)-172-sensitive currents were similar in the presence of PKI. However, inhibition of PKA by PKI or ORCC, and CFTR by DIDS and CFTR(inh)-172, respectively, resulted in reduction of Cl^- currents. This is clear evidence of PKA involvement in the regulation of Cl^- channels.

In the same manner as with PKI, the cells were pre-exposed to CsA (1 μM) (an inhibitor of CaN) to evaluate whether CaN affects the regulation of ion current through Cl^- channels. Fig. 3-10 shows that pre-treatment with CsA followed by FSK/IBMX resulted in very low inward and outward Cl^- current conductance in PMA-treated monocytic THP-1 cells. DIDS and CFTR(inh)-172-sensitive currents were similar in the presence of CsA. However, inhibition of CaN by CsA or ORCC, and CFTR by DIDS and CFTR(inh)-172, respectively, resulted in reduction of Cl^- currents. This shows that CsA is involved in the regulation Cl^- channels.

An interesting finding is the fact that the ion currents recorded were lowest in cells exposed to PKI or CsA followed by FSK/IBMX compared to those stimulated with FSK/IBMX only. It should also be noted that no significant difference was found between currents recorded from PKI or CsA-exposed cells and the remaining currents after

exposure to a combination of CFTR(inh)-172 and DIDS. This indicates the crucial role of PKA and CaN in regulating CFTR and ORCC.

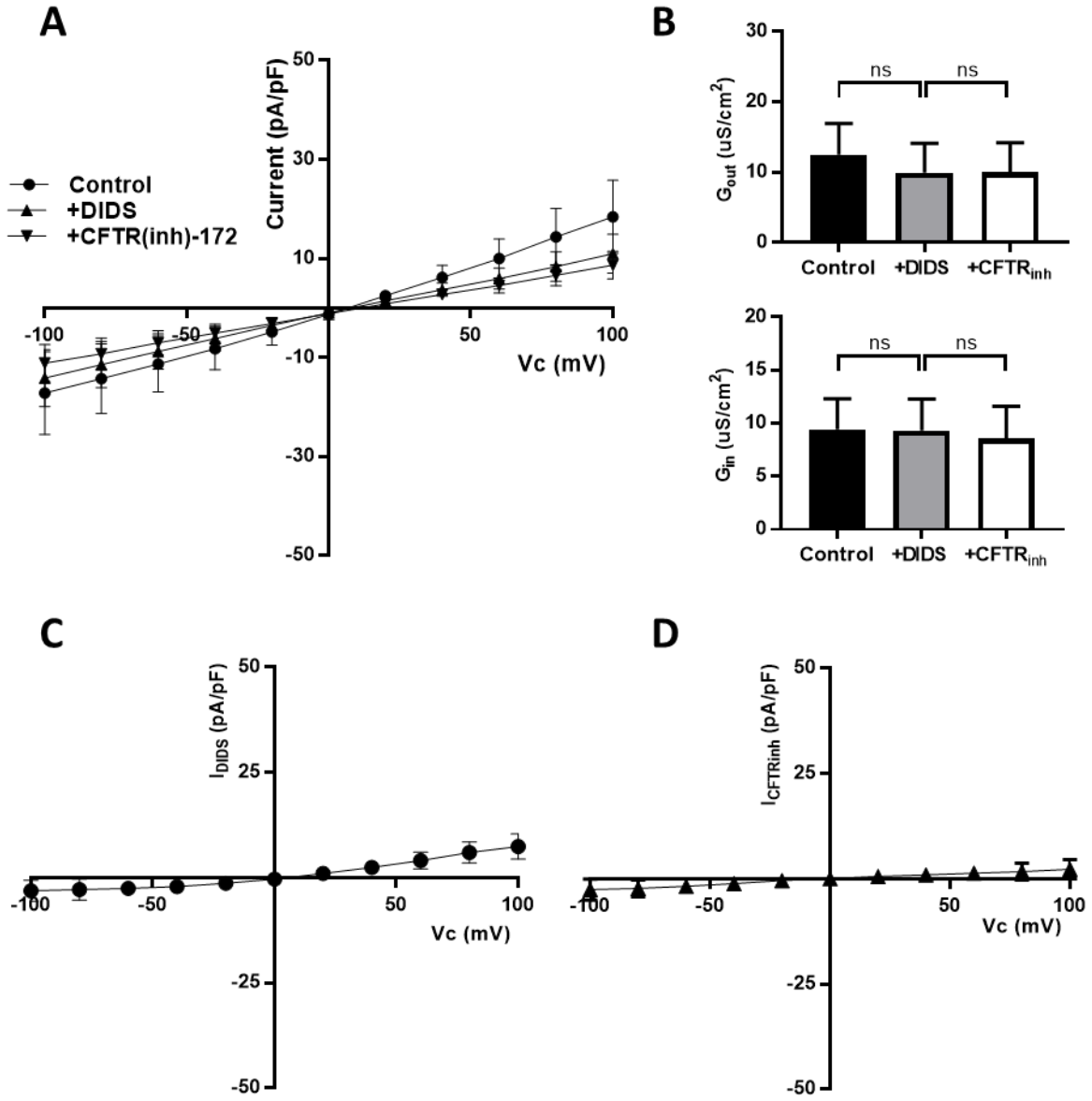

Figure 3-9. Lack of DIDS and CFTR(inh)-172 sensitive currents in PMA-treated THP-1 cells stimulated with PKI/FSK/IBMX.

Whole cell currents recorded from PMA-treated THP-1 cells pre-incubated with PKI (100 nM) for 30 min followed by incubation with FSK (10 μM), IBMX (100 μM) + PKI for 30 min to activate DIDS-sensitive Cl^- channels (ORCC) and CFTR channels. **(A)** Circles on the I-V curve signify currents recorded under control conditions. Squares signify currents recorded in the presence of DIDS (500 μM). Triangles signify current recorded in the presence of CFTR(inh)-172 (10 μM). **(B)** Indicates the mean G_{out} and G_{in} under control conditions, in the presence of DIDS, and in the presence of CFTR(inh)-172. The I-V curve **(C)** shows the lack of DIDS-sensitive currents (I_{DIDS}) and **(D)** shows the lack of CFTR(inh)-172-sensitive currents ($I_{CFTRinh}$). Data are presented as mean ± SEM. (n=10). ^{ns} indicates a non-significant difference.

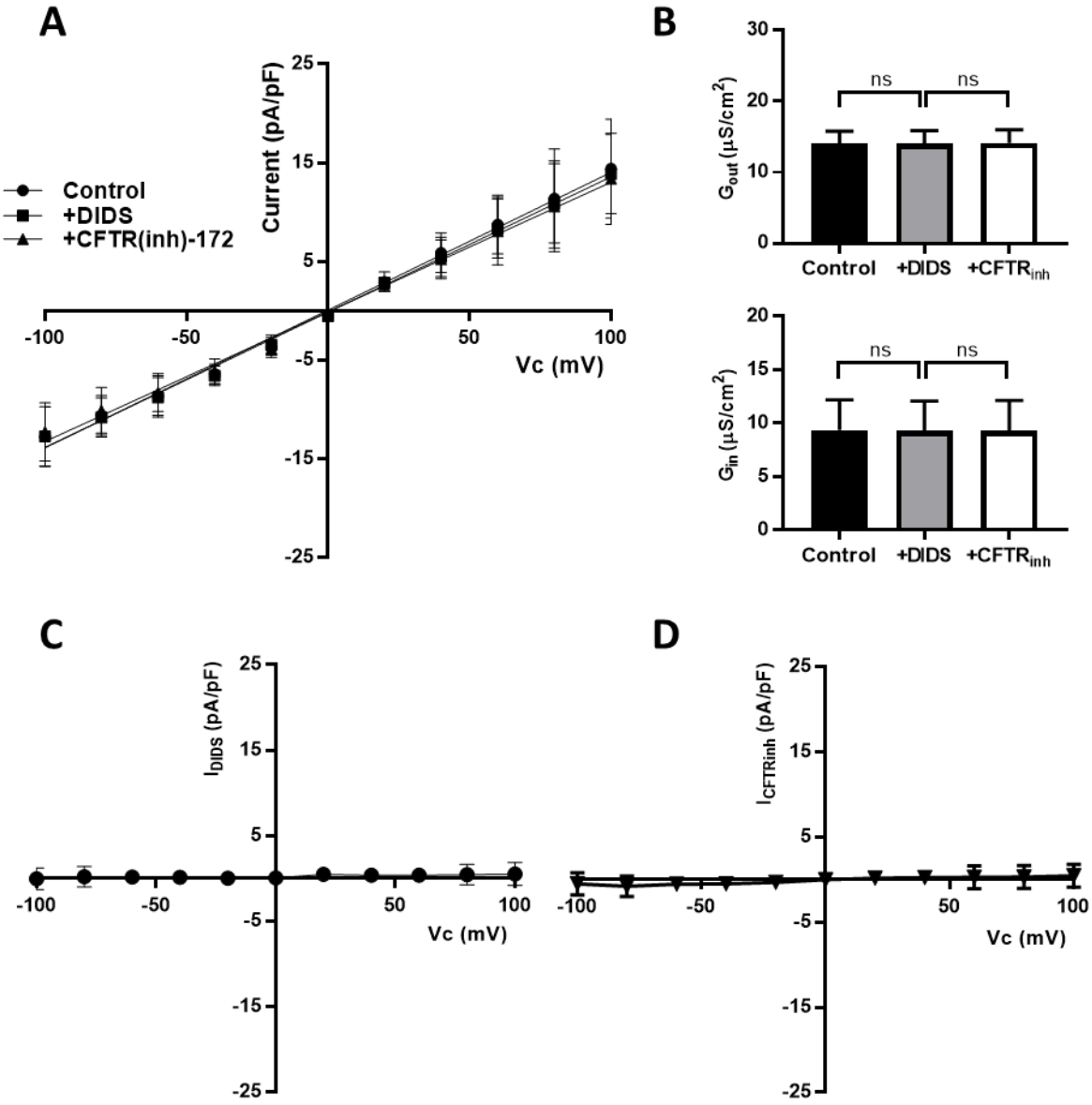

Figure 3-10. Lack of DIDS and CFTR(inh)-172-sensitive currents in PMA-treated THP-1 cells stimulated with CsA/FSK/IBMX.

Whole cell currents recorded from PMA-treated THP-1 cells pre-incubated with CsA (1 μM) for 30 min followed by incubation with FSK (10 μM), IBMX (100 μM) + CsA for 30 min to stimulate DIDS-sensitive Cl^- channels (ORCC) and CFTR channels. **(A)** Circles on the I-V curve signify currents recorded under control conditions. Squares signify currents recorded in the presence of DIDS (500 μM). Triangles signify current recorded in the presence of CFTR(inh)-172 (10 μM). **(B)** Indicates mean G_{out} and G_{in} under control conditions, in the presence of DIDS, and in the presence of CFTR(inh)-172. The I-V curve **(C)** shows the lack of DIDS-sensitive currents (I_{DIDS}), and **(D)** shows the lack of CFTR(inh)-172-sensitive currents ($I_{CFTRinh}$). Data are presented as mean ± SEM. (n=10). ^{ns} indicates a non-significant difference.

The findings presented in this chapter thus indicate that FSK/IBMX stimulates Cl^- current conductance in PMA-treated monocytic THP-1 cells, and that this Cl^- current is sensitive to DIDS (500 μM) and CFTR(inh)-172 (10 μM). Moreover, by using 100 nM of PKI or 1 μM of CsA, it has been confirmed in this current study that PKA and CaN play a role in FSK/IBMX stimulation of the Cl^- channels. An investigation into the effect of PKI, CsA, DIDS and CFTR(inh)-172 on HPBMs was also conducted to ascertain whether a difference occurs in their response compared to the PMA-treated monocytic THP-1 cells. The effect of DIDS (500 μM) and CFTR(inh)-172 (10 μM) exposure on FSK/IBMX stimulated ion current conductance was evaluated for HPBMs. The stimulated cells exposed to DIDS and CFTR(inh)-172 showed significantly lower inward and outward ion current conductance compared to the unexposed cells (see Fig. 3-11). In addition, pre-exposure of the cells to PKI or CsA also resulted in total reduction of FSK/IBMX-stimulated Cl^- currents, irrespective of whether the cells were exposed to DIDS/CFTR(inh)-172 (see Fig. 3-12 and Fig. 3-13). This may indicate that PKA and CaN are involved in the regulatory pathways of CFTR and ORCC. As observed for PMA-treated monocytic THP-1 cells, the Cl^- currents recorded were lower for all HPBMs in cells exposed to PKI or CsA compared to those that were only exposed to CFTR(inh)-172 and DIDS.

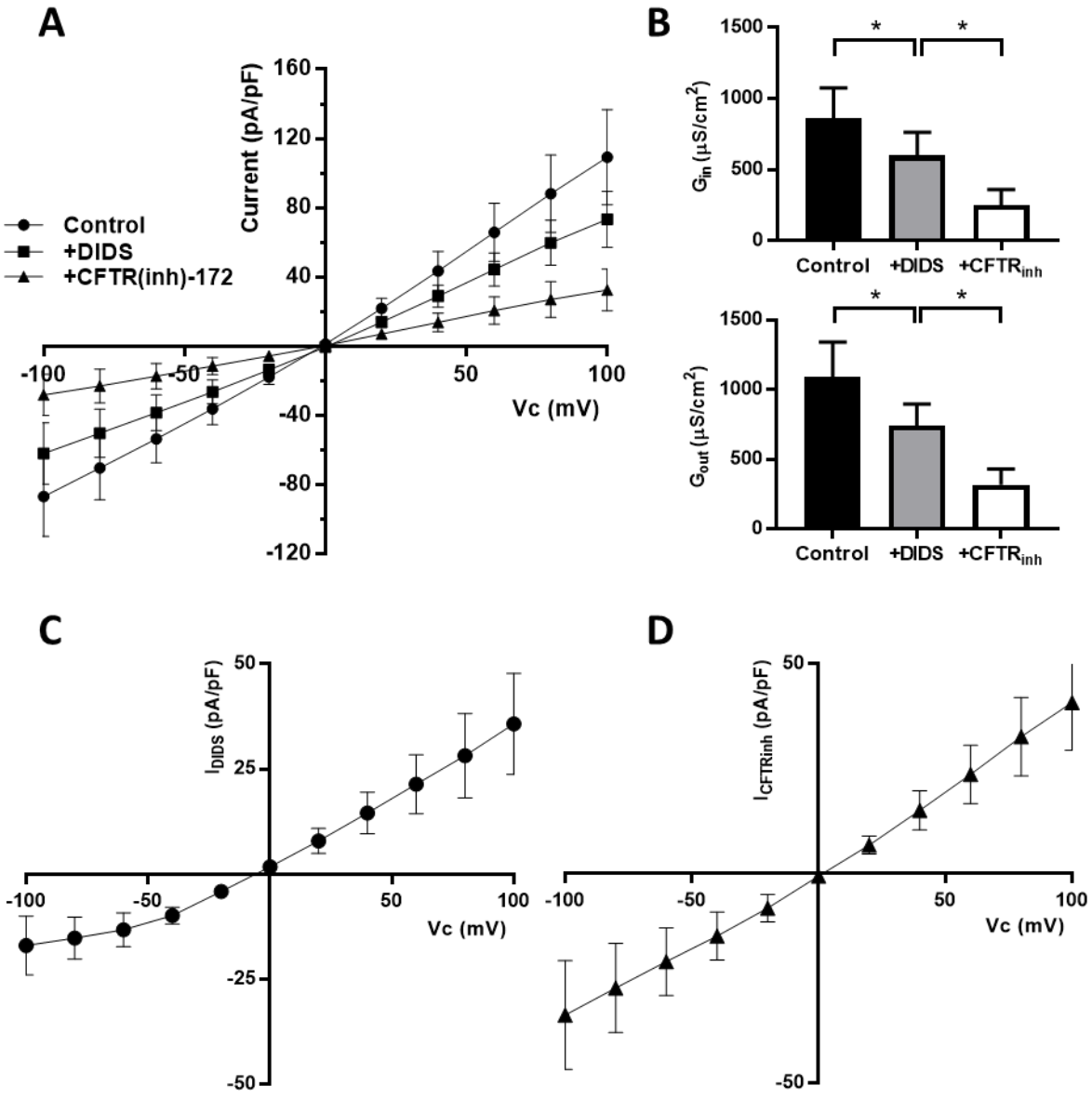

Figure 3-11. DIDS and CFTR(inh)-172-inhibited Cl^- flux in HPBMs stimulated with FSK/IBMX.

Whole cell currents recorded from HPBMs pre-incubated with FSK (10 µM) and IBMX (100 µM) for 30 min to activate DIDS-sensitive Cl^- channels (ORCC) and CFTR channels. **(A)** Circles on the I-V curve signify currents recorded under control conditions. Squares signify currents remaining after the addition of DIDS (500 µM). Triangles signify current remaining after the addition of CFTR(inh)-172 (10 µM). **(B)** Indicates the mean G_{out} and G_{in} under control conditions, in the presence of DIDS, and in the presence of CFTR(inh)-172. The I-V curve **(C)** shows the DIDS-sensitive outwardly-rectifying currents (I_{DIDS}), and **(D)** shows the ohmic CFTR currents ($I_{CFTRinh}$). Data are presented as mean ± SEM. (n=12). * indicates a significant difference.

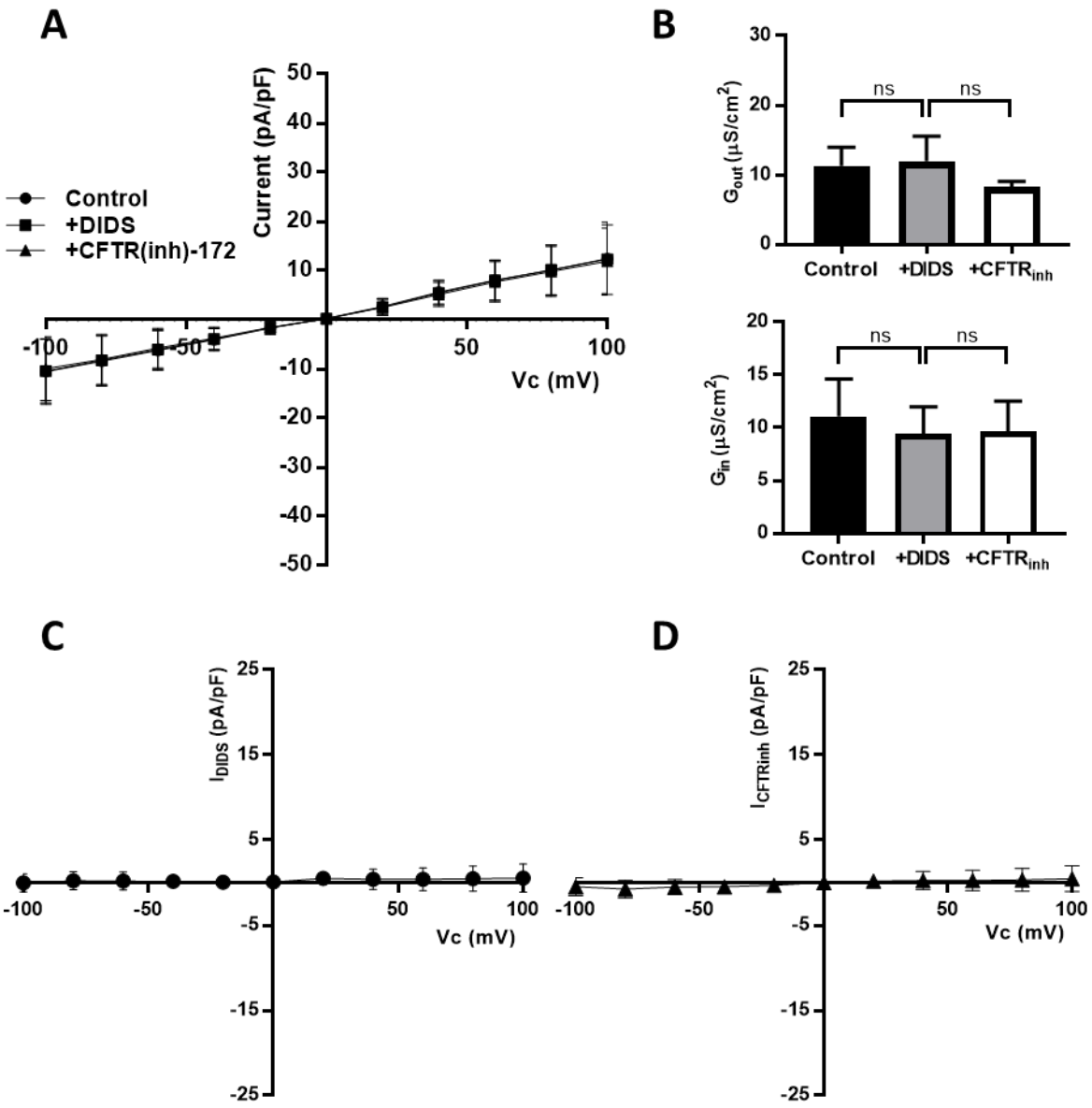

Figure 3-12. Lack of DIDS and CFTR(inh)-172-sensitive currents in HPBMs stimulated with PKI/FSK/IBMX.

Whole cell currents recorded from HPBMs pre-incubated with PKI (100 nM) for 30 min followed by incubation with FSK (10 µM), IBMX (100 µM) + PKI for 30 min to activate DIDS-sensitive Cl^- channels (ORCC) and CFTR channels. **(A)** Circles on the I-V curve signify currents recorded under control conditions. Squares signify currents recorded in the presence of DIDS (500 µM). Triangles signify currents recorded in the presence of CFTR(inh)-172 (10 µM). **(B)** Indicates mean G_{out} and G_{in} under control conditions, in the presence of DIDS, and in the presence of CFTR(inh)-172. The I-V curve **(C)** shows the lack of DIDS sensitive currents (I_{DIDS}), and **(D)** shows the lack of CFTR(inh)-172-sensitive currents ($I_{CFTRinh}$). Data are presented as mean ± SEM. (n=10). ^{ns} indicates a non-significant difference.

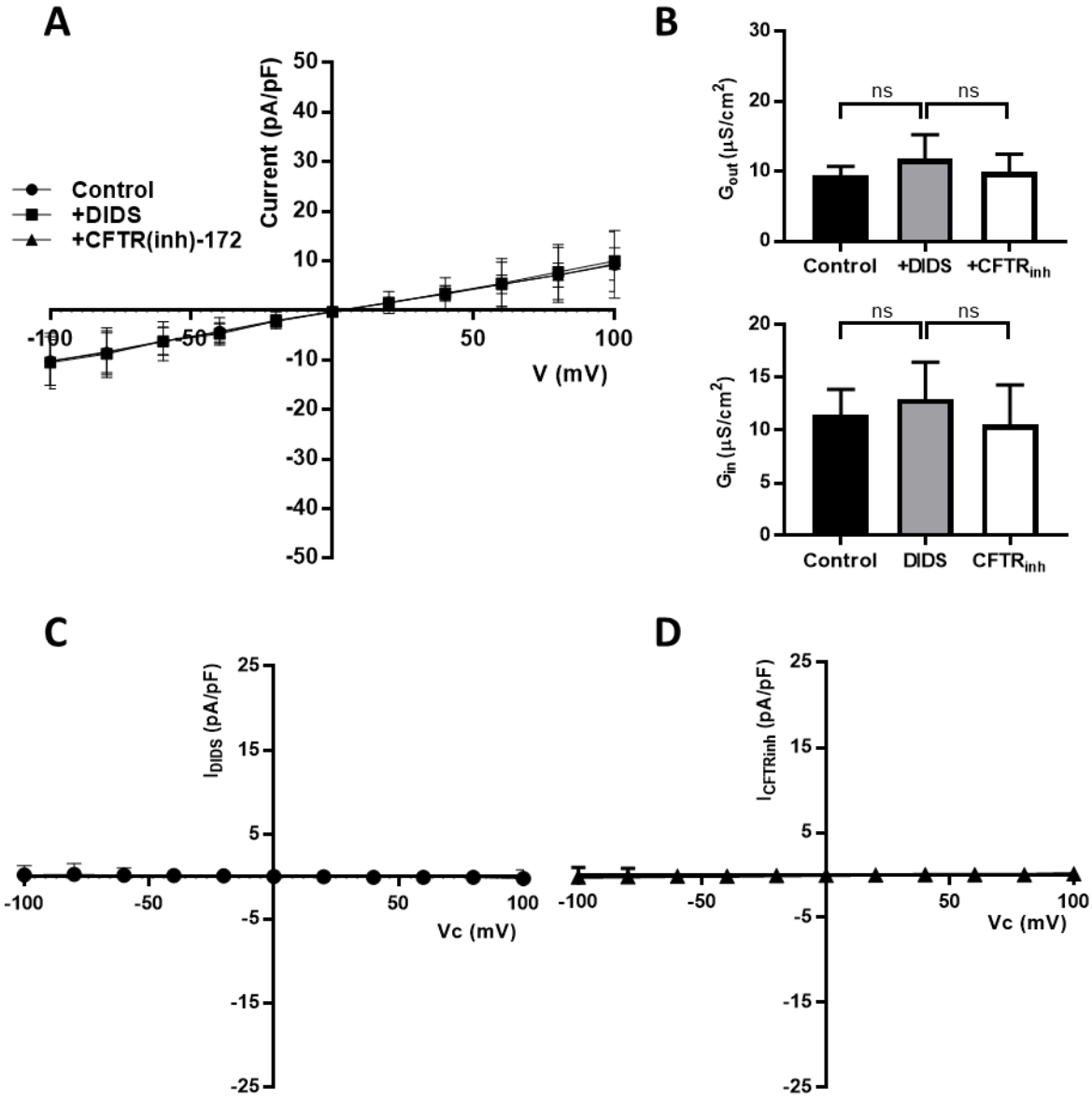

Figure 3-13. Lack of DIDS and CFTR(inh)-172-sensitive currents in HPBMs stimulated with CsA/FSK/IBMX.

Whole cell currents recorded from HPBMs pre-incubated with CsA (1 μM) for 30 min followed by incubation with FSK (10 μM), IBMX (100 μM) + CsA for 30 min to stimulate DIDS-sensitive Cl^- channels (ORCC) and CFTR channels. **(A)** Circles on the I-V curve signify currents recorded under control conditions. Squares signify currents recorded in the presence of DIDS (500 μM). Triangles signify currents recorded in the presence of CFTR(inh)-172 (10 μM). **(B)** Mean G_{out} and G_{in} under control conditions, in the presence of DIDS, and in the presence of CFTR(inh)-172. The I-V curve **(C)** shows the lack of DIDS-sensitive currents (I_{DIDS}), and **(D)** shows the lack of CFTR(inh)-172-sensitive currents ($I_{CFTRinh}$). Data are presented as mean ± SEM. (n=10). ^{ns} indicates a non-significant difference.

3.7 DISCUSSION

The interaction between CaN, S100A10 and AnxA2 has been demonstrated in the literature in the 16HBE14o$^-$ cell line (44), hence our choice of 16HBE14o$^-$ cell lines as the positive control. In addition, secretion defects with respect to CFTR have been well-studied using the 16HBE14o$^-$ cell line (172). Data from this study has demonstrated the interaction between S100A10, AnxA2 and CaN in 16HBE14o$^-$ cell lines, PMA-treated monocytic THP-1 cells and HPBMs. THP-1 cells used in this study were briefly exposed to PMA to differentiate them into monocytes as their phenotypic characteristic is similar to that of human promonocytes (see chapter 2, section 2.2.1.4). This was required because expression of cytokines, such as TNF-α and IL-1β, in response to stimuli, such as LPS, is greater in monocytes compared to promonocytes (208), and low levels of cytokine expression may be difficult to quantify.

S100A10 and AnxA2 have been shown to play important roles in the response of immune cells to inflammatory signals. For instance, S100A10 was shown by O'Connell, Surette (209) to mediate plasminogen-dependent invasion of macrophages in response to thioglycolate induced inflammation. AnxA2, on the other hand, was demonstrated to activate macrophages and stimulate production of certain inflammatory cytokine, such as IL-6, TNF-α, and IL-1β, via phosphorylation of MAPK and translocation of NF-κB into the nucleus (210). Therefore, PMA-treated monocytic THP-1 cells are suitable cells to study S100A10 and AnxA2 signalling pathways and their possible relationship to Cl^- secretion and pro-inflammatory cytokine release. However, the undifferentiated THP-1 cell line was found to express only AnxA2 and CaN, not S100A10. In addition to this, whole cell currents recorded from undifferentiated the THP-1 cell line showed an absence of Cl^- channel currents when stimulated with FSK and IBMX. Based on this knowledge, undifferentiated THP-1 cell lines for the study of the role of Cl^- channels or S100A10

signalling effects were excluded from further experiments. That said, they may still be useful for studies on S100A10-independent signalling in future work.

A further interesting finding was the detection of additional bands with the CaN antibodies, suggesting two possible isoforms of CaN in PMA-treated monocytic THP-1 cells and HPBMs. A study using kidney cells from streptozotocin induced diabetic mice showed differential expression of 3 calceneurin A isoforms; CaN-Aα, β, and γ, in the kidney cells based on disease progression, particularly in the endothelial cells of the glomeruli (211). Evidence exists in the literature that monocytes and macrophages express CaN-Aα (212), but whether they express the β and γ isoforms is currently unknown. Our observation could thus lay the foundations for future work investigating which of these isoforms is responsible for CaN activities in cell secretion and other cellular processes.

Activation of CaN occurs for various reasons, one of which is truncation in brain cells (213) and through binding to calmodulin (CaM) in renal tubule epithelial cells dependent on the intracellular Ca^{2+} level (214). However, activation of CaN by phosphorylation has not been widely studied. One recent study focusing on the virulence of *Aspergillus fumigatus* showed that CaN is activated by phosphorylation in serine-proline rich regions (215). Another study showed activation of a CaN like phosphatase in 16HBE14o$^-$ by PKA phosphorylation (44). These studies have thus provided evidence for the activation of CaN by phosphorylation and the effect of this activation on cell secretion.

Prior to this study, a similar study into the role of the cAMP/PKA pathway in the activation of CFTR ion transport was conducted via the stimulation of 16HBE14o$^-$ cell lines with 10 μM of FSK and 100 μM of IBMX, with and without 100 nM of PKI (44). In a later study, 50 μM of FSK was used to stimulate PKA to investigate the influence of phosphodiesterase 3 and 4 in regulating cAMP/PKA activities (216). Accordingly, the

conditions required to alter the interaction between S100A10, AnxA2 and CaN after stimulation were essentially optimised. Treatment of 16HBE14o$^-$ cell lines with 10 μM of FSK and 100 μM of IBMX stimulates cAMP/PKA activities. This results in the phosphorylation of downstream proteins in the cAMP/PKA pathway (including CaN), as explained earlier. This explains its use in this study as a positive control. The results presented in this chapter have provided evidence that there is interaction between S100A10 and CaN. Moreover, interaction between CaN and AnxA2 was observed in both PMA-treated monocytic THP-1 cells and 16HBE14o$^-$ cell lines. The interactions between AnxA2 and S100A10 with CaN in PMA-treated monocytic THP-1 cells was confirmed.

CFTR is one of the main ion channels that mediates transport of Cl^- in epithelial cells. Defects in this protein channel result in the defects in ion transportation which have been observed in CF (217). Studies have shown that CFTR is highly expressed in monocytes and macrophages with crucial functional roles (146, 218, 219). In fact, expression of defective CFTR has been demonstrated by some studies to affect immune activities of these cells (147, 220). Interestingly, CFTR is not the only channel responsible for Cl^- transport. ORCCs are a group of channels known to mediate Cl^- flux out of cells. This group of channels plays a crucial role in maintaining the Cl^- required for cellular homeostasis. Anoctamin 6, a well-characterised component of ORCC, is known to be highly expressed in macrophages and plays a role in mediating macrophage innate immune response downstream of the P2X7 receptor signalling pathway (221). Inhibition of CFTR and other ORCC by CFTR(inh)-172 and DIDS essentially shows that FSK/IBMX-induced Cl^- current is suppressed upon inhibition of CFTR and ORCC.

By investigating Cl^- transport in PMA-treated monocytic THP-1 cells, it was found that inhibition of the Cl^- channels with CFTR(inh)-172 and DIDS resulted in drops in the recorded ion transport, indicative of low Cl^- flux through the cells. CFTR is known to

control DIDS-sensitive ORCC currents (44, 222). Our finding, that exposure of the monocytes to CFTR inhibitor post exposure to DIDS causes additional suppression in the Cl^- flux, indicates that CFTR(inh)-172 causes a cumulative inhibition of Cl^- in addition to DIDS. Since there is evidence that CFTR interacts with ORCCs, inhibition of both Cl^- may have resulted in abrogation of Cl^- transport, as suggested by the findings of Jovov, Ismailov (223), showing that ORCC requires functional CFTR for its activation.

In PMA-treated monocytic THP-1 cells and HPBMs, functional evaluation of cAMP/PKA and CaN-dependent roles in CFTR ion transport using PKI and CsA has shown that pre-exposure to PKI or CsA has the same effect on the cells unexposed to CFTR(inh)-172 and DIDS as those which had been exposed to these inhibitors. In addition, pre-exposure of the cells to PKI or CsA resulted in inhibition of Cl^- flux more than 20-fold in the DIDS and CFTR(inh)-172 exposed cells and 100-fold in the control unexposed cells when compared to the cells which had not been exposed to either PKI or CsA. The reason for this observation could be that PKI and CsA blocked Cl^- movement by inhibiting FSK/IBMX-dependent induction of Cl^- currents. As such, the Cl^- flux became insensitive to CFTR(inh)-172 and DIDS, indicating that both CFTR and ORCC were not activated. It was suggested by Borthwick, McGaw (44) that complex formation between S100A10, AnxA2 and CaN could be regulating Cl^- transport. This conclusion is consistent with the findings of this present study. We have confirmed that PKI and CsA inhibited Cl^- movement is similarly observed when using a combination of CFTR(inh)-172 and DIDS, indicating that PKA/CaN may regulate CFTR and DIDS-sensitive ORCC.

3.8 CONCLUSION

Interaction of S100A10 with CaN, and AnxA2 with CaN has been confirmed in 16HBE14o$^-$ cell lines (as a control), PMA-treated monocytic THP-1 cells, and HPBMs. Both monocyte types were used in the studies presented in the following chapters. Our preliminary results have shown two probable isoforms of CaN in PMA-treated monocytic THP-1 cells and HPBMs. The distinct likelihood of interactions between AnxA2 and CaN, and between S100A10 and CaN has been confirmed. It has also been shown that Cl^- transport is stimulated by FSK/IBMX, and that inhibition of CFTR and DIDS-sensitive ORCC results in inhibition of the ion current observed.

3.8.1 SUMMARY OF KEY FINDINGS

1. CaN, AnxA2, S100A10 and CFTR likely form multiprotein complex via activation of cAMP/PKA pathway in human epithelial cells (16HBE14o$^-$), PMA-treated monocytic THP-1 cells and HPBMs.
2. FSK/IBMX induces Cl^- conductance in PMA-treated monocytic THP-1 cells and HPBMs.
3. cAMP/PKA/CaN pathway is involved in the FSK/IBMX activation of Cl^- conductance as PKI and CsA prevented activation of ORCC and CFTR in response to FSK/IBMX.

CHAPTER 4

P. aeruginosa regulation of CFTR and ORCC-mediated Cl^- transport, and impacted bacterial phagocytosis and survival in monocyte and macrophage

4 INTRODUCTION

With CF, CFTR plays a major role in disease pathogenesis due to defects in ion transport which eventually results in dehydration of the airway epithelia and subsequent thickening of the mucus lining. The thickened mucus lining creates a difficult environment to facilitate mucocilliary clearance of trapped bacteria, resulting in multiple infections that often lead to death (224). The innate immune system is the first line of defence against infections and it is known to be often dysfunctional in CF development in terms of defects in pathogen sensing, leukocyte recruitment and defective phagocytosis (225). Immune cells, such as macrophages and dendritic cells, are activated after encountering pathogen-associated molecular pattern (PAMP), such as the bacteria LPS, to activate phagocytosis of the bacteria (122). In addition, macrophages and monocytes have been shown to induce expression of Cl^- channels, such as chloride intracellular channel proteins (CLIC), upon LPS stimulation. In addition, the induction of CLIC has been found to also induce gene transcription of IL-1β and activation of NLRP3 inflammasome (226).

Microbial phagocytosis involving macrophages and monocytes is a fundamental characteristic of the innate immune system as it is the first line of defence against pathogens. After ingestion and internalisation of bacterial cells, the phagosome undergoes a series of changes involving fusion of the late phagosome with the lysosome. This forms a phagolysosome with an acidic pH (227). The phagolysosome is also rich in proteolytic enzymes, which in combination with the acidic pH, ensures that the targeted bacteria are killed. Cl^- have been linked, to some extent, to the regulation of phagosomal acidity, but evidence linking specific Cl^- channels to lowering of the phagosomal pH is scant. CFTR is a Cl^- channel that is ubiquitously expressed in different cells including macrophages and epithelial cells (228).

Several microbes, such as *Mycobacterium tuberculosis* and *Legionella pneumophila*, have developed mechanisms, including the prevention of phagolysosome formation, to weaken the phagosomal pathway. This ensures their survival and promotes infection and sepsis (229). Generally, macrophages initiate phagocytosis upon coming in contact with PAMP such as LPS. We hypothesise that *P. aeruginosa* uses this same mechanism to alter the phagocytotic ability of macrophages and monocytes by altering Cl^- transport to change the acidity of the phagolysosome.

4.1 AIMS OF THE STUDY

This study thus aims to determine whether LPS stimulation can alter Cl^- flux in monocytes and whether inhibition of Cl^- flux (in relation to our study) affects the ability of macrophages and monocytes to phagocytose *P. aeruginosa.*

4.2 INDUCTION OF Cl^- CHANNEL ACTIVITIES BY BACTERIAL LPS STIMULATION

In the previous chapter, the role of PKA in the formation of a multiprotein complex comprising CaN, AnxA2 and S100A10, and the role of the protein complex in regulating Cl^- flux in PMA-treated monocytic THP-1 cells and HPBMs were investigated. To understand the specific role played by the ion currents and the Cl^- channels, especially during bacterial infection as observed during CF, the conductance of Cl^- currents across PMA-treated monocytic THP-1 cells that were stimulated with LPS from *P. aeruginosa* was investigated after exposure of the cells to CFTR(inh)-172, an inhibitor of CFTR known to chemically recreate CFTR deficiency in CF. PMA-treated monocytic THP-1 cells were primed with LPS from *P. aeruginosa* for 30 min. They were then exposed to DIDS and then CFTR(inh)-172 to measure Cl^- currents. As indicated in Fig. 4-1, exposure of PMA-treated monocytic THP-1 cells to LPS resulted in generation of both inward and outward ion currents compared to control THP-1 monocytes that were unstimulated with LPS. These ion currents were significantly suppressed upon exposure of the cells to DIDS ($p \leq 0.05$). Further exposure to CFTR(inh)-172 resulted in significant suppression of both inward and outward ion currents when compared with DIDS exposure alone ($p \leq 0.05$).

After discovering that LPS induced Cl^- currents were inhibited by DIDS and CFTR(inh)-172, PMA-treated monocytic THP-1 cells were stimulated with LPS and pre-incubated with and without PKI and CsA prior to being exposed to DIDS and CFTR(inh)-172 (see Fig. 4-2 and 4-3). This was done to investigate the effect of PKA signalling and the role of CaN in LPS-induced Cl^- flux. It was found that pre-exposure of the PMA-treated monocytic THP-1 cells to PKI (100 nM) or CsA (1 μM) inhibited the Cl^- currents and resulted in insensitivity to DIDS and CFTR(inh)-172 inhibitory actions in the PMA-treated monocytic THP-1. This suggests a crucial role for CaN and PKA in CFTR and ORCC-mediated Cl^- flux in these monocytes.

Measurements taken from whole-cell patches exposed to DIDS and CFTR(inh)-172 after pre-incubation with PKI or CsA showed no significant reduction in either the inward or outward Cl^- current conductances when compared with the control group unexposed to PKI or CsA but exposed to LPS only. Interestingly, exposure of the PMA-treated monocytic THP-1 cells to either PKI or CsA resulted in reduction in the whole cell currents by almost 2-fold in all exposure groups causing an insensitivity to both DIDS and CFTR(inh)-172. In addition, total cell currents were less than those of the Cl^- currents recorded in the absence of PKI or CsA (Fig. 4-1).

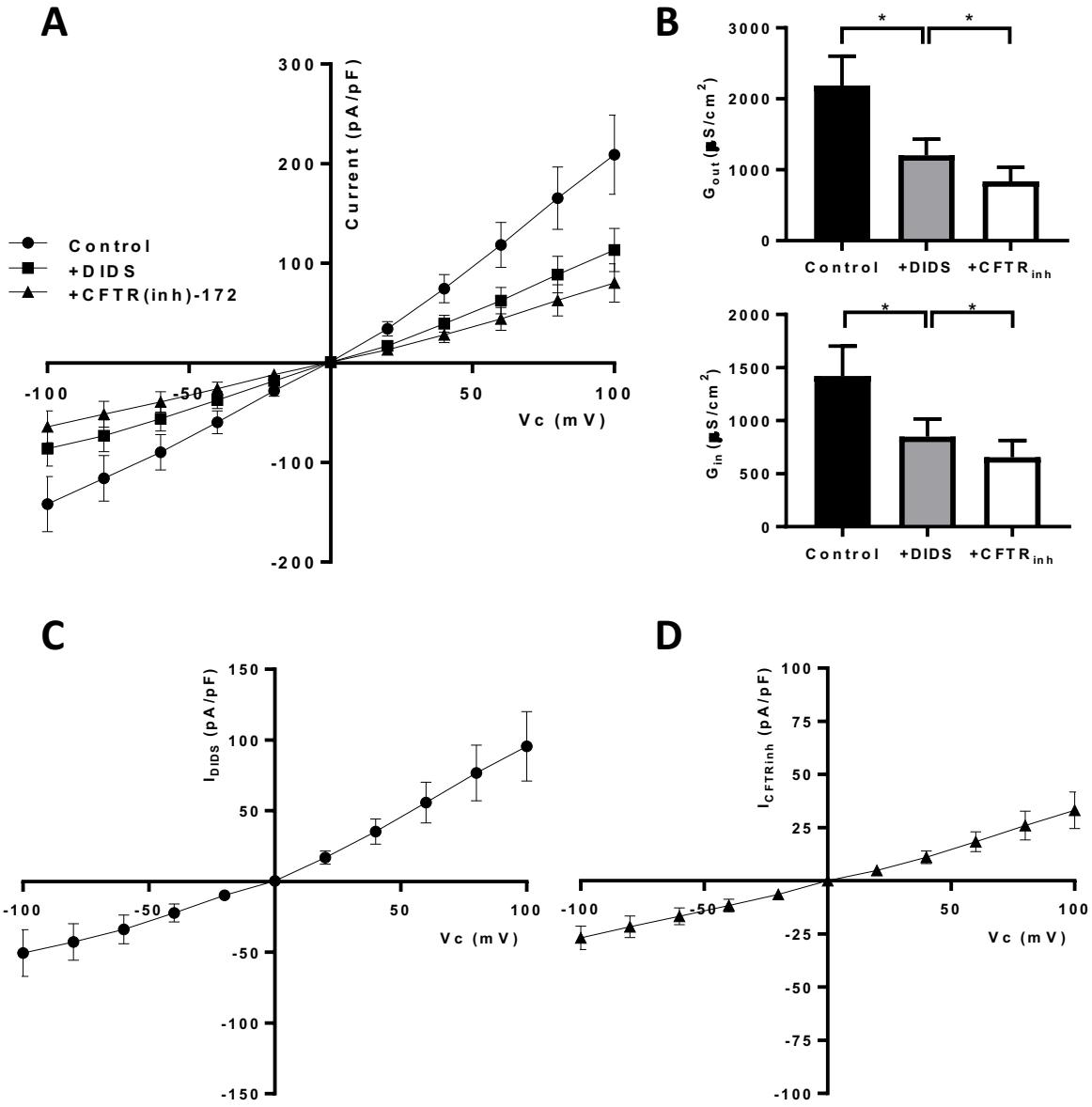

Figure 4-1. DIDS and CFTR(inh)-172-inhibited Cl^- flux in PMA-treated monocytic THP-1 cells stimulated with LPS from *P. aeruginosa*.

Whole cell currents recorded from PMA-treated monocytic THP-1 cells pre-incubated with LPS from *P. aeruginosa* (30 µg/ml) for 30 min to activate DIDS-sensitive Cl^- channels (ORCC) and CFTR channels. **(A)** Circles on the I-V curve signify currents recorded under control conditions. Squares signify currents remaining after addition of DIDS (500 µM). Triangles signify current remaining after addition of CFTR(inh)-172 (10 µM). **(B)** Indicates the mean G_{out} and G_{in} under control conditions, in the presence of DIDS, and in the presence of CFTR(inh)-172. The I-V curve **(C)** shows the DIDS-sensitive outwardly-rectifying currents (I_{DIDS}), and **(D)** shows the ohmic CFTR currents ($I_{CFTRinh}$). Data are presented as mean ± SEM. (n=19). * is $p \leq 0.05$.

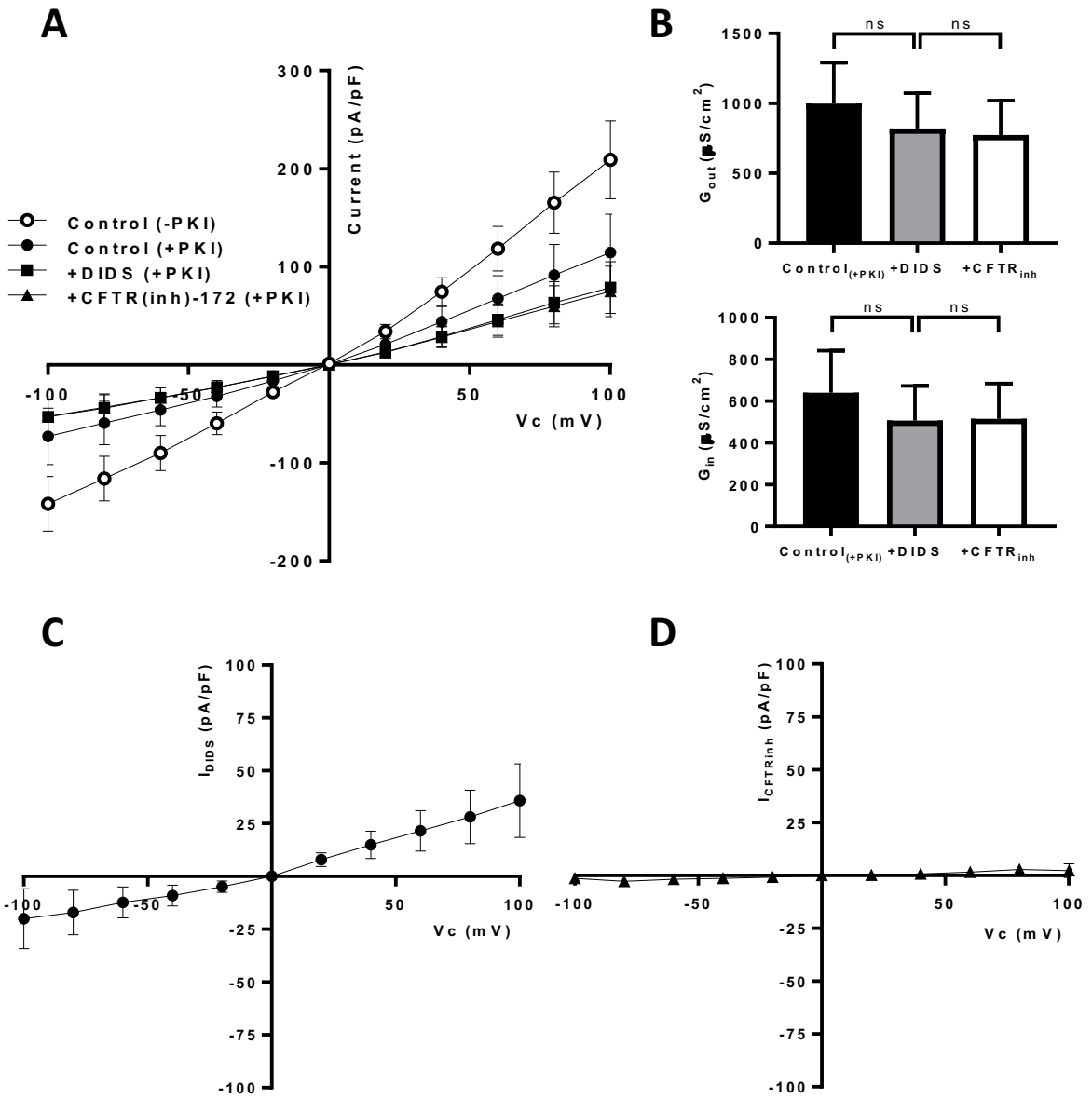

Figure 4-2. Lack of DIDS and CFTR(inh)-172-sensitive currents in PMA-treated monocytic THP-1 cells stimulated with PKI and LPS from *P. aeruginosa*.

Whole cell currents recorded from PMA-treated monocytic THP-1 cells pre-incubated with PKI (100 nM) for 30 min followed by incubation with LPS from *P. aeruginosa* (30 µg/ml) + PKI for 30 min to stimulate DIDS-sensitive Cl^- channels (ORCC) and CFTR channels. **(A)** Circles on the I-V curve signify currents recorded under control conditions (without and with PKI, respectively). Squares signify currents recorded in the presence of DIDS (500 µM). Triangles signify current recorded in the presence of CFTR(inh)-172 (10 µM). **(B)** Indicates the mean G_{out} and G_{in} under control conditions, in the presence of DIDS, and in the presence of CFTR(inh)-172. The I-V curve **(C)** shows the lack of DIDS-sensitive currents (I_{DIDS}), and **(D)** shows the lack of CFTR(inh)-172-sensitive currents ($I_{CFTRinh}$). Data are presented as mean ± SEM. (n=10). ^{ns} indicates a non-significant difference.

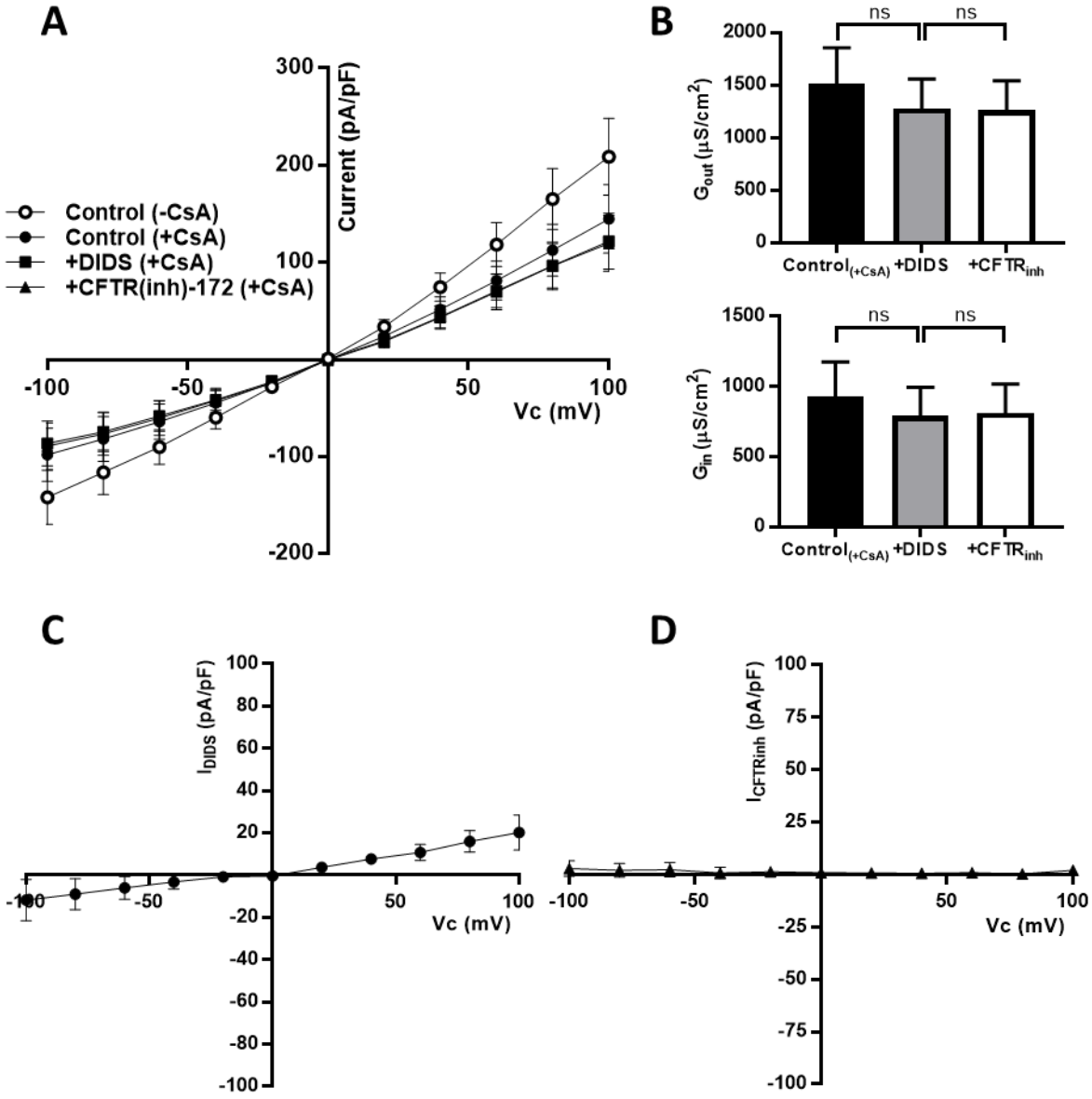

Figure 4-3. Lack of DIDS and CFTR(inh)-172-sensitive currents in PMA-treated monocytic THP-1 cells stimulated with CsA and LPS from *P. aeruginosa*.

Whole cell currents recorded from PMA-treated monocytic THP-1 cells pre-incubated with CsA (1 µM) for 30 followed by incubation with LPS from *P. aeruginosa* (30 µg/ml) + CsA for 30 min to stimulate DIDS-sensitive Cl^- channels (ORCC) and CFTR channels. **(A)** Circles on the I-V curve signify currents recorded under control conditions (without and with CsA, respectively). Squares signify currents recorded in the presence of DIDS (500 µM). Triangles signify currents recorded in the presence of CFTR(inh)-172 (10 µM). **(B)** Indicates the mean G_{out} and G_{in} under control conditions, in the presence of DIDS, and in the presence of CFTR(inh)-172. The I-V curve **(C)** shows the lack of DIDS-sensitive currents (I_{DIDS}), and **(D)** shows the lack of CFTR(inh)-172-sensitive currents ($I_{CFTRinh}$). Data are presented as mean ± SEM. (n=10). ^{ns} indicates a non-significant difference.

Following the finding that *P. aeruginosa* LPS induces Cl^- in PMA-treated monocytic THP-1 cells, testing was conducted to ascertain whether this flux is induced by other bacteria. This was done by exposing the PMA-treated monocytic THP-1 cells to LPS from *E. coli* (see Fig. 4-4). Contrary to our expectation, findings here signified that *E. coli* LPS was unable to induce Cl^- both in the presence or absence of CFTR(inh)-172 or DIDS stimulation. This indicates that not all bacteria LPS may induce Cl^- activation, and this may provide an explanation for *P. aeruginosa* infection being more common in CF (see Fig. 1-7).

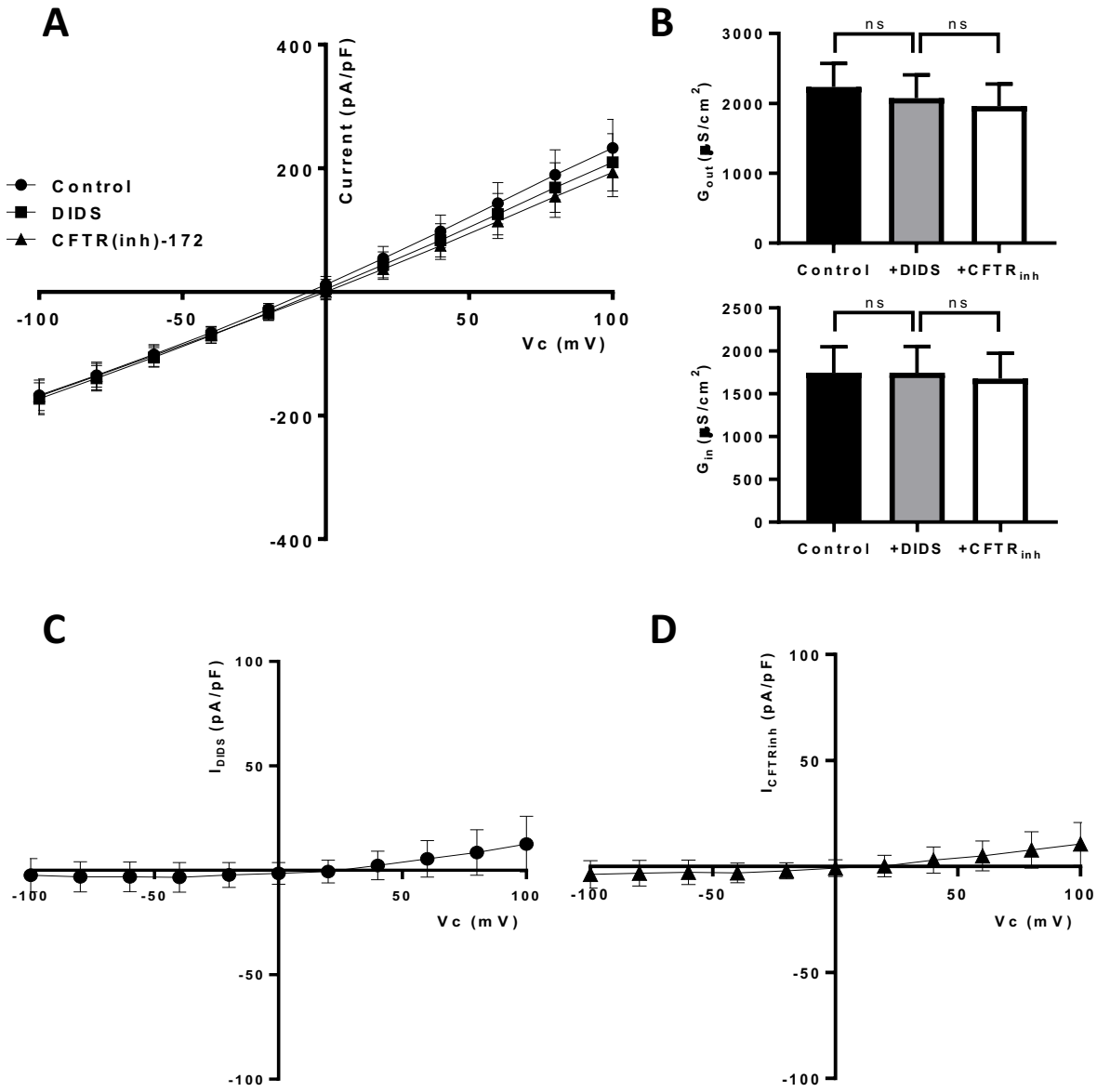

Figure 4-4. Lack of effect of DIDS and CFTR(inh)-172 in PMA-treated monocytic THP-1 cells pre-stimulated with LPS from *E. coli*.

Whole cell currents recorded from PMA-treated monocytic THP-1 cells pre-incubated with LPS from *E. coli* (10 µg/ml) for 30 min to activate DIDS-sensitive Cl^- channels (ORCC) and CFTR channels. **(A)** Circles on the I-V curve signify currents recorded under control conditions. Squares signify currents recorded in the presence of DIDS (500 µM). Triangles signify currents recorded in the presence of CFTR(inh)-172 (10 µM). **(B)** Indicates the mean G_{out} and G_{in} under control conditions, in the presence of DIDS, and in the presence of CFTR(inh)-172. The I-V curve **(C)** shows the lack of DIDS-sensitive currents (I_{DIDS}), and **(D)** shows the lack of CFTR(inh)-172-sensitive currents ($I_{CFTRinh}$). Data are presented as mean ± SEM. (n=22). ^{ns} indicates a non-significant difference.

It has been demonstrated in this study that LPS stimulation may activate CFTR and ORCC mediated Cl^- flux in PMA-treated monocytic THP-1 cells (as a cell line). On this basis, it is necessary to confirm this finding in HPBMs. After establishing the response of PMA-treated monocytic THP-1 cells to Cl^- current inhibition in response to PKI and CsA, the same experiments were therefore repeated using HPBMs. The HPBMs were first exposed to LPS for 30 min before being tested in a patch clamp and exposed to DIDS followed by CFTR(inh)-172. The outward and inward Cl^- flux were recorded and measured. As indicated in Fig. 4-5, pre-exposure of the HPBMs to LPS alone resulted in large total currents. Moreover, the currents were sensitive to DIDS and CFTR(inh)-172 which means that both channels (CFTR and DIDS-sensitive ORCC) are activated by LPS.

After determining the effect of DIDS and CFTR(inh)-172 on the LPS stimulated Cl^- currents, the effects of both PKA/cAMP and CaN activities on the HPBMs were investigated since the cell line (PMA-treated monocytic THP-1 cells) experiments proved that LPS activation of CFTR and ORCC requires PKA and CaN. To do this, the HPBMs were pre-incubated with PKI (100 nM) or CsA (1 μM) after being stimulated with LPS. The cells were then exposed to DIDS and subsequently CFTR(inh)-172 during the patch experiment while Cl^- currents were recorded and measured. As a control, HPBMs that were unexposed to PKI or CsA, but only LPS were used to determine the baseline effect of LPS on Cl^- currents. As shown in Fig. 4-6 and Fig. 4-7, PKI and CsA were able to suppress the Cl^- currents with no significant difference in both inward and outward Cl^- flux. However, when compared with HPBMs that were or were not exposed (control) to only DIDS and CFTR(inh)-172 in Fig. 4-5, the suppression of Cl^- currents induced by PKI and CsA was approximately 3 times the level of those not exposed to PKI and CsA. This suggests that PKI and CsA may have an influence on the Cl^- channels stimulated

with LPS. This in turn indicates that LPS-dependent activation of CFTR and ORCC may operate through the PKA and CaN pathway.

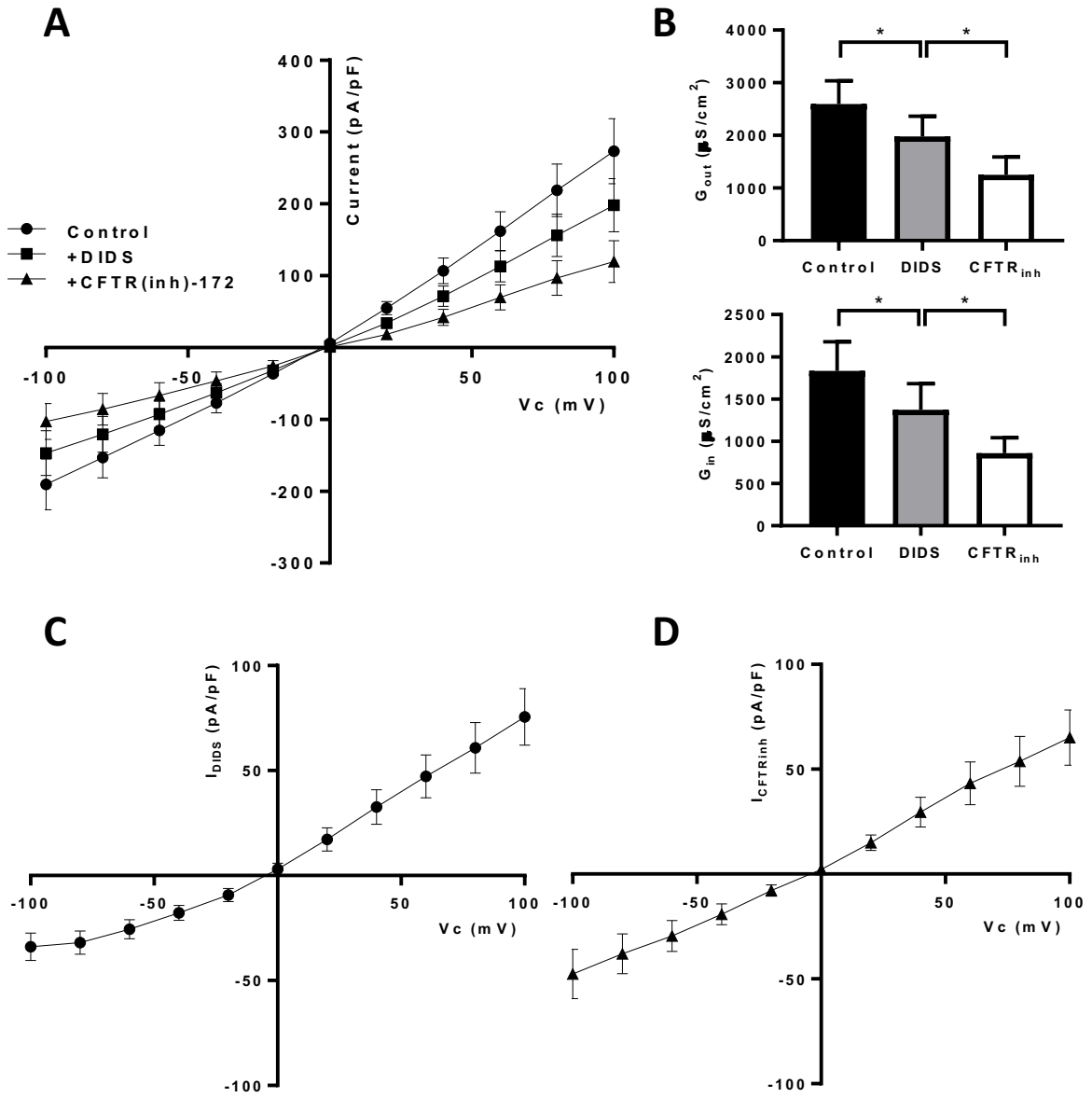

Figure 4-5. DIDS and CFTR(inh)-172-inhibited Cl^- flux in HPBMs stimulated with LPS from *P. aeruginosa*.

Whole cell currents recorded from HPBMs pre-incubated with LPS from *P. aeruginosa* (30 µg/ml) for 30 min to activate DIDS-sensitive Cl^- channels (ORCC) and CFTR channels. **(A)** Circles on the I-V curve signify currents recorded under control conditions. Squares signify currents remaining after addition of DIDS (500 µM). Triangles signify currents remaining after addition of CFTR(inh)-172 (10 µM). **(B)** Indicates the mean G_{out} and G_{in} under control conditions, in the presence of DIDS, and in the presence of CFTR(inh)-172. The I-V curve **(C)** shows the DIDS-sensitive outwardly-rectifying currents (I_{DIDS}), and **(D)** shows the ohmic CFTR currents ($I_{CFTRinh}$). Data are presented as mean ± SEM. (n=20). * is $p \leq 0.05$.

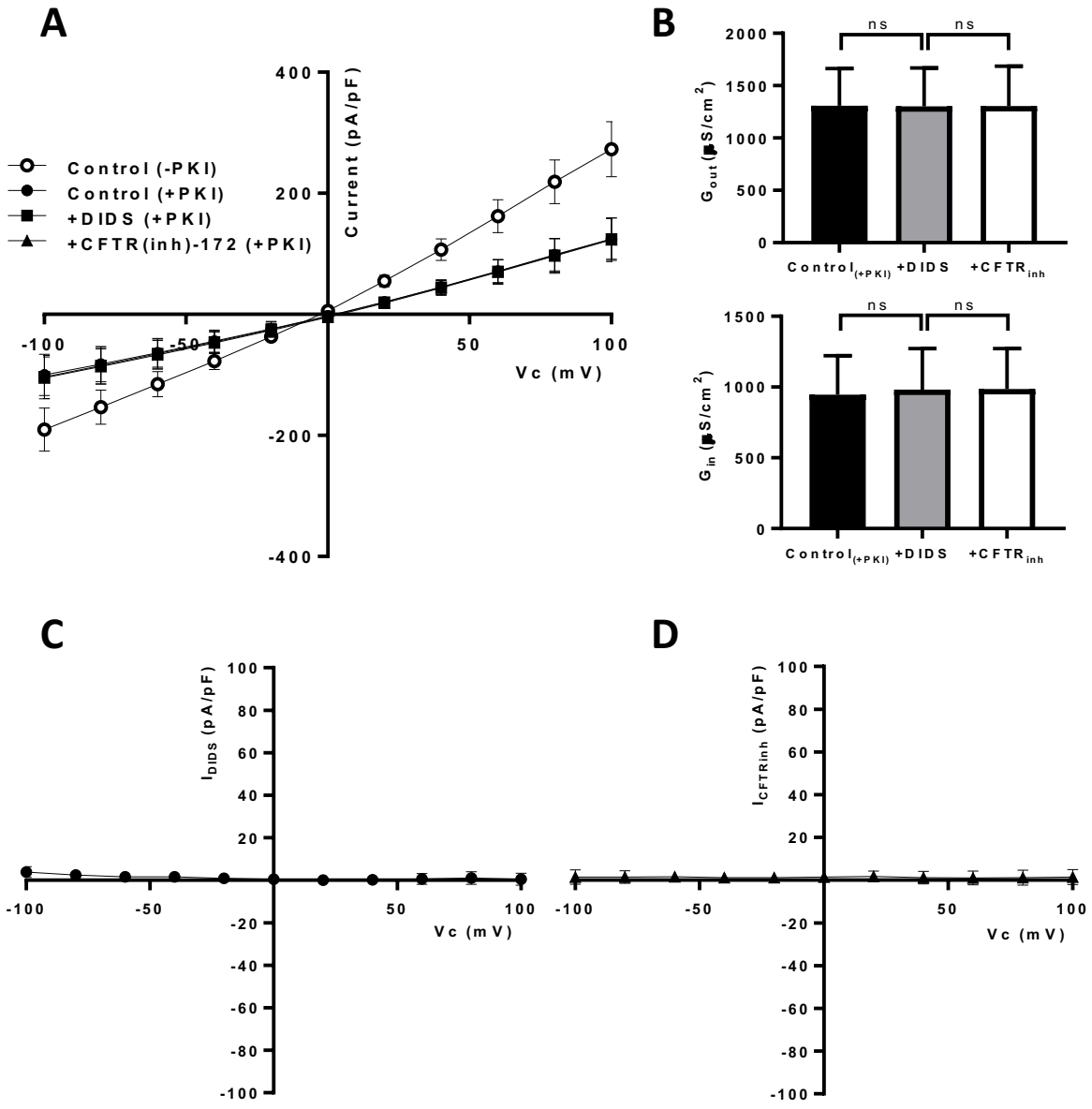

Figure 4-6. Lack of DIDS and CFTR(inh)-172-sensitive currents in HPBMs stimulated with PKI and LPS from *P. aeruginosa*.

Whole cell currents recorded from HPBMs pre-incubated with PKI (100 nM) for 30 min followed by incubation with LPS from *P. aeruginosa* (30 µg/ml) + PKI for 30 min to stimulate DIDS-sensitive Cl^- channels (ORCC) and CFTR channels. **(A)** Circles on the I-V curve signify currents recorded under control conditions (without and with PKI, respectively). Squares signify currents recorded in the presence of DIDS (500 µM). Triangles signify currents recorded in the presence of CFTR(inh)-172 (10 µM). **(B)** Indicates the mean G_{out} and G_{in} under control conditions, in the presence of DIDS, and in the presence of CFTR(inh)-172. The I-V curve **(C)** shows the lack of DIDS-sensitive currents (I_{DIDS}), and **(D)** shows the lack of CFTR(inh)-172-sensitive currents ($I_{CFTRinh}$). Data are presented as mean ± SEM. (n=11). ^{ns} indicates a non-significant difference.

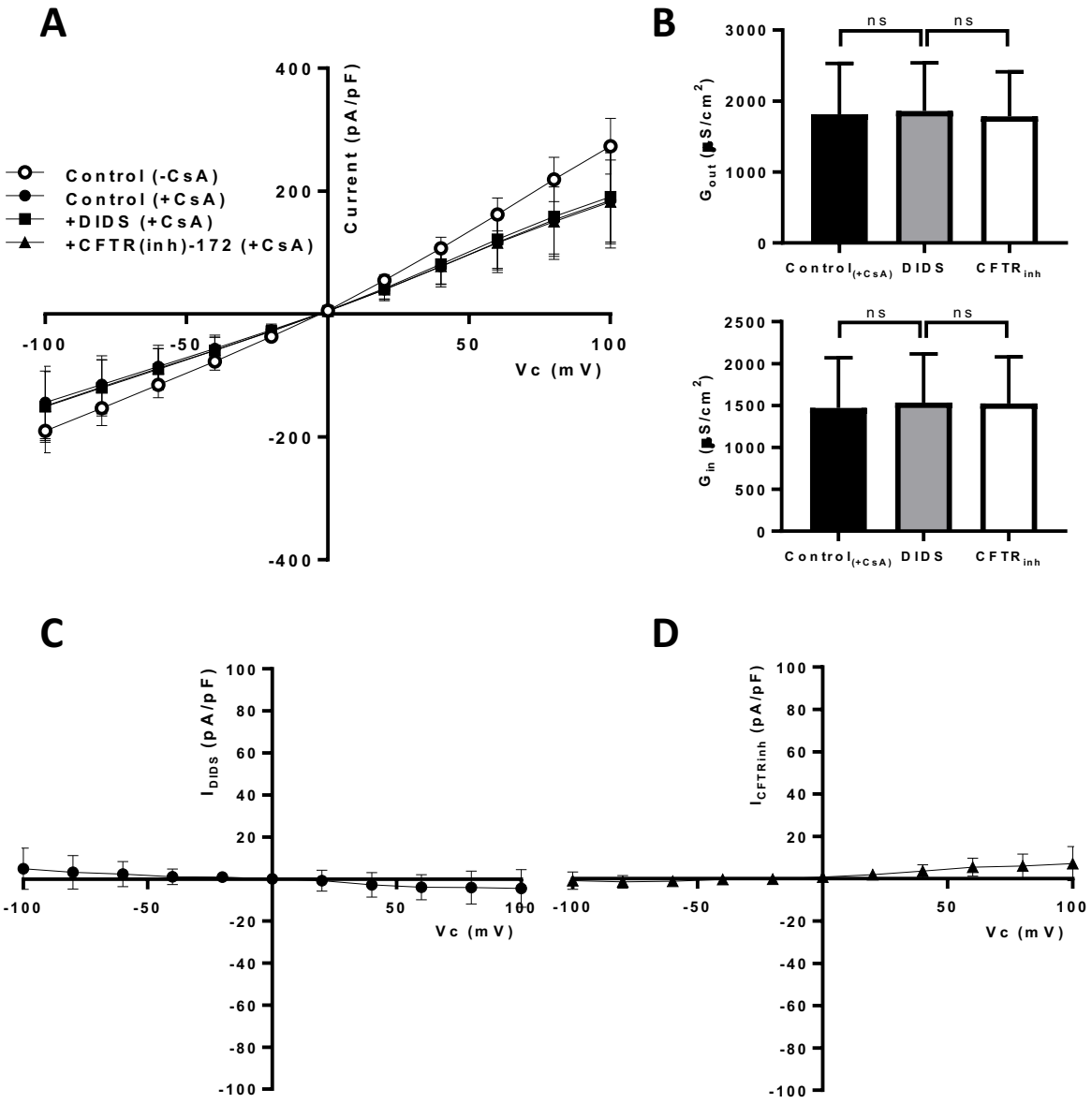

Figure 4-7. Lack of DIDS and CFTR(inh)-172-sensitive currents in HPBMs stimulated with CsA and LPS from *P. aeruginosa*.

Whole cell currents recorded from HPBMs pre-incubated with CsA (1 μM) for 30 min followed by incubation with LPS from *P. aeruginosa* (30 μg/ml) + CsA for 30 min to stimulate DIDS-sensitive Cl^- channels (ORCC) and CFTR channels. **(A)** Circles on the I-V curve signify currents recorded under control conditions (without and with CsA, respectively). Squares signify currents recorded in the presence of DIDS (500 μM). Triangles signify current recorded in the presence of CFTR(inh)-172 (10 μM). **(B)** Mean G_{out} and G_{in} under control conditions, in the presence of DIDS and the presence of CFTR(inh)-172. The I-V curve **(C)** shows the lack of DIDS-sensitive currents (I_{DIDS}), and **(D)** signifys lack of CFTR(inh)-172-sensitive currents ($I_{CFTRinh}$). Data are presented as mean ± SEM. (n=12). ^{ns} indicates a non-significant difference.

4.3 THE INFLUENCE OF Cl^- CHANNEL INHIBITION ON THE FUNCTIONING OF MONOCYTES AND MACROPHAGES DURING INFECTION

After establishing the effect of LPS and the possible impact of PKA and CaN on Cl^- current in PMA-treated monocytic THP-1 cells and HPBMs, the physiological role played by CaN on phagocytosis in PMA-treated monocytic THP-1 cells and HPBMs-derived macrophages (MDMs) was investigated using live *P. aeruginosa* bacterial cells to infect the target cells. Firstly, PMA-treated monocytic THP-1 cells were infected with *P. aeruginosa* and the cells divided into five different groups for analysis of phagocytosis and survival of *P. aeruginosa*: i) control cells infected with only *P. aeruginosa*; ii) cells infected after pre-exposure to DIDS (500 μM); iii) cells infected after pre-exposure to CFTR(inh)-172 (10 μM); iv) cells infected after pre-exposure to a combination of both CFTR(inh)-172 and DIDS; and v) cells infected after pre-exposure to CsA (1 μM). As shown in Fig. 4-8, exposure of the PMA-treated monocytic THP-1 cells to only *P. aeruginosa* (control) caused a higher level of phagocytotic ability of the cells. However, pre-exposure to either DIDS or CFTR(inh)-172 significantly reduced the phagocytotic ability of the PMA-treated monocytic THP-1 cells 3-fold ($p < 0.0001$). However, pre-exposure to CsA had no significant effect on phagocytotic activities of these monocytes when compared with the control group.

To conduct analysis of the survival of phagocytosed *P. aeruginosa*, PMA-treated monocytic THP-1 cells were infected with *P. aeruginosa* PAO1 at MOI 10 for 2 hours. After infection, cells were washed and extracellular bacteria were killed with gentamicin (200 μg/ml, 1 hour). Cells were then incubated in media containing CFTR(inh)-172 (10 μM), DIDS (500 μM), a combination of both, or CsA (1 μM) for different time intervals. Phagocytosed *P. aeruginosa* in control monocytes were found to survive for the least time of up to 18 hours. At 0 hours, uninfected PMA-treated monocytic THP-1 cells showed the presence of no bacteria, confirming the experiment had worked as expected.

P. aeruginosa-infected PMA-treated monocytic THP-1 cells, on the other hand, showed evidence of a significant amount of bacterial colony. At 4 hours however, there was no significant difference in survival of *P. aeruginosa* based on the CFU counted. This indicates that the effect of the inhibitors has not initiated at this time point. At 10 hours, cells exposed to both CFTR(inh)-172 and DIDS showed evidence of a significantly higher number of bacterial CFU when compared with the control unexposed group while PMA-treated monocytic THP-1 cells exposed to either CFTR(inh)-172, DIDS or CsA showed an insignificant difference. Interestingly, at 18 hours, only CsA exposed PMA-treated monocytic THP-1 cells evidenced significant suppression of phagocytosed *P. aeruginosa* survival compared to the unexposed control group (see Fig. 4-9).

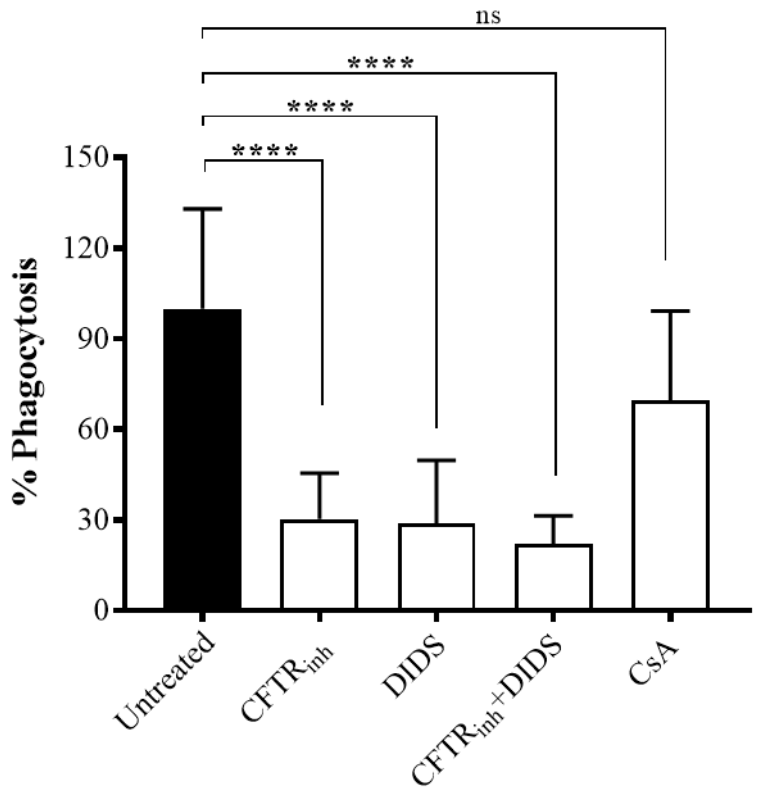

Figure 4-8. Impact of pre-treatment of PMA-treated monocytic THP-1 cells with CFTR(inh)-172, DIDS and CsA on the phagocytosis of *P. aeruginosa.*

PMA-treated monocytic THP-1 cells were treated with CFTR(inh)-172 (10 μM), DIDS (500 μM), a combination thereof, or CsA (1 μM) for 30 min. Cells were then infected with *P. aeruginosa* PAO1 at MOI 10 for 2 hours. After infection, cells were washed with PBS and extracellular bacteria were killed with gentamicin (200ug/ml, 1 hour). Cells were lysed with 2% saponin to release the phagocytosed bacteria and the lysate was plated on agar. The number of phagocytosed bacteria was quantified by colony counting. CFTR(inh)-172, DIDS and a combination of both significantly reduced the phagocytosis of *P. aeruginosa* ($p < 0.0001$) while CsA had a slight but not significant effect. **** and ^{ns} indicate $p < 0.0001$ and non-significant, respectively. Data is represented as mean ± SEM of n=7.

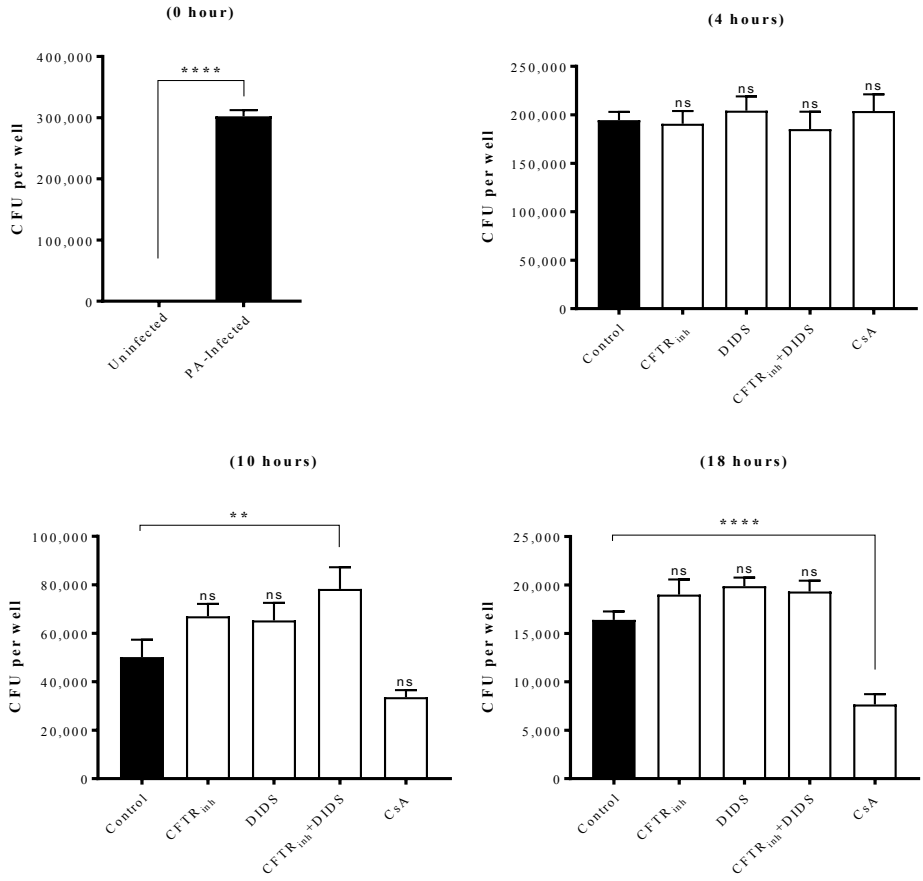

Figure 4-9. Survival of phagocytosed *P. aeruginosa* (+/- CFTR(inh)-172, DIDS, a combination of both, and CsA) by PMA-treated monocytic THP-1 cells.

PMA-treated monocytic THP-1 cells were infected with *P. aeruginosa* PAO1 at MOI 10 for 2 hours. After infection, cells were washed with PBS and extracellular bacteria were killed with gentamicin (200 μg/ml, 1 hour). Cells were incubated in media containing CFTR(inh)-172 (10 μM), DIDS (500 μM), a combination thereof, and CsA (1 μM) for up to 18 hours. At different time points, cells were lysed with 2% saponin to release the phagocytosed bacteria and the lysate was plated on agar. The number of surviving phagocytosed bacteria was quantified by colony counting at 0, 4, 10 and 18 hours. ** is $p < 0.01$ and **** is $p < 0.0001$. ^{ns} indicates non-significant. Data is represented as mean ± SEM of n=7.

In the same manner as with the PMA-treated monocytic THP-1 cells, the experiment was repeated using MDMs since HPBMs adherence to the plate is weak and will not withstand the several washings required by this procedure (data not shown). Firstly, MDMs were infected with *P. aeruginosa* and divided into four different groups before the phagocytosis and survival assays were carried out: i) control MDMs infected with only *P. aeruginosa*; ii) cells infected with *P. aeruginosa* and exposed to DIDS; iii) cells infected with *P. aeruginosa* and exposed to CFTR(inh)-172; iv) cells infected with *P. aeruginosa* and exposed to DIDS and CFTR(inh)-172; and v) cells infected with *P. aeruginosa* and exposed to CsA. As shown in Fig. 4-10, untreated MDMs infected with *P. aeruginosa* evidenced a higher level of phagocytotic ability. Exposure to either DIDS or CFTR(inh)-172 or both DIDS and CFTR(inh)-172 significantly reduced the phagocytotic ability of the MDMs 2-fold ($p < 0.0001$). On the contrary, exposure to CsA resulted in no significant effect on the phagocytotic activities of the control group.

This was also reflected in the survival assay of the *P. aeruginosa* after infection of MDM. At 0 hours, uninfected MDMs group did not signify any bacterial growth while the group infected with *P. aeruginosa* showed evidence of significant bacteria colony formation. At 4 hours, as observed in the PMA-treated monocytic THP-1 cells, only cells exposed to both CFTR(inh)-172 and DIDS had a significantly higher rate of *P. aeruginosa* colony survival compared to the control group. At 10 hours, all groups showed no significant CFU survival compared to the control groups. Unlike with PMA-treated monocytic THP-1 cells at 18 hours, only the DIDS-exposed group showed a significantly higher rate of CFU survival compared with the control group ($p < 0.01$) (see Fig. 4-11).

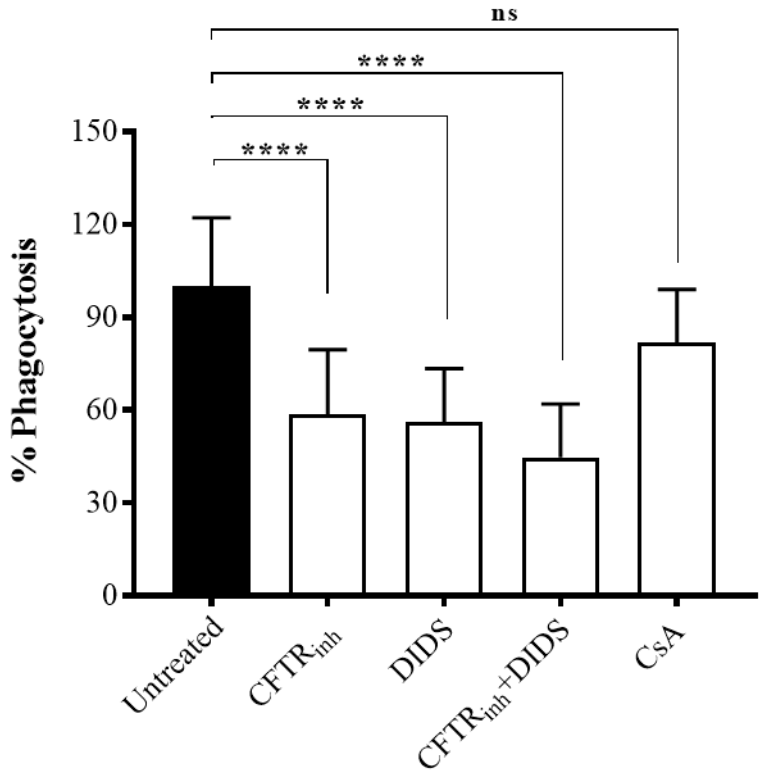

Figure 4-10. Impact of pre-treatment of MDMs with CFTR(inh)-172, DIDS or CsA on the phagocytosis of *P. aeruginosa.*

MDMs were treated with CFTR(inh)-172 (10 μM), DIDS (500 μM), a combination thereof, or CsA (1 μM) for 30 min. Cells were then infected with *P. aeruginosa* PAO1 at MOI 10 for 2 hours. After infection, cells were washed with PBS and extracellular bacteria were killed with gentamicin (200 μg/ml, 1 hour). Cells were lysed with 2% saponin to release the phagocytosed bacteria and the lysate was plated on agar. The number of phagocytosed bacteria was quantified by colony counting. CsA has a slight effect. ^{ns} indicates non-significant and **** is $p < 0.0001$. Data is represented as mean ± SEM of n=10.

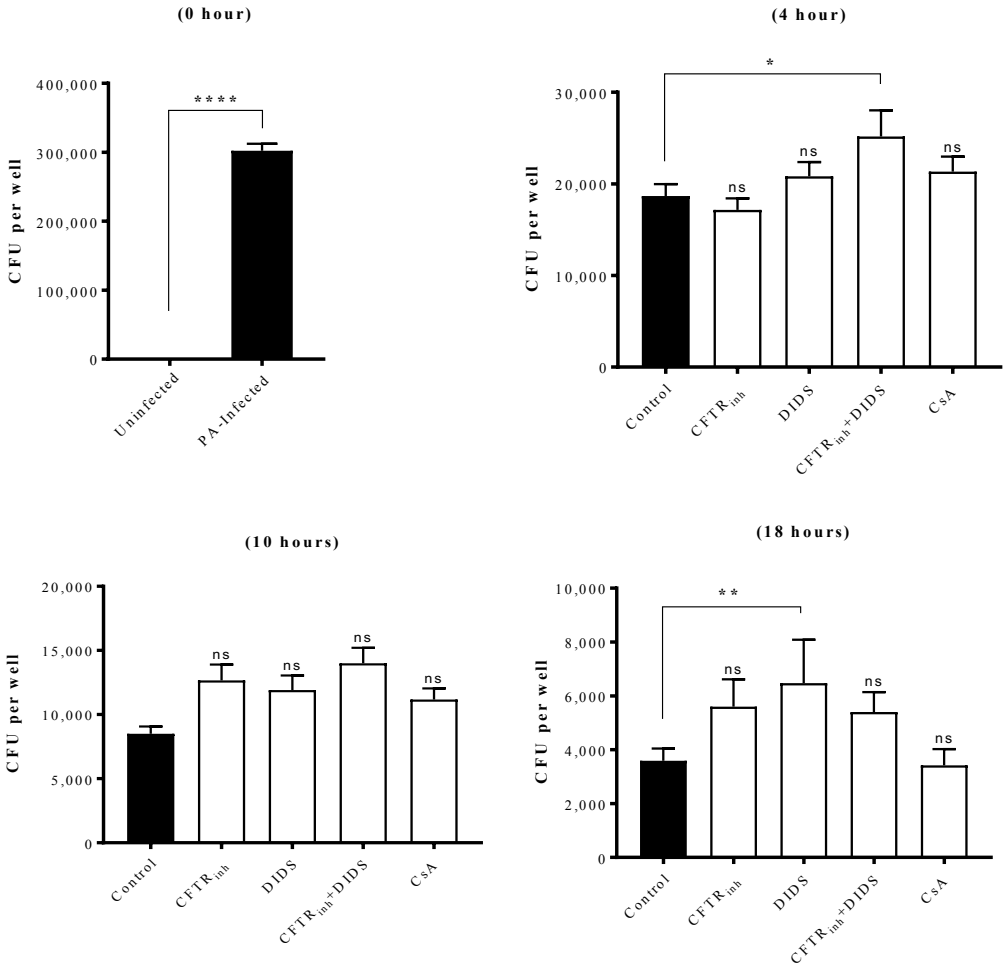

Figure 4-11. Survival of phagocytosed *P. aeruginosa* (+/- CFTR(inh)-172, DIDS, combination of both, or CsA) by MDMs.

MDMs were infected with *P. aeruginosa* PAO1 at MOI 10 for 2 hours. After infection, cells were washed with PBS and extracellular bacteria were killed with gentamicin (200 μg/ml, 1 hour). Cells were incubated in media containing CFTR(inh)-172 (10 μM), DIDS (500 μM), a combination thereof, or CsA (1 μM) for up to 18 hours. At different time points, cells were lysed with 2% saponin to release the phagocytosed bacteria and the lysate was plated on agar. The number of surviving phagocytosed bacteria was quantified by colony counting at 0, 4, 10 and 18 hours. ^{ns} indicates non-significant. * is $p \leq 0.05$, ** is $p < 0.001$ and **** is $p < 0.0001$. Data is represented as mean ± SEM of n=10

4.4 DISCUSSION

S100A10 and AnxA2 interaction is known to be crucial to CFTR function. This study has established the formation of a multi-protein complex consisting of CFTR, AnxA2, S100A10 and CaN and the functional relevance of this complex in the regulation of Cl^- current conductance in PMA-treated monocytic THP-1 cells and HPBMs. Thus, this study shows functional relevance of the complex in mediating Cl^- transport in these immune cells. In addition, intracellular Cl^- concentration plays a role in monocyte and macrophage function, especially phagocytosis. As such, it is important to study the physiological consequences of this protein complex in terms of functioning of immune cells, the induction of Cl^- currents by LPS, and specifically the role played by Cl^- channels, such as CFTR and ORCC, and the multi-protein complex, in influencing LPS induced Cl^- ion current. A previous study demonstrated the role of AnxA2-S100A10 in immune activation by inducing macrophage activation via toll like receptor 4 (TLR4)-mediated activities (230). This present study has shown that LPS from *P. aeruginosa* was able to induce Cl^- flux in both PMA-treated monocytic THP-1 cells and HPBMs. LPS is known to be a regulator of ion transport, especially in epithelial cells, and it has been previously shown that LPS from *P. aeruginosa* stimulates Cl^- transport in Calu-3 epithelial cells and inhibits Na^+ transport across mouse tracheal epithelium (192). *E. coli* LPS, on the other hand, has been shown to induce expression of Ca^{2+} activated Cl^- channels (CaCC) in human airway epithelia cells (191). The results of this present study show that inhibition of Cl^- channels using DIDS and CFTR(inh)-172 results in reduction in the Cl^- current recorded across the cell membrane for both PMA-treated monocytic THP-1 cells and HPBMs. This suggests that inhibition of CFTR as caused by CFTR(inh)-172 (to mimic CFTR defects in CF) results in Cl^- transport inhibition in monocytes. This finding is supported by existing studies which have reported a reduction in Cl^- currents in cells exposed to CFTR(inh)-172. For instance, Kopeikin et al. (231) have shown that

in Chinese Hamster Ovary (CHO) cells, CFTR(inh)-172 inhibits ion transport through CFTR by increasing the channel closing time and reducing the opening time. Melis et al. (232) provided further evidence by showing CFTR(inh)-172 suppressed Cl^- transport in murine renal cells. They concluded that this is highly specific for CFTR. In a similar vein, it was demonstrated in murine cardiomyocytes that DIDS can significantly block Cl^- currents (233). This observed Cl^- transport inhibition may have a functional impact on the innate immune response of monocytes and macrophages since impairment of macrophage phagocytotic ability has been previously reported in CF macrophages (234). This Cl^- flux inhibition in response to DIDS may be significant since there are many Cl^- channels that are DIDS-sensitive and may also be linked with CF. For instance, the ClCs are a group of ion channels that are ORCCs, one of which includes ClC2, which plays a crucial role in transepithelial fluid secretion (235). ClC4 is another ORCC that is known to colocalise with CFTR on the apical side of epithelial cell membrane. This ORCC may have a considerable effect on mediating Cl^- across the cell since knockdown of its mRNA resulted in more than 50% inhibition of Cl^- flux being recorded (236).

The role of PKA and CaN in influencing LPS-induced ion transport was investigated by inhibiting both PKA and CaN. It was found that PKA and CaN inhibition results in both the complete inhibition of Cl^- flux in PMA-treated monocytic THP-1 cells and HPBMs, and insensitivity of these cells Cl^- channels inhibitors. Lack of DIDS and CFTR(inh)-172-sensitive currents and no significant changes in the inward and outward records upon adding the inhibitors indicate that ORCC and CFTR may not have been activated due to the inhibition of CsA and PKI. Taken together, these findings indicate that both PKA and CaN influence Cl^- movement through Cl^- channels, possibly by interacting with other elements involved in the pathway including CFTR or Cl^- channels that are sensitive to DIDS. Indeed, if these inhibitors had no effect on the CFTR and ORCC mediated ion

transport, one would expect the ion currents recorded to be similar to when the monocytes were not exposed to PKI or CsA. This further confirms the possibility of the multiprotein complex comprising CaN and CFTR being responsible for this physiological suppression of Cl^- flux in a cAMP/PKA-dependent manner. It has been previously shown that CFTR(inh)-172 can suppress cAMP-stimulated Cl^- conductance (237, 238), further confirming crosstalk between CFTR and cAMP in facilitating Cl^- transport.

Bacterial infection accounts for the highest percentage of mortality in CF, with *P. aeruginosa* being the predominant specific cause of infection-dependent death globally (239). Mutations of *CFTR* are associated with severe lung disease aggravated by bacterial colonisation. This dysfunction in CF patients causes hyper susceptibility to *P. aeruginosa* colonisation and secondary infection caused by *S. aureus* (240, 241). In normal airways and lungs, bacterial infection is combatted via the innate immune response which sends monocytes and macrophages to the site of infection. This is coupled with mucocilliary clearance of the airway epithelia (225). However, it is known that Cl^- transport dysfunction results in drying up of the ASL, affecting mucocilliary clearance. Through the combination of defective mucocilliary clearance and incapacitation and dysfunction of the innate immune response, disease or sepsis is aggravated, leading to persistent bacterial infection. Indeed, CF macrophages have been demonstrated to exhibit defective phagocytotic ability (234), which obviously results in increased survival of colonising bacteria. Our investigation into the phagocytotic ability of PMA-treated monocytic THP-1 cells and MDMs has shown that exposure of these cells to DIDS and CFTR(inh)-172 results in significant inhibition of the ability of monocytes to phagocytose *P. aeruginosa* with some of the ingested bacterial cells surviving phagocytosis. This finding suggests that defective Cl^- conductance may have a negative effect on the ability of these monocytes to engulf and kill bacterial cells. A previous study concluded that Cl^- channels

are important factors in the regulation of macrophage phagosomal milieu through regulation of phagosomal acidification and Cl^- influx through specific Cl^- channels including Cl^- intracellular channels (CLIC) and CFTR (242). An additional study using neutrophils showed that Cl^- transport in and out of the phagosome helps maintain the acidity of the phagosome due to formation of hypochloric acid (HOCl). This helps to kill the bacterial cells that have been phagocytosed (243). Nicotinamide adenine dinucleotide phosphate (NADPH) oxidase-generated electrons cause induction of ROS in the phagosome, and the ROS are then converted into peroxide by superoxide dismutase. The peroxide in the presence of Cl^- is then converted by myeloperoxidase into HOCl (244). This could provide the reason for a considerable number of the *P. aeruginosa* having survived in CF for so long after they might have been phagocytosed: the phagosome of the monocytes and MDMs were not acidic enough to induce bacterial cell death due to the inhibition of Cl^- channels activities. As such, it is possible that bacteria such as *P. aeruginosa* are able to survive the action of immune cells such as macrophages, monocytes and neutrophils through this mechanism.

As previously stated, CaN, AnxA2, S100A10 and CFTR are known to interact as a multi-protein complex. In addition, cAMP signalling may influence CFTR and ORCC activities based on additive inhibition of Cl^- conductance observed in monocytes exposed to CFTR(inh)-172/DIDS and PKI or CsA. Thus, CFTR functions that require cAMP signalling are likely to be influenced by CaN. This may also involve ORCCs since evidence in the literature shows that ORCCs may also be regulated by cAMP activities (222). Moreover, functional CFTR has been previously shown to be required for activation of ORCCs in a PKA-dependent manner (223). As such, this interaction or crosstalk between ORCC and CFTR may play a crucial role in the signalling of the multiprotein complex comprising cAMP, CaN, S100A10 and CFTR. CsA is known as an

immunosuppressor and thus may affect the ability of immune cells' antimicrobial activities. This hypothesis was tested by investigating the exposure of both PMA-treated monocytic THP-1 cells and MDMs to CsA. This study found that there is a non-significant difference in the phagocytotic ability of both PMA-treated monocytic THP-1 cells and MDMs. It is possible that co-exposure of the monocytes to CsA and the Cl^- channel inhibitors may be required to affect the phagocytotic ability of the monocytes since it was established that CsA and the channel inhibitors significantly suppressed Cl^- flux when compared with the channel inhibitors alone. However, CsA exposure did not affect the survival of *P. aeruginosa* that had been phagocytosed by the MDMs in contrast to THP-1 monocytes. This can be explained by the differing response of PMA-treated monocytic THP-1 cells and MDMs to *P. aeruginosa* LPS in activation of the MDM under the conditions explored. It is known that macrophages show differing responses to LPS in comparison to monocytes under differing conditions. For example, Chanput et al. (245) showed that both MDMs and THP-1 monocytes possess different gene expression profiles to LPS stimulation under different immune-modulating compounds. Moreover, Sharif et al. (246) showed that LPS stimulation of THP-1 monocytes, MDMs and HPBMs result in a time-dependent difference in NF-κβ induced gene expression profiles in these cell types.

In summary, LPS induces Cl^- flux and the inhibition of Cl^- flux is seen to affect the phagocytotic ability of the immune cells used here. This may indicate that *P. aeruginosa* is inducing Cl^- via its LPS as a survival mechanism since it is recorded in the literature that several gram-negative bacteria, including *P. aeruginosa*, have strict dependence on Cl^- for growth and survival (247). This Cl^- flux has also been demonstrated to be crucial to neutrophil phagocytosis as engagement of the neutrophil membrane receptors by specific antigens results in induction of Cl^- secretion (248). The requirement of both

immune cells and *P. aeruginosa* for Cl^- for immune response and survival respectively seem conflicting. However, *P. aeruginosa* may be maintaining secretion of Cl^- at levels that are adequate for its survival.

4.5 CONCLUSION

In summary, we have established that LPS from *P. aeruginosa* can induce Cl^- conductance in both PMA-treated monocytic THP-1 cells and HPBMs and that this observed Cl^- movement is inhibited upon exposure to Cl^- channel inhibitors CFTR(inh)-172 (for CFTR) and DIDS (for ORCC). The possible role of PKA and CaN in LPS-dependent Cl^- conductance was also established based on the inhibition of LPS activation of Cl^- conductance by CsA and PKI. In addition, inhibition of Cl^- conductance in PMA-treated monocytic THP-1 cells and MDMs resulted in inhibition of the phagocytotic and the killing ability of these immune cells. This provides a possible explanation for the survival of *P. aeruginosa* as seen in CF.

4.5.1 SUMMARY OF KEY FINDINGS

1. LPS from *P. aeruginosa* induces Cl^- conductance in both PMA-treated monocytic THP-1 cells and HPBMs. This activation is sensitive to DIDS and CFTR(inh)-172.
2. PKA and CaN are involved in the observed *P. aeruginosa* LPS-activated Cl^- conductance.
3. Inhibition of Cl^- conductance inhibits PMA-treated monocytic THP-1 cells and MDMs phagocytotic ability.
4. *P. aeruginosa* have higher survival in MDMs than PMA-treated monocytic THP-1 cells when Cl^- conductance is inhibited.

CHAPTER 5

The role of Cl^- channels and cAMP/PKA/CaN in the release of cytokine by monocytes

5 INTRODUCTION

The CFTR channel is involved in ion transport and regulates fluid retention across the epithelial layer of the airway and the lungs. Patients found to have mutations in this ion channel express a dysfunctional CFTR protein that is unable to transport Cl^-. As such, these patients suffer from a dry and sticky epithelial surface owing to the dysfunction in the ability of the epithelial surface to retain fluid for optimal mucus secretion. The sticky surface thus provides an ideal environment for trapped bacteria to thrive due to poor elimination or antibacterial activities. This leads to infection and inflammatory response (249). In addition to the issues of excess fluid retention, the specific mutation in *CFTR*, F508Δ, causes improper folding of the protein and accumulation of the dysfunctional protein in addition to impaired ion transport (250). All these induce epithelial cell stress and activation of inflammatory responses. In addition to this, Cl^- transport, especially via CFTR, has been recently shown to modulate expression of specific Cl^- sensitive genes (251). As such, defects in CFTR may affect expression of such genes with severe physiological consequences.

A more direct involvement of the CFTR channel with the immune system has been reported in alveolar macrophages where LPS stimulation of the macrophages were found to induce expression of CFTR (219). The same study also concluded that mutation in CFTR or its inhibition in alveolar macrophages resulted in increased production of TNF-α, NF-κβ and expression of p38 MAPK. Additional studies have indicated increased intracellular Ca^{2+} levels, oxidative stress and activation of MAPK-AP and IKK-NF-κβ pathways in response to impaired Cl^- transport by CFTR (252-254).

In terms of the immune response of the body, monocytes are found circulating in the blood stream. These monocytes are sent to infected tissue and differentiate into macrophages which then serve as the first line of defence against pathogens. There is

evidence that when presented with LPS from *P. aeruginosa*, such macrophages – if they express deficient CFTR – produce high levels of cytokines (219). In addition, *P. aeruginosa* is responsible for the majority of infections and complications in CF patients. This bacteria often causes chronic infection and inflammation (255). Thus, in this study, LPS used was derived from *P. aeruginosa* to induce an inflammatory response in HPBMs. However, it is known that monocytes do not induce IL-1β secretion unless stimuli, such as nigericin or ATP, are used. This is because a stimulus is required to activate the caspase 1-dependent inflammasome pathway needed for proteolytic activation of IL-1 into IL-1β (256). This study has confirmed that nigericin is required as a stimulus to activate induction of IL-1β and TNF-α by HPBMs. To impair Cl^- transport, as seen in CF patients, the HPBMs were exposed to CFTR(inh)-172, which is a specific inhibitor of CFTR channels. In addition, to study the possible involvement of other Cl^- channels in pro-inflammatory cytokine release, DIDS was used to inhibit a proportion of ORCC. It is noteworthy that CFTR is not the only channel responsible for Cl^- transport with biological importance. ORCC is another group of Cl^- channels distinct from CFTR but which share the role of mediating Cl^- transport (257). ORCC inhibition has been implicated in inflammatory responses. This suggests that they play an important role in inflammation management. For example, DIDS inhibition of ORCC has been shown to result in inhibition of IL-12 expression (258). Another study has shown that blockage of ORCC may induce increased mucus secretion mediated by a resultant expression of pro-inflammatory cytokines (259).

5.1 AIM OF THIS STUDY

The main aim of this study is to investigate the role of PKA/CaN-regulated Cl^- channels in the release of the inflammatory cytokine IL-1β (and TNF-α as a control) by HPBMs.

5.2 Effect of CFTR(inh)-172, DIDS, PKI and CsA on the viability of HPBMs

To determine the potential effect on the viability of HPBMs, Cl^- channels (CFTR and ORCC) were inhibited at certain time points. The cells were exposed to CFTR(inh)-172 (10 μM) and DIDS (500 μM), inhibitors of CFTR and ORCC, respectively. Fig. 5-1A shows that for all the time points studied, there was no significant reduction in cell viability of the HPBMs for either inhibitor. The concentrations investigated for each of the inhibitors remained the same for other existing studies done within the time considered.

The effect of nigericin – an inducer of caspase-1 mediated proteolysis of IL-1 into IL-1β – on viability of HPBMs was tested. HPBMs were also exposed to CaN inhibitor (CsA at 1 μM) and protein kinase A inhibition (PKI at 100 nM) to check the effect of PKI and CsA on the cell viability. As shown in Fig. 5-1B, both CsA (1 μM) and PKI (100 nM) had no effect on cell viability at all the time-points studied when compared with the control.

It was shown by Gaidt et al. (2016) that partially differentiated THP-1 monocytes do not induce IL-1β secretion in response to LPS, except when the cells are primed with nigericin. Therefore, the effect of nigericin on the viability of HPBMs was examined in this study and no significant reduction in the cell viability was found (Fig. 5-1C). The possibility that HPBMs release IL-1β on exposure to LPS and other chemicals used in this study was also investigated: none of the reagents explored resulted in IL-1β release when compared with the control (LPS only). However, exposure of the HPBMs to a combination of LPS and nigericin resulted in highly significant induction of IL-1β release ($p < 0.0001$) (see Fig. 5-2).

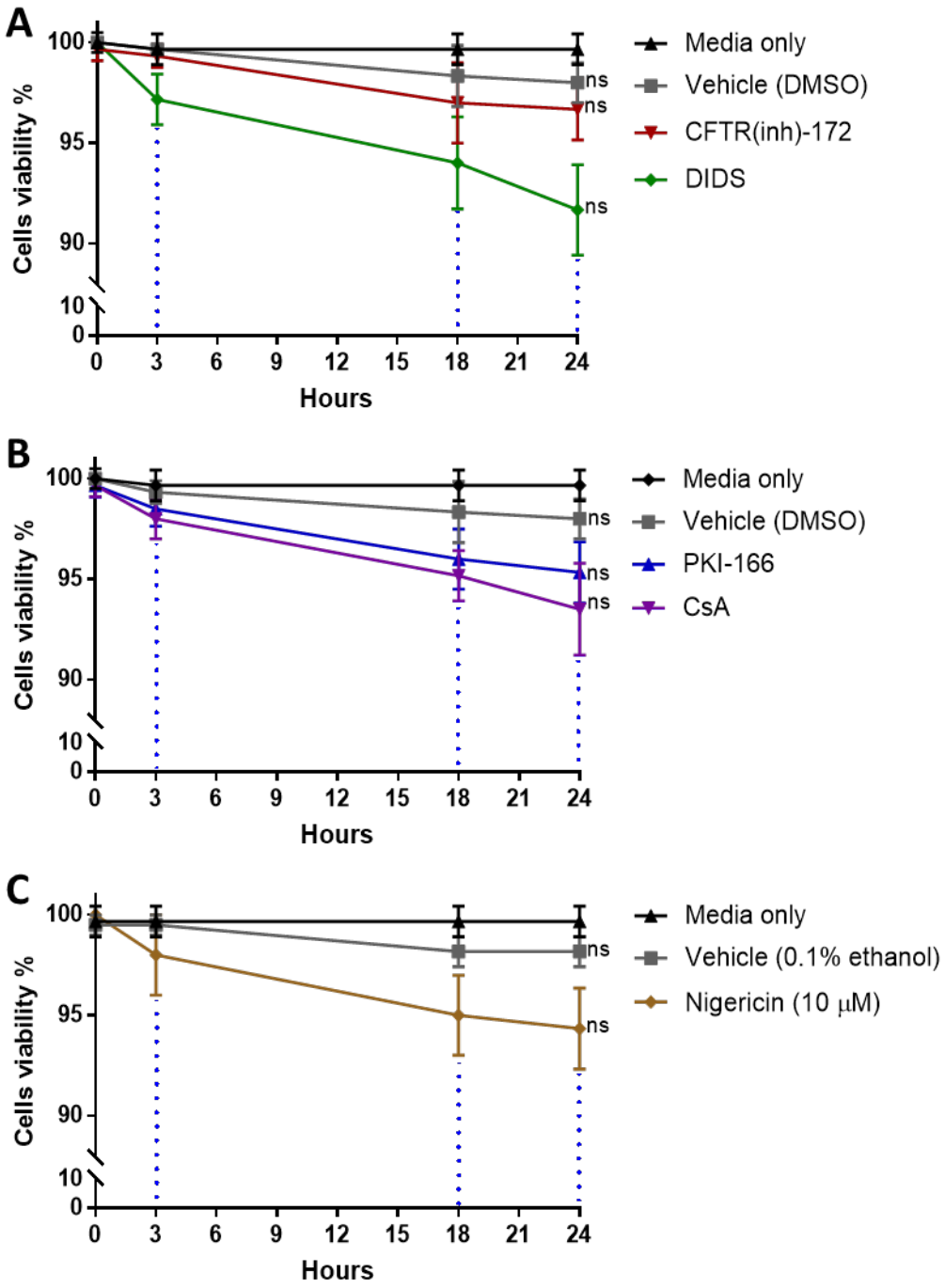

Figure 5-1. Effect of CFTR(inh)-172, DIDS, PKI, CsA and nigericin on viability of HPBMs.

HPBMs were seeded in 96 well plates overnight and then incubated with **(A)** vehicle (0.2% DMSO), CFTR(inh)-172 (10 μM), 4,4′-Diisothiocyanatostilbene-2,2′-disulfonic acid disodium salt hydrate (DIDS) at 500 μM; **(B)** cAMP-dependent protein kinase A inhibitor (PKI) at 100 nM and Cyclosporin A (CsA) at 1 μM; **(C)** Vehicle (0.1% ethanol) and 10 μM of nigericin. Cell viability was measured colorimetrically with MTS-based assay after 3, 18 and 24 hours at 490 nm. The results represent mean ± SEM from n=3 independent biological repeats. All samples were run in triplicate. ^{ns} indicates a non-significant difference.

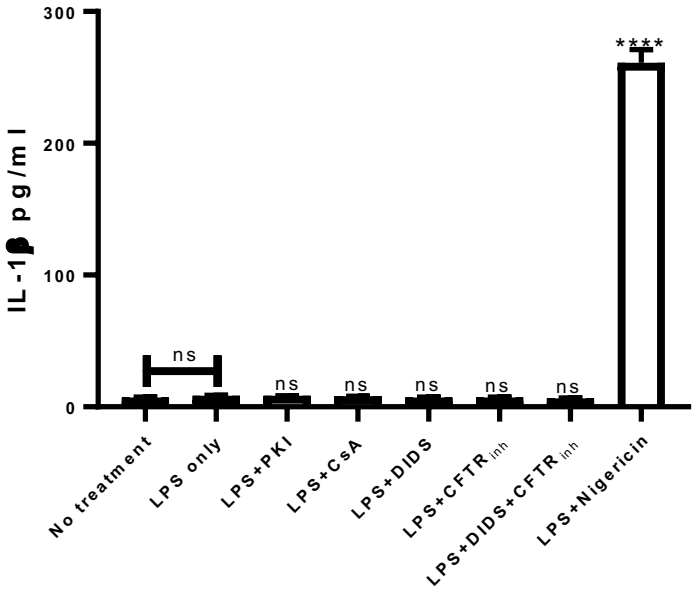

Figure 5-2. Impact of nigericin on IL-1β production in HPBMs.

HPBMs were primed with LPS from *P. aeruginosa* (30 μg/ml) for 2 hours and then incubated with nigericin (10 μM), PKI (100 nM), CsA (1 μM), DIDS (500 μM), CFTR(inh)-172 (10 μM) or both DIDS & CFTR(inh)-172 for 1 more hour then the supernatant was collected. IL-1β in supernatant was measured using ELISA (R&D Systems, MN, US). The statistical analysis was performed using one-way ANOVA with Bonferroni correction for multiple comparisons. (n=6 independent biological repeats). All samples were run in triplicate. ^{ns} and **** indicate non-significant and $p < 0.0001$, respectively. $CFTR_{inh}$ indicates CFTR(inh)-172.

5.3 THE EFFECT OF PKA, CAN AND Cl^- CHANNEL INHIBITION ON IL-1B SECRETION

The data gathered from chapter 3 shows that PKA, CaN, and CFTR contributes to FSK/IBMX mediated Cl^- transport in HPBMs. Based on this finding, the effect of Cl^- transport on inflammatory responses of HPBMs to LPS extracted from *P. aeruginosa* was investigated. First, the effect of FSK/IBMX on LPS-induced inflammatory response in HPBMs was investigated (see Fig. 5-3A). Exposure to LPS only resulted in no effect on IL-1β secretion. The same is true of exposure of the HPBMs to LPS with FSK/IBMX or FSK/IBMX followed by nigericin. However, exposure to LPS followed by nigericin only resulted in a significant increase in IL-1β secretion. Interestingly, this secretion was further enhanced significantly when cells were pre-incubated with FSK/IBMX plus LPS for 2 hours before exposure to nigericin for a further 1 hour. This suggests that in HPBMs, cAMP plays an important role in the LPS-induced inflammatory response to nigericin (see Fig. 5-3).

To explore a role for CaN and PKA in inflammatory response of the HPBMs, the cells were either pre-treated with CsA, an inhibitor of CaN, or PKI, a PKA inhibitor, before exposure of the cells to LPS, FSK/IBMX and nigericin. Fig. 5-3A shows that exposure to FSK/IBMX, CsA, PKI and LPS in absence of nigericin did not result in any recognisable level of IL-1β secretion. However, pre-treatment of HPBMs with CsA or PKI for 30 mins before priming with LPS/nigericin plus FSK/IBMX for 2 hours followed by exposure to nigericin resulted in a drop in IL-1β secretion back to the level of LPS/nigericin only (Fig. 5-3B). This suggests that CaN and PKA may not play any role in LPS induced IL-1β secretion but only inhibits cAMP/PKA activity in HPBMs as both inhibitors could only suppress the effect of FSK/IBMX.

In the same manner as described previously, the role of CFTR and ORCC in LPS-induced inflammatory response was investigated. Fig. 5-3B shows that inhibition of CFTR

activity using CFTR(inh)-172 at 10 μM resulted in significant suppression of LPS/FSK/IBMX induced IL-1β secretion ($p < 0.0001$). However, this suppression was greater when the cells were exposed to either DIDS alone or a combination of DIDS and CFTR(inh)-172 ($p < 0.0001$). This finding suggests that Cl^- flux via CFTR and ORCC plays a vital role in LPS induced inflammatory response and IL-1β.

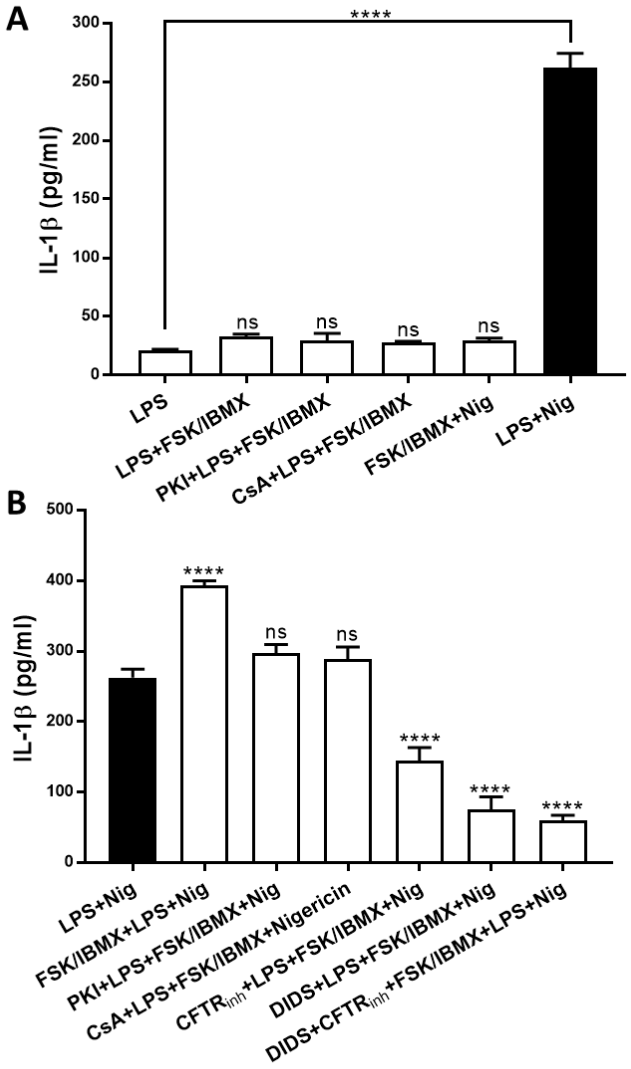

Figure 5-3. Treatment with FSK/IBMX-enhanced LPS/nigericin-dependent IL-1β release in HPBMs.

HPBMs were **(A)** primed with LPS from *P. aeruginosa* (30 μg/ml) for 3 hours; or LPS, FSK (10 μM) and IBMX (100 μM) for 3 hours; or pre-incubated with PKI (100 nM) or CsA (1 μM) for 30 min before being primed with LPS and FSK/IBMX for 3 hours; or FSK/IBMX for 2 hours followed by incubation with 10 μM nigericin (Nig) for 1 hour. **(B)** HPBMs primed with LPS only for 2 hours followed by Nig for 1 hour were used as a control. Cells were stimulated with FSK/IBMX and LPS for 2 hours followed by Nig for 1 hour; or pre-incubated with CsA or PKI for 30 min before being primed with LPS and FSK/IBMX for 2 hours followed by Nig for 1 hour; or pre-incubated with 10 μM of CFTR(inh)-172, DIDS (500 μM) or combination of DIDS & CFTR(inh)-172 for 30 min before being primed with LPS and FSK/IBMX for 2 hours followed by Nig for 1 hour. The release of IL-1β was evaluated using ELISA (R&D Systems, MN, US). The statistical analysis was performed using one-way ANOVA with Bonferroni correction for multiple comparisons. The results represent mean ± SEM from n=3 independent biological repeats. All samples were run in triplicate. ^{ns} and **** signify non-significant and $p < 0.001$, respectively.

5.4 Further characterisation of the impact of CFTR(inh)-172 and DIDS induction of IL-1b and TNF-a secretion using flow cytometry

We sought to further validate the results outlined in the previous section using a different approach. Thus, to further investigate the effects of DIDS-sensitive ORCC-mediated ion transport on IL-1β and TNF-α secretion, HPBMs were exposed to varying concentrations of DIDS before exposure to LPS and nigericin. Secretion of IL-1β and TNF-α was analysed using flow cytometry. Fig. 5-4A shows a dose-dependent decrease in IL-1β release from HPBMs treated with DIDS. Compared with the control (LPS and nigericin only), the decrease in IL-1β release was significant when the cells were exposed to DIDS concentrations above 62.5 μM with the highest response at 500 μM. On the other hand, when compared with control cells exposed to LPS and nigericin only, there was a steady dose-dependent increase in TNF-α secretion from DIDS 31.25 μM to 500 μM with the highest release at 500 μM (see Fig. 5-4B). Similarly, the increase in TNF-α was significant from 62.5 μM to 500 μM. These findings show that while inhibition of ORCC channel suppresses induction of IL-1β, it has a stimulatory effect on TNF-α.

Similarly, the effect of CFTR inhibition (CFTR(inh)-172) on IL-1β and TNF-α secretion was analysed using flow cytometry. HPBMs were pre-treated with varying concentrations of CFTR(inh)-172 from 1.5 μM to 30 μM and were co-stimulated with LPS and nigericin. Fig. 5-5 shows that at concentrations above 5 μM CFTR(inh)-172 there was a dose-dependent significant reduction in IL-1β secretion. On the other hand, a significant reduction in TNF-α secretion was observed when cells were treated with 2.5 to 30 μM CFTR(inh)-172 with TNF-α secretion being very sensitive to CFTR(inh)-172 exposure based on response at 2.5 μM. This indicates that CFTR inhibition inhibits IL-1β secretion, but unlike ORCC inhibition, it also inhibits the secretion of TNF-α.

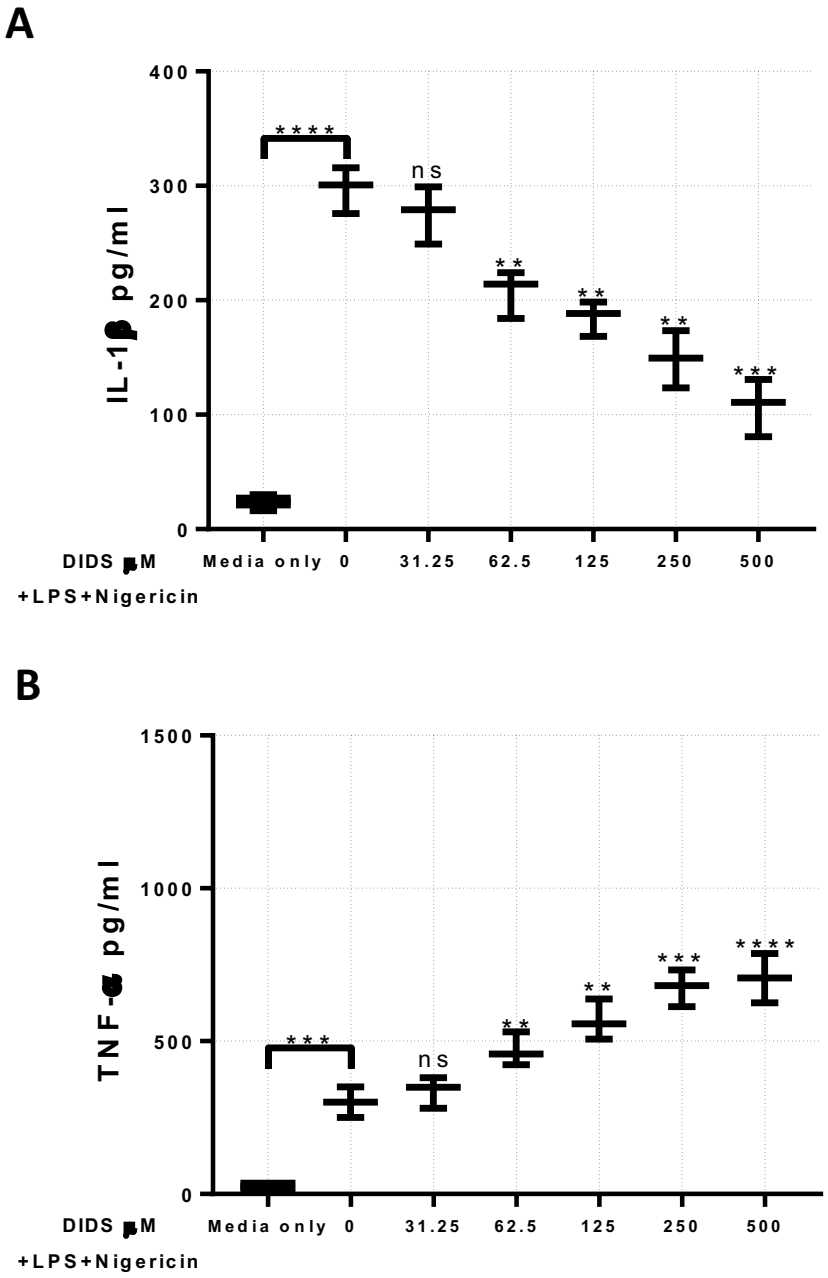

Figure 5-4. Dose-response curve of the impact of DIDS on IL-1β and TNF-α production by HPBMs.

HPBMs were pre-incubated with DIDS at 0, 31.25, 62.5, 125, 250 and 500 μM for 30 min before being primed with LPS from *P. aeruginosa* (30 μg/ml) for 2 hours followed by nigericin (10 μM) for 1 hour. The release of **(A)** IL-1β and **(B)** TNF-α was measured with a cytometric bead array (CBA) system from BD Bioscience (Jan jose, Ca, US). Statistical analysis was conducted using one-way ANOVA. (± SEM from n=3 independent biological repeats). All samples were run in triplicate. ^{ns}, **, *** and **** signify non-significant, $p < 0.01$, $p < 0.001$ and $p < 0.0001$, respectively.

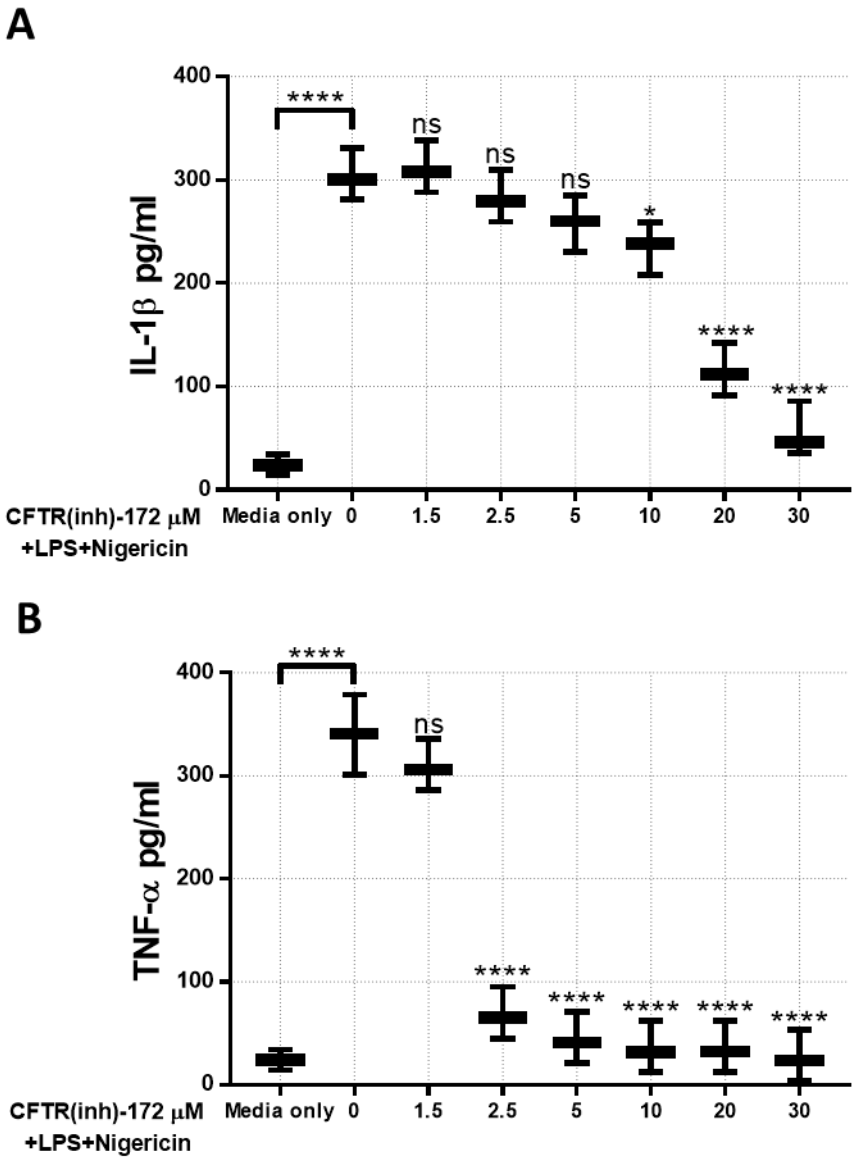

Figure 5-5. Dose-response curve of the impact of CFTR(inh)-172 (0-30 μM) on IL-1β and TNF-α production by HPBMs.

HPBMs were pre-incubated with CFTR(inh)-172 at 0, 1.5, 2.5, 5, 10, 20 and 30 μM for 30 min before being primed with LPS from *P. aeruginosa* (30 μg/ml) for 2 hours followed by nigericin (10 μM) for 1 hour. The release of **(A)** IL-1β and **(B)** TNF-α was measured using a cytometric bead array (CBA) system from BD Bioscience (Jan jose, Ca, US). Statistical analysis was conducted using one-way ANOVA. (± SEM from n=3 independent biological repeats and all samples were run in triplicate). ^{ns}, * and **** signify non-significant, $p \leq 0.05$ and $p < 0.001$, respectively.

A difference in the responses of HPBMs to both DIDS and CFTR(inh)-172 with respect to TNF-α secretion was noticed. As a result of this difference, the combined effect of both CFTR(inh)-172 and DIDS on the cells was examined. As was done previously, HPBMs were exposed to a combination of CFTR(inh)-172 (10 μM) and DIDS (500 μM) and then primed and stimulated with LPS (30 μg/ml) and nigericin (10 μM). This was followed by analysis of IL-1β and TNF-α secretion using flow cytometry (see Fig. 5-6A and C) and with ELISA for IL-1β secretion as a confirmation (see Fig. 5-6B). As expected, Fig. 5-6A shows that LPS/nigericin alone significantly induced secretion of IL-1β ($p < 0.0001$) and that CFTR(inh)-172 significantly reduced LPS/nigericin-induced secretion of IL-1β ($p \leq 0.05$). Furthermore, there was a highly significant reduction in IL-1β secretion when the HPBMs were pre-exposed to DIDS alone ($p < 0.01$), and both DIDS and CFTR(inh)-172 ($p < 0.0001$) prior to stimulation with LPS/nigericin. This result was verified by collecting supernatant from the cells (under the same condition) for ELISA analysis: although CFTR(inh)-172 or DIDS alone significantly inhibited IL-1β secretion ($p \leq 0.05$) and ($p < 0.01$), respectively (see Fig. 5-6B), a combination of both CFTR(inh)-172 and DIDS had an additive effect and resulted in further inhibition of IL-1β secretion ($p < 0.0001$) (see Fig. 5-6B).

With regard to TNF-α, treatment with LPS/nigericin induced significant secretion ($p < 0.001$) in HPBMs compared to untreated control cells. However, CFTR(inh)-172 only significantly inhibited TNF-α secretion ($p \leq 0.05$) while a combination of CFTR(inh)-172 and DIDS had no impact on the level of TNF-α secretion when compared to cells treated with LPS/nigericin alone. Exposure of HPBMs to DIDS alone resulted in a significant increase ($p < 0.0001$) in TNF-α secretion (see Fig. 5-6C). These findings suggest that while both CFTR and ORCC play a role in regulation of TNF-α secretion, the impact of the two channels is inversely correlated.

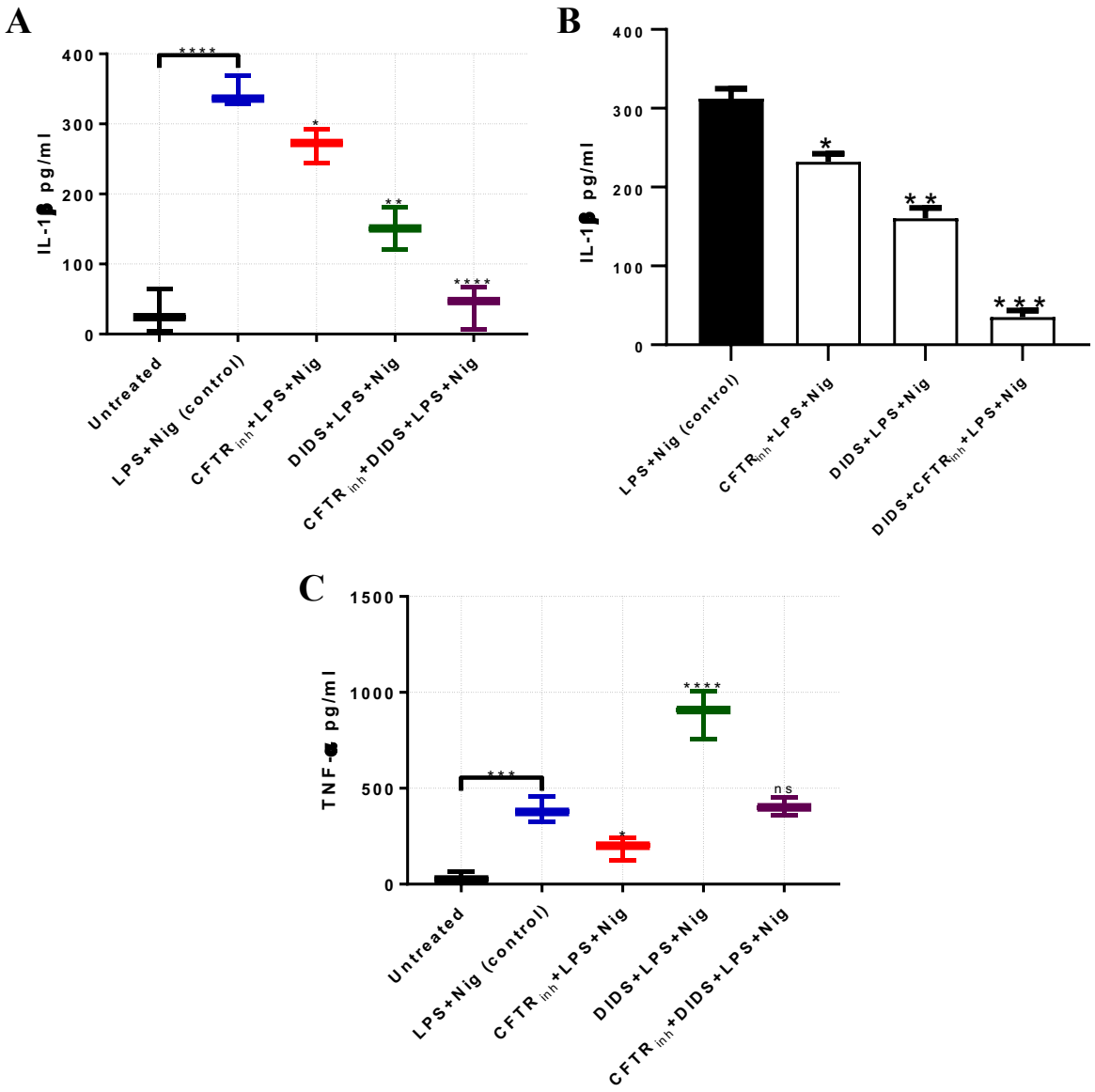

Figure 5-6. Impact of DIDS-sensitive ORCC and CFTR channels on LPS/nigericin-dependent IL-1β and TNF-α production by HPBMs.

HPBMs were pre-incubated with CFTR(inh)-172 at 10 µM, DIDS at 500 µM, or a combination of CFTR(inh)-172 and DIDS for 30 min before being primed with LPS from *P. aeruginosa* (30 µg/ml) for 2 hours followed by nigericin (Nig) at 10 µM for 1 hour. Cells primed with LPS only followed by nigericin were used as a control. The release of IL-1β was measured using a cytometric bead array (CBA) **(A)** system from BD Bioscience and the results confirmed using ELISA (R&D Systems, MN, US) **(B)**. The release of TNF-α was also measured using a cytometric bead array (CBA) system from BD Bioscience **(C)**. The statistical analysis was performed using unpaired *t*-test and one-way ANOVA. (± SEM from n=4 independent biological repeats. All samples were run in triplicate). ^{ns}, *, **, *** and **** signify non-significant, $p \leq 0.05$, $p < 0.01$, $p < 0.001$ and $p < 0.0001$, respectively. $CFTR_{inh}$ indicates CFTR(inh)-172.

5.5 PKI AND CYCLOSPORIN A (CSA)-ENHANCED LPS/NIGERICIN-INDUCED IL1-B SECRETION

We have demonstrated that inhibition of CFTR-mediated ion transport inhibits IL-1β secretion. However, CFTR is known to be regulated by protein kinase A (PKA) and PKC (260). Thus, we investigated whether inhibition of PKA and CaN would impact LPS/Nigericin induced IL-1β secretion. HPBMs were pre-exposed to PKA inhibitor (PKI) or CaN inhibitor (CsA) before stimulation with LPS/nigericin, and the secretion of IL-1β was measured using ELISA and flow cytometry. As shown in Fig. 5-7A1-2 and B1-2, flow cytometric and ELISA analyses indicate that treatment of the HPBMs with PKI and LPS alone did not significantly induce IL-1β secretion compared to the control. Interestingly, a slight enhancement in LPS/nigericin-induced IL-1β secretion in cells pre-exposed to PKI or CsA was observed ($p \leq 0.05$). On the other hand, as regards TNF-α, pre-incubation of HPBMs with either PKI or CsA and LPS/nigericin resulted in significant enhancement of LPS/nigericin-induced TNF-α secretion compared to the control (see Fig. 5-7A3 and B3). This shows that inhibition of PKA or CaN impacts the effect of LPS in inducing inflammatory responses in HPBMs as opposed to our hypothesis that inhibition of both CaN and PKA would result in suppression of inflammatory response since CsA and PKI were able to block Cl^- transport mediated by CFTR and DIDS-sensitive ORCC.

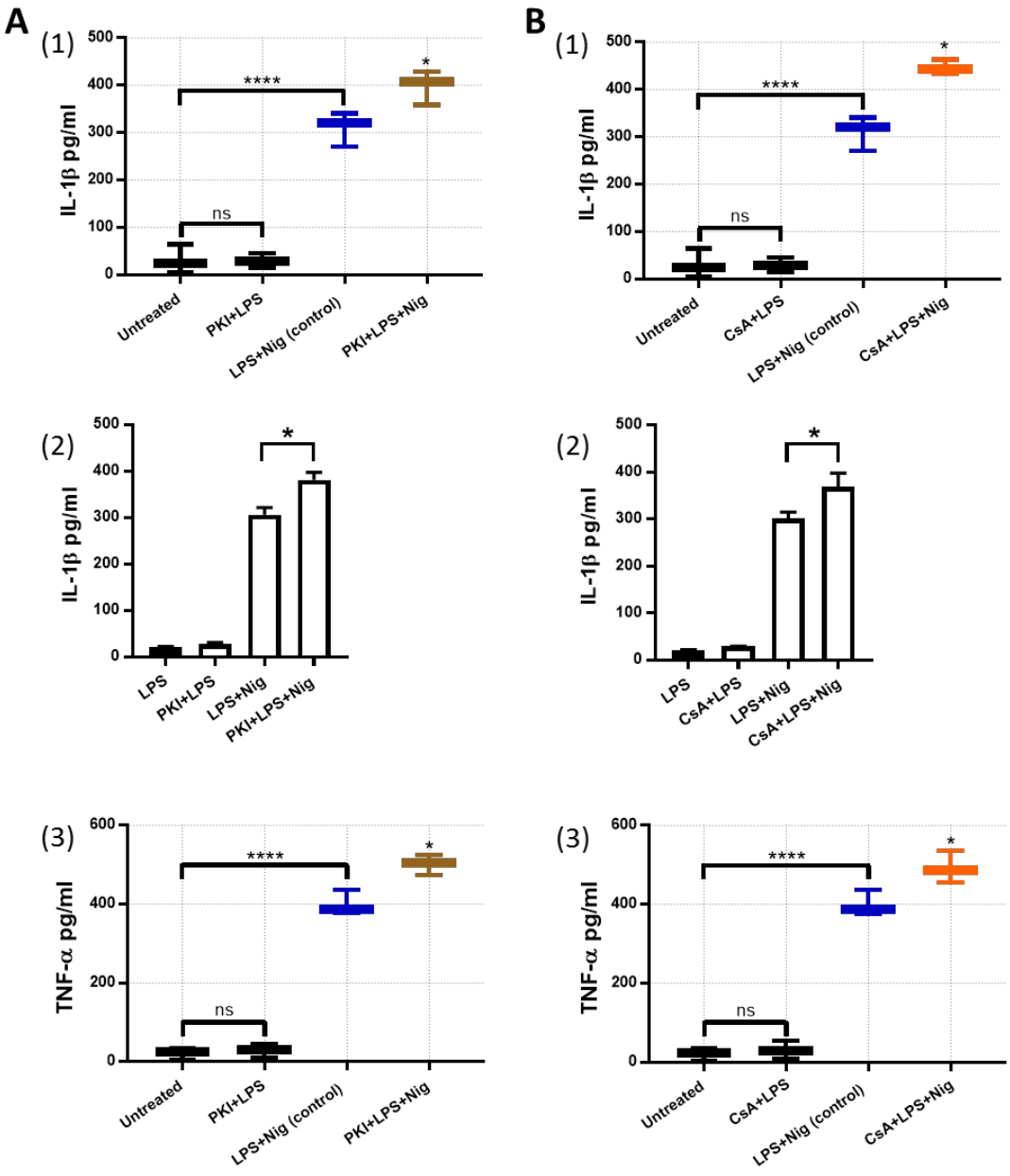

Figure 5-7. Pre-treatment with PKI or CsA-induced LPS/nigericin-dependent IL-1β and TNF-α release by HPBMs.

HPBMs were pre-incubated with 100 nM of PKI **(A)** or 1 µM of CsA **(B)** for 30 min before being primed with LPS from *P. aeruginosa* (30 µg/ml) for 2 hours followed by incubation with nigericin (Nig) at 10 µM for 1 hour. Cells primed with LPS only followed by nigericin were used as control. The release of IL-1β **(A1 and B1)** and TNF-α **(A3 and B3)** were measured using a cytometric bead array (CBA) system from BD Bioscience. The experiment was repeated biologically to validate the release of IL-1β and was measured using ELISA (R&D Systems, MN, US) for confirmation **(A2 and B2)**. The statistical analysis was performed using one-way ANOVA. (± SEM from n=6 independent biological repeats. All samples were run in triplicate). ^{ns}, * and **** signify non-significant, $p \leq 0.05$ and $p < 0.001$, respectively.

5.6 A COMBINATION OF BOTH CFTR(INH)-172 AND DIDS BLOCKS PKI ENHANCEMENT OF IL-1B AND TNF-A SECRETION, BUT NOT CFTR(INH)-172 OR DIDS ALONE

After showing that PKI and CsA enhance LPS/nigericin-induced secretion of IL-1β and TNF-α, the effect of inhibition of ORCC, CFTR or both on the secretion of the inflammatory molecules was investigated. To do this, HPBMs were primed with LPS and nigericin to induce expression of the inflammatory molecules, after which the cells were exposed to either of DIDS, or CFTR(inh)-172, or a combination of both in the presence of PKI. These cells were then analysed using flow cytometry. The results shown in Fig. 5-8 indicate that exposure of the HPBMs to DIDS did not affect the PKI impact in enhancing LPS/nigericin-dependent IL-1β induction.

After discovering that DIDS had no effect on PKI enhancing effect on the inflammatory response of LPS/nigericin, the effect of CFTR(inh)-172 on HPBMs stimulated with PKI/LPS/nigericin was investigated. Just as with DIDS, pre-exposure of the cells primed with PKI/LPS/nigericin to CFTR(inh)-172 also had no effect on IL-1β induction compared to cells unexposed to CFTR(inh)-172 (see Fig. 5-8). However, exposure of the HPBMs to CFTR(inh)-172 in the presence of PKI and DIDS resulted in a significant drop in IL-1β level ($p < 0.0001$) (see Fig. 5-8).

As shown in Fig. 5-9, PKI significantly induced secretion of TNF-α compared to unexposed HPBMs. Interestingly, exposure of the HPBMs to DIDS did not affect PKI-dependent induction of TNF-α. However, CFTR(inh)-172 or combination of both CFTR(inh)-172 and DIDS significantly suppressed PKI-dependent enhancement of TNF-α secretion ($p < 0.0001$) (see Fig. 5-9).

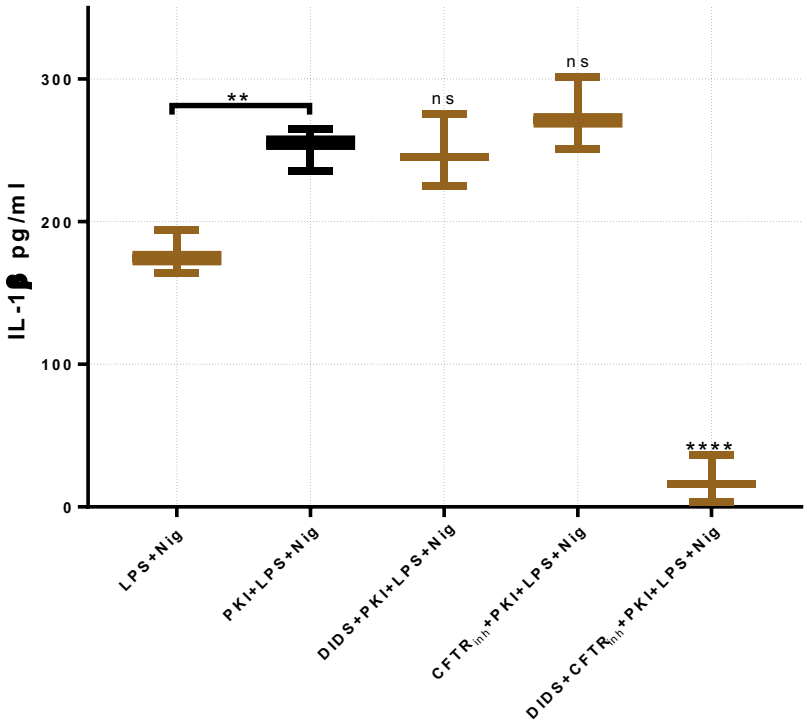

Figure 5-8. The role of DIDS-sensitive ORCC and CFTR channels in PKI/LPS/nigericin-dependent IL-1β release by HPBMs.

HPBMs primed with *P. aeruginosa* LPS only followed by nigericin (Nig) were used as the control. Cells were pre-incubated with PKI (100 nM), PKI and DIDS (500 µM), PKI and CFTR(inh)-172 (10 µM), or PKI and combination of both DIDS and CFTR(inh)-172 for 30 min before being primed with LPS from *P. aeruginosa* (30 µg/ml) for 2 hours followed by nigericin (Nig) at 10 µM for 1 hour. The release of IL-1β was measured using a cytometric bead array (CBA) system from BD Bioscience. The statistical analysis was conducted using one-way ANOVA with Bonferroni correction for multiple comparisons. (± SEM from n=3 independent biological repeats. All samples were run in triplicate). ^{ns}, ** and **** signify non-significant, $p \leq 0.01$ and $p < 0.0001$, respectively. $CFTR_{inh}$ indicates CFTR(inh)-172.

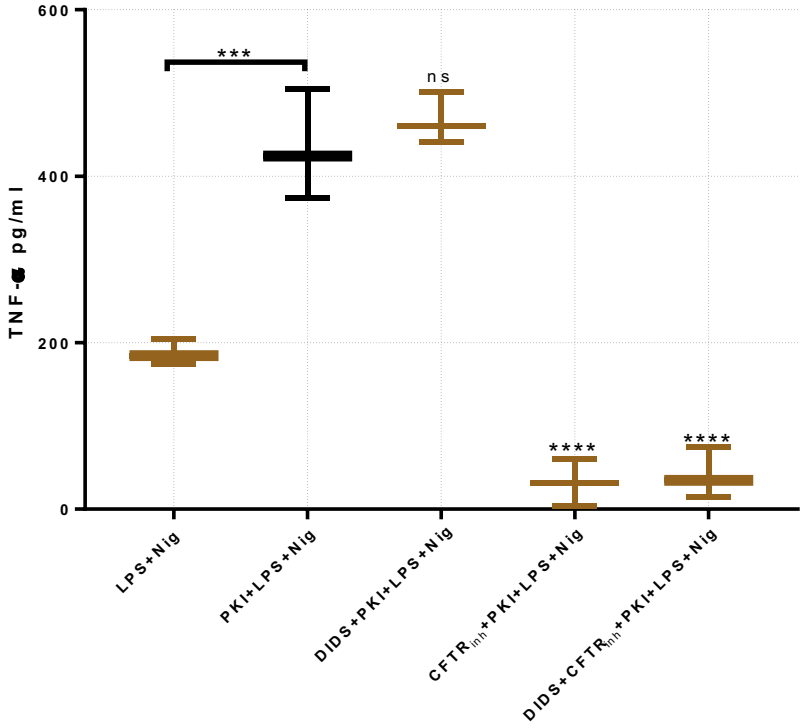

Figure 5-9. The role of DIDS-sensitive ORCC and CFTR channels in PKI/LPS/nigericin-dependent TNF-α release by HPBMs.

HPBMs primed with *P. aeruginosa* LPS only followed by nigericin (Nig) were used as the control. Cells were pre-incubated with PKI (100 nM), PKI and DIDS (500 µM), PKI and CFTR(inh)-172 (10 µM), or PKI and combination of both DIDS and CFTR(inh)-172 for 30 min before being primed with LPS from *P. aeruginosa* (30 µg/ml) for 2 hours followed by nigericin (Nig) at 10 µM for 1 hour. The release of TNF-α was measured using a cytometric bead array (CBA) system from BD Bioscience. The statistical analysis was conducted using one-way ANOVA with Bonferroni correction for multiple comparisons. (± SEM from n=3 independent biological repeats. All samples were run in triplicate). ^{ns}, *** and **** signify non-significant, $p < 0.001$ and $p < 0.0001$, respectively. $CFTR_{inh}$ indicates CFTR(inh)-172.

Following an investigation of the effect of DIDS and CFTR inhibitor on PKI-dependent induction of IL-1β and TNF-α secretion in HPBMs, the effect of both inhibitors on CsA-dependent elevation of both IL-1β and TNF-α secretion was investigated. As described previously, HPBMs were exposed to CsA and pre-treated with either DIDS or CFTR(inh)-172 or a combination of both before being primed with LPS and nigericin. As shown in Fig. 5-10, the flow cytometric analysis indicated that exposure of the cells to DIDS or CFTR(inh)-172 and post-treatment with CsA did not have any effect on IL-1β induction. However, combinational pre-exposure of the LPS/nigericin-primed cells to CsA and both CFTR(inh)-172 and DIDS resulted in significant suppression of IL-1β induction ($p < 0.0001$) (see Fig. 5-10).

Evaluation of the impact of DIDS and CFTR(inh)-172 on the CsA-mediated induction of TNF-α secretion showed that DIDS exposure did not affect the CsA-dependent TNF-α induction (Fig. 5-11). Contrastingly, CFTR(inh)-172 and a combination of CFTR(inh)-172 and DIDS did significantly inhibit CsA-dependent TNF-α induction ($p < 0.0001$) (see Fig. 5-11).

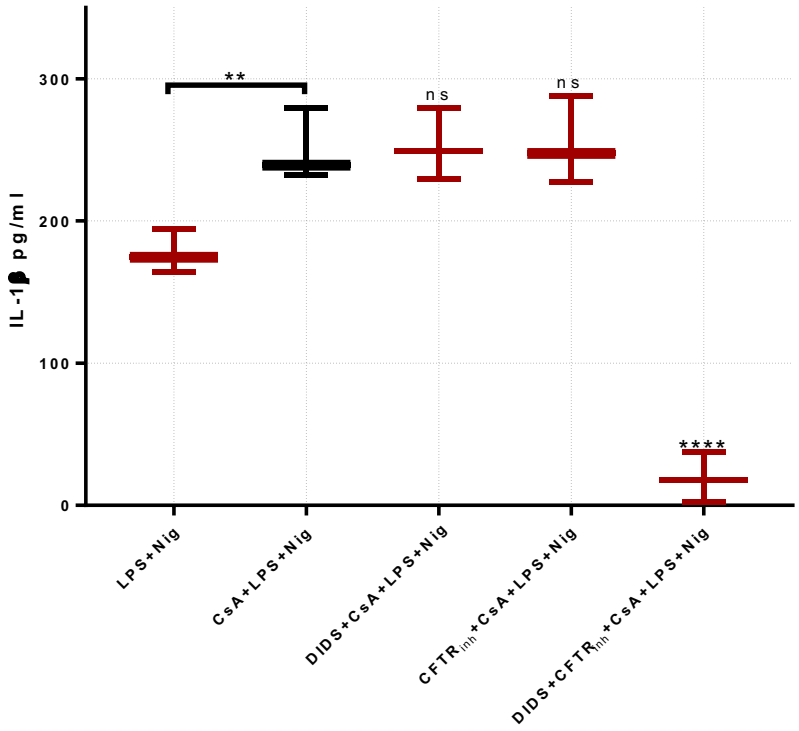

Figure 5-10. The effect of DIDS-sensitive ORCC and CFTR channels on CsA/LPS/nigericin-dependent IL-1β release by HPBMs.

HPBMs primed with *P. aeruginosa* LPS only followed by nigericin (Nig) were used as the control. Cells were pre-incubated with CsA (1 µM), CsA and DIDS (500 µM), CsA and CFTR(inh)-172 (10 µM), or CsA and a combination of both DIDS and CFTR(inh)-172 for 30 min before being primed with LPS from *P. aeruginosa* (30 µg/ml) for 2 hours followed by nigericin (Nig) at 10 µM for 1 hour. The release of IL-1β was measured using a cytometric bead array (CBA) system from BD Bioscience. The statistical analysis was conducted using one-way ANOVA with Bonferroni correction for multiple comparisons. (± SEM from n=3 independent biological repeats. All samples were run in triplicate). ^{ns}, ** and **** signify non-significant, $p \leq 0.01$ and $p < 0.0001$, respectively. $CFTR_{inh}$ indicates CFTR(inh)-172.

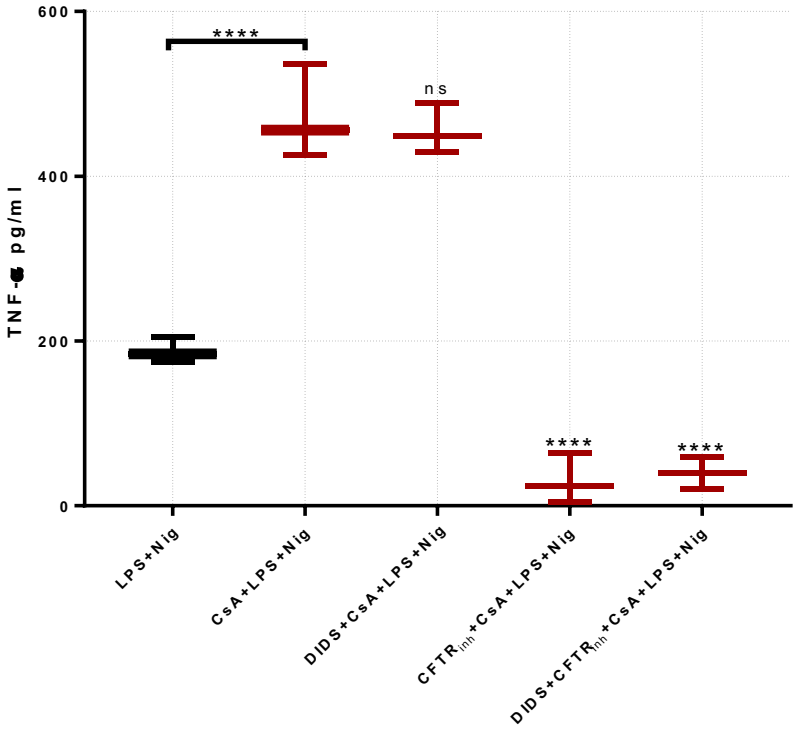

Figure 5-11. The effect of DIDS-sensitive ORCC and CFTR channels on CsA/LPS/nigericin-dependent TNF-α release by HPBMs.

HPBMs primed with *P. aeruginosa* LPS only followed by nigericin (Nig) were used as the control. Cells were pre-incubated with CsA (1 µM), CsA and DIDS (500 µM), CsA and CFTR(inh)-172 (10 µM), or CsA and a combination of both DIDS and CFTR(inh)-172 for 30 min before being primed with LPS from *P. aeruginosa* (30 µg/ml) for 2 hours followed by nigericin (Nig) at 10 µM for 1 hour. The release of TNF-α was measured using a cytometric bead array (CBA) system from BD Bioscience. The statistical analysis was conducted using one-way ANOVA with Bonferroni correction for multiple comparisons. (± SEM from n=3 independent biological repeats. All samples were run in triplicate). ^{ns} and **** signify non-significant and $p < 0.0001$, respectively. $CFTR_{inh}$ indicates CFTR(inh)-172.

5.7 DISCUSSION

In the initial phase of this study, the impact of these inhibitors (PKI, CsA, CFTR(inh)-172 and DIDS) on cell viability at maximum concentrations possible was investigated to establish a time-point effective enough to inhibit ion transport but not so high that it would significantly affect cell viability. It was found that all the inhibitors did not significantly affect cell viability even after 24 hours of exposure. Following this finding, the dose-dependent inflammatory responses of the LPS/nigericin-primed HPBMs in the presence of the varying concentrations of CFTR(inh)-172 and DIDS was examined. Our findings showed a dose-dependent decrease in IL-1β for both DIDS and CFTR(inh)-172. In the same manner, pre-treatment of the cells with CFTR(inh)-172 resulted in significant reductions in the TNF-α level while pre-exposure to DIDS alone increased TNF-α secretion. This finding shows inhibition of ORCC ion transport stimulates TNF-α secretion but not IL-1β.

These findings are supported by the findings of Perregaux et al. (261), who show that DIDS inhibits IL-1β post-translational processing, resulting in reduced IL-1β secretion in T cells. Moreover, a more recent study showed that DIDS protects neuronal cell injury by inhibiting gene expression of IL-1β (262). This could mean that ion transports through ORCC may help in mediating secretion of IL-1β by enhancing post-translational processing of its mRNA. However, DIDS-induced inhibition of anion transport enhances secretion of TNF-α, which indicates an inverse association between TNF-α secretion and anion transport mediated by DIDS-sensitive ORCC. In another study, chemical inhibition of CFTR was shown not to affect IL-1β induction in THP-1 cells that were primed with ATP (263). At this point, the reason for this difference is unknown. However, the use of live *P. aeruginosa* rather than the *P. aeruginosa*-extracted LPS for monocyte infection could have resulted in the higher inflammatory response observed by Tang et al. (263).

This only explains induction of IL-1β, not TNF-α. It was found that TNF-α induction was suppressed in response to CFTR(inh)-172 but increased upon exposure of the HPBMs to DIDS. This is clearly in contrast to the findings of Gao and Su (219), who found that CFTR plays a role in the acute inflammatory response of alveolar and peritoneal macrophages as inhibition of CFTR in these cells resulted in a marked increase in TNF-α secretion. However, the difference in cell type may be the cause of the different response observed in our study since monocytes are known to have differing responses to LPS-induced inflammatory response compared to macrophages (264). However, a previous study has shown that 500 μM DIDS, as used in this study, resulted in induction of TNF-α secretion in PMA-differentiated macrophages (265). A possible reason for this could be that Cl^- conductance through Cl^- channels other than the ORCC is capable of inducing the observed TNF-α induction.

TNF-α is also known to have multiple roles in regulation of cellular homeostasis. TNF-α has been used to induce NF-kβ inflammation in response to *P. aeruginosa* infection of airway epithelial cells after CFTR inhibition (266). In addition to this, Oprins et al. (267) and (268) showed that, in the human colonic cancer cell line HT29cl.19A and a porcine intestinal cell line, TNF-α induces ion transport due to a rise in PKC level in the phospholipase D (PLD) pathway. Interestingly, a previous study has also shown that PMA induces PLD expression in a NF-kβ-dependent manner in colon cancer cells (269). As such, different unknown factors in this complex signalling involving TNF-α may be contributing to the varying responses observed based on the feedback regulatory loop due to PMA stimulation. The increased TNF-α induction in response to DIDS may represent the inflammation seen in CF as ORCC defects have been reported in tissue sections from CF patients (270). However, the opposite observation in response to CFTR inhibition may

mean that CFTR does not play a role in TNF-α secretion in the HPBMs while other Cl^- channels that are sensitive to DIDS may be sufficient to cause TNF-α induction.

cAMP and PKA are both important components of the signalling pathway involved in IL-1β secretion (271), and we have previously shown that PKA and CaN play a role in DIDS-sensitive ORCC and CFTR-dependent ion transport (see chapter 3). Interestingly, previous studies have shown that PKA and CFTR are required for ORCC activity, further linking the two Cl^- channels functionally in the cAMP/PKA signalling pathway (270, 223). Thus, the role of PKA and CaN in the inflammatory response of HPBMs upon exposure to LPS from *P. aeruginosa* was investigated. It was first investigated whether activation of CaN by FSK/IBMX would enhance IL-1β induction since FSK/IBMX is an inducer of CaN. It was found that CaN activation by FSK/IBMX did indeed induce more IL-1β secretion. It was also confirmed that CaN inhibition by CsA in the presence of FSK/IBMX significantly suppressed IL-1β induction. In addition, DIDS and CFTR(inh)-172, together and individually, significantly suppressed IL-1β induction in the presence of CsA. It was then investigated whether inhibition of CaN would result in suppression of IL-1β and what impact CFTR(inh)-172 and DIDS would have on this. It was found that inhibition of CaN produced the same response both in presence of CFTR(inh)-172 together with DIDS and also both individually. This was the first suggestion that the inflammatory response may be independent of CaN. It was also discovered that inhibition of cAMP/PKA-dependent activities by PKI resulted in a significant increase in secretion of both IL-1β and TNF-α in HPBMs primed with LPS/nigericin, showing that cAMP/PKA are likely inhibitors of the inflammatory response. This contradicts the report of Oprins et al. (267) and (272) who found that PKA inhibition resulted in inhibition of TNF-α activities. In addition, CsA, an inhibitor of CaN, also resulted in enhancement of LPS/nigericin-dependent IL-1β and TNF-α release by HPBMs. This result shows that

cAMP/PKA signalling through CaN may cause a slight enhancement of IL-1β and TNF-α secretion. This further confirms the result from exposure to PKI. On the contrary, inhibition of protein kinase A by PKI has been previously shown to result in suppression of LPS-induced IL-1β secretion in peritoneal macrophages (273). In fact, another study showed that PKA activation resulted in inhibited expression of both TNF-α and IL-1β in macrophages (274) while another study also reported inhibited expression of TNF-α upon PKA inhibition (275). The reason for the contrasting observation in our study is unknown at this point, but these findings also suggest that CFTR interaction with PKA/CaN may be necessary for CFTR ion transport in CF but not the inflammatory response.

Other factors which may be responsible for the contrasting findings in our pro-inflammatory cytokines releases study were also investigated. Hence, involvement of other Cl^- channels in this respect, as well as whether PKA and CaN are involved in this pathway, were investigated by evaluating the role of DIDS-sensitive ORCC in addition to CFTR-dependent ion transport. It was found that exposure to CFTR(inh)-172 alone, and both CFTR(inh)-172 and DIDS totally blocked IL-1β and TNF-α induction, irrespective of PKI or CsA exposure. This finding shows that PKA/CaN signalling does not influence DIDS-sensitive ORCC and CFTR for the secretion of both IL-1β and TNF-α in HPBMs. Inhibition of PKA and CaN signalling by PKI and CsA resulted in a slight enhancement of LPS/nigericin-dependent pro-inflammatory cytokine release. However, these inflammatory responses were completely blocked by inhibiting CFTR and ORCC channels. This could mean that the observed inflammatory response is independent of PKA signalling since inhibition of PKA alone resulted in enhancement of IL-1β and TNF-α secretion while inhibition of CFTR and ORCC was the stimulus that blocked this inflammatory response. This provides an alternative pathway for Cl^- transport not requiring PKA or CaN signalling for inflammation, contrary to what was expected based

on evidence in the literature - cAMP/PKA or CaN mediates phosphorylation of CFTR on several residues to activate CFTR ion transport (172, 35). The reason for this variation is not known but may be the result of different responses between monocytes and macrophages as these cells are known to have differing responses to LPS effects (276). While the concentration of PKI and CsA used in this study may be high enough to partially inhibit DIDS-sensitive ORCC and CFTR, other pathways involving CaN may have been activated as CaN inhibition by CsA is known to have multiple effects which are poorly understood (277). As such, the concentrations of CsA and PKI were enough to inhibit the function of CFTR and ORCC (as seen in chapter 4, 4.2), but may need to be increased to totally block cytokine release from the HPBMs, as seen with CFTR(inh)-172 and DIDS, and cell viability must be taken in the account for higher concentrations. In addition to this, nigericin was used to induce proteolysis and maturation of pro-IL-1β into IL-1β. Nigericin is a potassium ionophore and the increase in intracellular concentration of K^+ in response to nigericin could have perturbed the Ca^{2+} balance, resulting in IL-1β secretion. Nigericin is also known to induce activation of NALP3 inflammasome: NALP3 activation is known to be highly active in monocytes (278). This could be the reason for the contrasting findings for PKI and CsA between this and previous studies.

CFTR(inh)-172 alone was able to block CsA-dependent and PKI-dependent enhancement of TNF-α secretion. Interestingly, inhibition of Cl^- transport by CFTR(inh)-172 alone and in combination with DIDS blocked CsA mediated enhancement of TNF-α secretion while IL-1β secretion was only blocked by combination of both CFTR(inh)-172 and DIDS. The reason for IL-1β secretion not being affected by CFTR inhibition is not known, but the requirement of CFTR inhibition for suppression of TNF-α suggests CaN interaction with CFTR may be sufficient for CFTR-dependent TNF-α release while the ORCCs may be required for IL-1β.

5.8 CONCLUSION

In conclusion, we have shown that CFTR in healthy HPBMs plays a role in secretion of both IL-1β and TNF-α independent of PKA signalling. Findings from this study also showed suppressed secretion of LPS-induced IL-1β and TNF-α upon chemical inhibition of CFTR-mediated Cl^- transport. Additionally, inhibition of CaN and PKA stimulated secretion of LPS induced IL-1β and TNF-α in an attempt to mimick CFTR deficiency seen in CF. This finding could be due to the compensatory or alternative pathways to IL-1β and TNF-α secretion being activated, likely due to the use of nigericin to induce IL-1β secretion. However, expected CsA-induced suppression of the inflammatory cytokines is likely activated by CFTR and DIDS-sensitive ORCC.

5.8.1 SUMMARY OF KEY FINDINGS

1. LPS alone did not induce IL-1β secretion in HPBMs except in the presence of nigericin as stimulus.
2. FSK/IBMX enhanced LPS/nigericin-dependent IL-1β release in HPBMs. This was inhibited by exposure of the HPBMs to CFTR(inh)-172, DIDS, or both.
3. DIDS alone showed no reduction in LPS/nigericin-dependent TNF-α release while CFTR(inh)-172 and DIDS together blocked IL-1β secretion. The CFTR inhibitor alone or in combination with DIDS blocked TNF-α secretion by HPBMs.
4. PKI and CsA enhanced LPS/nigericin-induced IL-1β and TNF-α secretion by HPBMs.
5. A combination of CFTR(inh)-172 and DIDS can inhibit the PKI and CsA-induced IL-1β secretion while CFTR(inh)-172 alone, and both CFTR(inh)-172 and DIDS, blocked PKI and CsA-induced TNF-α secretion by HPBMs.

CHAPTER 6

The role of cAMP/EPAC in the release of cytokine and bacterial phagocytosis by monocytes

6 INTRODUCTION

CFTR is the main channel found on the apical membrane of airway and intestinal epithelial cells, a channel which mediates Cl^- transport in a PKA-dependent manner (279). Several studies investigating Cl^- secretion have investigated PKA as a downstream signalling factor of cAMP. Two major pathways are known to be responsible for mediating cAMP downstream signalling. One is the cAMP-PKA signalling and the other is the cAMP-EPAC signalling. EPAC proteins are of two types (EPAC1 and EPAC2) and are known to be expressed in macrophages, monocytes, lymphocytes, neutrophils, eosinophils and platelets. These proteins have also been demonstrated to be strongly associated with immune responses such as cytokine release and phagocytosis (280). Binding of EPAC to cAMP activates a PKA-independent pathway though certain small G proteins – Rap1, Rap2 and Rab3A (281, 282). Many cellular processes that have been previously believed to be PKA-dependent are now known to also be effected through EPAC signalling (283). For example, a cAMP stimulating agent, the glucagon-like peptide I (GLP1), is known to stimulate insulin secretion in β cells of the pancreas both through the EPAC and PKA signalling pathways. However, the signalling through EPAC is linked to Ca^{2+} signalling, as EPAC is known to influence voltage-dependent Ca^{2+} channels. This creates a Ca^{2+} flux across the cell membrane (284). Interestingly, Ca^{2+} signalling is linked to intracellular cAMP levels, and EPAC-related Ca^{2+} secretion is known to occur through the activation of CaN, a Ca^{2+}-sensitive protein phosphatase (285). Thus, this may be one of the ways cAMP and EPAC interact in the same signalling pathway.

cAMP is a major regulator of Cl^- secretion. FSK and IBMX, which elevate the intracellular level of cAMP through modulating the activities of adenylate cyclase and the EPAC activator 8-pCPT-2'-O'-Me-cAMP – a cAMP analogue used to investigate

PKA independent Cl^- secretion – have both been used to stimulate cAMP signalling (286, 287). However, it appears that cAMP elevation or FSK stimulation may not be acting via PKA since Ca^{2+} intracellular levels may also be raised in response to FSK stimulation. Petrucci, Cervia (288) showed that, in rat pituitary tumour cells, stimulation of the cells by FSK increases intracellular secretion of Ca^{2+}. In addition, Hoque, Woodward (287) showed that, in the T84 cell line, stimulation of the cells with EPAC activator and FSK increases Ca^{2+} and Cl^- secretion, suggesting a link between EPAC and Cl^- secretion.

Based on the findings presented in Chapter 5 of this study, that Cl^- secretion and its influence on cytokine release may be independent of PKA, **this chapter aims** to investigate the role of the alternative cAMP-dependent signalling involving EPAC protein in regulating Cl^- dependent cytokine expression in HPBMs and its role in phagocytosis by MDMs.

6.1 THE PATHWAY INVOLVING cAMP BUT NOT PKA MAY BE REQUIRED FOR THE OBSERVED INFLAMMATORY RESPONSE

The findings presented thus far in this thesis show that protein kinase A inhibitor (PKI) did not inhibit LPS/nigericin-induced IL-1β release but in fact increased it. In addition, FSK/IBMX increased IL-1β release (see chapter 5) and we can conclude that FSK/IBMX activates cAMP signalling which has PKA and EPAC as downstream factors due to results confirming that FSK/IBMX stimulation of Cl^- flux was inhibited by both PKI and CsA (see chapter 3). Our expectations were to see PKI inhibit IL-1β release. However, the contradictory result, that PKI stimulated LPS/nigericin-induced IL-1β release even in the presence of CFTR(inh)-172 or DIDS, led to the conclusion that another factor may be involved in a cAMP-dependent and PKA-independent pathway for IL-1β release involving CFTR. Based on this, the possibility of cAMP acting in this pathway through activation of EPAC in the release of IL-1β was investigated. Firstly, the involvement of EPAC protein on IL-1β secretion was confirmed by investigating the effect of EPAC activation on IL-1β secretion in LPS/nigericin-primed HPBMs. The HPBMs were treated with 10 μM of the EPAC activator 8-pcpt-2'-o-me-camp, a cAMP analogue, prior to their being primed with LPS/nigericin. Although exposure of the HPBMs to EPAC analogue and nigericin alone induced IL-1β release, this release was significantly lower than LPS/nigericin-induced IL-1β secretion, as demonstrated in chapter 5 (section 5.3). This was done to confirm that the cAMP analogue is unable to influence IL-1β secretion as was done for the effect of nigericin on inducing IL-1β release (chapter 5, section 5.3). Significant induction of IL-1β secretion was observed for the HPBMs that were exposed to EPAC activator and LPS/nigericin when compared with LPS/nigericin-exposed HBPMs ($p < 0.01$) However, exposure to PKI (100 nM), in addition to the cAMP analogue, showed no effect on the IL-1β secretion (Fig. 6-1A). This suggests that PKI did not have any effect on the HPBMs in the presence of the cAMP analogue. In addition to

this, exposure of the HPBMs to the cAMP analogue and 10 μM CFTR(inh)-172 resulted in significant suppression of IL-1β induction when compared to HPBMs exposed to the cAMP analogue alone ($p < 0.001$). Interestingly, exposure of the HPBMs to DIDS (500 μM) or both CFTR(inh)-172 and DIDS resulted in further suppression of IL-1β secretion ($p < 0.0001$). However, exposure of the HPBMs to DIDS resulted in insensitivity to CFTR(inh)-172 effects (Fig. 6-1B).

After confirming that EPAC activation induced IL-1β secretion, we proceeded to investigate cAMP-dependent and PKA-independent effects on the HPBMs by first treating the cells with different combinations of LPS/nigericin, FSK (10 μM)/IBMX (100 μM), CFTR(inh)-172 (10 μM), DIDS (500 μM), PKI (100 nM), CsA (1 μM) and EPAC inhibitor (ESI-09) at 10 μM (Fig. 6-2). Findings show that 10 μM of ESI-09 was unable to inhibit FSK/IBMX-induced IL-1β release. The LPS/nigericin-induced release of IL-1β was confirmed to be independent of both PKA and CaN, as PKI and CsA showed no effect on LPS/nigericin-induced release of IL-1β. On the contrary, CFTR or DIDS alone or together in addition to ESI-09 (10 μM) and FSK/IBMX significantly suppressed IL-1β release ($p < 0.01$). This effect is likely to be due to CFTR(inh)-72 and DIDS but not ESI-09 since 10 μM of ESI-09 was not be able to inhibit FSK/IBMX-induced IL-1β release.

As 10 μM of ESI-09 was unable to inhibit IL-1β release, the concentration was increased to 25 μM based on the evidence that 25 μM of ESI-09 inhibits both EPAC1 and EPAC2 (289). HBPMs were then exposed to LPS/nigericin, FSK/IBMX, and 25 μM of ESI-09 with and without PKI. A significant suppression of IL-1β release was observed for HPBMs exposed to a combination of LPS/nigericin, FSK/IBMX and ESI-09 when compared with the group exposed to only LPS/nigericin and FSK/IBMX ($p < 0.01$). It was also found that exposure of the HPBMs to a combination of LPS/nigericin, PKI (100 nM) and FSK/IBMX resulted in significant suppression of IL-1β release compared to the cells exposed to only FSK/IBMX and LPS/nigericin ($p \leq 0.05$). This confirms that

cAMP/PKA signalling and FSK/IBMX stimulation occur via the same pathway. However, PKI did not have any effect on IL-1β induction due to exposure of the HPBMs to ESI-09 and FSK/IBMX (Fig. 6-3), which indicates PKA is not required for EPAC's role in IL-1β release.

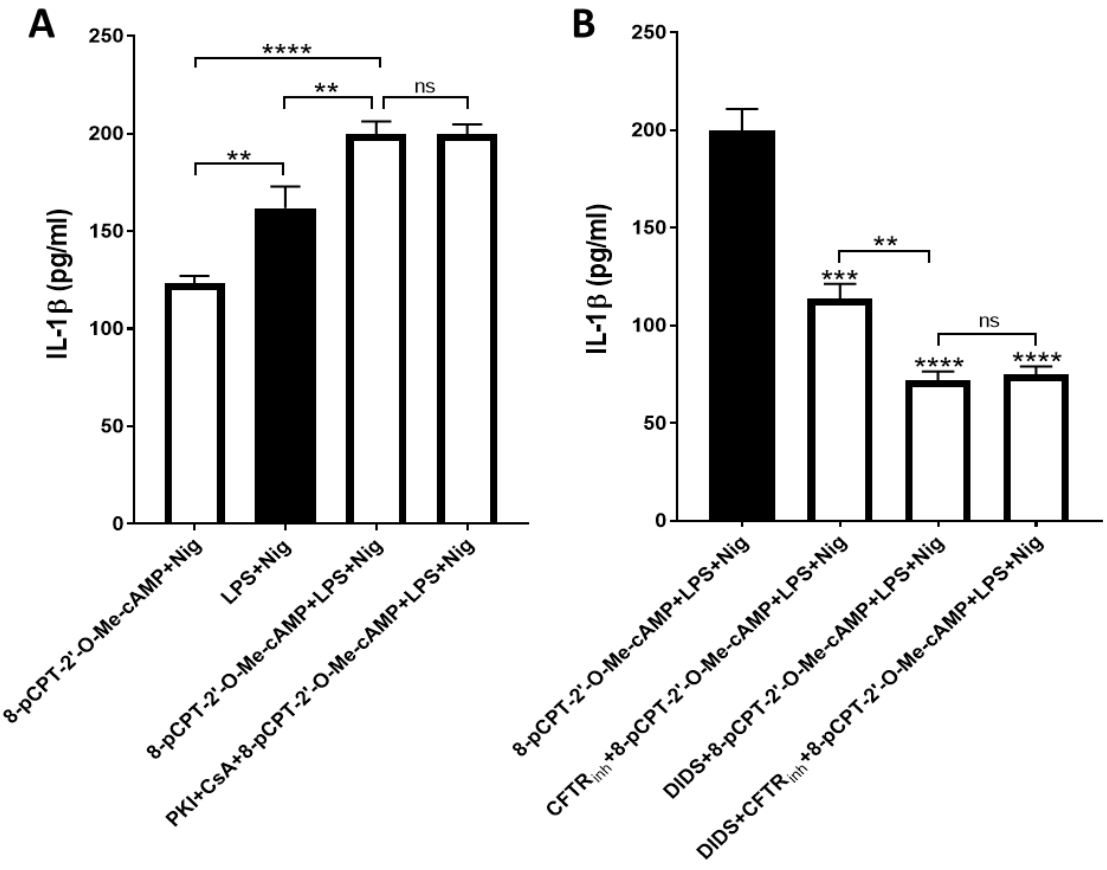

Figure 6-1. Pre-treatment with 8-pCPT-2'-O-Me-cAMP enhanced LPS/nigericin-dependent IL-1β production by HPBMs in presence and absence of CsA/PKI.

HPBMs were pre-incubated with 8-pCPT-2'-O-Me-cAMP (EPAC activator) at 10 μM with and without **(A)** protein kinase A inhibitor (PKI at 100 nM), CaN inhibitor (CsA at 1 μM), **(B)** DIDS (500 μM), CFTR(inh)-172 (10 μM) or a combination of both DIDS & CFTR(inh)-172 for 30 min before being primed with LPS from *P. aeruginosa* (30 μg/ml) for 2 hours followed by nigericin (10 μM) for 1 hour. Cells stimulated with LPS and followed by nigericin were used as a control. The release of IL-1β was measured by ELISA (R&D Systems, MN, US). The statistical analysis was performed using unpaired *t*-test and one-way ANOVA with Bonferroni correction for multiple comparisons. The results represent mean ± SEM from n=3 independent biological repeats; all samples were run in triplicate. **, ***, **** and ^{ns} signify $p < 0.01$, $p < 0.001$, $p < 0.0001$ and a non-significant difference, respectively.

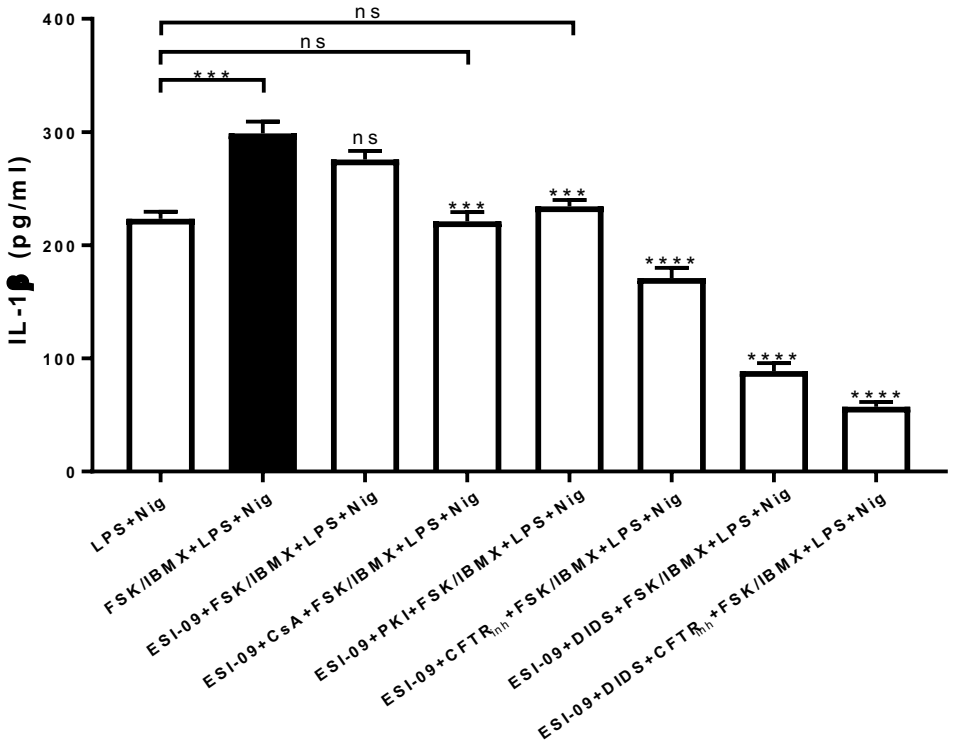

Figure 6-2. EPAC1 inhibition (using ESI-09 at 10 μM) showed no significant effect on FSK/IBMX/LPS/nigericin-dependent IL-1β release by HPBMs in presence or absence of PKI and CsA.

HPBMs were pre-incubated with ESI-09 (10 μM) with and without CaN inhibitor (CsA at 1 μM), protein kinase A inhibitor (PKI at 100 nM), CFTR(inh)-172 (10 μM), DIDS (500 μM), or a combination of both CFTR(inh)-172 and DIDS for 30 min before being primed with FSK (10 μM)/IBMX (10 μM)/LPS from *P. aeruginosa* (30 μg/ml) for 2 hours followed by 10 μM nigericin (Nig) for 1 hour. The release of IL-1β was measured by ELISA (R&D Systems, MN, US). The statistical analysis was performed using unpaired *t*-test and one-way ANOVA with Bonferroni correction for multiple comparisons. The results represent mean ± SEM from n=3 independent biological repeats; all samples were run in triplicate. *** indicates $p < 0.001$, **** indicates $p < 0.0001$ and ^{ns} indicates a non-significant difference.

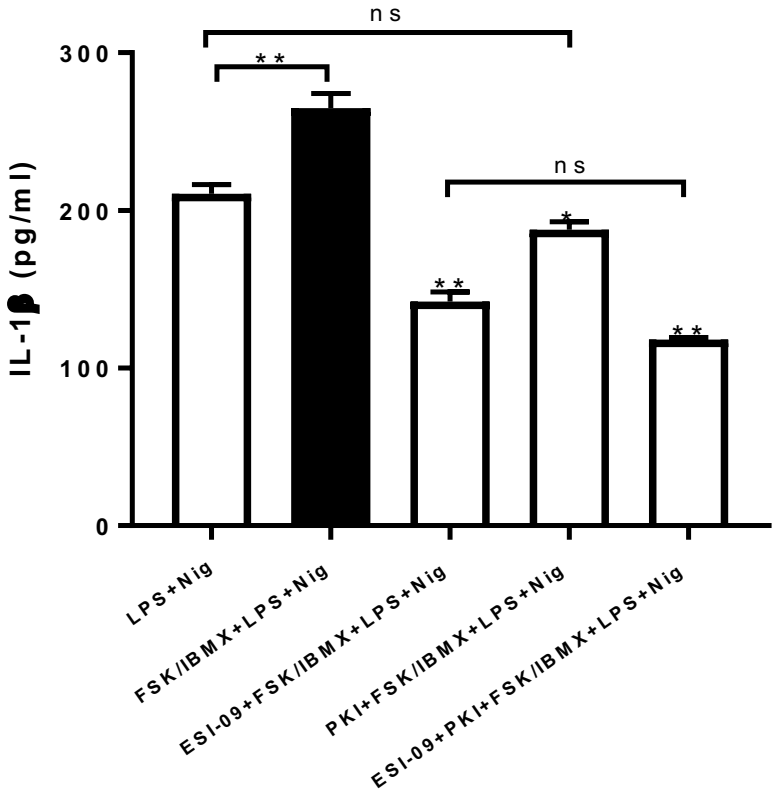

Figure 6-3. EPAC2 inhibition (using ESI-09 at 25 μM) reduced FSK/IBMX/LPS/nigericin-dependent IL-1β release by HPBMs in presence and absence of PKI.

HPBMs were pre-incubated with ESI-09 (25 μM), protein kinase A inhibitor (PKI at 100 nM) or a combination of both for 30 min before being primed with FSK (10 μM)/IBMX (100 μM)/LPS from *P. aeruginosa* (30 μg/ml) for 2 hours followed by 10 μM nigericin (Nig) for 1 hour. The release of IL-1β was measured by ELISA (R&D Systems, MN, US). The statistical analysis was performed using unpaired *t*-test and one-way ANOVA with Bonferroni correction for multiple comparisons. The results represent mean ± SEM from n=3 independent biological repeats; all samples were run in triplicate. * indicates $p \leq 0.05$, ** indicates $p < 0.01$ and ^{ns} indicates a non-significant difference.

ESI-09 at 10 μM is known to inhibit EPAC1. At 25 μM, the inhibitor has been shown to inhibit both EPAC1 and EPAC2 (289). It was found in this current study that 25 μM ESI-09 can inhibit FSK/IBMX-induced IL-1β secretion but that at 10 μM, ESI-09 exhibited no effect on IL-1β release. We proceeded to investigate the effect of 10 μM ESI-09 on inhibition of PKA and CaN by PKI and CsA, respectively, on IL-1β release. It was found that neither PKI nor CsA affected ESI-09 inhibition of IL-1β release (Fig. 6-4A). The concentration of ESI-09 was then increased to 25 μM and its effect at this concentration was investigated in the presence of PKI and CsA, separately. ESI-09 at 25 μM was found to significantly inhibit the PKI-stimulated effect on IL-1β (Fig. 6-4B). This experiment was repeated for HPBMs exposed to CsA and PKI, and even though both CsA and PKI enhanced LPS/nigericin induced IL-1β secretion, 25 μM of ESI-09 significantly suppressed this effect in the HBPMs ($p < 0.01$) (Fig. 6-4C).

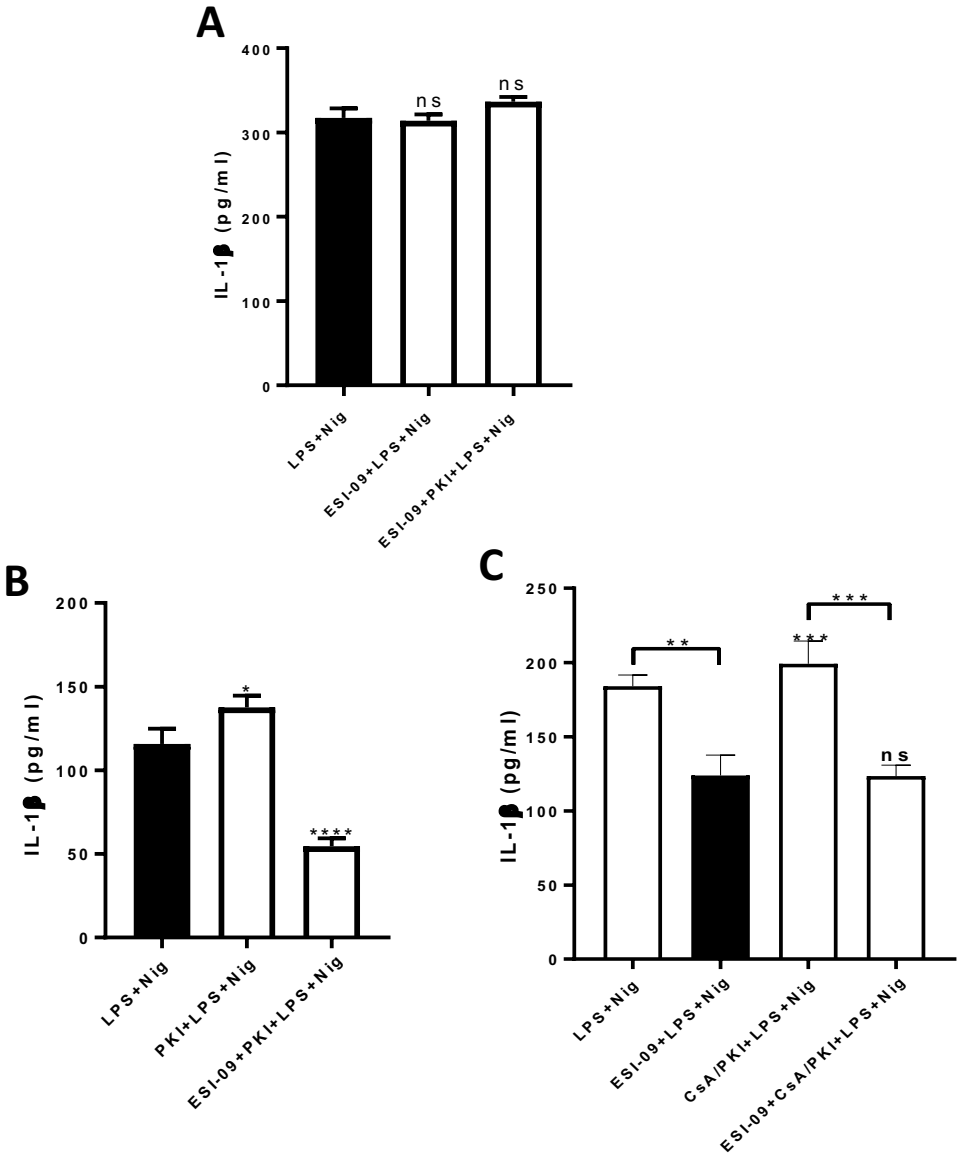

Figure 6-4. Inhibition of EPAC2, but not EPAC1, reduced LPS/nigericin-dependent IL-1β release by HPBMs in a PKA-independent manner.

(A) HPBMs were pre-incubated with ESI-09 (10 μM) with and without protein kinase A inhibitor (PKI at 100 nM) for 30 min, **(B)** HPBMs were pre-incubated with PKI (100 nM) with and without ESI-09 (25 μM) for 30 min, and **(C)** HPBMs were pre-incubated with ESI-09 (25 μM) for 30 min with and without a combination of CsA (1 μM) and PKI (100 nM) before being primed with LPS from *P. aeruginosa* (30 μg/ml) for 2 hours followed by 10 μM nigericin (Nig) for 1 hour. The release of IL-1β was measured by ELISA (R&D Systems, MN, US). The statistical analysis was performed using one-way ANOVA with Bonferroni correction for multiple comparisons. The results represent mean ± SEM from n=3 independent biological repeats; all samples were run in triplicate. * indicates $p \leq 0.05$, ** indicates $p < 0.01$, *** indicates $p < 0.001$, **** indicates $p < 0.001$ and ^{ns} indicates a non-significant difference.

6.2 THE EFFECT OF EPAC INHIBITION ON THE VIABILITY OF HPBM CELLS AND IL-1B SECRETION

It was initially found that 10 μM of ESI-09 was unable to inhibit EPAC activity in IL-1β release. However, when the concentration was increased to 25 μM, an inhibitory effect on EPAC-induced IL-1β release was observed. This high concentration resulted in our investigation of the effect of varying ESI-09 concentrations on cell viability of HPBMs for 3 hours. It was observed that ESI-09 at concentrations below 50 μM did not induce significant reduction in HPBMs viability. However, exposure of the HPBMs to ESI-09 concentrations ≥ 50 μM resulted in significant reduction in monocyte cell viability ($p < 0.005$) (Fig. 6-5A). A longer time point of 24 hrs was then considered for the 25 μM concentration to ascertain whether this would affect cell viability. It was discovered that 25 μM of ESI-09 does not affect the cell viability even after 24 hrs (Fig. 6-5B). This allowed the establishment of the concentration of ESI-09 to be used in subsequent assays studying its effect on cell viability.

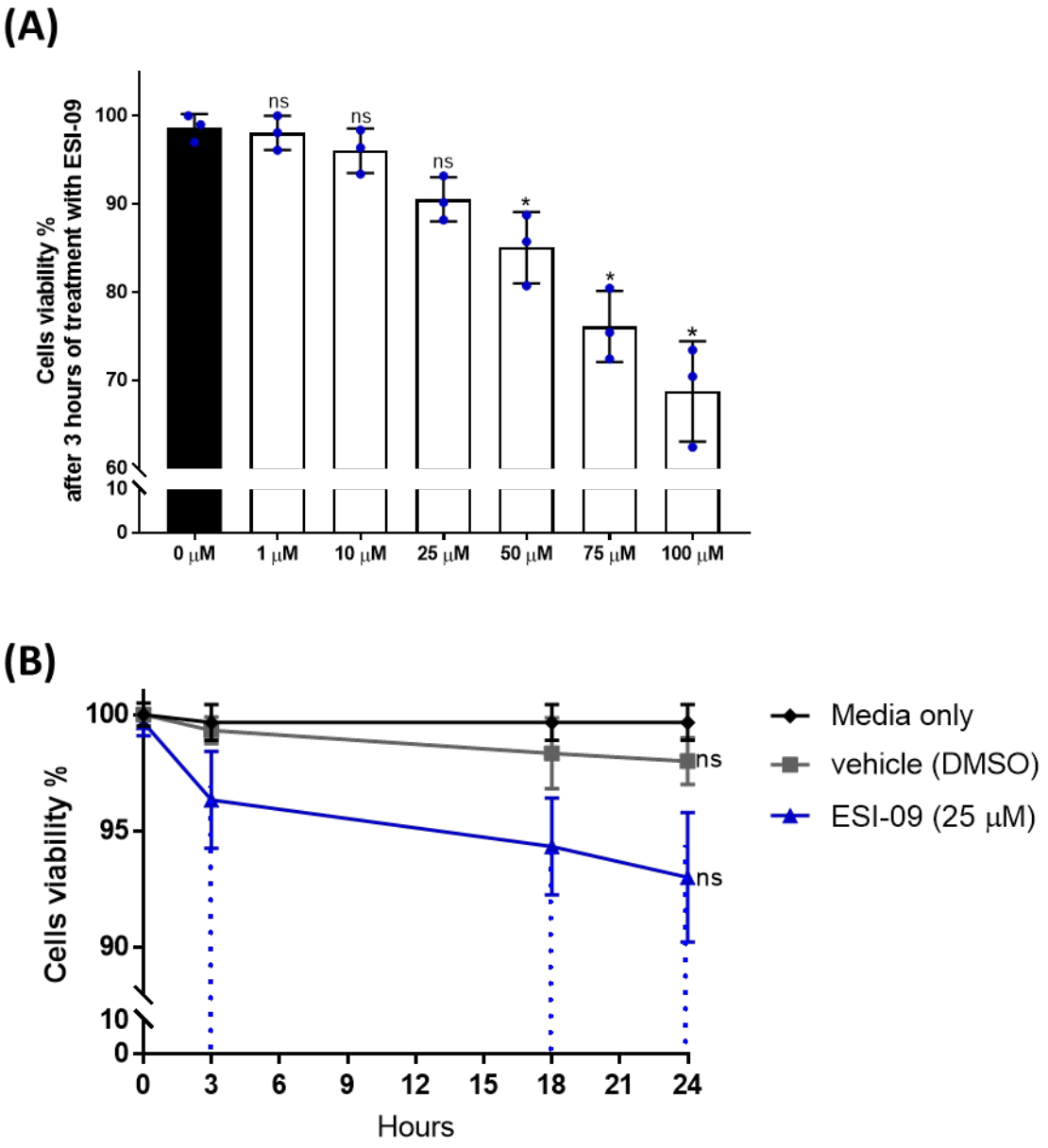

Figure 6-5. EPAC inhibitor (ESI-09) did not significantly affect the viability of HPBMs.

HPBMs pre-incubated with different concentrations of ESI-09 (EPAC inhibitor) at 0, 1, 10, 25, 50, 75, 100 μM for 3 hours followed by 10% MTS **(A)**. Cells were pre-treated with 25 μM of ESI-09 for 3, 18, 24 hours followed by 10% of MTS **(B)**. The absorbance was measured at 490nm (colorimetrically). The results represent mean ± SEM from n=3 independent biological repeats; all samples were run in triplicate. ^{ns} and * indicate a non-significant difference and $p \leq 0.05$, respectively.

6.3 THE INFLUENCE OF EPAC ON CFTR/ORCC-MEDIATED IL-1B AND TNF-A RELEASE IN HPBMS

To further establish a concentration-dependent role for EPAC protein in the inflammatory response of HPBMs to LPS/nigericin, the HPBMs were exposed to varying concentrations of ESI-09, after which they were primed with LPS/nigericin. We observed a dose dependent reduction in IL-1β secretion (Fig. 6-6A and B) and found, using ELISA, that concentrations ≥ 25 μM induced significant suppression of IL-1β secretion ($p < 0.01$).

As a confirmatory experiment for the ELISA analysis on expression of IL-1β in response to different doses of ESI-09 (Fig. 6-6A), IL-1β secretion was measured using CBA flow cytometry. The results showed that ESI-09 induced a significant suppression of IL-1β secretion at concentrations ≥ 15 μM (Fig. 6-6B). For TNF-α, CBA flow cytometric analysis also showed that ESI-09 induced a dose-dependent reduction in TNF-α secretion with significant reduction at ESI-09 concentrations ≥ 15 μM (Fig. 6-6C).

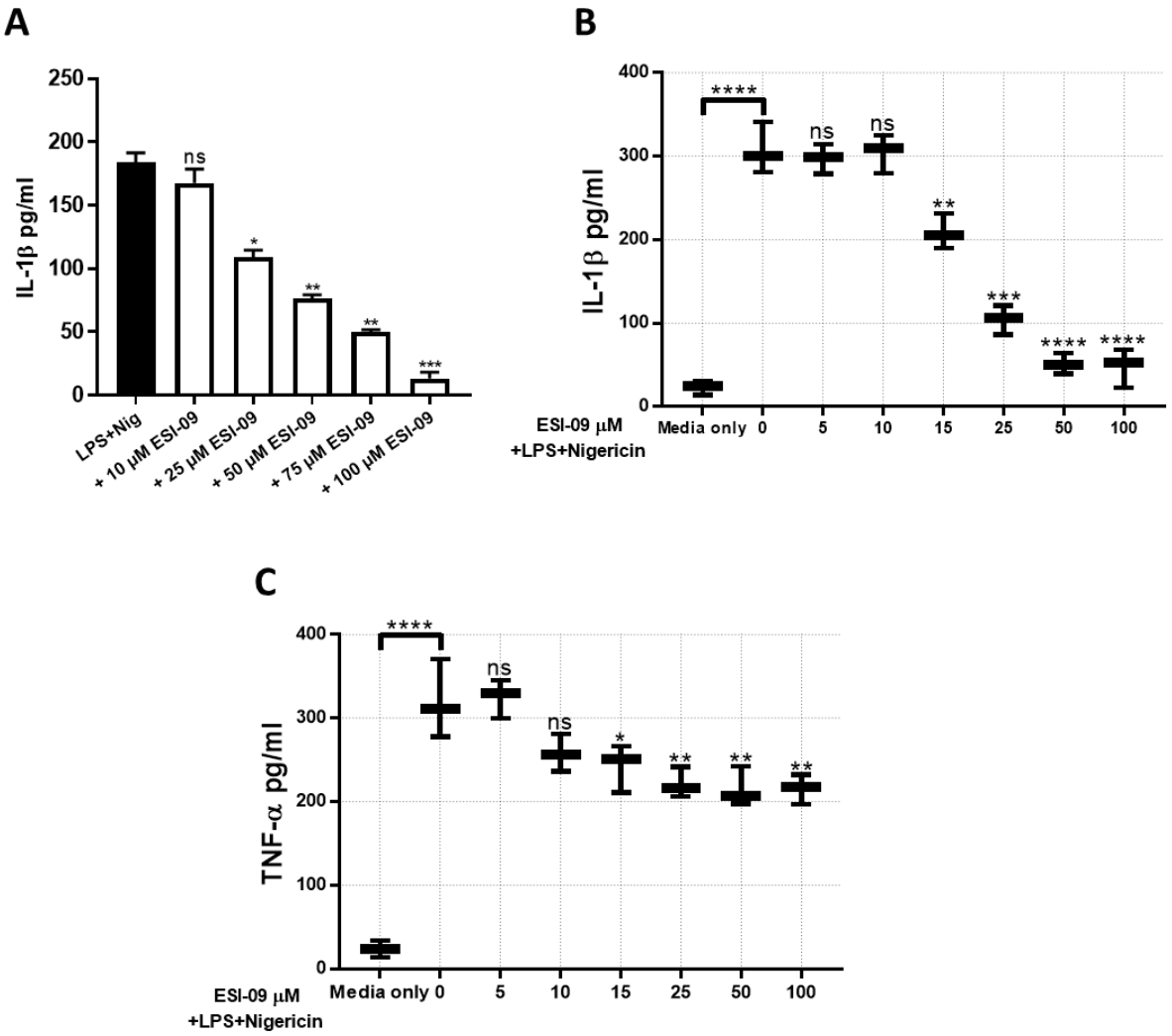

Figure 6-6. ESI-09 (EPAC inhibitor) dose-dependently suppressed IL-1β and TNF-α production by HPBMs.

HPBMs pre-incubated with ESI-09 at 0, 5, 10, 15, 25, 50 and 100 μM for 30 min before being primed with LPS from *P. aeruginosa* (30 μg/ml) for 2 hours, followed by nigericin (Nig) at 10 μM for 1 hour. The release of IL-1β was measured by ELISA **(A)**. The experiment was repeated biologically for confirmation with different doses and the release of IL-1β and TNF-α was measured using a cytometric bead array (CBA) system from BD Bioscience **(B and C)**. The inhibitory potency of ESI-09 on IL-1β and TNF-α release was compared with cytotoxicity: ESI-09 was not cytotoxic up to concentration of 25 μM. The statistical analysis was performed using one-way ANOVA. The results represent mean ± SEM from n=3 independent biological repeats; all samples were run in triplicate. *, **, *** and **** signify $p \leq 0.05$, $p < 0.01$, $p < 0.001$ and $p < 0.0001$ respectively. ^{ns} indicates a non-significant difference.

Fig. 6-3 shows that ESI-09 (25 μM) significantly attenuates LPS/nigericin-dependent IL-1β production by HPBMs. Furthermore, co-exposure of the HPBMs to both ESI-09 and CFTR(inh)-172 (10 μM) or ESI-09 and DIDS (500 μM) resulted in highly significant suppression of IL-1β secretion compared to CFTR(inh)-172 ($p < 0.0001$) or DIDS ($p \leq 0.05$) alone (Fig. 6-7). This suggests that the impact of EPAC on IL-1β secretion in HPBMs occurs through both Cl^- channel-dependent and -independent pathways. On the other hand, Fig. 6-6C shows that ESI-09 also significantly attenuates LPS/nigericin-dependent TNF-α production by HPBMs. However, in contrast to IL-1β release, TNF-α production is inversely correlated in the presence of CFTR(inh)-172 or DIDS and that CFTR(inh)-172 significantly inhibits whilst DIDS significantly enhances production. Co-exposure with ESI-09 and chloride channel inhibitors [ESI-09 and CFTR(inh)-172, ESI-09 and DIDS, or ESI-09 and both CFTR(inh)-172 and DIDS] resulted in highly significant suppression of TNF-α secretion (Fig. 6-8). This suggests that while EPAC and Cl^- channels (CFTR and DIDS-sensitive ORCC) play an important role in cytokine release, regulation of the cytokine release by EPAC or the Cl^- channels occurs through distinct and discrete pathways.

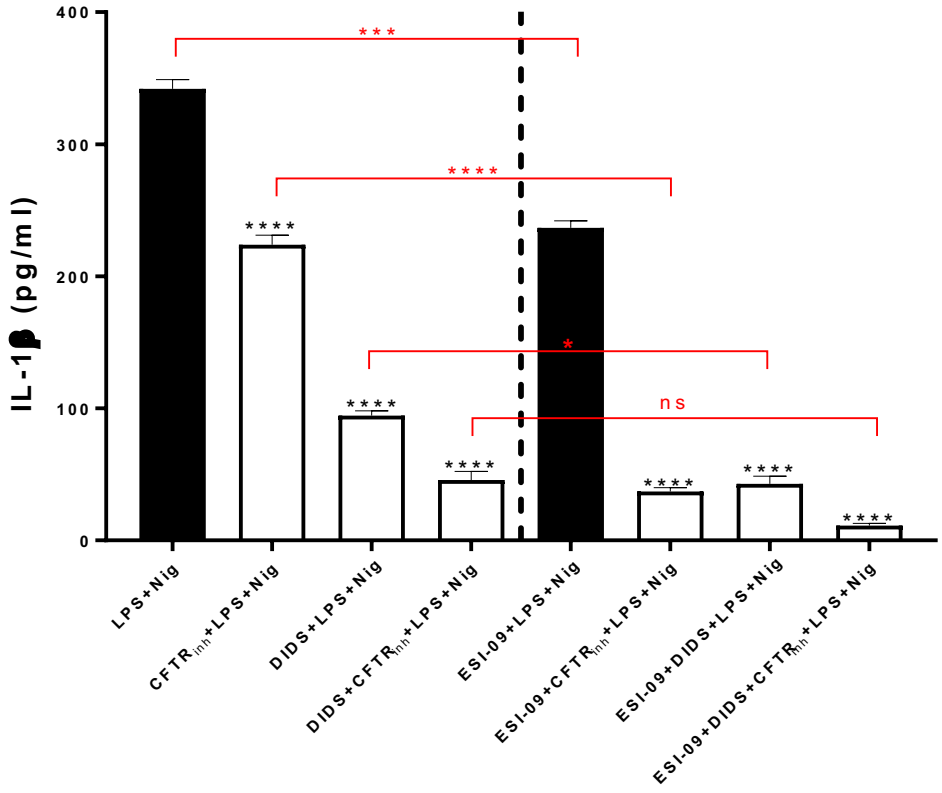

Figure 6-7. Inhibition of EPAC2 and Cl^- channels completely blocked LPS/nigericin-dependent IL-1β production by HPBMs.

HPBMs were pre-incubated with CFTR(inh)-172 (10 µM), DIDS (500 µM) or a combination of both DIDS and CFTR(inh)-172 for 30 min without and with EPAC inhibitor (ESI-09 at 25 µM) before being primed with LPS from *P. aeruginosa* (30 µg/ml) for 2 hours, followed by nigericin (Nig) at 10 µM for 1 hour. Pre-treatment with ESI-09/DIDS/CFTR(inh)-172 blocked LPS/Nig-dependent release of IL-1β ($p < 0.0001$). The release of IL-1β was measured by ELISA (R&D Systems, MN, US). The statistical analysis was performed using unpaired *t*-test and one-way ANOVA with Bonferroni correction for multiple comparisons. The results represent mean ± SEM from n=3 independent biological repeats; all samples were run in triplicate. ^{ns}, *, *** and **** signify a non-significant difference, $p \leq 0.05$, $p < 0.001$ and $p < 0.0001$, respectively.

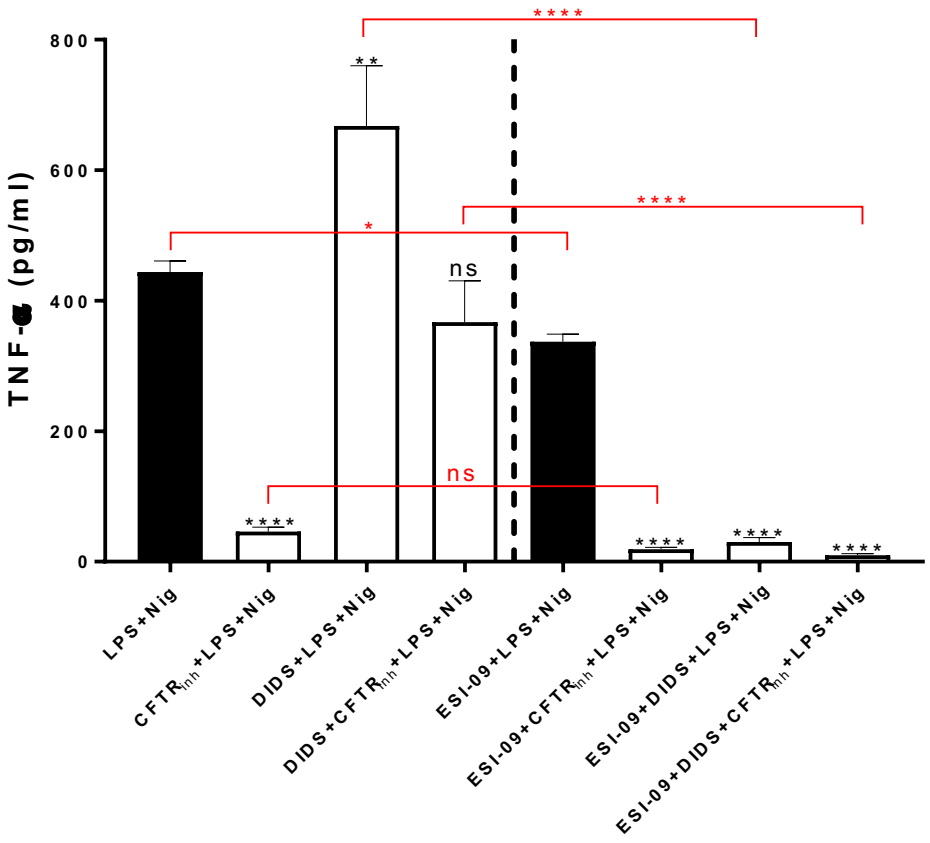

Figure 6-8. Inhibition of EPAC2 and Cl^- channels completely blocked LPS/nigericin-dependent TNF-α production by HPBMs.

HPBMs were pre-incubated with CFTR(inh)-172 (10 µM), DIDS (500 µM) or a combination of both DIDS and CFTR(inh)-172 for 30 min without and with EPAC inhibitor (ESI-09 at 25 µM) before being primed with LPS from *P. aeruginosa* (30 µg/ml) for 2 hours, followed by nigericin (Nig) at 10 µM for 1 hour. Pre-treatment with ESI-09/DIDS/CFTR(inh)-172 blocked LPS/Nig-dependent release of TNF-α ($p < 0.0001$). The release of TNF-α was measured using a cytometric bead array (CBA) system from BD Bioscience (Jan jose, Ca, US). The statistical analysis was performed using unpaired *t*-test and one-way ANOVA with Bonferroni correction for multiple comparisons. The results represent mean ± SEM from n=3 independent biological repeats; all samples were run in triplicate. ^{ns}, *, ** and **** signify a non-significant difference, $p \leq 0.05$, $p < 0.001$ and $p < 0.0001$, respectively.

6.4 THE ROLE OF EPAC2 IN PMA-TREATED MONOCYTIC THP-1 CELLS AND MDMS BACTERIAL PHAGOCYTOSES

It has been found in this current study that EPAC2 inhibition suppresses IL-1β release while activation of the protein causes secretion of IL-1β. This thus suggests a clear role for EPAC2 in the inflammatory response of HPBMs. Since inflammation is a necessary requirement during defence against pathogens, the role of EPAC in immune cell bacterial phagocytosis was investigated in both PMA-treated monocytic THP-1 cells and MDMs. Inhibition of EPAC2 in PMA-treated monocytic THP-1 cells was found to cause a significant inhibition of the cells' ability to phagocytose *P. aeruginosa*, as shown in Fig. 6-9. The CFU count from bacteria phagocytosed by ESI-09-exposed PMA-treated monocytic THP-1 cells was significantly lower than in the control group unexposed to ESI-09 ($p < 0.0001$). A survival analysis of the bacterial cells was also carried out after collection for up to 18 hrs. It was found that the percentage of surviving *P. aeruginosa* in the PMA-treated monocytic THP-1 cells group exposed to ESI-09 (25 μM) was lower for all time points observed than in the control group unexposed to ESI-09. This indicates that ESI-09 exposure resulted in reduced survival of the phagocytosed *P. aeruginosa* (Fig. 6-10). In the same manner, the phagocytotic ability of MDMs was also investigated upon exposure to ESI-09. MDMs that were exposed to ESI-09 also evidenced significantly deficient phagocytosis of *P. aeruginosa* when compared with the control unexposed group ($p < 0.0001$) (Fig. 6-11). As observed for the PMA-treated monocytic THP-1 cells, survival analysis of the phagocytosed *P. aeruginosa* by MDMs exposed to ESI-09 (25 μM) was also lower for all the time points investigated compared to unexposed MDMs, although significant reduction in the bacterial survival was observed at 18 hours post incubation ($p < 0.0001$) (Fig. 6-12). The observed reduced survival rate of the *P. aeruginosa* in the immune cells exposed to ESI-09 was thus likely due to the low number of bacterial cells cultured, a consequence of the deficient phagocytosis.

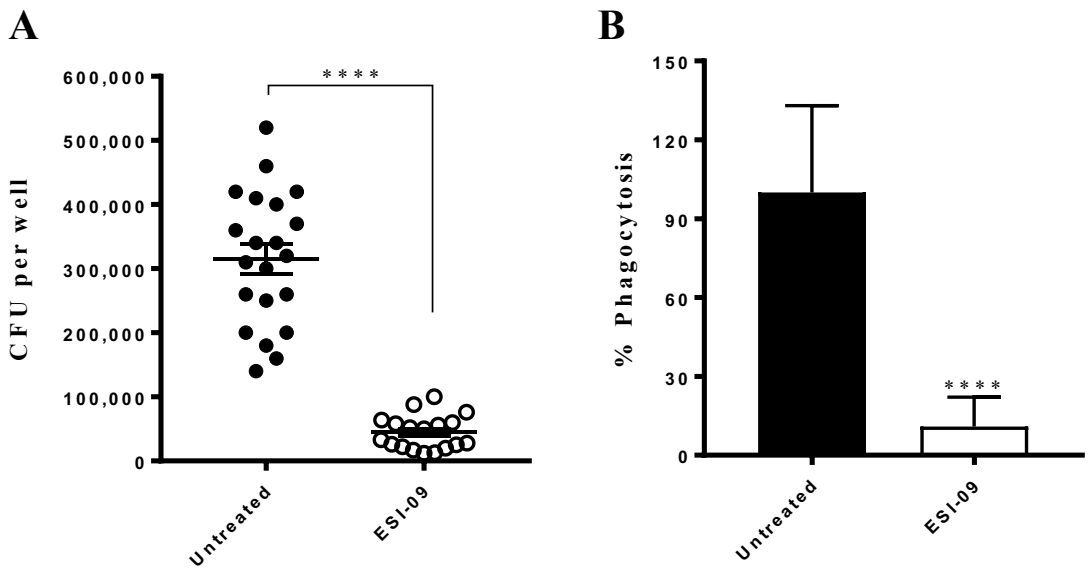

Figure 6-9. Pre-treatment with ESI-09 (25 µM) inhibited the phagocytosis of *P. aeruginosa* by PMA-treated monocytic THP-1 cells.

PMA-treated monocytic THP-1 cells were treated with ESI-09 (EPAC inhibitor) at 25 µM for 30 min. Cells were then infected with *P. aeruginosa* PAO1 at MOI 10 for 2 hours. After infection, cells were washed with PBS and extracellular bacteria were killed with gentamicin (200 ug/ml, 1 hour). Cells were lysed with 2% saponin to release the phagocytosed bacteria and the lysate was plated on agar. The number of phagocytosed bacteria was quantified by colony counting (**A**) and as a percentage (**B**). ESI-09 significantly reduced the phagocytosis of *P. aeruginosa* ($p < 0.0001$). Data is presented as mean ± SEM for n=7.

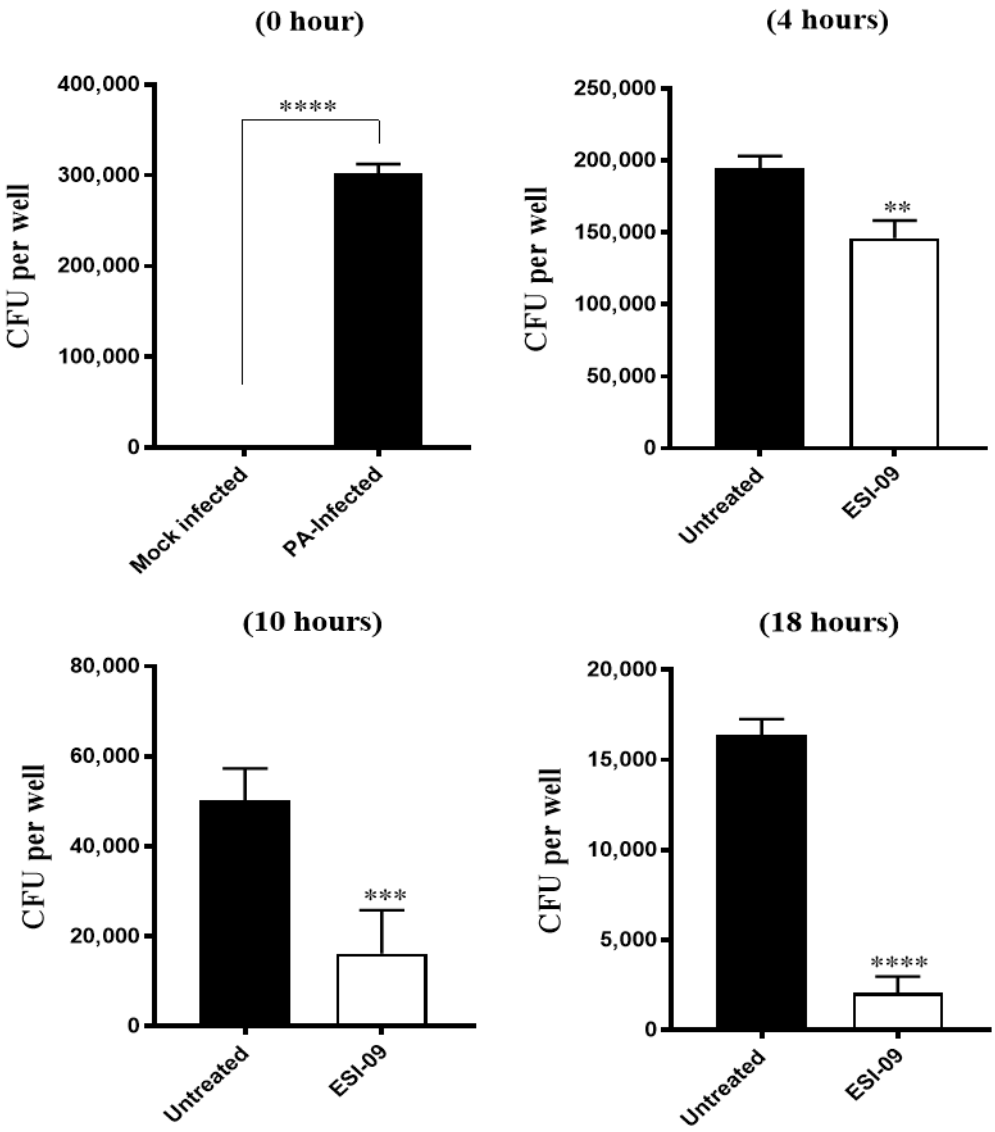

Figure 6-10. EPAC2 inhibition resulted in less survival of phagocytosed *P. aeruginosa* by PMA-treated monocytic THP-1 cells.

PMA-treated monocytic THP-1 cells were infected with *P. aeruginosa* PAO1 at MOI 10 for 2 hours. After infection, cells were washed with PBS and extracellular bacteria were killed with gentamicin (200 μg/ml, 1 hour). Cells were incubated in media containing ESI-09 (EPAC inhibitor) at 25 μM for up to 18 hours. At different time points, cells were lysed with 2% saponin to release the phagocytosed bacteria and the lysate was plated on agar. The number of surviving phagocytosed bacteria was quantified by colony counting at 0, 4, 10 and 18 hours. ESI-09 enhanced the clearance of *P. aeruginosa* after 18 hours ($p < 0.0001$). n= 5 to 6 (± SEM).

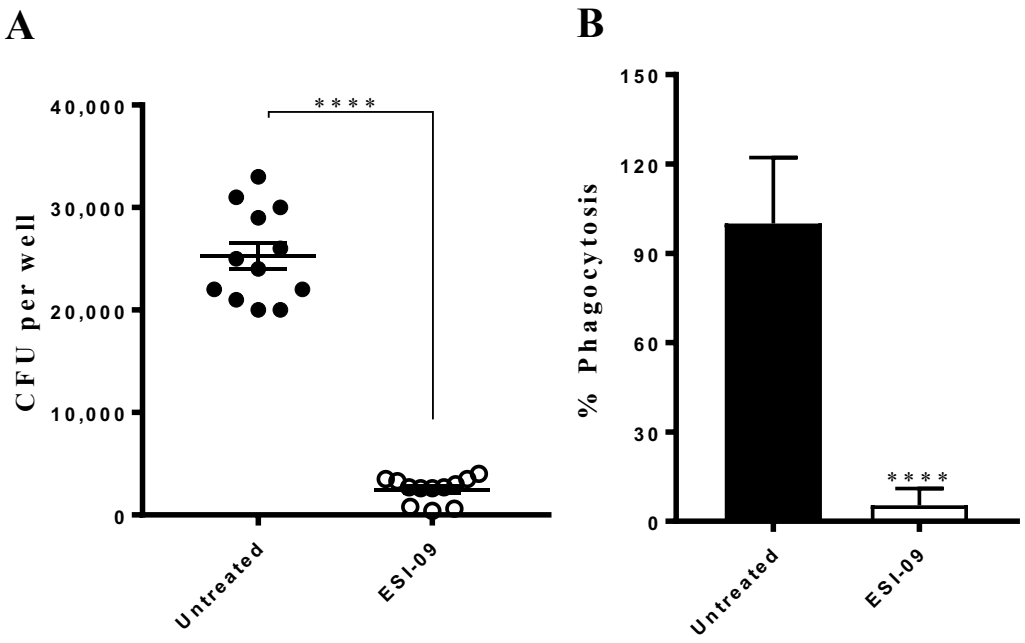

Figure 6-11. Pre-treatment with ESI-09 (25 µM) inhibited the phagocytosis of *P. aeruginosa* by MDMs.

MDMs were treated with ESI-09 (EPAC inhibitor) at 25 µM for 30 min. Cells were then infected with *P. aeruginosa* PAO1 at MOI 10 for 2 hours. After infection, cells were washed with PBS and extracellular bacteria were killed with gentamicin (200 ug/ml, 1 hour). Cells were lysed with 2% saponin to release the phagocytosed bacteria and the lysate was plated on agar. The number of phagocytosed bacteria was quantified by colony counting (**A**) and as percentage (**B**). ESI-09 significantly reduced the phagocytosis of *P. aeruginosa* ($p < 0.0001$). n=10 (± SEM).

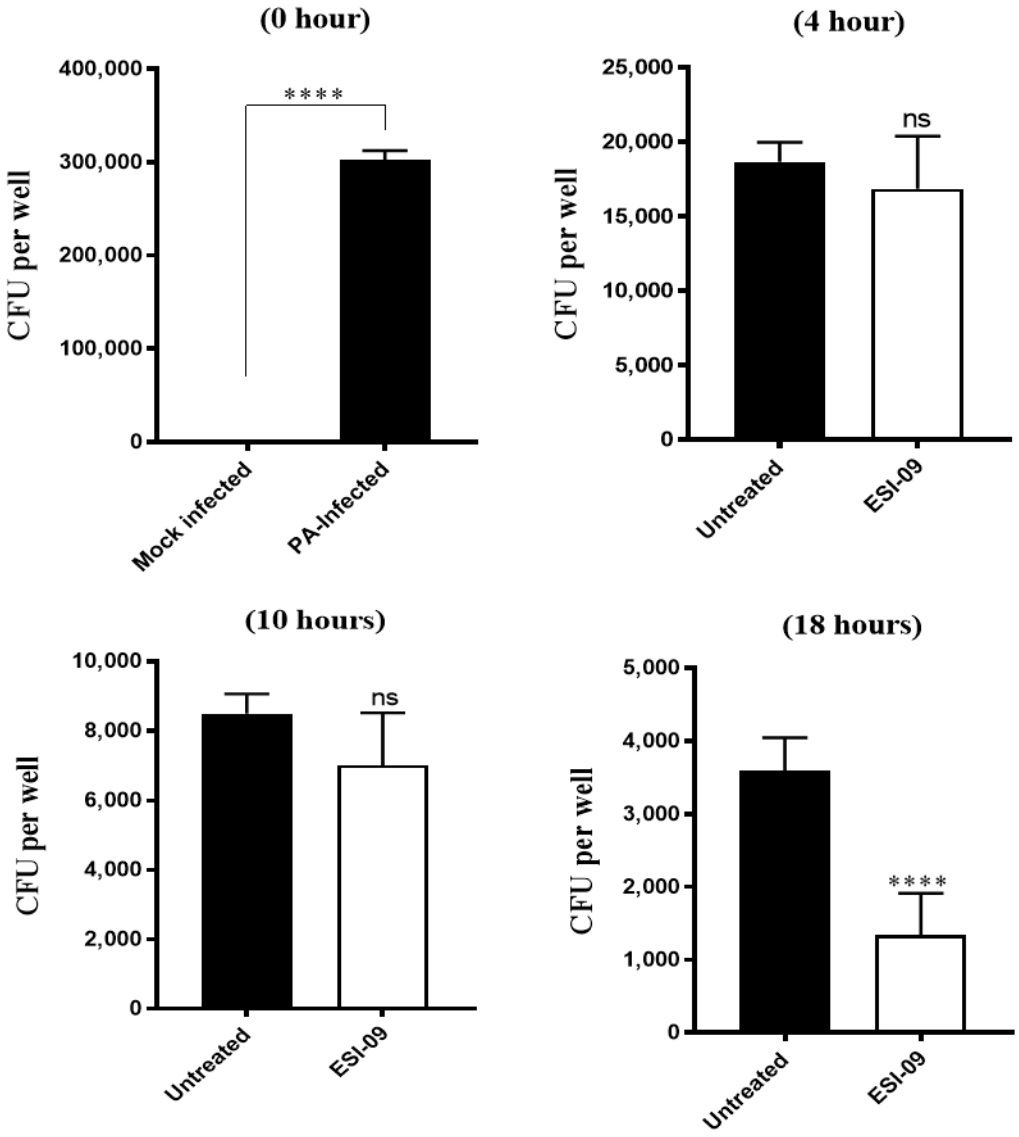

Figure 6-12. EPAC2 inhibition resulted in less survival of phagocytosed *P. aeruginosa* by MDMs.

MDMs were infected with *P. aeruginosa* PAO1 at MOI 10 for 2 hours. After infection, cells were washed with PBS and extracellular bacteria were killed with gentamicin (200 µg/ml, 1 hour). Cells were incubated in media containing ESI-09 (EPAC inhibitor) at 25 µM 4, 10 and 18 hours. At different time points, cells were lysed with 2% saponin to release the phagocytosed bacteria and the lysate was plated on agar. The number of surviving phagocytosed bacteria was quantified by colony counting of survival after 0, 4, 10 and 18 hours. ESI-09 enhanced the clearance of *P. aeruginosa* after 18 hours ($p < 0.001$). n=6 (± SEM).

6.5 CONFIRMING THE ROLE OF EPAC2 IN CFTR/ORCC-MEDIATED INFLAMMATORY RESPONSE

It was unclear whether the observed inhibition of IL-1β release in response to exposure to 25 μM of ESI-09 was due to the inhibition of EPAC1 and EPAC2 together since this concentration is known to inhibit both. The specific role for EPAC2 in IL-1β inhibition that was observed was evaluated by exposing the HBPMs to varying concentrations of ESI-05 (a specific inhibitor for EPAC2 and not EPAC1) for a dose-dependent effect on IL-1β release. Findings showed a dose-dependent decrease in IL-1β with significant suppression in IL-1β release occurring at an ESI-05 concentration of 10 μM (Fig. 6-13A). After determining the dose-dependent effect of ESI-05 on IL-1β suppression, the HPBMs were exposed to 25 μM of ESI-05 in the presence and absence of CFTR(inh)-172, DIDS and both. The HBPMs were exposed to 25 μM ESI-05 – a concentration used in previous studies and shown to be non-toxic to the cells (290, 291) – alone and in combination with CFTR(inh)-172 (10 μM) and/or DIDS (500 μM). The release of IL-1β was then measured using ELISA. A significant inhibition of IL-1β release was observed when the HBPMs were exposed to ESI-05 and CFTR(inh)-172 or DIDS or both ($p < 0.0001$) (Fig. 6-13B). This confirms that EPAC2 is involved in the suppression of IL-1β that was observed upon exposure of the HPBMs to 25 μM of ESI-09.

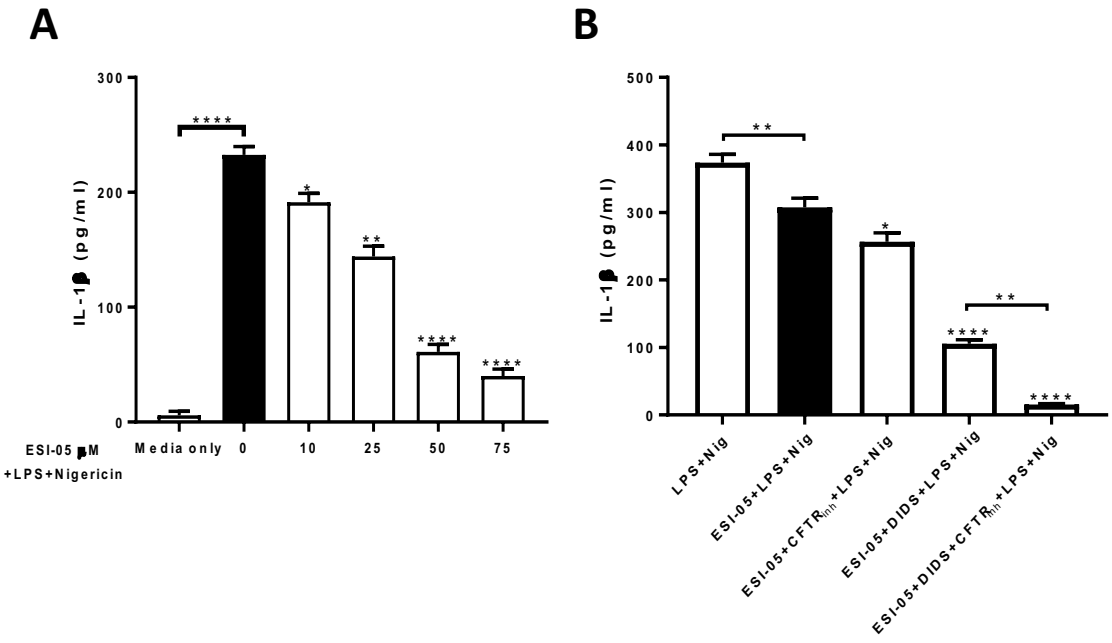

Figure 6-13. (A) ESI-05 (EPAC2 inhibitor) dose-dependently suppressed IL-1β production by HPBMs and (B) confirmation of ESI-05 inhibitory role on IL-1β release in presence and absence of DIDS/CFTR(inh).

(A) HPBMs pre-incubated with ESI-05 at 0, 10, 25, 50 and 75 μM for 30 min before being primed with LPS from *P. aeruginosa* (30 μg/ml) for 2 hours, followed by nigericin (Nig) at 10 μM for 1 hour. **(B)** HPBMs were pre-incubated with CFTR(inh)-172 (10 μM), DIDS (500 μM) or a combination of both DIDS and CFTR(inh)-172 for 30 min with ESI-05 (25 μM) before being primed with LPS from *P. aeruginosa* (30 μg/ml) for 2 hours, followed by Nig at 10 μM for 1 hour. The release of IL-1β was measured using ELISA (R&D Systems, MN, US). The statistical analysis was performed using one-way ANOVA. The results represent mean ± SEM from n=3 independent biological repeats; all samples were run in triplicate. *, ** and **** signify $p \leq 0.05$, $p < 0.001$ and $p < 0.0001$, respectively.

6.6 THE INFLUENCE OF EPAC2 AND Ca^{2+} ON THE INFLAMMATORY RESPONSE OF HPBMS

In this present study, it has thus far been demonstrated that EPAC2 inhibition by ESI-09 and ESI-05 significantly inhibits secretion of IL-1β. It has also been shown in this research that CaN inhibition by CsA does not inhibit IL-1β release by HPBMs. In addition, ESI-09 significantly inhibits *P. aeruginosa* phagocytoses by MDMs. Chapter 5 concluded that CsA inhibition of CaN does not show any effect on the phagocytotic ability of both PMA-treated monocytic THP-1 cells and MDMs. As a confirmation of the possible role of PKA-independent CaN (possibly Ca^{2+}/CaN) in the release of IL-1β, HPBMs were exposed to 1,2-bis(o-aminophenoxy)ethane-N,N,N′,N′-tetraacetic acid-acetoxymethyl ester (BAPTA-AM), a metal ion chelator that is highly specific for Ca^{2+}, in a dose-dependent manner. The effect of BAPTA-AM concentration on IL-1β secretion by HPBMs was measured using ELISA. As shown in Fig. 6-14A, a dose-dependent decrease in IL-1β secretion was observed upon exposure of the HPBMs to BAPTA-AM from 1 μM to 10 μM. However, the effect of BAPTA-AM on IL-1β secretion plateaued between 5 and 10 μM with no additional inhibition up to 75 μM (data not shown).

After establishing that Ca^{2+} chelation inhibited IL-1β secretion, the HPBMs were then exposed to BAPTA-AM (10 μM) in combination with 500 μM of DIDS, 10 μM of CFTR(inh)-172, or a combination of both with the addition of ESI-05 (25 μM), as shown in Fig. 6-14B. It was found in this current study that BAPTA-AM exposure resulted in a highly significant reduction in IL-1β secretion ($p < 0.0001$). In addition to this, BAPTA-AM exposure caused the HPBMs to be insensitive to their exposure to CFTR(inh)-172, DIDS and ESI-05.

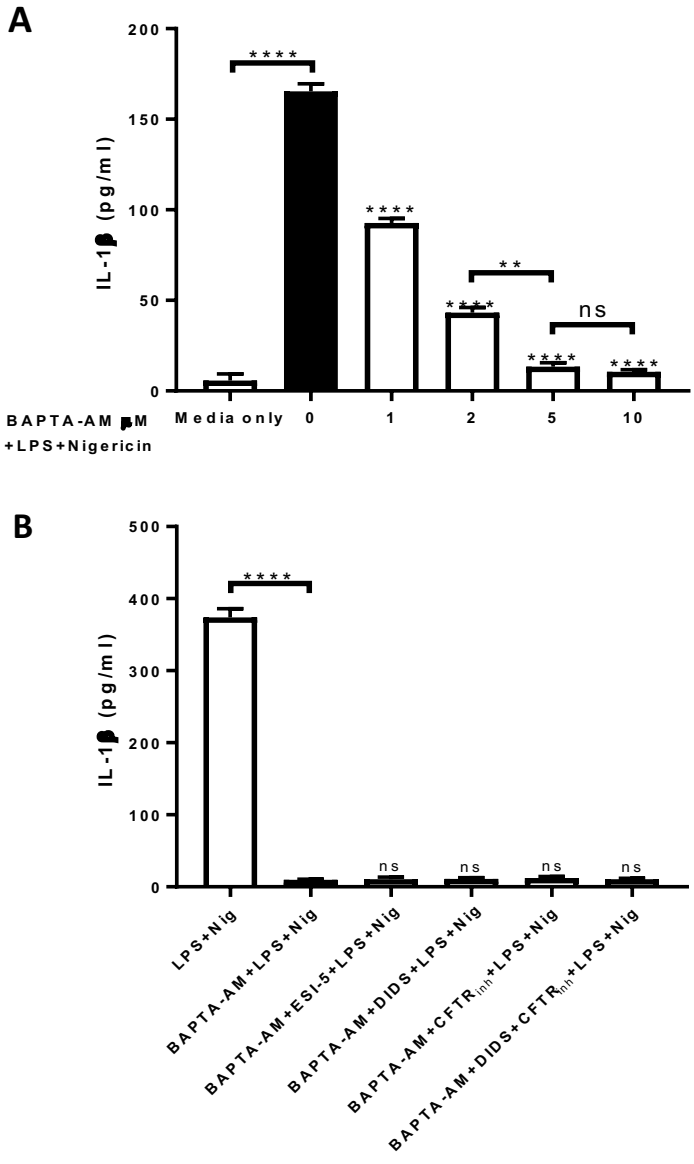

Figure 6-14. (A) BAPTA-AM (Ca^{2+} chelator) dose-dependently suppressed IL-1β production by HPBMs and (B) Ca^{2+} chelation blocked LPS/nigericin-dependent IL-1β production by HPBMs in the presence and absence of ESI-05, DIDS and CFTR(inh)-172.

(A) HPBMs pre-incubated with BAPTA-AM at 0, 1, 2, 5 and 10 μM for 30 min before being primed with LPS from *P. aeruginosa* (30 μg/ml) for 2 hours followed by nigericin (Nig) at 10 μM for 1 hour. **(B)** HPBMs were pre-incubated with CFTR(inh)-172 (10 μM), DIDS (500 μM) or a combination of both DIDS and CFTR(inh)-172 for 30 min with BAPTA-AM (10 μM) before being primed with LPS from *P. aeruginosa* (30 μg/ml) for 2 hours followed by Nig at 10 μM for 1 hour. The release of IL-1β was measured using ELISA (R&D Systems, MN, US). The statistical analysis was performed using one-way ANOVA. The results represent mean ± SEM from n=3 independent biological repeats; all samples were run in triplicate. ^{ns}, ** and **** indicate a non-significant, $p < 0.001$ and $p < 0.0001$, respectively.

6.7 THE ROLE OF Ca^{2+} AND EPAC2 IN *P. AERUGINOSA* PHAGOCYTOSIS

After confirming that EPAC2 inhibition by ESI-05 and Ca^{2+} chelation by BAPTA-AM individually inhibited the secretion of IL-1β by HPBMs, we proceeded to investigate the effect of these drugs (ESI-05 and BAPTA-AM) on *P. aeruginosa* phagocytosis by the MDMs since HPBMs cannot adhere to the plate following the several washings required by this procedure. As such, MDMs were exposed to either of ESI-05 (25 μM) or BAPTA-AM (10 μM) then the cells were infected with *P. aeruginosa*, after which the rate of phagocytosis was measured as previously described in this study (see chapter 2, section 2.2.8). It was found out that both ESI-05 and BAPTA-AM significantly inhibited phagocytosis of *P. aeruginosa* by MDMs, as shown in Fig. 6-15 ($p < 0.0001$ and 0.01, respectively).

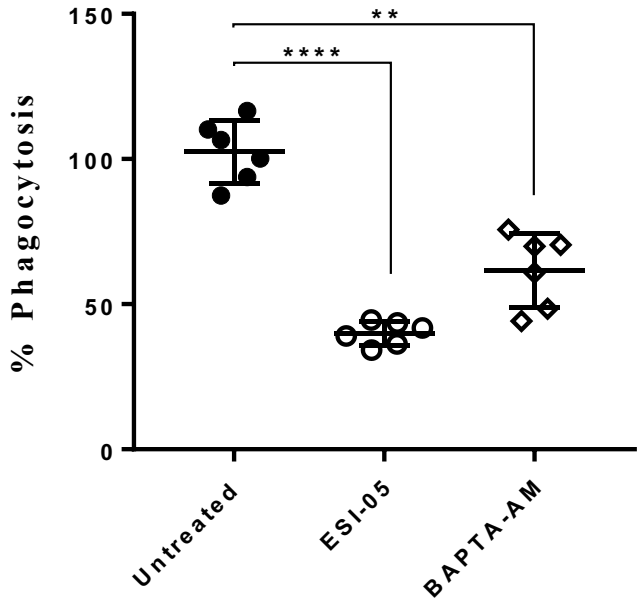

Figure 6-15. Inhibition of EPAC2 and chelation of Ca^{2+} reduced the phagocytosis of *P. aeruginosa* by MDMs.

MDMs were pre-treated with ESI-05 (EPAC2 inhibitor) at 25 μM or BAPTA-AM (Ca^{2+} chelator) at 10 μM for 30 min. Cells were then infected with *P. aeruginosa* PAO1 at MOI 10 for 2 hours. After infection, cells were washed with PBS and extracellular bacteria were killed with gentamicin (200 μg/ml, 1 hour). Cells were lysed with 2% saponin to release the phagocytosed bacteria and the lysate was plated on agar. The number of phagocytosed bacteria was quantified by colony counting and presented as a percentage. ** indicates $p < 0.01$ and **** indicates $p < 0.0001$. Data is represented as mean ± SEM for n=6.

6.8 DISCUSSION

There is evidence in the literature indicating ion transport plays a crucial role during the inflammatory response (292-294). Perhaps, activation of the immune response via the innate immune system is largely dependent on interaction/movement of ions such as Ca^{2+} and Cl^- with/proteins such as CaN and CFTR. It has been shown in chapter 5 of this study that inhibition of cAMP dependent PKA signalling and CaN activities induced secretion of pro-inflammatory cytokines, IL-1β and TNF-α. However, due to the disparity between our findings and that of other studies, we proceeded to further investigate other pathways that may be responsible for the results observed.

In this study, we first confirmed that CaN and PKA have no influence on cAMP induced secretion of IL-1β and TNF-α using cAMP analogue to stimulate cAMP production since we have found that CaN and PKI do not influence LPS induced inflammatory response upon cAMP stimulation by FSK/IBMX (see chapter 5). Subsequently, cAMP signalling and the role this signalling plays during secretion of IL-1β and TNF-α was evaluated. The findings showed that LPS/nigericin-induced IL-1β secretion was enhanced in the presence of FSK/IBMX, contradicting the findings of previous studies. Challier et al. (295) observed a significant suppression in IL-1β and TNF-α secretion in monocyte derived dendritic cells stimulated with LPS when they were exposed to FSK/IBMX. This may be due to the altered cytokine expression profile of dendritic cells compared with HPBMs. Exposure of the HPBMs to ESI-09 in the presence of FSK/IBMX showed significant suppression of IL-1β when compared to exposure to only FSK/IBMX. This indicates that EPAC activation may require cAMP in stimulating IL-1β and could have resulted from an increase in the intracellular Ca^{2+} concentration. Metrich et al. (65) showed that CaN is a downstream target for EPAC protein signalling and this pathway may have been utilised in the HPBMs to serve as a feedback loop to further activate CaN. This activation would then raise Ca^{2+} levels to induce cAMP association with EPAC and

stimulate IL-1β expression totally independently of PKA. The hypothesis that this may be occurring independently of PKA was tested by exposing HPBMs to a combination of ESI-09, LPS/nigericin and FSK/IBMX, with and without PKI exposure. It was found that there was no significant difference in the IL-1β secretion under these two conditions. This finding suggests that PKA does not play a role in the observed inflammatory response in influencing the expression of the pro-inflammatory cytokines. In addition, this finding also showed that cAMP signalling is acting independently of PKA activation since FSK/IBMX, which raises intracellular cAMP levels, resulted in induced IL-1β secretion. As such, it was hypothesised that pathways involving cAMP, but not PKA, may be required for the observed inflammatory response.

To test the above hypothesis, we investigated the possible role of EPAC protein which acts as a guanine nucleotide exchange factor (GEF) for specific G proteins (such as GTPases) after its activation by cAMP independent of PKA (296). EPAC activation is known to be facilitated by a rise in intracellular concentration of Ca^{2+} (297), which hints at possible crosstalk between pathways involving CaN and EPAC. Of more interest is the finding that induction of cytokine secretion could be driven by EPAC activation independent of PKA and instead through the activation of the EPAC/RAP1 pathway (298). In addition to this, another study demonstrated that vascular endothelial barrier function is maintained by EPAC1 in a PKA-independent manner (299).

The investigation is still ongoing on the role of EPAC2 expression and its regulatory role in CFTR/ORCC-mediated ion transport and the immune response to *P. aeruginosa*. It was discovered here that inhibition of EPAC using ESI-09 before HPBMs were primed with LPS/nigericin resulted in suppression of IL-1β, whereas upon exposure to EPAC activator 8-pCPT-2'-O-Me-cAMP – a cAMP analogue – there was significant release of IL-1β when compared to that secreted by the HPBMs that were only stimulated with LPS/nigericin. This finding indicates a clear role for EPAC proteins in the secretion of

LPS/nigericin-induced IL-1β and that EPACs role occurs in a cAMP-dependent manner. It should be noted that we used ESI-09 at concentrations of 10 μM and 25 μM which are known to inhibit EPAC1 and EPAC2, respectively (289). Our findings showed inhibition of IL-1β release at 25 μM, a concentration known to inhibit both EPAC1 and EPAC2. To confirm the role of EPAC2, we investigated the effect of the EPAC2-specific inhibitor, ESI-05, on CFTR/ORCC-mediated IL-1β release and discovered the same result indicating that EPAC2 has a role in IL-1β secretion. Interestingly, Tan, Nackley (300) have shown that, in RAW cell lines (a macrophage cell line), EPAC activation can induce secretion of IL-1β. Aronoff et al. (274) showed that EPAC1 and not PKA activation suppresses TNF-α expression in alveolar macrophages. Additionally, it was discovered that inhibition of EPAC, PKA and CaN resulted in no net difference in the observed responses compared to when only EPAC was inhibited. This confirms that the pathway used by EPAC is independent of PKA and likely Ca^{2+} dependent. To confirm if Ca^{2+} plays any role in the cytokine secretion was dependent or independent of EPAC1 and EPAC2, BAPTA-AM (a highly selective chelator of Ca^{2+}) confirmed that Ca^{2+} chelation can block secretion of IL-1β independent of any other factors. This was concluded due to treatment of HPBMs with BAPTA-AM (10 μM), resulting in insensitivity to Cl^- channels and EPAC inhibitors.

EPAC activation with 8-pCPT-2'-O-Me-cAMP was found to result in stimulation of IL-1β secretion by HPBMs, and this is in agreement with the findings of Sokolowska, Chen (301) who showed that EPAC agonist stimulated LPS-induced IL-1β secretion in MDMs. In addition, Roscioni, Kistemaker (302) have also demonstrated that the EPAC agonist induced IL-8 dependent inflammatory responses in human smooth muscle cells. Interestingly, expression of both IL-8 and IL-1β is known to occur in response to NF-κβ activation (303), indicating that EPAC induction of IL-1β may be a consequence of activation of a complex inflammatory response that induces expression of other

inflammatory cytokines such as that involving NF-κβ. This, in addition to the inhibition of IL-1β secretion by ESI-05 and ESI-09, indicated that EPAC2 is crucial factor that is required for IL-1β inflammatory response. In addition, BAPTA-AM and ESI-05 also inhibited phagocytosis of *P. aeruginosa* in MDMs, further confirming the link between phagocytosis and the cytokine expression observed in previous chapters.

Considering the abrogation of IL-1β secretion upon Ca^{2+} chelation by BAPTA-AM, there is evidence of suppression of EPAC activity upon inhibition of Ca^{2+}/calmodulin-dependent kinase II (CaMKII) (304), indicating a link between Ca^{2+} and EPAC activity. This link may or may not involve CaN but may also involve the activity of CaMKII. The involvement of CaMKII and not CaN may explain the reason for the lack of inhibition of IL-1β secretion due to CaN inhibition by CsA (see chapter 5) and in the presence of EPAC agonist. In support of this, Ainscough, Gerberick (305) have shown that nigericin-induced IL-1β processing requires the activity of Calmodulin (CaM) activation by Ca^{2+} in PMA-treated monocytic THP-1 cells.

It was also discovered that both DIDS and CFTR(inh)-172 were able to suppress IL-1β release in the presence of both LPS/nigericin and ESI-09 or EPAC agonist 8-pCPT-2'-O-Me-cAMP. This finding shows that ORCC and CFTR play a prominent role in suppressing cytokine secretion in conjunction with EPAC. Other downstream signalling involving EPAC activation may also play a role in the observed response. The association of EPAC with cAMP and its subsequent activation is known to result in the opening of chloride channel transporters (ClC-3), a transporter for chloride ions (306). It is also known that the ClC family of proteins are inhibited by DIDS (307). Based on this, it is possible that inhibition of EPAC resulted in closing up of the ClC channel. It is also possible that the effects of DIDS activities on both the ClCs and ORCC may have resulted in the total shut down of chloride ion transport, resulting in suppression of IL-1β secretion. These findings indicate that the secretion inflammatory response in HPBMs is

dependent on interaction between EPAC and CFTR. It is also likely that this interaction requires Ca^{2+} through the activity of CaMKII or a Ca^{2+} protein which may or may not involve CaN. The implication of this in CF is that deficient CFTR could result in dysregulation in its interaction with EPAC or CaM, resulting in a suppressed inflammatory response. In addition, since IL-1β secretion is known to be regulated by the NLRP3 inflammasome, the findings of this study are supported by those of Lee, Subramanian (308) who demonstrated that the NLRP3 inflammasome activites are tightly regulated by cAMP and Ca^{2+}. As such, utilisation of cAMP for EPAC activation in stabilisation of CFTR membrane localisation along with inflammasome activation by cAMP and Ca^{2+} are likely the facilitators of the ion flux that drives IL-1β secretion.

Although it is supposed that cytokine expression is raised in response to deficient CFTR (and its associated pathway) during infection in CF, it is possible that the contrasting results obtained in this present research were as a result of investigating cytokine expression only in response to Cl^- channels inhibition in addition to inhibition/activation of other factors such as EPAC and CaN. However, investigation of cytokine expression during or post *P. aeruginosa* infection in combination to inhibition of the Cl^- channels as it occurs in CF may be a better representative of the conditions found in CF. Palomo, Marchiol (309) have shown that *P. aeruginosa* infection of a F508Δ-CFTR mouse resulted in increased expression of IL-1β. Exposure of *P. aeruginosa*-infected HPBMs or MDMs to CFTR(inh)-172, DIDS, CsA, BAPTA-AM and ESI-05/ESI-09 may have resulted in the aggravated inflammatory response.

6.9 CONCLUSION

This chapter has shown that EPAC plays a role in LPS-induced inflammatory response in HBPMs. However, this likely occurs in a PKA-independent manner requiring an alternative pathway, likely involving interaction between Ca^{2+}-associating proteins, such as CaM or CaMKII and EPAC, with contribution from other chloride channels, such as the ClCs, in addition to CFTR and ORCCs. This proposes a role for Ca^{2+} and EPAC during LPS-induced inflammatory responses involving different pathways with different stimuli to result in the same cellular response. However, the observed inflammatory response in CF may be better investigated by evaluating the cytokine expression in *P. aeruginosa*-infected immune cells that have been exposed to Cl^- channel inhibitors.

6.9.1 SUMMARY OF KEY FINDINGS

1. EPAC is responsible for cAMP-dependent CFTR/ORCC-mediated IL-1β release in HBPMs.
2. Ca^{2+} is strongly required by CFTR for secretion IL-1β in HBPMs.
3. Defects in signalling of EPAC or Ca^{2+} affects phagocytotic ability of MDMs on *P. aeruginosa*.
4. Inhibition of EPAC affects survival of phagocytosed *P. aeruginosa* in MDMs.

CHAPTER 7

General Discussion

7 GENERAL DISCUSSION

7.1 cAMP/PKA-DEPENDENT CFTR, S100A10 AND ANXA2 COMPLEX SECRETION OF Cl^- IS FACILITATED BY CAN

The initial phase of this study aimed to investigate the interactions between S100A1, AnxA2 and CaN in immune cells and the roles played by this interaction in CFTR-mediated Cl^- transport. Previous research has already shown that S100A10 and AnxA2 are Ca^{2+} interacting proteins that form an octameric protein complex on the cytosolic part of the cell membrane in different cell types, including neuroendocrine and epithelial cells. They are also known to influence Ca^{2+}-regulated cellular processes (310). In addition to this, AnxA2-S100A10 has been demonstrated to form a functional complex with CFTR (44). CaN, on the other hand, interacts with Ca^{2+} through its utilisation of the Ca^{2+}-binding protein (CaM) as a co-factor. It is believed that CaN may be required to mobilise formation of S100A10/AnxA2/CFTR multiprotein complexes, the formation of which is done in a cAMP/PKA-dependent manner. This multiprotein complex is known to enable CFTR Cl^- secretion, with a likely role in the immune response of CF sufferers. CF patients are known to have deficient CFTR-mediated Cl^- transport coupled with a heightened inflammatory response (249). Based on this knowledge, we investigated the interaction of these proteins in PMA-treated monocytic THP-1 cells and HPBMs. Our results showed that these proteins indeed interact in these cells. Although there is very little evidence in terms of the role played by CFTR-mediated Cl^- in the immune response, especially in terms of its impact on CF, evidence is now increasing that Cl^- transport by channels such as CLIC play a role in inducing inflammasome activation (226). In a similar manner, CFTR complex formation alongside CFTR regulation of ORCC and consequent Cl^- secretion may have an important role in the immune response. There is an indication in the literature that THP-1 cell lines are not matured monocytes. This conclusion is based on the cytokine expression profile and the phenotypic outlook of the cell line (208). As

such, THP-1 monocytes are normally pre-treated briefly with PMA to induce adherence and cytokine expression similar to that of matured monocytes. PMA activates protein kinase C (PKC), which also activates B-Raf, an oncogene involved in cell division and differentiation, to induce monocyte differentiation into macrophages (311). Based on this disparity, the expression of S100A10 was investigated in non-PMA-treated THP-1 cell lines. It was thus confirmed that the cells do not express S100A10, making it impossible for formation of S100A10, AnxA2 and CFTR multiprotein complexes. The formation of S100A10, AnxA2 and CFTR multiprotein complexes in PMA-treated monocytic THP-1 cells suggests a link between the protein complex and cytokine expression in immune cells.

ORCCs are a group of Cl^- channels that are expressed in epithelial cells and certain immune cells. They are found on the basolateral surface of the plasma membrane in epithelial cells (312, 221). These channels are known to be regulated by CFTR (270), making the combined effect of both ORCC and CFTR important in Cl^- secretion with possible physiological consequences in CF. Our investigation into CFTR and ORCC-mediated Cl^- secretion in PMA-treated monocytic THP-1 cells and HPBMs showed that Cl^- flux through these channels is facilitated by cAMP as we found that FSK/IBMX-stimulated Cl^- was inhibited by CFTR(inh)-172 and DIDS. This could mean that an increase in FSK/IBMX induced cAMP levels that mediate Cl^- transport through CFTR, confirming the requirement of cAMP signalling for CFTR-mediated Cl^- transport. In addition, we found that CaN alone plays a cAMP/PKA-dependent role in facilitating the Cl^- flux through CFTR and ORCC since inhibition of both PKA and CaN inhibited FSK/IBMX-induced Cl^- current in these cells. A previous study has shown that CaN is activated by PKA through phosphorylation of egulator of CaN (RCAN1) (313), explaining why CaN did not influence Cl^- secretion in the absence of FSX/IBMX in our study. As such, CaN activity in inducing Cl^- here may have occurred due to the complex

formed by S100A10, AnxA2 and CFTR. To support this finding, an investigation into the Cl^- flux in non-PMA treated THP-1 cell line was conducted, concluding that the cells do not exhibit any Cl^- flux upon stimulation with FSK/IBMX and treatment with CFTR(inh)-172 and DIDS. This could possibly be a result of the factor responsible for the non-expression of S100A10 in the non-PMA-treated cells.

7.2 LPS INDUCED Cl^- FLUX THROUGH CFTR AND ORCC INFLUENCES *P. AERUGINOSA* PHAGOCYTOSIS AND SURVIVAL OF PHAGOCYTOSED BACTERIAL CELLS

One of the consequences of immune cells encountering PAMPs or DAMPs is activation of signalling cascade, which eventually leads to immune responses for defence. Thus, dysfunction in these signalling cascades may lead to failure in activating the defence mechanisms of the immune system. Cl^- secretion has been previously linked to innate immune activation in a study that showed that flagellin from *P. aeruginosa* induced Cl^- secretion in Calu-3 airway epithelia cell lines (192). LPS, being the main constituent of the outer membrane of Gram negative bacteria, such as *P. aeruginosa*, is the main factor that is responsible for provoking the immune response. Detection of LPS by TLR4-MD2 protein complex is made possible by enhancement of LPS presence through its binding with the LPS binding protein (LBP) and CD14. Detection of LPS by TLR4 thus results in activation of the MAPK pathway, expression of NF-kβ regulated genes, and production of pro-inflammatory cytokines (150). Furthermore, LPS has been shown to induce Cl^- secretion. In fact, LPS from *P. aeruginosa* has been demonstrated to induce Cl^- secretion via CFTR in human bronchial epithelial cell lines (314). Taken together, these findings suggest a strong link between Cl^- secretion and immune response.

Here, we evaluated the impact of LPS on inducing Cl^- flux through CFTR and ORCC in PMA-treated monocytic THP-1 cells and HPBMs. It was found that LPS does induce Cl^- flux and that this ion flux was facilitated through CFTR and ORCC. This was based on

the finding that CFTR(inh)-172 and DIDS both inhibited Cl^- flux induced by LPS. As found in the initial investigation focus of this thesis, S100A10 and AnxA2 complex formation is likely involved in mediating Cl^- flux through CFTR by the multiprotein complexes formed. It is possible that this multiprotein complex of S100A10, AnxA2, CFTR and CaN is stimulated into activity by LPS to mediate Cl^- movement through CFTR with a functional consequence of inducing the immune response. This is supported by a previous finding that the S100A10 and AnxA2 complex plays a role in activating macrophages through the activities of TLR4 (210, 230). As such, LPS binding to TLR4 may also be linked with S100A10 and AnxA2 interaction with TLR4 in a complex process required to elicit an immune response to bacterial antigens.

One of the hypotheses of this thesis is that CFTR interaction with AnxA2-S100A10 complex requires a CaN phosphatase activity to activate CFTR ion transport and cell secretion. We successfully demonstrated that CaN is required for ion flux through CFTR and ORCC. Not only is CaN required, it was also found out that cAMP/PKA signalling is required. Upon stimulation with LPS, it was found that CaN and PKA are required to facilitate LPS induced Cl^- flux in both PMA-treated monocytic THP-1 cells and HPBMs. In addition, exposure of the cells to PKI or CsA resulted in insensitivity of the cells to CFTR or ORCC inhibition by CFTR(inh)-172 and DIDS, respectively. This insensitivity of CFTR current upon exposure to PKI or CsA shows the importance of PKA/CaN to CFTR-dependent functions. Since CFTR is a regulator of ORCC, CaN inhibition results in dysfunction of CFTR regulation of ORCC, rendering both channels non-functional in terms of Cl^- movements across the cell membrane.

Upon contact of immune cells such as monocytes and macrophages with LPS, the cell membrane of the immune cells reshapes and invaginates to initiate cell membrane kinetic that causes the pathogen expressing the LPS to be phagocytosed. These bacterial cells are engulfed into phagosomes while the immune cells initiate secretion of chemicals that

cause the death of bacterial cells. One such chemical has been found to be Cl^- (315). Chronologically, phagocytosis is initiated prior to Cl^- secretion, indicating that phagocytosis may be a requirement for Cl^- secretion in phagosomes to maintain the acidic pH level that is required for bacterial cell death. As such, the observed inhibited Cl^- secretion may have occurred due to defective phagocytotic processes. However, mutations in CFTR as seen in CF result in dysfunctional CFTR activities. This causes inhibition of Cl^- flux; the first and most studied physiological consequence of CFTR mutation. It thus appears likely that Cl^- is responsible for initiating phagocytosis. Based on this assumption, the effect of CFTR(inh)-172 on phagocytosis of *P. aeruginosa* by PMA-treated monocytic THP-1 cells and MDMs was investigated in this present study. Inhibition of Cl^- flux by CFTR(inh)-172 and DIDS not only inhibited phagocytosis in both cell types, it also resulted in increased survival of phagocytosed bacterial cells. This finding indicates a link between phagocytosis and Cl^- flux in these immune cells and that defects in Cl^- flux may be responsible for both defective phagocytosis and ineffective induction of bacterial cell death in the phagosome. Aiken, Painter (243) have shown that Cl^- is essential for maintenance of acidity of the neutrophil phagosome for efficient killing of bacterial cells. In addition to this, ClC has been demonstrated ex vivo to colocalise with lysosomal and endosomal in *E. coli*-infected Drosophilia macrophages (227). Interestingly, Cl^- transport by ClC in maturing phagosomes have been proposed to be essential for release of Ca^{2+} by TRPML, a transmembrane Ca^{2+} channel, to facilitate the transfer of phagocytic cargo for lysosomal degradation (316). Taken together, these findings show that Cl^- transport may not only be essential for maintaining acidity of phagosomes to enhance bacterial cell killing, it may also be essential for intracellular transport for the cell to successfully degrade the content of the phagosome in the lysosome to complete the bacterial clearance process.

7.3 Inhibition of Cl^- flux through CFTR and ORCC results in reduction of pro-inflammatory cytokines

Aside from phagocytosis of pathogens, one other method immune cells use to activate the body's defence system against foreign pathogens is secretion of pro-inflammatory cytokines that serve to recruit other immune cells to the site of infection for effective eradication of the disease-causing microbes (180). These cytokines include IL-1β and TNF-α, which are mainly produced by monocytes and macrophages in the correct amounts for effective inflammatory response. However, when produced in excessive amounts, either due to deregulated signalling or due to excessive engagement of immune cells with highly immunogenic substances, septic shock may occur, which is highly common in CF patients (317, 318).

Our investigations have shown that a multiprotein complex interaction occurs between CFTR and both S100A10 and AnxA2 in a cAMP/PKA/CaN-dependent manner and facilitates Cl^- flux through CFTR. Cl^- channels have long been linked to inflammatory responses defining the distinction between normal and pathologic conditions in processes where Cl^- secretion is regulated by signaling involving Ca^{2+}, cAMP and cGMP (319). It is also known that ClC-2 is upregulated and phosphorylated in inflammatory bowel disease to maintain Cl^- influx into the bowel for transporting Na^{2+} and water out of the intestinal lumen. This causes constipation and inflammation (320). Inflammatory studies involving the activities of CFTR in CF have shown that TNF-α is a mediator of inflammation in CF through its regulatory activity of CFTR mRNA transcript stability. Similarly, IL-1β is known to regulate steady state expression of CFTR mRNA and protein production (321). In addition, chemical inhibition of CFTR or mutation in *CFTR* in alveolar macrophages has been shown to result in inflammatory responses involving TNF-α and NF-κβ (219). Unfortunately, studies linking the Cl^- transport of CFTR with inflammatory responses are limited.

Our investigation into induction of inflammation in primary monocytes has shown that *P. aeruginosa*-derived LPS induced IL-1β and TNF-α secretion. It was also found that FSK/IBMX stimulates secretion of LPS/nigericin-induced IL-1β. It is also known that FSK/IBMX stimulate cAMP signalling, which is required by CFTR. To further corroborate if the cAMP facilitated PKA activation of CFTR as well as a possible role for CaN phosphatase activity in this, PKI and CsA, which are inhibitors of PKA and CaN, were found to enhance IL-1β and TNF-α secretion. Inhibition of CFTR and ORCC mediated Cl^- transport with selective inhibitors was also found to have an opposite effect by inhibiting IL-1β and TNF-α secretion. CF airways are normally characterised by heightened inflammation upon CFTR dysfunction (249), indicating a contrasting phenomenon to our findings and expectations that CFTR and ORCC inhibition would result in increased secretion of IL-1β and TNF-α while PKA and CaN inhibition would suppress the inflammatory response. Based on this, it was initially thought that an alternative pathway may be involved in the observed response. Further investigation showed that pre-incubtion of the HPBMs with CFTR(inh)-172 and DIDS resulted in insensitivity to the normal effects of PKI and CsA on IL-1β and TNF-α secretion. This was the first hint that PKA activation of CFTR may not be required for CFTR and ORCC-mediated inflammatory responses since inhibition of the Cl^- channels was dominant in inhibiting inflammatory responses that were otherwise enhanced by PKA and CaN inhibition. It was thus deduced that CaN and PKA do play a role in inflammatory responses, but they both act in an independent pathway from CFTR and ORCC. This would indicate that CFTR and ORCC may be using another cAMP-activated protein since we have clearly shown that FSK/IBMX stimulates IL-1β secretion. In addition to this, CFTR and ORCC may also require another Ca^{2+}-associated protein aside from CaN. Although the functional assay of CFTR showed that it is regulated by CaN, this interaction, despite playing a role in Cl^- secretion, may not be required for inflammatory

responses. However, it may facilitate the recruitment of other Ca^{2+} associated proteins, such as CaM or CaMKII, for CFTR-mediated inflammatory responses.

7.4 cAMP/EPAC IS A PROTEIN FACILITATING CFTR AND ORCC-DEPENDENT INFLAMMATORY RESPONSES

We confirmed the role of CFTR and ORCC in pro-inflammatory cytokines release by HPBMs and found that inhibition of cAMP/PKA and CaN pathway does not affect the release of cykotines. We thus decided to investigate other factors and relevant pathways that may be responsible for the observed suppression of IL-1β and TNF-α secretion upon inhibition of CFTR and ORCC. Two main pathways that are known to involve activity of cAMP downstream signalling are those of PKA and EPAC proteins. Based on this knowledge, the role of EPAC protein in inflammatory responses involving CFTR and ORCC was investigated since EPAC is a cAMP-activated protein that does not require PKA activity.

EPACs are implicated in variety of secretory pathways, some of which include secretion of insulin in the pancreatic β-cells, secretion of progesterone by luteinizing human granulosa cells and acrosomal exocytosis during activation of the sperm head (297). PKA activation by cAMP results in phosphorylation of PKA substrates; however, EPAC acts as GEFs upon activation by cAMP, resulting in distinct pathwyas and differing mechanisms of action between PKA and EPAC. For example, the role of EPAC in insulin secretion involves its cAMP-dependent activation of Rap1, a small GTPase, which results in exocytosis of the pancreatic β-cells with increased release of Ca^{2+} through ryanodine-sensitive Ca^{2+} channels to mediate insulin secretion (322).

Evidence from the literature that EPAC signaling requires Ca^{2+} (284) and evidence that EPAC activation stabilises CFTR at the plasma membrane (323) are strong indications that EPAC plays an important role in CFTR-mediated physiological processes. As such,

we first investigated the effect of EPAC1 inhibition on release of pro-inflammatory molecules and found that ESI-09 (10 μM) does not affect IL-1β release, suggesting that a compensatory action of another EPAC-like protein in IL-1β secretion upon EPAC1 inhibition. Subsequently, we investigated the impact of EPAC2 inhibition (using a higher dose of ESI-09) on cytokine release and demonstrated a dose-dependent inhibition of IL-1β and TNF-α secretion. We also investigated the effect of EPAC2 inhibition (using ESI-09 at 25 μM) on FSK/IBMX-induced IL-1β. It should be noted that FSK/IBMX also stimulates intracellular Ca^{2+}. As expected, it was found that ESI-09 at 25 μM here does in fact inhibit FSK/IBMX activity. Conversely, EPAC agonist 8-pCPT-2'-O-Me-cAMP enhanced the secretion of IL-1β, in agreement with the findings of Tan, Nackley (300), and this enhancement was not affected by either of PKI or CsA, further suggesting that PKA and CaN are not required. However, CFTR(inh)-172 and/or DIDS does inhibit EPAC agonist-stimulated IL-1β production, suggesting EPAC may be associated with CFTR/ORCC for IL-1β secretion. There is evidence in the literature regarding the role of EPAC in CFTR-mediated Cl^- secretion. Hoque, Woodward (287) have demonstrated that EPAC activation by 8-pCPT-2'-O-Me-cAMP stimulates Cl^- secretion through CFTR in the T84 colon carcinoma cell line in a cAMP- and Ca^{2+}-dependent manner. In addition to this, Sheikh, Koley (324) demonstrated that depletion of EPAC1 and inhibition of the KCNN4c channel, a Ca^{2+} activated K^+ channel in the T84 cell line, significantly blocked cAMP-mediated Cl^- secretion through CFTR. They also showed that Cl^- secretion through CFTR is cAMP-dependent and PKA-independent. KCNN4c channel is known to produce a driving force for Cl^- secretion during diarrhea. As such, interaction between EPAC and KCNN4c and the Cl^- secretion may suggest a role for EPAC in the inflammatory response in diarrhea involving Cl^- secretion.

It was also found that EPAC1 inhibition results in insensitivity of HPBMs to the effect of both PKA and CaN inhibition, further suggesting that neither EPAC1 nor PKA/CaN are involved in cytokine release. This indicates that cAMP elevation is used to activate EPAC, which then aids the stabilisation of CFTR for release of IL-1β. Furthermore, inhibition of IL-1β and TNF-α by CFTR(inh)-172 or DIDS after EPAC2 inhibition led to suppression of cytokine release. This indicates that both CFTR/ORCC and EPAC2 may be acting in the same pathway due to the additive effect of the inhibitors to these proteins. The finding that EPAC2 and CFTR/ORCC may interact in the same pathway led to the assumption that cAMP activities as required by EPAC occur in this pathway.

In summary, IL-1β secretion mediated by CFTR in HPBMs requires activity of EPAC, especially EPAC2. However, FSK/IBMX stimulation, ESI-09/05 reduction and BAPTA-AM inhibition of IL-1β suggests the requirement of Ca^{2+}. The requirement for Ca^{2+} was also confirmed by the complete abrogation of IL-1β secretion after chelation of Ca^{2+} by BAPTA-AM in the presence of CFTR/ORCC blockers, ESI-09 or ESI-05. The involvement of Ca^{2+} in IL-1β release has been previously shown to be mediated through the P2X7 receptor, a nucleotide receptor that mediates ATP-induced cellular changes such as CFTR (325). As such, CFTR-mediated release of IL-1β may involve the P2X7 receptor in addition to Ca^{2+} and EPAC. The requirement of Ca^{2+} by CFTR may also be via other proteins, such as CaM or CaMKII, since our investigation has ruled out involvement of CaN. Although CaN forms a complex with CFTR, it may help recruit CaM or CaMKII for IL-1β release. It should be noted that Ca^{2+}/CaM-dependent protein phosphatase interaction with CaN are involved in IL-1β secretion during neuroinflammation (326).

Phagocytotic activities in the innate immune system are a major defence mechanism of immune cells such as monocytes and macrophages. In CF, inadequate mucocilliary clearance caused by both the sticky nature of the epithelia upon dysfunctional Cl^-

transport and ASL accumulation account for the sustained infections that aggravate the disease. Additionally, dysfunctional phagocytotic activities of macrophages and monocytes also contribute to sepsis and inflammation observed in CF. This is due to phagocytosis of apoptotic cells in the lungs and airways, playing a crucial role in maintaining lung homeostasis and combatting inflammation (327). We have shown in this current study that inhibition of CFTR and ORCC inhibits the phagocytotic ability of PMA-treated monocytic THP-1 cells and HPBMs-derived macrophages. CsA however, does not in any way affect cytokine release or immune cell phagocytosis, indicating that CaN is not required. Our finding that EPAC2 may play a role in cytokine release prompted our investigation into its role in PMA-treated monocytic THP-1 cells and MDMs phagocytosis of *P. aeruginosa*. Inhibition of EPAC2 significantly inhibits the phagocytosis of *P. aeruginosa* by PMA-treated monocytic THP-1 cells and MDMs. Coupled with this, BAPTA-AM treatment of MDMs also significantly inhibits the phagocytotic ability. Taken altogether, these findings must mean that Ca^{2+} and EPAC either directly or indirectly result in CFTR stabilisation, maintaining the Cl^- transport and cytokines release through other Ca^{2+}-activated proteins such as CaM. However, inhibition of EPAC2 or CFTR could have abrogated the interaction between these proteins, resulting in suppressed cytokine release and dysfunctional phagocytosis.

However, it was expected that chemical inhibition of CFTR should result in inflammation or increased cytokines release, as observed in CF. One explanation for our findings is a possible lack of contribution of bacterial cells in the experimental set up during CFTR/ORCC inhibition. In CF, the airway is colonised with apoptotic cells and bacteria which are antigens that can greatly promote inflammation. LPS alone may not be sufficient for cytokine release during CFTR/ORCC inhibition. As such, whole bacterial cell infection of CFTR(inh)-172 and DIDS-treated HPBMs may better represent the condition in CF.

There is also evidence in the literature that EPAC plays a role in macrophage phagocytosis. Kim, Moon (328) showed that EPAC activation by 8-pCPT-2'-O-Me-cAMP can induce macrophage phagocytosis of serum (C3bi)-opsonized zymosans, which are PAMPs found on fungi such as yeast. In addition, Scott, Harris (329) demonstrated that β2-Agonists and corticosteroids inhibited neutrophil phagocytosis of *Staphylococcus aureus*. However, EPAC activation by 8-pCPT-2'-O-Me-cAMP successfully reversed this impairment. Coupled with the CFTR stabilising function of EPAC at the plasma membrane demonstrated by Lobo, Amaral (323) and the findings in this study and those of previous ones that Cl^- and CFTR play a role in ensuring successful phagocytosis, EPAC stabilisation of CFTR may be the key factor ensuring the Cl^- flux needed for the phagocytosis.

7.5 CONCLUSION

This thesis has demonstrated interaction between S100A10, AnxA2 and CaN in both 16HBE14o$^-$ cell lines (as a control) and PMA-treated monocytic THP-1 cells. This multiprotein complex is believed to facilitate Cl^- transport by CFTR and ORCC in a cAMP/PKA-dependent manner. It was also demonstrated that LPS from *P. aeruginosa* induces Cl^- conductance in both PMA-treated monocytic THP-1 cells and HPBMs through CFTR and ORCC with the possible influence of PKA and CaN. The first link between Cl^- conductance and immune cell phagocytosis was established as inhibition of Cl^- conductance in PMA-treated monocytic THP-1 cells and MDMs. This resulted in inhibition of the phagocytotic ability of the immune cells and enhanced survival of the bacteria, as seen in CF. It was also shown that CFTR and ORCC mediates cytokines release in HPBMs; however, this was independent of PKA and CaN signalling and likely via cAMP/EPAC pathway. Further investigation showed that while Ca^{2+} is required for cytokine release, Ca^{2+} is likely needed for EPAC activation to stabilise CFTR in

regulating cytokine release, or the Ca^{2+} may be utilised by Ca^{2+}-activated proteins, such as CaM or CaMKII, other than CaN.

7.6 FUTURE WORK

One of the aims of this study was to delineate the role of the CaN and AnxA2-S100A10 multiprotein complex on physiological functions of CFTR such as in Cl^- transport and cytokine release. While we have been able to show that CFTR does mediate Cl^- conductance upon LPS stimulation of primary monocytes, PMA-treated monocytic THP-1 cell and HPBMs with the aid of CaN and PKA, CaN and PKA does not seem to be involved in CFTR-mediated cytokine release.

Our findings indicate that EPAC2 is the facilitator of CFTR-mediated cytokine release upon exposure to LPS from *P. aeruginosa*. Our findings show that chemical inhibition of CFTR and ORCC result in inhibited cytokine release, in contrast to the inflammatory conditions observed in CF. As such, a study investigating the effect of chemical inhibition of CFTR and ORCC on immune cells that are infected with *P. aeruginosa* and not only stimulated with LPS may be required to better represent the conditions in CF. This is due to the complex interactions between apoptotic cells, bacteria and immune cells which are responsible for the inflammatory responses in CF.

Investigation of the protein expression of EPAC1 and EPAC2 by western blot is required as a confirmatory experiment to the confocal microscopy under different conditions, including LPS stimulation and exposure to EPAC and CFTR/ORCC inhibitors. A knockout cell line or knockdown HPBMs of EPAC1 and EPAC2 are also required as negative controls for further confirmation and to better understand cytokine expression during chemical inhibition of CFTR and ORCC in the absence of EPAC1 and EPAC2.

One unexpected result was the finding that CaN is not required for cytokine release by CFTR. Therefore, knockout cell line or knockdown HPBMs of CaN can be used to

investigate the causes and implications of this finding. However, we found that Ca^{2+} is strongly required for CFTR-mediated cytokine release. As such, investigation is also necessary into the role of Ca^{2+} by investigating which protein utilises Ca^{2+}. CaM inhibitors can thus be used to evaluate if CaM is recruited by Ca^{2+} into this pathway for cytokine release.

Anoctamin 6 (ANO6), also known as TMEM16F, was recently identified as an essential component of the ORCC which is also involved in epithelial anion transport. Its knockdown in mouse airways leads to a CF-like phenotype, reflecting the importance of anoctamins for airway anion secretion (222). As such, creating a knockdown cell line may help create a CF condition for better investigation of cytokine release/inflammatory responses.

8 BIBLIOGRAPHY

1. Neher E, Sakmann B. Single-channel currents recorded from membrane of denervated frog muscle fibres. Nature. 1976;260(5554):799.
2. Jentsch TJ. Discovery of CLC transport proteins: cloning, structure, function and pathophysiology. J Physiol. 2015.
3. Niemeyer BA, Mery L, Zawar C, Suckow A, Monje F, Pardo LA, et al. Ion channels in health and disease. 83rd Boehringer Ingelheim Fonds International Titisee Conference. EMBO reports. 2001;2(7):568-73.
4. Jentsch TJ, Stein V, Weinreich F, Zdebik AA. Molecular structure and physiological function of chloride channels. Physiological reviews. 2002;82(2):503-68.
5. Puljak L, Kilic G. Emerging roles of chloride channels in human diseases. Biochim Biophys Acta. 2006;1762(4):404-13.
6. Valverde MA. ClC channels: leaving the dark ages on the verge of a new millennium. Current opinion in cell biology. 1999;11(4):509-16.
7. Duran C, Thompson CH, Xiao Q, Hartzell HC. Chloride channels: often enigmatic, rarely predictable. Annual review of physiology. 2010;72:95-121.
8. Forgac M. Vacuolar ATPases: rotary proton pumps in physiology and pathophysiology. Nature reviews Molecular cell biology. 2007;8(11):917-29.
9. Hartzell C, Putzier I, Arreola J. Calcium-activated chloride channels. Annual review of physiology. 2005;67:719-58.
10. Gadsby DC, Vergani P, Csanady L. The ABC protein turned chloride channel whose failure causes cystic fibrosis. Nature. 2006;440(7083):477-83.
11. Sosnay PR, Siklosi KR, Van Goor F, Kaniecki K, Yu H, Sharma N, et al. Defining the disease liability of variants in the cystic fibrosis transmembrane conductance regulator gene. Nat Genet. 2013;45(10):1160-7.
12. Anderson MP, Sheppard DN, Berger HA, Welsh MJ. Chloride channels in the apical membrane of normal and cystic fibrosis airway and intestinal epithelia. The American journal of physiology. 1992;263(1 Pt 1):L1-14.
13. Riordan JR, Rommens JM, Kerem B, Alon N, Rozmahel R, Grzelczak Z, et al. Identification of the cystic fibrosis gene: cloning and characterization of complementary DNA. Science. 1989;245(4922):1066-73.
14. Cant N, Pollock N, Ford RC. CFTR structure and cystic fibrosis. The international journal of biochemistry & cell biology. 2014;52:15-25.
15. Linsdell P. Relationship between anion binding and anion permeability revealed by mutagenesis within the cystic fibrosis transmembrane conductance regulator chloride channel pore. The Journal of physiology. 2001;531(Pt 1):51-66.
16. Sorum B, Torocsik B, Csanady L. Asymmetry of movements in CFTR's two ATP sites during pore opening serves their distinct functions. eLife. 2017;6.
17. Mall MA, Galietta LJ. Targeting ion channels in cystic fibrosis. Journal of cystic fibrosis : official journal of the European Cystic Fibrosis Society. 2015;14(5):561-70.
18. Corradi V, Vergani P, Tieleman DP. Cystic Fibrosis Transmembrane Conductance Regulator (CFTR): CLOSED AND OPEN STATE CHANNEL MODELS. The Journal of biological chemistry. 2015;290(38):22891-906.
19. Hobbs CA, Da Tan C, Tarran R. Does epithelial sodium channel hyperactivity contribute to cystic fibrosis lung disease? The Journal of physiology. 2013;591(18):4377-87.
20. Chen JH, Stoltz DA, Karp PH, Ernst SE, Pezzulo AA, Moninger TO, et al. Loss of anion transport without increased sodium absorption characterizes newborn porcine cystic fibrosis airway epithelia. Cell. 2010;143(6):911-23.

21. Winter MC, Sheppard DN, Carson MR, Welsh MJ. Effect of ATP concentration on CFTR Cl- channels: a kinetic analysis of channel regulation. Biophysical journal. 1994;66(5):1398-403.
22. Berger HA, Anderson MP, Gregory RJ, Thompson S, Howard PW, Maurer RA, et al. Identification and regulation of the cystic fibrosis transmembrane conductance regulator-generated chloride channel. The Journal of clinical investigation. 1991;88(4):1422-31.
23. Sheppard DN, Welsh MJ. Structure and function of the CFTR chloride channel. Physiological reviews. 1999;79(1 Suppl):S23-45.
24. Seibert FS, Chang XB, Aleksandrov AA, Clarke DM, Hanrahan JW, Riordan JR. Influence of phosphorylation by protein kinase A on CFTR at the cell surface and endoplasmic reticulum. Biochimica et biophysica acta. 1999;1461(2):275-83.
25. Rich DP, Gregory RJ, Anderson MP, Manavalan P, Smith AE, Welsh MJ. Effect of deleting the R domain on CFTR-generated chloride channels. Science (New York, NY). 1991;253(5016):205-7.
26. Li C, Ramjeesingh M, Wang W, Garami E, Hewryk M, Lee D, et al. ATPase activity of the cystic fibrosis transmembrane conductance regulator. The Journal of biological chemistry. 1996;271(45):28463-8.
27. Wang Y, Wrennall JA, Cai Z, Li H, Sheppard DN. Understanding how cystic fibrosis mutations disrupt CFTR function: from single molecules to animal models. The international journal of biochemistry & cell biology. 2014;52:47-57.
28. Meng X, Clews J, Kargas V, Wang X, Ford RC. The cystic fibrosis transmembrane conductance regulator (CFTR) and its stability. Cellular and molecular life sciences : CMLS. 2017;74(1):23-38.
29. Quinton PM. Physiological basis of cystic fibrosis: a historical perspective. Physiological reviews. 1999;79(1 Suppl):S3-s22.
30. Toczylowska-Maminska R, Dolowy K. Ion transporting proteins of human bronchial epithelium. Journal of cellular biochemistry. 2012;113(2):426-32.
31. Schwiebert EM, Kizer N, Gruenert DC, Stanton BA. GTP-binding proteins inhibit cAMP activation of chloride channels in cystic fibrosis airway epithelial cells. Proceedings of the National Academy of Sciences of the United States of America. 1992;89(22):10623-7.
32. Kunzelmann K, Schreiber R, Boucherot A. Mechanisms of the inhibition of epithelial Na(+) channels by CFTR and purinergic stimulation. Kidney international. 2001;60(2):455-61.
33. Hryciw DH, Guggino WB. Cystic fibrosis transmembrane conductance regulator and the outwardly rectifying chloride channel: a relationship between two chloride channels expressed in epithelial cells. Clinical and experimental pharmacology & physiology. 2000;27(11):892-5.
34. Moran O. Model of the cAMP activation of chloride transport by CFTR channel and the mechanism of potentiators. Journal of theoretical biology. 2010;262(1):73-9.
35. Bozoky Z, Ahmadi S, Milman T, Kim TH, Du K, Di Paola M, et al. Synergy of cAMP and calcium signaling pathways in CFTR regulation. Proc Natl Acad Sci U S A. 2017;114(11):E2086-E95.
36. Scott JD, Dessauer CW, Tasken K. Creating order from chaos: cellular regulation by kinase anchoring. Annual review of pharmacology and toxicology. 2013;53:187-210.
37. Farinha CM, Swiatecka-Urban A, Brautigan DL, Jordan P. Regulatory Crosstalk by Protein Kinases on CFTR Trafficking and Activity. Frontiers in chemistry. 2016;4:1.
38. Egan M, Flotte T, Afione S, Solow R, Zeitlin PL, Carter BJ, et al. Defective regulation of outwardly rectifying Cl- channels by protein kinase A corrected by insertion of CFTR. Nature. 1992;358(6387):581-4.

39. Chappe V, Hinkson DA, Howell LD, Evagelidis A, Liao J, Chang XB, et al. Stimulatory and inhibitory protein kinase C consensus sequences regulate the cystic fibrosis transmembrane conductance regulator. Proc Natl Acad Sci U S A. 2004;101(1):390-5.
40. Carson MR, Travis SM, Welsh MJ. The two nucleotide-binding domains of cystic fibrosis transmembrane conductance regulator (CFTR) have distinct functions in controlling channel activity. Journal of Biological Chemistry. 1995;270(4):1711-7.
41. Mocsai A, Ruland J, Tybulewicz VL. The SYK tyrosine kinase: a crucial player in diverse biological functions. Nat Rev Immunol. 2010;10(6):387-402.
42. Luz S, Kongsuphol P, Mendes AI, Romeiras F, Sousa M, Schreiber R, et al. Contribution of casein kinase 2 and spleen tyrosine kinase to CFTR trafficking and protein kinase A-induced activity. Molecular and cellular biology. 2011;31(22):4392-404.
43. Treharne KJ, Xu Z, Chen J-H, Best OG, Cassidy DM, Gruenert DC, et al. Inhibition of protein Kinase CK2 closes the CFTR Cl-channel, but has no effect on the cystic fibrosis mutant ΔF508-CFTR. Cellular Physiology and Biochemistry. 2009;24(5-6):347-60.
44. Borthwick LA, McGaw J, Conner G, Taylor CJ, Gerke V, Mehta A, et al. The formation of the cAMP/protein kinase A-dependent annexin 2-S100A10 complex with cystic fibrosis conductance regulator protein (CFTR) regulates CFTR channel function. Molecular biology of the cell. 2007;18(9):3388-97.
45. Borthwick LA, Riemen C, Goddard C, Colledge WH, Mehta A, Gerke V, et al. Defective formation of PKA/CnA-dependent annexin 2-S100A10/CFTR complex in DeltaF508 cystic fibrosis cells. Cellular signalling. 2008;20(6):1073-83.
46. Crabtree GR. Generic signals and specific outcomes: signaling through Ca2+, calcineurin, and NF-AT. Cell. 1999;96(5):611-4.
47. Dittmer PJ, Dell'Acqua ML, Sather WA. Ca2+/calcineurin-dependent inactivation of neuronal L-type Ca2+ channels requires priming by AKAP-anchored protein kinase A. Cell reports. 2014;7(5):1410-6.
48. Rebholz H, Nishi A, Liebscher S, Nairn AC, Flajolet M, Greengard P. CK2 negatively regulates Gαs signaling. Proceedings of the National Academy of Sciences. 2009;106(33):14096-101.
49. Li H, Rao A, Hogan PG. Interaction of calcineurin with substrates and targeting proteins. Trends in cell biology. 2011;21(2):91-103.
50. Suzuki J, Bayna E, Li HL, Molle ED, Lew WY. Lipopolysaccharide activates calcineurin in ventricular myocytes. Journal of the American College of Cardiology. 2007;49(4):491-9.
51. Jennings C, Kusler B, Jones PP. Calcineurin inactivation leads to decreased responsiveness to LPS in macrophages and dendritic cells and protects against LPS-induced toxicity in vivo. Innate immunity. 2009;15(2):109-20.
52. Reddy MM, Quinton PM. Deactivation of CFTR-Cl conductance by endogenous phosphatases in the native sweat duct. Am J Physiol. 1996;270(2 Pt 1):C474-80.
53. Travis SM, Berger HA, Welsh MJ. Protein phosphatase 2C dephosphorylates and inactivates cystic fibrosis transmembrane conductance regulator. Proc Natl Acad Sci U S A. 1997;94(20):11055-60.
54. Muimo R. Regulation of CFTR function by annexin A2-S100A10 complex in health and disease. Gen Physiol Biophys. 2009;28 Spec No Focus:F14-9.
55. Perretti M, Flower RJ. Annexin 1 and the biology of the neutrophil. Journal of leukocyte biology. 2004;76(1):25-9.
56. Gerke V, Creutz CE, Moss SE. Annexins: linking Ca2+ signalling to membrane dynamics. Nature reviews Molecular cell biology. 2005;6(6):449-61.

57. Grindheim AK, Saraste J, Vedeler A. Protein phosphorylation and its role in the regulation of Annexin A2 function. Biochim Biophys Acta. 2017;1861(11 Pt A):2515-29.
58. Zhang S, Yu M, Guo Q, Li R, Li G, Tan S, et al. Annexin A2 binds to endosomes and negatively regulates TLR4-triggered inflammatory responses via the TRAM-TRIF pathway. Scientific reports. 2015;5:15859.
59. Swisher JF, Burton N, Bacot SM, Vogel SN, Feldman GM. Annexin A2 tetramer activates human and murine macrophages through TLR4. Blood. 2010;115(3):549-58.
60. Monterisi S, Favia M, Guerra L, Cardone RA, Marzulli D, Reshkin SJ, et al. CFTR regulation in human airway epithelial cells requires integrity of the actin cytoskeleton and compartmentalized cAMP and PKA activity. Journal of cell science. 2012;125(Pt 5):1106-17.
61. Lobo MJ, Amaral MD, Zaccolo M, Farinha CM. EPAC1 activation by cAMP stabilizes CFTR at the membrane by promoting its interaction with NHERF1. J Cell Sci. 2016;129(13):2599-612.
62. Parnell E, Smith BO, Palmer TM, Terrin A, Zaccolo M, Yarwood SJ. Regulation of the inflammatory response of vascular endothelial cells by EPAC1. British journal of pharmacology. 2012;166(2):434-46.
63. Sharma N, LaRusch J, Sosnay PR, Gottschalk LB, Lopez AP, Pellicore MJ, et al. A sequence upstream of canonical PDZ-binding motif within CFTR COOH-terminus enhances NHERF1 interaction. American journal of physiology Lung cellular and molecular physiology. 2016;311(6):L1170-l82.
64. Sun F, Hug MJ, Bradbury NA, Frizzell RA. Protein kinase A associates with cystic fibrosis transmembrane conductance regulator via an interaction with ezrin. The Journal of biological chemistry. 2000;275(19):14360-6.
65. Metrich M, Lucas A, Gastineau M, Samuel JL, Heymes C, Morel E, et al. Epac mediates beta-adrenergic receptor-induced cardiomyocyte hypertrophy. Circulation research. 2008;102(8):959-65.
66. Li H, Pink MD, Murphy JG, Stein A, Dell'Acqua ML, Hogan PG. Balanced interactions of calcineurin with AKAP79 regulate Ca2+–calcineurin–NFAT signaling. Nature structural & molecular biology. 2012;19(3):337-45.
67. Lezoualc'h F, Fazal L, Laudette M, Conte C. Cyclic AMP Sensor EPAC Proteins and Their Role in Cardiovascular Function and Disease. Circulation Research. 2016;118(5):881-97.
68. Pilewski JM, Frizzell RA. Role of CFTR in airway disease. Physiol Rev. 1999;79(1 Suppl):S215-55.
69. Roth EK, Hirtz S, Duerr J, Wenning D, Eichler I, Seydewitz HH, et al. The K+ channel opener 1-EBIO potentiates residual function of mutant CFTR in rectal biopsies from cystic fibrosis patients. PLoS One. 2011;6(8):e24445.
70. Wang J, Haanes KA, Novak I. Purinergic regulation of CFTR and Ca(2+)-activated Cl(-) channels and K(+) channels in human pancreatic duct epithelium. Am J Physiol Cell Physiol. 2013;304(7):C673-84.
71. Klein H, Abu-Arish A, Trinh NT, Luo Y, Wiseman PW, Hanrahan JW, et al. Investigating CFTR and KCa3.1 Protein/Protein Interactions. PLoS One. 2016;11(4):e0153665.
72. Kumar S, Tana A, Shankar A. Cystic fibrosis--what are the prospects for a cure? European journal of internal medicine. 2014;25(9):803-7.
73. Collins FS. Cystic fibrosis: molecular biology and therapeutic implications. Science (New York, NY). 1992;256(5058):774-9.
74. Rowe SM, Miller S, Sorscher EJ. Cystic fibrosis. The New England journal of medicine. 2005;352(19):1992-2001.

75. Illing EA, Woodworth BA. Management of the upper airway in cystic fibrosis. Current opinion in pulmonary medicine. 2014;20(6):623-31.
76. Cutting GR. Cystic fibrosis genetics: from molecular understanding to clinical application. Nat Rev Genet. 2015;16(1):45-56.
77. National Guideline A. National Institute for Health and Care Excellence: Clinical Guidelines. Cystic Fibrosis: Diagnosis and management. London: National Institute for Health and Care Excellence (UK)
Copyright (c) National Institute for Health and Care Excellence 2017.; 2017.
78. MacKenzie T, Gifford AH, Sabadosa KA, Quinton HB, Knapp EA, Goss CH, et al. Longevity of patients with cystic fibrosis in 2000 to 2010 and beyond: survival analysis of the Cystic Fibrosis Foundation patient registry. Annals of internal medicine. 2014;161(4):233-41.
79. Quon BS, Rowe SM. New and emerging targeted therapies for cystic fibrosis. BMJ (Clinical research ed). 2016;352:i859.
80. Shukla SD, Budden KF, Neal R, Hansbro PM. Microbiome effects on immunity, health and disease in the lung. Clinical & translational immunology. 2017;6(3):e133.
81. Stoltz DA, Meyerholz DK, Welsh MJ. Origins of cystic fibrosis lung disease. The New England journal of medicine. 2015;372(4):351-62.
82. Haq IJ, Gray MA, Garnett JP, Ward C, Brodlie M. Airway surface liquid homeostasis in cystic fibrosis: pathophysiology and therapeutic targets. Thorax. 2016;71(3):284-7.
83. Derichs N, Jin BJ, Song Y, Finkbeiner WE, Verkman AS. Hyperviscous airway periciliary and mucous liquid layers in cystic fibrosis measured by confocal fluorescence photobleaching. FASEB journal : official publication of the Federation of American Societies for Experimental Biology. 2011;25(7):2325-32.
84. Pezzulo AA, Tang XX, Hoegger MJ, Abou Alaiwa MH, Ramachandran S, Moninger TO, et al. Reduced airway surface pH impairs bacterial killing in the porcine cystic fibrosis lung. Nature. 2012;487(7405):109-13.
85. Gelfond D, Borowitz D. Gastrointestinal complications of cystic fibrosis. Clinical gastroenterology and hepatology : the official clinical practice journal of the American Gastroenterological Association. 2013;11(4):333-42; quiz e30-1.
86. Lewis C, Blackman SM, Nelson A, Oberdorfer E, Wells D, Dunitz J, et al. Diabetes-related mortality in adults with cystic fibrosis. Role of genotype and sex. American journal of respiratory and critical care medicine. 2015;191(2):194-200.
87. Cutting GR. Modifier genes in Mendelian disorders: the example of cystic fibrosis. Annals of the New York Academy of Sciences. 2010;1214:57-69.
88. Taylor-Robinson DC, Thielen K, Pressler T, Olesen HV, Diderichsen F, Diggle PJ, et al. Low socioeconomic status is associated with worse lung function in the Danish cystic fibrosis population. The European respiratory journal. 2014;44(5):1363-6.
89. Kopp BT, Sarzynski L, Khalfoun S, Hayes D, Jr., Thompson R, Nicholson L, et al. Detrimental effects of secondhand smoke exposure on infants with cystic fibrosis. Pediatric pulmonology. 2015;50(1):25-34.
90. Zielenski J, Tsui LC. Cystic fibrosis: genotypic and phenotypic variations. Annual review of genetics. 1995;29:777-807.
91. Veit G, Avramescu RG, Chiang AN, Houck SA, Cai Z, Peters KW, et al. From CFTR biology toward combinatorial pharmacotherapy: expanded classification of cystic fibrosis mutations. Molecular biology of the cell. 2016;27(3):424-33.
92. Ward CL, Omura S, Kopito RR. Degradation of CFTR by the ubiquitin-proteasome pathway. Cell. 1995;83(1):121-7.
93. Kopito RR. Biosynthesis and degradation of CFTR. Physiological reviews. 1999;79(1 Suppl):S167-73.

94. Cui L, Aleksandrov L, Hou YX, Gentzsch M, Chen JH, Riordan JR, et al. The role of cystic fibrosis transmembrane conductance regulator phenylalanine 508 side chain in ion channel gating. The Journal of physiology. 2006;572(Pt 2):347-58.
95. Amaral MD, Farinha CM. Rescuing mutant CFTR: a multi-task approach to a better outcome in treating cystic fibrosis. Current pharmaceutical design. 2013;19(19):3497-508.
96. Castellani S, Favia M, Guerra L, Carbone A, Abbattiscianni AC, Di Gioia S, et al. Emerging relationship between CFTR, actin and tight junction organization in cystic fibrosis airway epithelium. Histology and histopathology. 2017;32(5):445-59.
97. Martin SL, Saint-Criq V, Hwang TC, Csanady L. Ion channels as targets to treat cystic fibrosis lung disease. Journal of cystic fibrosis : official journal of the European Cystic Fibrosis Society. 2017.
98. Elborn JS. Cystic fibrosis. Lancet (London, England). 2016;388(10059):2519-31.
99. Mall M, Grubb BR, Harkema JR, O'Neal WK, Boucher RC. Increased airway epithelial Na+ absorption produces cystic fibrosis-like lung disease in mice. Nature medicine. 2004;10(5):487-93.
100. John G, Yildirim AO, Rubin BK, Gruenert DC, Henke MO. TLR-4-mediated innate immunity is reduced in cystic fibrosis airway cells. Am J Respir Cell Mol Biol. 2010;42(4):424-31.
101. Boucher RC. An overview of the pathogenesis of cystic fibrosis lung disease. Advanced drug delivery reviews. 2002;54(11):1359-71.
102. Hollenhorst MI, Richter K, Fronius M. Ion transport by pulmonary epithelia. Journal of biomedicine & biotechnology. 2011;2011:174306.
103. Kim JK, Kim SS, Rha KW, Kim CH, Cho JH, Lee CH, et al. Expression and localization of surfactant proteins in human nasal epithelium. American journal of physiology Lung cellular and molecular physiology. 2007;292(4):L879-84.
104. Petrocheilou A, Papagrigoriou-Theodoridou M, Michos A, Doudounakis SE, Loukou I, Kaditis A. Early-Life Pseudomonas aeruginosa Infection in Cystic Fibrosis and Lung Disease Progression. Global pediatric health. 2017;4:2333794x17738465.
105. Rogers GB, Hart CA, Mason JR, Hughes M, Walshaw MJ, Bruce KD. Bacterial diversity in cases of lung infection in cystic fibrosis patients: 16S ribosomal DNA (rDNA) length heterogeneity PCR and 16S rDNA terminal restriction fragment length polymorphism profiling. Journal of clinical microbiology. 2003;41(8):3548-58.
106. Filkins LM, Hampton TH, Gifford AH, Gross MJ, Hogan DA, Sogin ML, et al. Prevalence of streptococci and increased polymicrobial diversity associated with cystic fibrosis patient stability. Journal of bacteriology. 2012;194(17):4709-17.
107. Gilligan PH. Infections in patients with cystic fibrosis: diagnostic microbiology update. Clinics in laboratory medicine. 2014;34(2):197-217.
108. Alvarez-Ortega C, Harwood CS. Responses of Pseudomonas aeruginosa to low oxygen indicate that growth in the cystic fibrosis lung is by aerobic respiration. Molecular microbiology. 2007;65(1):153-65.
109. Schobert M, Jahn D. Anaerobic physiology of Pseudomonas aeruginosa in the cystic fibrosis lung. International journal of medical microbiology : IJMM. 2010;300(8):549-56.
110. Boucher RC. New concepts of the pathogenesis of cystic fibrosis lung disease. The European respiratory journal. 2004;23(1):146-58.
111. Sibley CD, Duan K, Fischer C, Parkins MD, Storey DG, Rabin HR, et al. Discerning the complexity of community interactions using a Drosophila model of polymicrobial infections. PLoS pathogens. 2008;4(10):e1000184.
112. Bragonzi A, Farulla I, Paroni M, Twomey KB, Pirone L, Lore NI, et al. Modelling co-infection of the cystic fibrosis lung by Pseudomonas aeruginosa and Burkholderia

cenocepacia reveals influences on biofilm formation and host response. PLoS One. 2012;7(12):e52330.
113. Bhagirath AY, Li Y, Somayajula D, Dadashi M, Badr S, Duan K. Cystic fibrosis lung environment and Pseudomonas aeruginosa infection. BMC Pulm Med. 2016;16(1):174.
114. Wat D, Gelder C, Hibbitts S, Cafferty F, Bowler I, Pierrepoint M, et al. The role of respiratory viruses in cystic fibrosis. Journal of cystic fibrosis : official journal of the European Cystic Fibrosis Society. 2008;7(4):320-8.
115. Chotirmall SH, O'Donoghue E, Bennett K, Gunaratnam C, O'Neill SJ, McElvaney NG. Sputum Candida albicans presages FEV(1) decline and hospital-treated exacerbations in cystic fibrosis. Chest. 2010;138(5):1186-95.
116. Heijerman H. Infection and inflammation in cystic fibrosis: a short review. Journal of cystic fibrosis : official journal of the European Cystic Fibrosis Society. 2005;4 Suppl 2:3-5.
117. Nichols DP, Chmiel JF. Inflammation and its genesis in cystic fibrosis. Pediatric pulmonology. 2015;50 Suppl 40:S39-56.
118. Mott LS, Park J, Murray CP, Gangell CL, de Klerk NH, Robinson PJ, et al. Progression of early structural lung disease in young children with cystic fibrosis assessed using CT. Thorax. 2012;67(6):509-16.
119. Lyczak JB, Cannon CL, Pier GB. Lung infections associated with cystic fibrosis. Clinical microbiology reviews. 2002;15(2):194-222.
120. Fritzsching B, Zhou-Suckow Z, Trojanek JB, Schubert SC, Schatterny J, Hirtz S, et al. Hypoxic epithelial necrosis triggers neutrophilic inflammation via IL-1 receptor signaling in cystic fibrosis lung disease. American journal of respiratory and critical care medicine. 2015;191(8):902-13.
121. Stick S, Tiddens H, Aurora P, Gustafsson P, Ranganathan S, Robinson P, et al. Early intervention studies in infants and preschool children with cystic fibrosis: are we ready? The European respiratory journal. 2013;42(2):527-38.
122. Bruscia EM, Bonfield TL. Cystic Fibrosis Lung Immunity: The Role of the Macrophage. J Innate Immun. 2016;8(6):550-63.
123. Bragonzi A, Horati H, Kerrigan L, Lore NI, Scholte BJ, Weldon S. Inflammation and host-pathogen interaction: Cause and consequence in cystic fibrosis lung disease. Journal of cystic fibrosis : official journal of the European Cystic Fibrosis Society. 2017.
124. Cigana C, Lore NI, Riva C, De Fino I, Spagnuolo L, Sipione B, et al. Tracking the immunopathological response to Pseudomonas aeruginosa during respiratory infections. Scientific reports. 2016;6:21465.
125. Courtney JM, Ennis M, Elborn JS. Cytokines and inflammatory mediators in cystic fibrosis. Journal of cystic fibrosis : official journal of the European Cystic Fibrosis Society. 2004;3(4):223-31.
126. Dinarello CA. Anti-inflammatory Agents: Present and Future. Cell. 2010;140(6):935-50.
127. Downey DG, Bell SC, Elborn JS. Neutrophils in cystic fibrosis. Thorax. 2009;64(1):81-8.
128. Moser C, Johansen HK, Song Z, Hougen HP, Rygaard J, Hoiby N. Chronic Pseudomonas aeruginosa lung infection is more severe in Th2 responding BALB/c mice compared to Th1 responding C3H/HeN mice. APMIS : acta pathologica, microbiologica, et immunologica Scandinavica. 1997;105(11):838-42.
129. Moser C, Hougen HP, Song Z, Rygaard J, Kharazmi A, Hoiby N. Early immune response in susceptible and resistant mice strains with chronic Pseudomonas aeruginosa lung infection determines the type of T-helper cell response. APMIS : acta pathologica, microbiologica, et immunologica Scandinavica. 1999;107(12):1093-100.

130. Moser C, Kjaergaard S, Pressler T, Kharazmi A, Koch C, Hoiby N. The immune response to chronic Pseudomonas aeruginosa lung infection in cystic fibrosis patients is predominantly of the Th2 type. APMIS : acta pathologica, microbiologica, et immunologica Scandinavica. 2000;108(5):329-35.
131. Ulrich M, Worlitzsch D, Viglio S, Siegmann N, Iadarola P, Shute JK, et al. Alveolar inflammation in cystic fibrosis. Journal of cystic fibrosis : official journal of the European Cystic Fibrosis Society. 2010;9(3):217-27.
132. Ratner D, Mueller C. Immune responses in cystic fibrosis: are they intrinsically defective? American journal of respiratory cell and molecular biology. 2012;46(6):715-22.
133. Strieter RM, Kunkel SL, Showell HJ, Remick DG, Phan SH, Ward PA, et al. Endothelial cell gene expression of a neutrophil chemotactic factor by TNF-alpha, LPS, and IL-1 beta. Science (New York, NY). 1989;243(4897):1467-9.
134. Su X, Looney MR, Su HE, Lee JW, Song Y, Matthay MA. Role of CFTR expressed by neutrophils in modulating acute lung inflammation and injury in mice. Inflammation research : official journal of the European Histamine Research Society [et al]. 2011;60(7):619-32.
135. Morris MR, Doull IJ, Dewitt S, Hallett MB. Reduced iC3b-mediated phagocytotic capacity of pulmonary neutrophils in cystic fibrosis. Clinical and experimental immunology. 2005;142(1):68-75.
136. Gao L, Broughman JR, Iwamoto T, Tomich JM, Venglarik CJ, Forman HJ. Synthetic chloride channel restores glutathione secretion in cystic fibrosis airway epithelia. American journal of physiology Lung cellular and molecular physiology. 2001;281(1):L24-30.
137. Chen J, Jiang XH, Chen H, Guo JH, Tsang LL, Yu MK, et al. CFTR negatively regulates cyclooxygenase-2-PGE(2) positive feedback loop in inflammation. Journal of cellular physiology. 2012;227(6):2759-66.
138. Friard J, Tauc M, Cougnon M, Compan V, Duranton C, Rubera I. Comparative Effects of Chloride Channel Inhibitors on LRRC8/VRAC-Mediated Chloride Conductance. Front Pharmacol. 2017;8:328.
139. Cheng G, Ramanathan A, Shao Z, Agrawal DK. Chloride channel expression and functional diversity in the immune cells of allergic diseases. Curr Mol Med. 2008;8(5):401-7.
140. Huang F, Zhang H, Wu M, Yang H, Kudo M, Peters CJ, et al. Calcium-activated chloride channel TMEM16A modulates mucin secretion and airway smooth muscle contraction. Proc Natl Acad Sci U S A. 2012;109(40):16354-9.
141. Sondo E, Caci E, Galietta LJ. The TMEM16A chloride channel as an alternative therapeutic target in cystic fibrosis. The international journal of biochemistry & cell biology. 2014;52:73-6.
142. Vishwanath S, Ramphal R, Guay CM, DesJardins D, Pier GB. Respiratory-mucin inhibition of the opsonophagocytic killing of Pseudomonas aeruginosa. Infection and immunity. 1988;56(9):2218-22.
143. Belchamber KBR, Donnelly LE. Macrophage Dysfunction in Respiratory Disease. Results and problems in cell differentiation. 2017;62:299-313.
144. Sajjan U, Thanassoulis G, Cherapanov V, Lu A, Sjolin C, Steer B, et al. Enhanced susceptibility to pulmonary infection with Burkholderia cepacia in Cftr(-/-) mice. Infection and immunity. 2001;69(8):5138-50.
145. Zaman MM, Gelrud A, Junaidi O, Regan MM, Warny M, Shea JC, et al. Interleukin 8 secretion from monocytes of subjects heterozygous for the deltaF508 cystic fibrosis transmembrane conductance regulator gene mutation is altered. Clinical and diagnostic laboratory immunology. 2004;11(5):819-24.

146. Di A, Brown ME, Deriy LV, Li C, Szeto FL, Chen Y, et al. CFTR regulates phagosome acidification in macrophages and alters bactericidal activity. Nat Cell Biol. 2006;8(9):933-44.
147. Del Porto P, Cifani N, Guarnieri S, Di Domenico EG, Mariggio MA, Spadaro F, et al. Dysfunctional CFTR alters the bactericidal activity of human macrophages against Pseudomonas aeruginosa. PLoS One. 2011;6(5):e19970.
148. Lamothe J, Valvano MA. Burkholderia cenocepacia-induced delay of acidification and phagolysosomal fusion in cystic fibrosis transmembrane conductance regulator (CFTR)-defective macrophages. Microbiology (Reading, England). 2008;154(Pt 12):3825-34.
149. Kim MJ, Cheng G, Agrawal DK. Cl- channels are expressed in human normal monocytes: a functional role in migration, adhesion and volume change. Clinical and experimental immunology. 2004;138(3):453-9.
150. Park BS, Lee JO. Recognition of lipopolysaccharide pattern by TLR4 complexes. Exp Mol Med. 2013;45:e66.
151. Hallows KR, Kobinger GP, Wilson JM, Witters LA, Foskett JK. Physiological modulation of CFTR activity by AMP-activated protein kinase in polarized T84 cells. American journal of physiology Cell physiology. 2003;284(5):C1297-308.
152. Tarique AA, Sly PD, Holt PG, Bosco A, Ware RS, Logan J, et al. CFTR-dependent defect in alternatively-activated macrophages in cystic fibrosis. Journal of cystic fibrosis : official journal of the European Cystic Fibrosis Society. 2017;16(4):475-82.
153. Bruscia EM, Zhang PX, Ferreira E, Caputo C, Emerson JW, Tuck D, et al. Macrophages directly contribute to the exaggerated inflammatory response in cystic fibrosis transmembrane conductance regulator-/- mice. American journal of respiratory cell and molecular biology. 2009;40(3):295-304.
154. Bauernfeind FG, Horvath G, Stutz A, Alnemri ES, MacDonald K, Speert D, et al. Cutting edge: NF-kappaB activating pattern recognition and cytokine receptors license NLRP3 inflammasome activation by regulating NLRP3 expression. Journal of immunology (Baltimore, Md : 1950). 2009;183(2):787-91.
155. Lee S, Suh GY, Ryter SW, Choi AM. Regulation and Function of the Nucleotide Binding Domain Leucine-Rich Repeat-Containing Receptor, Pyrin Domain-Containing-3 Inflammasome in Lung Disease. American journal of respiratory cell and molecular biology. 2016;54(2):151-60.
156. Brodsky IE, Monack D. NLR-mediated control of inflammasome assembly in the host response against bacterial pathogens. Seminars in immunology. 2009;21(4):199-207.
157. Franchi L, Eigenbrod T, Munoz-Planillo R, Nunez G. The inflammasome: a caspase-1-activation platform that regulates immune responses and disease pathogenesis. Nature immunology. 2009;10(3):241-7.
158. Muruve DA, Petrilli V, Zaiss AK, White LR, Clark SA, Ross PJ, et al. The inflammasome recognizes cytosolic microbial and host DNA and triggers an innate immune response. Nature. 2008;452(7183):103-7.
159. Provoost S, Maes T, Pauwels NS, Vanden Berghe T, Vandenabeele P, Lambrecht BN, et al. NLRP3/caspase-1-independent IL-1beta production mediates diesel exhaust particle-induced pulmonary inflammation. Journal of immunology (Baltimore, Md : 1950). 2011;187(6):3331-7.
160. Petrilli V, Papin S, Dostert C, Mayor A, Martinon F, Tschopp J. Activation of the NALP3 inflammasome is triggered by low intracellular potassium concentration. Cell death and differentiation. 2007;14(9):1583-9.

161. Kawana N, Yamamota Y, Kino Y, Satoh J. Molecular Network of NLRP3 Inflammasome Activation-Responsive Genes in a Human Monocyte Cell Line. Austin Journal of Clinical Immunology. 2014;1(4).
162. Arend WP, Palmer G, Gabay C. IL-1, IL-18, and IL-33 families of cytokines. Immunological reviews. 2008;223:20-38.
163. Broz P, von Moltke J, Jones JW, Vance RE, Monack DM. Differential requirement for Caspase-1 autoproteolysis in pathogen-induced cell death and cytokine processing. Cell host & microbe. 2010;8(6):471-83.
164. Tang A, Sharma A, Jen R, Hirschfeld AF, Chilvers MA, Lavoie PM, et al. Inflammasome-mediated IL-1beta production in humans with cystic fibrosis. PloS one. 2012;7(5):e37689.
165. Dinarello CA. Interleukin-1 in the pathogenesis and treatment of inflammatory diseases. Blood. 2011;117(14):3720-32.
166. Basu R, Whitley SK, Bhaumik S, Zindl CL, Schoeb TR, Benveniste EN, et al. IL-1 signaling modulates activation of STAT transcription factors to antagonize retinoic acid signaling and control the TH17 cell-iTreg cell balance. Nature immunology. 2015;16(3):286-95.
167. de Luca A, Smeekens SP, Casagrande A, Iannitti R, Conway KL, Gresnigt MS, et al. IL-1 receptor blockade restores autophagy and reduces inflammation in chronic granulomatous disease in mice and in humans. Proceedings of the National Academy of Sciences of the United States of America. 2014;111(9):3526-31.
168. Gresnigt MS, van de Veerdonk FL. The role of interleukin-1 family members in the host defence against Aspergillus fumigatus. Mycopathologia. 2014;178(5-6):395-401.
169. Hartl D, Latzin P, Hordijk P, Marcos V, Rudolph C, Woischnik M, et al. Cleavage of CXCR1 on neutrophils disables bacterial killing in cystic fibrosis lung disease. Nature medicine. 2007;13(12):1423-30.
170. Coutinho CA, Marson FA, Marcelino AR, Bonadia LC, Carlin MP, Ribeiro AF, et al. TNF-alpha polymorphisms as a potential modifier gene in the cystic fibrosis. International journal of molecular epidemiology and genetics. 2014;5(2):87-99.
171. Charo IF, Ransohoff RM. The many roles of chemokines and chemokine receptors in inflammation. The New England journal of medicine. 2006;354(6):610-21.
172. Borthwick LA, Riemen C, Goddard C, Colledge WH, Mehta A, Gerke V, et al. Defective formation of PKA/CnA-dependent annexin 2–S100A10/CFTR complex in ΔF508 cystic fibrosis cells. Cellular Signalling. 2008;20(6):1073-83.
173. Little R, Muimo R, Robson L, Harris K, Grabowski PS. The Transient Receptor Potential Ion Channel TRPV6 Is Expressed at Low Levels in Osteoblasts and Has Little Role in Osteoblast Calcium Uptake. PLoS ONE. 2011;6(11):e28166.
174. Walters S, Mehta A. Epidemiology of cystic fibrosis. Cystic fibrosis. 2007;3:21-45.
175. Chappe V, Irvine T, Liao J, Evagelidis A, Hanrahan JW. Phosphorylation of CFTR by PKA promotes binding of the regulatory domain. The EMBO journal. 2005;24(15):2730-40.
176. Kallenberg L. Calcium signalling in secretory cells. Archives of physiology and biochemistry. 2000;108(5):385-90.
177. Hamidi H, Lilja J, Ivaska J. Using xCELLigence RTCA Instrument to Measure Cell Adhesion. Bio Protoc. 2017;7(24).
178. Bennett S, Breit SN. Variables in the isolation and culture of human monocytes that are of particular relevance to studies of HIV. J Leukoc Biol. 1994;56(3):236-40.

179. Elkord E, Williams PE, Kynaston H, Rowbottom AW. Human monocyte isolation methods influence cytokine production from in vitro generated dendritic cells. Immunology. 2005;114(2):204-12.
180. Arango Duque G, Descoteaux A. Macrophage cytokines: involvement in immunity and infectious diseases. Front Immunol. 2014;5:491.
181. Lopez S, Peiretti F, Morange P, Laouar A, Fossat C, Bonardo B, et al. Activation of plasminogen activator inhibitor-1 synthesis by phorbol esters in human promyelocyte HL-60--roles of PCKbeta and MAPK p42. Thrombosis and haemostasis. 1999;81(3):415-22.
182. Bass JJ, Wilkinson DJ, Rankin D, Phillips BE, Szewczyk NJ, Smith K, et al. An overview of technical considerations for Western blotting applications to physiological research. Scand J Med Sci Sports. 2017;27(1):4-25.
183. Aramburu J, Rao A, Klee CB. Calcineurin: from structure to function. Current topics in cellular regulation. 2000;36:237-95.
184. Jin L, Harrison SC. Crystal structure of human calcineurin complexed with cyclosporin A and human cyclophilin. Proc Natl Acad Sci U S A. 2002;99(21):13522-6.
185. Pereira L, Métrich M, Fernández- Velasco M, Lucas A, Leroy J, Perrier R, et al. The cAMP binding protein Epac modulates Ca2+ sparks by a Ca2+/calmodulin kinase signalling pathway in rat cardiac myocytes. The Journal of physiology. 2007;583(2):685-94.
186. Singer SJ, Nicolson GL. The fluid mosaic model of the structure of cell membranes. Science (New York, NY). 1972;175(4023):720-31.
187. Gershoni JM. Protein blotting: a manual. Methods Biochem Anal. 1988;33:1-58.
188. Aidley DJ, Stanfield PR. Ion channels: molecules in action: Cambridge University Press; 1996.
189. Hamill OP, Marty A, Neher E, Sakmann B, Sigworth FJ. Improved patch-clamp techniques for high-resolution current recording from cells and cell-free membrane patches. Pflugers Arch. 1981;391(2):85-100.
190. Ozaki N, Shibasaki T, Kashima Y, Miki T, Takahashi K, Ueno H, et al. cAMP-GEFII is a direct target of cAMP in regulated exocytosis. Nature cell biology. 2000;2(11):805-11.
191. Hauber HP, Goldmann T, Vollmer E, Wollenberg B, Hung HL, Levitt RC, et al. LPS-induced mucin expression in human sinus mucosa can be attenuated by hCLCA inhibitors. J Endotoxin Res. 2007;13(2):109-16.
192. Illek B, Fu Z, Schwarzer C, Banzon T, Jalickee S, Miller SS, et al. Flagellin-stimulated Cl- secretion and innate immune responses in airway epithelia: role for p38. American journal of physiology Lung cellular and molecular physiology. 2008;295(4):L531-42.
193. Cullen SP, Kearney CJ, Clancy DM, Martin SJ. Diverse activators of the NLRP3 inflammasome promote IL-1β secretion by triggering necrosis. Cell reports. 2015;11(10):1535-48.
194. Richter E, Ventz K, Harms M, Mostertz J, Hochgräfe F. Induction of macrophage function in human THP-1 cells is associated with rewiring of MAPK signaling and activation of MAP3K7 (TAK1) protein kinase. Frontiers in cell and developmental biology. 2016;4:21.
195. R&D-System. Human IL-1 beta/IL-1F2 Quantikine ELISA Kit [cited 2018 9th April 2018]. Available from: https://www.rndsystems.com/products/human-il-1-beta-il-1f2-quantikine-elisa-kit_dlb50.
196. BD-Biosciences. Human Inflammatory Cytokine Kit 2018 [Available from: http://www.bdbiosciences.com/us/applications/research/bead-based-immunoassays/cba-kits/human-inflammatory-cytokine-kit/p/551811.

197. Berczeli O, Vizvári E, Katona M, Török D, Szalay L, Rárosi F, et al. Novel Insight Into the Role of CFTR in Lacrimal Gland Duct Function in Mice. Investigative ophthalmology & visual science. 2018;59(1):54-62.
198. Li C, Naren AP. CFTR chloride channel in the apical compartments: spatiotemporal coupling to its interacting partners. Integr Biol (Camb). 2010;2(4):161-77.
199. Lee H-J, Zheng JJ. PDZ domains and their binding partners: structure, specificity, and modification. Cell Communication and Signaling : CCS. 2010;8:8-.
200. Bertrand CA, Frizzell RA. The role of regulated CFTR trafficking in epithelial secretion. Am J Physiol Cell Physiol. 2003;285(1):C1-18.
201. Brandherm I, Disse J, Zeuschner D, Gerke V. cAMP-induced secretion of endothelial von Willebrand factor is regulated by a phosphorylation/dephosphorylation switch in annexin A2. Blood. 2013;122(6):1042-51.
202. Lowenstein CJ, Morrell CN, Yamakuchi M. Regulation of Weibel-Palade body exocytosis. Trends in cardiovascular medicine. 2005;15(8):302-8.
203. Valentijn KM, van Driel LF, Mourik MJ, Hendriks GJ, Arends TJ, Koster AJ, et al. Multigranular exocytosis of Weibel-Palade bodies in vascular endothelial cells. Blood. 2010;116(10):1807-16.
204. Nilius B, Gerke V, Prenen J, Szucs G, Heinke S, Weber K, et al. Annexin II modulates volume-activated chloride currents in vascular endothelial cells. The Journal of biological chemistry. 1996;271(48):30631-6.
205. Kelley JL, Rozek MM, Suenram CA, Schwartz CJ. Activation of human blood monocytes by adherence to tissue culture plastic surfaces. Exp Mol Pathol. 1987;46(3):266-78.
206. Guo Y, Wilderman A, Zhang L, Taylor SS, Insel PA. Quantitative proteomics analysis of the cAMP/protein kinase A signaling pathway. Biochemistry. 2012;51(46):9323-32.
207. Ferguson RE, Carroll HP, Harris A, Maher ER, Selby PJ, Banks RE. Housekeeping proteins: a preliminary study illustrating some limitations as useful references in protein expression studies. Proteomics. 2005;5(2):566-71.
208. Daigneault M, Preston JA, Marriott HM, Whyte MK, Dockrell DH. The identification of markers of macrophage differentiation in PMA-stimulated THP-1 cells and monocyte-derived macrophages. PLoS One. 2010;5(1):e8668.
209. O'Connell PA, Surette AP, Liwski RS, Svenningsson P, Waisman DM. S100A10 regulates plasminogen-dependent macrophage invasion. Blood. 2010;116(7):1136-46.
210. Swisher JF, Khatri U, Feldman GM. Annexin A2 is a soluble mediator of macrophage activation. Journal of leukocyte biology. 2007;82(5):1174-84.
211. Gooch JL, Pergola PE, Guler RL, Abboud HE, Barnes JL. Differential expression of calcineurin A isoforms in the diabetic kidney. J Am Soc Nephrol. 2004;15(6):1421-9.
212. Kang YJ, Kusler B, Otsuka M, Hughes M, Suzuki N, Suzuki S, et al. Calcineurin negatively regulates TLR-mediated activation pathways. J Immunol. 2007;179(7):4598-607.
213. Liu F, Grundke-Iqbal I, Iqbal K, Oda Y, Tomizawa K, Gong CX. Truncation and activation of calcineurin A by calpain I in Alzheimer disease brain. J Biol Chem. 2005;280(45):37755-62.
214. Kubokawa M, Nakamura K, Komagiri Y. Interaction between Calcineurin and Ca2+/Calmodulin Kinase-II in Modulating Cellular Functions. Enzyme Research. 2011;2011.
215. Juvvadi PR, Gehrke C, Fortwendel JR, Lamoth F, Soderblom EJ, Cook EC, et al. Phosphorylation of calcineurin at a novel serine-proline rich region orchestrates hyphal growth and virulence in Aspergillus fumigatus. PLoS Pathog. 2013;9(8):e1003564.

216. Nunes AR, Sample V, Xiang YK, Monteiro EC, Gauda E, Zhang J. Effect of oxygen on phosphodiesterases (PDE) 3 and 4 isoforms and PKA activity in the superior cervical ganglia. Advances in experimental medicine and biology. 2012;758:287-94.
217. Hull J. Cystic fibrosis transmembrane conductance regulator dysfunction and its treatment. J R Soc Med. 2012;105 Suppl 2:S2-8.
218. Johansson J, Vezzalini M, Verze G, Caldrer S, Bolognin S, Buffelli M, et al. Detection of CFTR protein in human leukocytes by flow cytometry. Cytometry A. 2014;85(7):611-20.
219. Gao Z, Su X. CFTR regulates acute inflammatory responses in macrophages. QJM. 2015;108(12):951-8.
220. Sorio C, Buffelli M, Angiari C, Ettorre M, Johansson J, Vezzalini M, et al. Defective CFTR expression and function are detectable in blood monocytes: development of a new blood test for cystic fibrosis. PLoS One. 2011;6(7):e22212.
221. Ousingsawat J, Wanitchakool P, Kmit A, Romao AM, Jantarajit W, Schreiber R, et al. Anoctamin 6 mediates effects essential for innate immunity downstream of P2X7 receptors in macrophages. Nat Commun. 2015;6:6245.
222. Martins JR, Faria D, Kongsuphol P, Reisch B, Schreiber R, Kunzelmann K. Anoctamin 6 is an essential component of the outwardly rectifying chloride channel. Proceedings of the National Academy of Sciences. 2011;108(44):18168-72.
223. Jovov B, Ismailov, II, Berdiev BK, Fuller CM, Sorscher EJ, Dedman JR, et al. Interaction between cystic fibrosis transmembrane conductance regulator and outwardly rectified chloride channels. J Biol Chem. 1995;270(49):29194-200.
224. Tipirneni KE, Grayson JW, Zhang S, Cho D-Y, Skinner DF, Lim D-J, et al. Assessment of acquired mucociliary clearance defects using micro-optical coherence tomography. International forum of allergy & rhinology. 2017;7(9):920-5.
225. Hartl D, Gaggar A, Bruscia E, Hector A, Marcos V, Jung A, et al. Innate immunity in cystic fibrosis lung disease. J Cyst Fibros. 2012;11(5):363-82.
226. Domingo-Fernández R, Coll RC, Kearney J, Breit S, O'Neill LA. The intracellular chloride channel proteins CLIC1 and CLIC4 induce IL-1β transcription and activate the NLRP3 inflammasome. Journal of Biological Chemistry. 2017;292(29):12077-87.
227. Wong C-O, Gregory S, Hu H, Chao Y, Sepúlveda VE, He Y, et al. Lysosomal degradation is required for sustained phagocytosis of bacteria by macrophages. Cell host & microbe. 2017;21(6):719-30. e6.
228. Xu Y, Tertilt C, Krause A, Quadri LE, Crystal RG, Worgall S. Influence of the cystic fibrosis transmembrane conductance regulator on expression of lipid metabolism-related genes in dendritic cells. Respir Res. 2009;10:26.
229. Vergne I, Chua J, Lee H-H, Lucas M, Belisle J, Deretic V. Mechanism of phagolysosome biogenesis block by viable Mycobacterium tuberculosis. Proceedings of the National Academy of Sciences of the United States of America. 2005;102(11):4033-8.
230. Swisher JF, Burton N, Bacot SM, Vogel SN, Feldman GM. Annexin A2 tetramer activates human and murine macrophages through TLR4. Blood. 2010;115(3):549-58.
231. Kopeikin Z, Sohma Y, Li M, Hwang TC. On the mechanism of CFTR inhibition by a thiazolidinone derivative. J Gen Physiol. 2010;136(6):659-71.
232. Melis N, Tauc M, Cougnon M, Bendahhou S, Giuliano S, Rubera I, et al. Revisiting CFTR inhibition: a comparative study of CFTRinh -172 and GlyH-101 inhibitors. Br J Pharmacol. 2014;171(15):3716-27.
233. Wang L, Shen M, Guo X, Wang B, Xia Y, Wang N, et al. Volume-sensitive outwardly rectifying chloride channel blockers protect against high glucose-induced apoptosis of cardiomyocytes via autophagy activation. Sci Rep. 2017;7:44265.

234. Simonin-Le Jeune K, Le Jeune A, Jouneau S, Belleguic C, Roux PF, Jaguin M, et al. Impaired functions of macrophage from cystic fibrosis patients: CD11b, TLR-5 decrease and sCD14, inflammatory cytokines increase. PLoS One. 2013;8(9):e75667.
235. Wulff H. New light on the "old" chloride channel blocker DIDS. ACS Chem Biol. 2008;3(7):399-401.
236. Mohammad-Panah R, Ackerley C, Rommens J, Choudhury M, Wang Y, Bear CE. The chloride channel ClC-4 co-localizes with cystic fibrosis transmembrane conductance regulator and may mediate chloride flux across the apical membrane of intestinal epithelia. Journal of Biological Chemistry. 2002;277(1):566-74.
237. Pongkorpsakol P, Pathomthongtaweechai N, Srimanote P, Soodvilai S, Chatsudthipong V, Muanprasat C. Inhibition of cAMP-activated intestinal chloride secretion by diclofenac: cellular mechanism and potential application in cholera. PLoS Negl Trop Dis. 2014;8(9):e3119.
238. Benedetto R, Ousingsawat J, Wanitchakool P, Zhang Y, Holtzman MJ, Amaral M, et al. Epithelial Chloride Transport by CFTR Requires TMEM16A. Sci Rep. 2017;7(1):12397.
239. Parkins MD, Floto RA. Emerging bacterial pathogens and changing concepts of bacterial pathogenesis in cystic fibrosis. J Cyst Fibros. 2015;14(3):293-304.
240. Lovewell RR, Patankar YR, Berwin B. Mechanisms of phagocytosis and host clearance of Pseudomonas aeruginosa. American journal of physiology Lung cellular and molecular physiology. 2014;306(7):L591-603.
241. Zemanick ET, Accurso FJ. Cystic fibrosis transmembrane conductance regulator and pseudomonas. Am J Respir Crit Care Med. 2014;189(7):763-5.
242. Jiang L, Salao K, Li H, Rybicka JM, Yates RM, Luo XW, et al. Intracellular chloride channel protein CLIC1 regulates macrophage function through modulation of phagosomal acidification. Journal of Cell Science. 2012;125(22):5479-88.
243. Aiken ML, Painter RG, Zhou Y, Wang G. Chloride transport in functionally active phagosomes isolated from Human neutrophils. Free Radic Biol Med. 2012;53(12):2308-17.
244. Davies MJ. Myeloperoxidase-derived oxidation: mechanisms of biological damage and its prevention. J Clin Biochem Nutr. 2011;48(1):8-19.
245. Chanput W, Mes J, Vreeburg RA, Savelkoul HF, Wichers HJ. Transcription profiles of LPS-stimulated THP-1 monocytes and macrophages: a tool to study inflammation modulating effects of food-derived compounds. Food Funct. 2010;1(3):254-61.
246. Sharif O, Bolshakov VN, Raines S, Newham P, Perkins ND. Transcriptional profiling of the LPS induced NF-κB response in macrophages. BMC Immunology. 2007;8:1-.
247. Roessler M, Sewald X, Muller V. Chloride dependence of growth in bacteria. FEMS Microbiol Lett. 2003;225(1):161-5.
248. Busetto S, Trevisan E, Decleva E, Dri P, Menegazzi R. Chloride movements in human neutrophils during phagocytosis: characterization and relationship to granule release. J Immunol. 2007;179(6):4110-24.
249. Cantin AM, Hartl D, Konstan MW, Chmiel JF. Inflammation in cystic fibrosis lung disease: Pathogenesis and therapy. J Cyst Fibros. 2015;14(4):419-30.
250. Wang XR, Li C. Decoding F508del misfolding in cystic fibrosis. Biomolecules. 2014;4(2):498-509.
251. Valdivieso ÁG, Mori C, Clauzure M, Massip-Copiz M, Santa-Coloma TA. CFTR modulates RPS27 gene expression using chloride anion as signaling effector. Archives of Biochemistry and Biophysics. 2017;633:103-9.

252. Weber AJ, Soong G, Bryan R, Saba S, Prince A. Activation of NF-kappaB in airway epithelial cells is dependent on CFTR trafficking and Cl- channel function. American journal of physiology Lung cellular and molecular physiology. 2001;281(1):L71-8.
253. Tabary O, Boncoeur E, de Martin R, Pepperkok R, Clement A, Schultz C, et al. Calcium-dependent regulation of NF-(kappa)B activation in cystic fibrosis airway epithelial cells. Cell Signal. 2006;18(5):652-60.
254. Verhaeghe C, Remouchamps C, Hennuy B, Vanderplasschen A, Chariot A, Tabruyn SP, et al. Role of IKK and ERK pathways in intrinsic inflammation of cystic fibrosis airways. Biochem Pharmacol. 2007;73(12):1982-94.
255. Nichols D, Chmiel J, Berger M. Chronic inflammation in the cystic fibrosis lung: alterations in inter- and intracellular signaling. Clin Rev Allergy Immunol. 2008;34(2):146-62.
256. Gaidt MM, Ebert TS, Chauhan D, Schmidt T, Schmid-Burgk JL, Rapino F, et al. Human Monocytes Engage an Alternative Inflammasome Pathway. Immunity. 2016;44(4):833-46.
257. Martins JR, Faria D, Kongsuphol P, Reisch B, Schreiber R, Kunzelmann K. Anoctamin 6 is an essential component of the outwardly rectifying chloride channel. Proc Natl Acad Sci U S A. 2011;108(44):18168-72.
258. Hasko G, Deitch EA, Nemeth ZH, Kuhel DG, Szabo C. Inhibitors of ATP-binding cassette transporters suppress interleukin-12 p40 production and major histocompatibility complex II up-regulation in macrophages. J Pharmacol Exp Ther. 2002;301(1):103-10.
259. Ge N, Nakamura Y, Nakaya Y, Sone S. Interferon-gamma activates outwardly rectifying chloride channels in the human bronchial epithelial cell line BEAS-2B. J Med Invest. 2001;48(1-2):97-101.
260. Alzamora R, King JD, Jr., Hallows KR. CFTR regulation by phosphorylation. Methods Mol Biol. 2011;741:471-88.
261. Perregaux DG, Svensson L, Gabel CA. Tenidap and other anion transport inhibitors disrupt cytolytic T lymphocyte-mediated IL-1 beta post-translational processing. J Immunol. 1996;157(1):57-64.
262. Yao H, Felfly H, Wang J, Zhou D, Haddad GG. DIDS protects against neuronal injury by blocking Toll-like receptor 2 activated-mechanisms. J Neurochem. 2009;108(3):835-46.
263. Tang A, Sharma A, Jen R, Hirschfeld AF, Chilvers MA, Lavoie PM, et al. Inflammasome-Mediated IL-1β Production in Humans with Cystic Fibrosis. PLOS ONE. 2012;7(5):e37689.
264. Foster N, Lea SR, Preshaw PM, Taylor JJ. Pivotal advance: vasoactive intestinal peptide inhibits up-regulation of human monocyte TLR2 and TLR4 by LPS and differentiation of monocytes to macrophages. J Leukoc Biol. 2007;81(4):893-903.
265. Qiu MR. FUNCTIONAL AND MOLECULAR ASPECTS OF ION CHANNELS IN MACROPHAGES. Sydney, Australia: University of New South Wales, Sydney, Australia; 2003.
266. Perez A, Issler AC, Cotton CU, Kelley TJ, Verkman AS, Davis PB. CFTR inhibition mimics the cystic fibrosis inflammatory profile. American journal of physiology Lung cellular and molecular physiology. 2007;292(2):L383-95.
267. Oprins JC, van der Burg C, Meijer HP, Munnik T, Groot JA. Tumour necrosis factor alpha potentiates ion secretion induced by histamine in a human intestinal epithelial cell line and in mouse colon: involvement of the phospholipase D pathway. Gut. 2002;50(3):314-21.

268. Kandil HM, Berschneider HM, Argenzio RA. Tumour necrosis factor alpha changes porcine intestinal ion transport through a paracrine mechanism involving prostaglandins. Gut. 1994;35(7):934-40.
269. Kang DW, Park MH, Lee YJ, Kim HS, Kwon TK, Park W-S, et al. Phorbol Ester Up-regulates Phospholipase D1 but Not Phospholipase D2 Expression through a PKC/Ras/ERK/NFκB-dependent Pathway and Enhances Matrix Metalloproteinase-9 Secretion in Colon Cancer Cells. Journal of Biological Chemistry. 2008;283(7):4094-104.
270. Gabriel SE, Clarke LL, Boucher RC, Stutts MJ. CFTR and outward rectifying chloride channels are distinct proteins with a regulatory relationship. Nature. 1993;363(6426):263-8.
271. Schulte G, Fredholm BB. Signalling from adenosine receptors to mitogen-activated protein kinases. Cell Signal. 2003;15(9):813-27.
272. Frey RS, Rahman A, Kefer JC, Minshall RD, Malik AB. PKCzeta regulates TNF-alpha-induced activation of NADPH oxidase in endothelial cells. Circ Res. 2002;90(9):1012-9.
273. Ouyang X, Ghani A, Malik A, Wilder T, Colegio OR, Flavell RA, et al. Adenosine is required for sustained inflammasome activation via the A2A receptor and the HIF-1α pathway. Nature Communications. 2013;4:2909.
274. Aronoff DM, Canetti C, Serezani CH, Luo M, Peters-Golden M. Cutting edge: macrophage inhibition by cyclic AMP (cAMP): differential roles of protein kinase A and exchange protein directly activated by cAMP-1. J Immunol. 2005;174(2):595-9.
275. Bryn T, Mahic M, Enserink JM, Schwede F, Aandahl EM, Tasken K. The cyclic AMP-Epac1-Rap1 pathway is dissociated from regulation of effector functions in monocytes but acquires immunoregulatory function in mature macrophages. J Immunol. 2006;176(12):7361-70.
276. Guo Y, Zhao G, Tanaka S, Yamaguchi T. Differential responses between monocytes and monocyte-derived macrophages for lipopolysaccharide stimulation of calves. Cellular & molecular immunology. 2009;6(3):223-9.
277. Juhasz T, Matta C, Veress G, Nagy G, Szijgyarto Z, Molnar Z, et al. Inhibition of calcineurin by cyclosporine A exerts multiple effects on human melanoma cell lines HT168 and WM35. Int J Oncol. 2009;34(4):995-1003.
278. Pelegrin P, Surprenant A. Pannexin-1 couples to maitotoxin- and nigericin-induced interleukin-1beta release through a dye uptake-independent pathway. J Biol Chem. 2007;282(4):2386-94.
279. Frizzell RA, Hanrahan JW. Physiology of epithelial chloride and fluid secretion. Cold Spring Harb Perspect Med. 2012;2(6):a009563.
280. Grandoch M, Roscioni SS, Schmidt M. The role of Epac proteins, novel cAMP mediators, in the regulation of immune, lung and neuronal function. Br J Pharmacol. 2010;159(2):265-84.
281. de Rooij J, Rehmann H, van Triest M, Cool RH, Wittinghofer A, Bos JL. Mechanism of regulation of the Epac family of cAMP-dependent RapGEFs. J Biol Chem. 2000;275(27):20829-36.
282. Branham MT, Bustos MA, De Blas GA, Rehmann H, Zarelli VE, Trevino CL, et al. Epac activates the small G proteins Rap1 and Rab3A to achieve exocytosis. J Biol Chem. 2009;284(37):24825-39.
283. Bos JL. Epac proteins: multi-purpose cAMP targets. Trends Biochem Sci. 2006;31(12):680-6.
284. Kang G, Leech CA, Chepurny OG, Coetzee WA, Holz GG. Role of the cAMP sensor Epac as a determinant of KATP channel ATP sensitivity in human pancreatic β-cells and rat INS- 1 cells. The Journal of physiology. 2008;586(5):1307-19.

285. Purves GI, Kamishima T, Davies LM, Quayle JM, Dart C. Exchange protein activated by cAMP (Epac) mediates cAMP-dependent but protein kinase A-insensitive modulation of vascular ATP-sensitive potassium channels. J Physiol. 2009;587(Pt 14):3639-50.
286. Tang J, Bouyer P, Mykoniatis A, Buschmann M, Matlin KS, Matthews JB. Activated PKC{delta} and PKC{epsilon} inhibit epithelial chloride secretion response to cAMP via inducing internalization of the Na+-K+-2Cl- cotransporter NKCC1. J Biol Chem. 2010;285(44):34072-85.
287. Hoque KM, Woodward OM, van Rossum DB, Zachos NC, Chen L, Leung GP, et al. Epac1 mediates protein kinase A–independent mechanism of forskolin-activated intestinal chloride secretion. The Journal of general physiology. 2010;135(1):43-58.
288. Petrucci C, Cervia D, Buzzi M, Biondi C, Bagnoli P. Somatostatin-induced control of cytosolic free calcium in pituitary tumour cells. Br J Pharmacol. 2000;129(3):471-84.
289. Zhu Y, Chen H, Boulton S, Mei F, Ye N, Melacini G, et al. Biochemical and pharmacological characterizations of ESI-09 based EPAC inhibitors: defining the ESI-09 "therapeutic window". Sci Rep. 2015;5:9344.
290. Yang Z, Kirton HM, Al-Owais M, Thireau J, Richard S, Peers C, et al. Epac2-Rap1 Signaling Regulates Reactive Oxygen Species Production and Susceptibility to Cardiac Arrhythmias. Antioxid Redox Signal. 2017;27(3):117-32.
291. Yu X, Zhang Q, Zhao Y, Schwarz BJ, Stallone JN, Heaps CL, et al. Activation of G protein-coupled estrogen receptor 1 induces coronary artery relaxation via Epac/Rap1-mediated inhibition of RhoA/Rho kinase pathway in parallel with PKA. PLoS One. 2017;12(3):e0173085.
292. Eisenhut M. Changes in ion transport in inflammatory disease. J Inflamm (Lond). 2006;3:5.
293. Eisenhut M, Wallace H. Ion channels in inflammation. Pflugers Arch. 2011;461(4):401-21.
294. Peteranderl C, Sznajder JI, Herold S, Lecuona E. Inflammatory Responses Regulating Alveolar Ion Transport during Pulmonary Infections. Front Immunol. 2017;8:446.
295. Challier J, Bruniquel D, Sewell AK, Laugel B. Adenosine and cAMP signalling skew human dendritic cell differentiation towards a tolerogenic phenotype with defective CD8(+) T-cell priming capacity. Immunology. 2013;138(4):402-10.
296. Schmidt M, Dekker FJ, Maarsingh H. Exchange protein directly activated by cAMP (epac): a multidomain cAMP mediator in the regulation of diverse biological functions. Pharmacol Rev. 2013;65(2):670-709.
297. Cheng X, Ji Z, Tsalkova T, Mei F. Epac and PKA: a tale of two intracellular cAMP receptors. Acta biochimica et biophysica Sinica. 2008;40(7):651-62.
298. Sands WA, Woolson HD, Milne GR, Rutherford C, Palmer TM. Exchange protein activated by cyclic AMP (Epac)-mediated induction of suppressor of cytokine signaling 3 (SOCS-3) in vascular endothelial cells. Molecular and cellular biology. 2006;26(17):6333-46.
299. Cullere X, Shaw SK, Andersson L, Hirahashi J, Luscinskas FW, Mayadas TN. Regulation of vascular endothelial barrier function by Epac, a cAMP-activated exchange factor for Rap GTPase. Blood. 2005;105(5):1950-5.
300. Tan KS, Nackley AG, Satterfield K, Maixner W, Diatchenko L, Flood PM. β2 adrenergic receptor activation stimulates pro-inflammatory cytokine production in macrophages via PKA-and NF-κB-independent mechanisms. Cellular signalling. 2007;19(2):251-60.

301. Sokolowska M, Chen L-Y, Liu Y, Martinez-Anton A, Qi H-Y, Logun C, et al. Prostaglandin E2 inhibits NLRP3 inflammasome activation through EP4 receptor and intracellular cyclic AMP in human macrophages. The Journal of Immunology. 2015;194(11):5472-87.
302. Roscioni SS, Kistemaker LE, Menzen MH, Elzinga CR, Gosens R, Halayko AJ, et al. PKA and Epac cooperate to augment bradykinin-induced interleukin-8 release from human airway smooth muscle cells. Respir Res. 2009;10:88.
303. Li J, Moran T, Swanson E, Julian C, Harris J, Bonen DK, et al. Regulation of IL-8 and IL-1β expression in Crohn's disease associated NOD2/CARD15 mutations. Human molecular genetics. 2004;13(16):1715-25.
304. Hothi SS, Gurung IS, Heathcote JC, Zhang Y, Booth SW, Skepper JN, et al. Epac activation, altered calcium homeostasis and ventricular arrhythmogenesis in the murine heart. Pflugers Arch. 2008;457(2):253-70.
305. Ainscough JS, Gerberick GF, Kimber I, Dearman RJ. Interleukin-1β Processing Is Dependent on a Calcium-mediated Interaction with Calmodulin. Journal of Biological Chemistry. 2015;290(52):31151-61.
306. Holz GG. Epac: A new cAMP-binding protein in support of glucagon-like peptide-1 receptor-mediated signal transduction in the pancreatic beta-cell. Diabetes. 2004;53(1):5-13.
307. Matulef K, Maduke M. Side-dependent inhibition of a prokaryotic ClC by DIDS. Biophys J. 2005;89(3):1721-30.
308. Lee GS, Subramanian N, Kim AI, Aksentijevich I, Goldbach-Mansky R, Sacks DB, et al. The calcium-sensing receptor regulates the NLRP3 inflammasome through Ca2+ and cAMP. Nature. 2012;492(7427):123-7.
309. Palomo J, Marchiol T, Piotet J, Fauconnier L, Robinet M, Reverchon F, et al. Role of IL-1β in experimental cystic fibrosis upon P. aeruginosa Infection. PloS one. 2014;9(12):e114884.
310. Gabel M, Chasserot-Golaz S. Annexin A2, an essential partner of the exocytotic process in chromaffin cells. J Neurochem. 2016;137(6):890-6.
311. Qiao H, May JM. Macrophage differentiation increases expression of the ascorbate transporter (SVCT2). Free Radic Biol Med. 2009;46(8):1221-32.
312. Szkotak AJ, Man SF, Duszyk M. The role of the basolateral outwardly rectifying chloride channel in human airway epithelial anion secretion. Am J Respir Cell Mol Biol. 2003;29(6):710-20.
313. Kim SS, Lee EH, Lee K, Jo SH, Seo SR. PKA regulates calcineurin function through the phosphorylation of RCAN1: identification of a novel phosphorylation site. Biochemical and biophysical research communications. 2015;459(4):604-9.
314. Buyck JM, Verriere V, Benmahdi R, Higgins G, Guery B, Matran R, et al. P. aeruginosa LPS stimulates calcium signaling and chloride secretion via CFTR in human bronchial epithelial cells. J Cyst Fibros. 2013;12(1):60-7.
315. Wang G. Chloride flux in phagocytes. Immunological reviews. 2016;273(1):219-31.
316. Venkatachalam K, Wong C-O, Zhu MX. The role of TRPMLs in endolysosomal trafficking and function. Cell calcium. 2015;58(1):48-56.
317. Al- Khadra ES, Chau Kw, Barone CP, Colin AA. Invasive pneumonia and septic shock in infants as a presentation of cystic fibrosis with vitamin- deficiency. Pediatric pulmonology. 2012;47(7):722-6.
318. Grosse-Onnebrink J, Stehling F, Tschiedel E, Olivier M, Mellies U, Schmidt R, et al. Bacteraemia and fungaemia in cystic fibrosis patients with febrile pulmonary exacerbation: a prospective observational study. BMC Pulm Med. 2017;17(1):96.

319. Cucu D, Dima S-O. Ion channels involved in the inflammatory processes of the digestive system. Romanian Journal of Biochemistry. 2011;48(1):41-50.
320. Bi MM, Hong S, Zhou HY, Wang HW, Wang LN, Zheng YJ. Chloride Channelopathies of ClC-2. International Journal of Molecular Sciences. 2014;15(1):218-49.
321. Cafferata EG, González-Guerrico AM, Giordano L, Pivetta OH, Santa-Coloma TA. Interleukin-1β regulates CFTR expression in human intestinal T84 cells. Biochimica et Biophysica Acta (BBA)-Molecular Basis of Disease. 2000;1500(2):241-8.
322. Sabbatini ME, Chen X, Ernst SA, Williams JA. Rap1 activation plays a regulatory role in pancreatic amylase secretion. J Biol Chem. 2008;283(35):23884-94.
323. Lobo MJ, Amaral MD, Zaccolo M, Farinha CM. EPAC1 activation by cAMP stabilizes CFTR at the membrane by promoting its interaction with NHERF1. J Cell Sci. 2016;129(13):2599-612.
324. Sheikh IA, Koley H, Chakrabarti MK, Hoque KM. The Epac1 signaling pathway regulates Cl- secretion via modulation of apical KCNN4c channels in diarrhea. J Biol Chem. 2013;288(28):20404-15.
325. Gudipaty L, Munetz J, Verhoef PA, Dubyak GR. Essential role for Ca2+ in regulation of IL-1beta secretion by P2X7 nucleotide receptor in monocytes, macrophages, and HEK-293 cells. Am J Physiol Cell Physiol. 2003;285(2):C286-99.
326. Sama MA, Mathis DM, Furman JL, Abdul HM, Artiushin IA, Kraner SD, et al. Interleukin-1β-dependent Signaling between Astrocytes and Neurons Depends Critically on Astrocytic Calcineurin/NFAT Activity. The Journal of Biological Chemistry. 2008;283(32):21953-64.
327. Vandivier RW, Richens TR, Horstmann SA, deCathelineau AM, Ghosh M, Reynolds SD, et al. Dysfunctional cystic fibrosis transmembrane conductance regulator inhibits phagocytosis of apoptotic cells with proinflammatory consequences. American journal of physiology Lung cellular and molecular physiology. 2009;297(4):L677-86.
328. Kim JG, Moon MY, Kim HJ, Li Y, Song DK, Kim JS, et al. Ras-related GTPases Rap1 and RhoA collectively induce the phagocytosis of serum-opsonized zymosan particles in macrophages. J Biol Chem. 2012;287(7):5145-55.
329. Scott J, Harris GJ, Pinder EM, Macfarlane JG, Hellyer TP, Rostron AJ, et al. Exchange protein directly activated by cyclic AMP (EPAC) activation reverses neutrophil dysfunction induced by β2-agonists, corticosteroids, and critical illness. Journal of Allergy and Clinical Immunology. 2016;137(2):535-44.